UCID-17296 SUPPORTING DOCUMENTS FOR LLL AREA 27 (410 AREA) SAFETY ANALYSIS REPORTS NEVADA TEST SITE LAWRENCE LIVERMORE LABORATORY

UCID- 17296

Lawrence Livermore Laboratory

SUPPORTING DOCUMENTS FOR LLL AREA 27 (410 AREA) SAFETY ANALYSIS REPORTS NEVADA TEST SITE

Compiled by Byron N. Odell

February 1, 1977

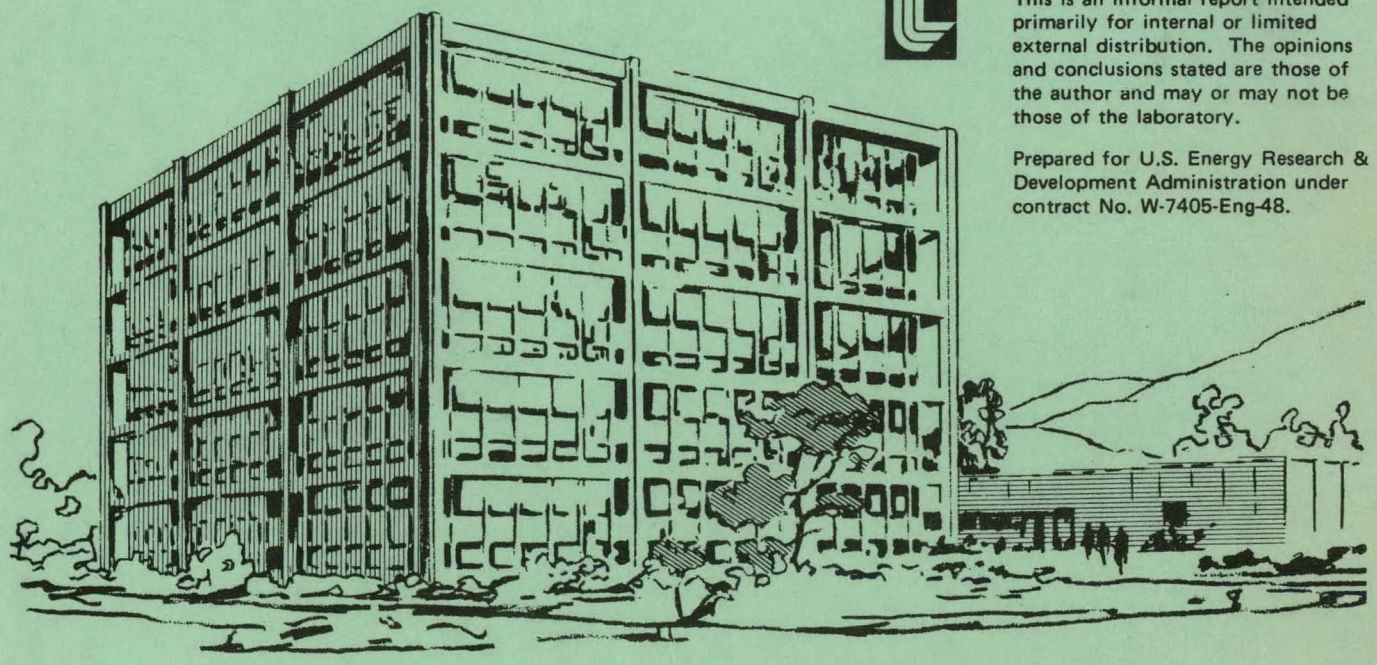

Prepared for U.S. Energy Research & Development Administration under contract No. W-7405-Eng-48.

DISCLAIMER

UCID-17296

SUPPORTING DOCUMENTS

FOR

LLL AREA 27 (410 AREA) SAFETY ANALYSIS REPORTS

NEVADA TEST SITE

February 1, 1977

Compiled by Byron N. Odell

INTRODUCTION

The following appendices are common to the LLL Safety Analysis Reports Nevada Test Site and are included here as supporting documents to those reports.

APPENDICES

A — Environmental Monitoring Report for the Nevada Test Site and Other Test Areas Used for Underground Nuclear Detonations, U. S. Environmental Protection Agency, Las Vegas, Rept. EMSL-LV-539-4 (1976)

B — Selected Census Information Around the Nevada Test Site, U. S. Environmental Protection Agency, Las Vegas, Rept. NERC-LV-539-8 (1973)

C — W. J. Hannon and H. L. McKague, An Examination of the Geology and Seismology Associated with Area 410 at the Nevada Test Site, Lawrence Livermore Laboratory, Livermore, Rept. UCRL-51830 (1975)

D — K. R. Peterson, Diffusion Climatology for Hypothetical Accidents in Area 410 of the Nevada Test Site, Lawrence Livermore Laboratory, Livermore, Rept. UCRL-52074 (1976)

E — J. R. McDonald, J. E. Minor, and K. C. Mehta, Development of a Design Basis Tornado and Structural Design Criteria for the Nevada Test Site, Nevada, Lawrence Livermore Laboratory, Livermore, Rept. UCRL-13668 (1975)

F — A. E. Stevenson, Impact Tests of Wind-Borne Wooden Missiles, Sandia Laboratories, Tonopah, Rept. SAND 76-0407 (1976)

G — Hydrology of the 410 Area (Area 27) at the Nevada Test Site

EMSL-LV-539-4

EMSL-LV-539-4

May 1976

ENVIRONMENTAL MONITORING REPORT FOR THE NEVADA TEST SITE AND OTHER TEST AREAS USED FOR UNDERGROUND NUCLEAR DETONATIONS

January through December 1975

by

Monitoring Operations Division
Environmental Monitoring and Support Laboratory
U.S. ENVIRONMENTAL PROTECTION AGENCY
Las Vegas, Nevada 89114

APRIL 1976

This work performed under a Memorandum of
Understanding No. AT(26-1)-539
for the
U.S. ENERGY RESEARCH & DEVELOPMENT ADMINISTRATION

This document is available to the public through the National Technical Information Service, U.S. Department of Commerce, Springfield, Virginia 22161.

EMSL-LV-539-4

May 1976

ENVIRONMENTAL MONITORING REPORT FOR THE NEVADA TEST SITE AND OTHER TEST AREAS USED FOR UNDERGROUND NUCLEAR DETONATIONS

January through December 1975

by

Monitoring Operations Division
Environmental Monitoring and Support Laboratory
U.S. ENVIRONMENTAL PROTECTION AGENCY
Las Vegas, Nevada 89114

APRIL 1976

This work performed under a Memorandum of
Understanding No. AT(26-1)-539
for the
U.S. ENERGY RESEARCH & DEVELOPMENT ADMINISTRATION

THIS PAGE

WAS INTENTIONALLY

LEFT BLANK

PREFACE

The Atomic Energy Commission (AEC) used the Nevada Test Site (NTS) from January 1951 through January 19, 1975, as an area for conducting nuclear detonations, nuclear rocket-engine development, nuclear medicine studies, and miscellaneous nuclear and non-nuclear experiments. Beginning on January 19, 1975, these responsibilities were transferred to the newly-formed U.S. Energy Research and Development Administration (ERDA). Atmospheric nuclear tests were conducted periodically from 1951 through October 30, 1958, at which time a testing moratorium was implemented. Since September 1, 1961, in accordance with the limited test ban treaty, all nuclear detonations have been conducted underground with the expectation of containment except for four slightly above-ground or shallow underground tests of Operation Dominic II and five nuclear earth-cratering experiments conducted under the Plowshare program.

The U.S. Public Health Service (PHS), from 1953 through 1970, and the U.S. Environmental Protection Agency (EPA), from 1970 to the present, have maintained facilities at the NTS or in Las Vegas, Nevada, for the purpose of providing an Off-Site Radiological Safety Program for the nuclear testing program. In addition, off-site surveillance has been provided by the PHS/EPA for nuclear explosive tests at places other than the NTS. Prior to 1953, the surveillance program was performed by the Los Alamos Scientific Laboratory and U.S. Army personnel.

The objective of the Program since 1953 has been to measure levels and trends of radioactivity in the off-site environment surrounding testing areas to assure that the testing is in compliance with existing radiation protection standards. To assess off-site radiation levels, routine sampling networks for milk, water, and air are maintained along with a dosimetry network and special sampling of food crops, soil, etc., as required. For the purpose of implementing protective actions, providing immediate radiation monitoring, and obtaining environmental samples rapidly after a release of radioactivity, mobile monitoring personnel are also placed in areas downwind of NTS or other test areas prior to each test.

In general, analytical results showing radioactivity levels above naturally occurring levels have been published in reports covering a test series or test project. Beginning in 1959 for reactor tests, and in 1962 for weapons tests, surveillance data for each individual test which released radioactivity off-site were reported separately. Commencing in January 1964, and continuing through December 1970, these individual reports for nuclear tests were also summarized and reported every 6 months. The individual analytical results for all routine or special milk samples were also included in the 6-month summary reports.

In 1971, the AEC implemented a requirement (ERDA Manual, Chapter 0513) for a comprehensive radiological monitoring report from each of the several contractors or agencies involved in major nuclear activities. The compilation

of these various reports since that time and their entry into the general literature serve the purpose of providing a single source of information concerning the environmental impact of nuclear activities. To provide more rapid dissemination of data, the monthly report of analytical results of all air data collected since July 1971, and all milk and water samples collected since January 1972, were submitted to the appropriate state health departments involved, and were also published in Radiation Data and Reports, a monthly publication of the EPA which was discontinued at the end of 1974.

Beginning with the first quarter of 1975, air and milk sample data have been reported quarterly. Dosimetry data were included beginning with the third quarter 1975.

Since 1962, PHS/EPA aircraft have also been used during nuclear tests to provide rapid monitoring and sampling for releases of radioactivity. Early aircraft monitoring data obtained immediately after a test are used to position mobile radiation monitoring personnel on the ground, and the results of airborne sampling are used to quantitate the inventories, diffusion, and transport of the radionuclides released. Beginning in 1971, all monitoring and sampling results by aircraft have been reported in effluent monitoring data reports in accordance with the ERDA Manual, Chapter 0513.

TABLE OF CONTENTS

LIST OF FIGURES

LIST OF TABLES

INTRODUCTION

Under a Memorandum of Understanding, No. AT(26-1)-539, with the U.S. Energy Research and Development Administration (ERDA), the U.S. Environmental Protection Agency (EPA), Environmental Monitoring and Support Laboratory-Las Vegas (EMSL-LV), continued its Off-Site Radiological Safety Program within the environment surrounding the Nevada Test Site (NTS) and at other sites designated by the ERDA during 1975. This report, prepared in accordance with the ERDA Manual, Chapter 0513, contains summaries of EMSL-LV sampling methods, analytical procedures, and the analytical results of environmental samples collected in support of ERDA nuclear testing activities. Where applicable, sampling data are compared to appropriate guides for external and internal exposures to ionizing radiation. In addition, a brief summary of pertinent and demographical features of the NTS and the NTS environs is presented for background information.

NEVADA TEST SITE

The major programs conducted at the NTS in the past have been nuclear weapons development, proof-testing and weapons safety, testing for peaceful uses of nuclear explosives (Project Plowshare), reactor/engine development for nuclear rocket and ram-jet applications (Projects Pluto and Rover), basic high-energy nuclear physics research, and seismic studies (Vela-Uniform). During this report period these programs were continued with the exception of Project Pluto, discontinued in 1964, and Project Rover, which was terminated in January 1973. No Plowshare nuclear tests were conducted at the NTS or any other site during this period. All nuclear weapons tests were conducted underground to minimize the possibility of the release of fission products to the atmosphere.

Site Location

The Nevada Test Site (Figures 1 and 2) is located in Nye County, Nevada, with its southeast corner about 90 km northwest of Las Vegas. The NTS has an area of about 3500 km^2 and varies from 40-56 km in width (east-west) and from 64-88 km in length (north-south). This area consists of large basins or flats about 900-1200 m above mean sea level (MSL) surrounded by mountain ranges 1800-2100 m MSL.

The NTS is nearly surrounded by an exclusion area collectively named the Nellis Air Force Range. The Range, particularly to the north and east, provides a buffer zone between the test areas and public lands. This buffer zone varies from 24-104 km between the test area and land that is open to the public. Depending upon wind speed and direction, this provides a delay of from 1/2 to more than 6 hours before any accidental release of airborne radioactivity could pass over public lands.

Climate

The climate of the NTS and surrounding area is variable, primarily due to altitude and the rugged terrain. Generally, the climate is referred to as Continental Arid. Throughout the year there is not sufficient water to support tree or crop growth without irrigation.

The climate may be classified by the types of vegetation which grow under these conditions. According to Houghton et al., this method, developed by Köppen in 1918, recognizes five basic climatic conditions as humid tropical, dry, humid mesothermal, humid microthermal, and polar (five-sixths of Nevada falls in the dry category). Köppen's classification of dry conditions is further subdivided on the basis of temperature and severity of drought. Table 1, from Houghton et al., summarizes the different characteristics of these climatic types in Nevada.

TABLE 1. CHARACTERISTICS OF CLIMATIC TYPES IN NEVADA

Climatic Type	Mean Temperature °C (°F) Winter	Summer	Annual Precipitation cm (inches) Total*	Snowfall	Dominant Vegetation	Percent of Area
Alpine tundra	-18° - -9° (0° - 15°)	4° - 10° (40° - 50°)	38 - 114 (15 - 45)	Medium to heavy	Alpine meadows	--
Humid Continental	-12° - -1° (10° - 30°)	10° - 21° (50° - 70°)	64 - 114 (25 - 45)	Heavy	Pine-fir forest	1
Subhumid continental	-12° - -1° (10° - 30°)	10° - 21° (50° - 70°)	30 - 64 (12 - 25)	Moderate	Pine or scrub woodland	15
Mid-latitude steppe	-7° - 4° (20° - 40°)	18° - 27° (65° - 80°)	15 - 38 (6 - 15)	Light to moderate	Sagebrush, grass, scrub	57
Mid-latitude desert	-7° - 4° (20° - 40°)	18° - 27° (65° - 80°)	8 - 20 (3 - 8)	Light	Greasewood, shadscale	20
Low-latitude desert	4° - 10° (40° - 50°)	27° - 32° (80° - 90°)	5 - 25 (2 - 10)	Negligible	Creosote bush	7

*Limits of annual precipitation overlap because of variations in temperature which affect the water balance.

As pointed out by Houghton et al., 90 percent of Nevada's population lives in areas with less than 25 cm of rain per year or in areas which would be classified as mid-latitude steppe to low-latitude desert regions.

According to Quiring, 1968, the NTS average annual precipitation ranges from about 10 cm at the 900-m altitude to around 25 cm on the plateaus. During the winter months, the plateaus may be snow-covered for periods of several days or weeks. Snow is uncommon on the flats. Temperatures vary considerably with elevation, slope, and local air currents. The average daily high (low) temperatures at the lower altitudes are around 10° (-4°) C in January and 35° (12°) C in July, with extremes of 44° and -26° C. Corresponding temperatures on the plateaus are 2° (-4°) C in January and 26° (18°) C in July with extremes of 38° and -29° C. Temperatures as low as -34° C and higher than 46° C have been observed at the NTS.

The direction from which winds blow, as measured on a 30-m tower at the Yucca observation station, is predominantly northerly except for the months of May through August when winds from the south-southwest predominate. Because of the prevalent mountain/valley winds in the basins, south to southwest winds predominate during daylight hours during most months. During the winter months southerly winds have only a slight edge over northerly winds for a few hours during the warmest part of the day. These wind patterns may be quite different at other locations on the NTS because of local terrain effects and differences in elevation (Quiring, 1968).

Geology and Hydrology

Geological and hydrological studies of the NTS have been in progress by the U.S. Geological Survey and various other institutions since 1956. Because of this continuing effort, including subsurface studies of numerous boreholes, the surface and underground geological and hydrological characteristics for much of the NTS are known in considerable detail. This is particularly true for those areas in which underground experiments are conducted. A comprehensive summary of the geology and hydrology of the NTS was published in 1968 as Memoir 110 by the Geological Society of America, entitled "Nevada Test Site."

There are two major hydrologic systems on the NTS (Figure 3). Groundwater in the northwestern part of NTS or in the Pahute Mesa has been reported (WASH-DRAFT, 1975) to travel somewhere between 2 and 80 m per year to the south and southwest toward the Ash Meadows discharge area in the Amargosa Desert. It is estimated that the groundwater to the east of the NTS moves from north to south at a rate not less than 2 nor greater than 220 m per year. Carbon-14 analyses of this eastern groundwater indicate that the lower velocity is nearer the true value. At Mercury Valley, in the extreme southern part of the NTS, the groundwater flow direction shifts to the southwest toward the Ash Meadows discharge area in the southeastern Amargosa Valley.

Depths of water on the NTS vary from about 100 m beneath the valleys in the southeastern part of the site to more than 600 m beneath the highlands to the north. Although much of the valley fill is saturated, downward movement of water is extremely slow. The primary aquifer in these formations is the Paleozoic carbonates which underlie the more recent tuffs and alluviums.

Land Use of NTS Environs

Figure 4 is a map of the off-NTS area showing general land use. A wide variety of uses, such as farming, mining, grazing, camping, fishing, and hunting, exists due to the variable terrain. For example, within a 300-km radius west of the NTS, elevations range from below sea level in Death Valley to 4420 m above MSL in the Sierra Nevada Range. Additionally, parts of two valleys of major agricultural importance (the Owens and San Joaquin) are included. The areas south of the NTS are more uniform since the Mojave Desert ecosystem (mid-latitude desert) comprises most of this portion of Nevada, California, and Arizona. The areas east of the NTS are primarily mid-latitude steppe with some of the older river valleys, such as the Virgin River Valley and Moapa Valley, supporting small-scale but intensive farming of a variety of crops by irrigation. Grazing is also common in this area, particularly to the northeast. The area north of the NTS is also mid-latitude steppe where the major agricultural-related activity is grazing of both cattle and sheep. Only areas of minor agricultural importance, primarily the growing of alfalfa hay, are found in this portion of the State within a distance of 300 km.

In the summer of 1974, a brief survey of home gardens around the NTS found that a majority of the residents grow or have access to locally grown fruits and vegetables. Approximately two dozen of the surveyed gardens within 30-80 km of the NTS boundary were selected for sampling. These gardens produce a variety of root, leaf, seed, and fruit crops.

The only industrial enterprises within the immediate off-NTS area are 25 active mines, as shown in Figure 4, and several chemical processing plants located near Henderson, Nevada. The number of employees for these operations varies from one person at several small mines to several hundred workers for the chemical plants at Henderson. Most of the individual mining operations involve less than 10 workers per mine; however, a few operations employ up to 100-150 workers.

The major body of water close to the NTS is Lake Mead, a man-made lake supplied by water from the Colorado River. Lake Mead supplies about 60 percent of the water used for domestic, recreational, and industrial purposes in the Las Vegas Valley and a portion of the water used by Southern California. Smaller reservoirs and lakes located in the area are primarily for irrigation and for livestock. In California, the Owens River and Haiwee Reservoir feed into the Los Angeles Aqueduct and are the major sources of domestic water for the Los Angeles area.

As indicated by Figure 4, there are many places scattered in all directions from the NTS where such recreational activities as hunting, fishing, and camping are enjoyed by both local residents and tourists. In general, the camping and fishing sites to the northwest, north, and northeast of the NTS are utilized throughout the year except for the winter months. Camping and fishing at locations southeast, south, and southwest are utilized throughout the year with the most extensive activities occurring during all months except the hot summer months. All hunting is generally restricted to various times during the last 6 months of the year.

Dairy farming is not extensive within the 300-km-radius area under discussion. From a survey of milk cows during this report period, 8700 dairy cows, 370 family goats, and 600 family cows were located. The family cows and goats are found in all directions around the test site (Figure 5), whereas the dairy cows (Figure 6) are located southeast of the test site (Moapa River Valley, Nevada; Virgin River Valley, Nevada; and Las Vegas, Nevada), northeast (Hiko and Alamo, Nevada, area), west-northwest (near Bishop, California), and southwest (near Barstow, California).

Population Distribution

The populated area of primary concern around the NTS is shown in Figure 7 as the area within a 300-km radius of the NTS Control Point (CP-1), except for the areas west of the Sierra Nevada Mountains and in the southern portion of San Bernardino County. Based upon the 1970 census and the projections for 1973 and 1974 by the U.S. Census Bureau, Figure 7 shows the population of counties in Nevada and pertinent portions of the States of Arizona, California, and Utah. Las Vegas and vicinity are the only major population centers within the inscribed area of Figure 7. With the assumption that the total populations of the counties bisected by the 300-km radius lie within the inscribed area, there is a population of about 520,000 people living within the area of primary concern, about 50 percent of which lives in the Las Vegas urbanized area. If the urbanized area is not considered in determining population density, there are about 0.7 people per km^2 (2 people per mi^2). For comparison, the United States (50 states, 1970 census) has a population density of 22 people per km^2, and the overall Nevada average is 1.5 people per km^2.

The off-site areas within about 80 km of NTS are predominantly rural. Several small communities are located in the area, the largest being in the Pahrump Valley. This rural community, with an estimated population of about 1800, is located about 72 km south of the NTS. The Amargosa Farm area has a population of about 300 and is located about 50 km southwest of the center of the NTS. The Spring Meadows Farm area is a relatively new development consisting of approximately 4000 m^2 with a population of about 60. This area is about 55 km south-southwest of the NTS. The largest town in the near off-site area is Beatty with a population of about 500; it is located about 65 km to the west of the site.

In the adjacent states, the Mojave Desert of California, which includes Death Valley National Monument, lies along the southwestern border of Nevada. The population in the Monument boundaries varies considerably from season to season with fewer than 200 permanent residents and tourists in the area during any given period in the summer months. However, during the winter as many as 12,000 tourists and campers can be in the area on any particular day during the major holiday periods. The largest town in this general area is Barstow, located 265 km south-southwest of the NTS, with a population of about 18,200. The Owens Valley, where numerous small towns are located, lies about 50 km west of Death Valley. The largest town in Owens Valley is Bishop, located 225 km west-northwest of the NTS, with a population of about 3600.

The extreme southwestern region of Utah is more developed than the adjacent part of Nevada. The largest town, Cedar City, with a population of 9900, is located 280 km east-northeast of the NTS. The next largest community is St. George, located 220 km east of the NTS, with a population of 8000.

The extreme northwestern region of Arizona is mostly undeveloped range land with the exception of that portion in the Lake Mead Recreation Area.

Several small retirement communities are found along the Colorado River, primarily at Lake Mojave and Lake Havasu. The largest town in the area is Kingman, located 280 km southeast of the NTS, with a population of about 7500.

OTHER TEST SITES

Table 2 lists the names, dates, locations, yields, depths, and purposes of all underground nuclear tests conducted at locations other than the NTS. No off-NTS nuclear tests were conducted during this report period.

SUMMARY

During 1975, the monitoring of gamma radiation levels in the environs of the NTS was continued through the use of an off-site network of radiation dosimeters and gamma-rate recorders. Concentrations of radionuclides in pertinent environmental media were also continuously or periodically monitored by established air, milk, and water sampling networks. Before each underground nuclear detonation, mobile radiation monitors, equipped with radiation monitoring instruments and sampling equipment, were on standby in off-NTS locations to respond to any accidental release of airborne radioactivity. An airplane was airborne near the test area at detonation time to undertake tracking and sampling of any release which might occur.

A total of about 22 curies (Ci) of radioactivity, primarily radioxenon, was reported by ERDA/NV as being released intermittently throughout the year. The only off-NTS indications of this radioactivity from test operations were low concentrations of xenon-133, krypton-85, and tritium (hydrogen-3) in various combinations, measured in air samples collected at Beatty, Diablo, Hiko, Indian Springs, and Las Vegas, Nevada. The concentrations at these locations when averaged over the year were less than 0.01 percent of the Concentration Guide of 1×10^{-7} microcuries per millilitre (μCi/ml) as listed in the ERDA Manual, Chapter 0524, for exposure to a suitable sample of the population. Based upon time-integrated concentrations of the nuclides at these locations, dose calculations, and population information, the whole-body gamma dose commitment to persons within 80 km of the NTS Control Point for test operations during this year was estimated to be 0.00065 man-rem. The highest dose commitment,* 0.062 man-rem occurred beyond 80 km of NTS at Las Vegas, Nevada, a location with a much higher population density than any within 80 km of NTS.

All other measurements of radioactivity made by the Off-Site Radiological Safety Program were attributed to naturally occurring radioactivity or atmospheric fallout and not related to underground nuclear test operations during this report period. Due to the absence of atmospheric tests by the People's Republic of China during 1975 and the reduction in fallout from all previous atmospheric tests, no radionuclides were detected in samples of the Air Surveillance Network (ASN). A decrease in the range and average of gamma radiation levels monitored by thermoluminescent dosimeters of the off-NTS Dosimetry Network was observed as compared to previous years. The decrease in average exposures was attributed to a combination of factors: the slightly lower response of the new 2271-G2 dosimeters which replaced the TL-12 dosimeters used previously; the unusually low levels of world-wide fallout observed during the year by the ASN; and the continuing decay of old fallout from atmospheric testing at the NTS during 1951 - 1958.

*The dose commitment (product of estimated average dose and population) at Las Vegas from 1 year's exposure to natural background radiation is about 9700 man-rem.

The Long-Term Hydrological Monitoring Program used for the monitoring of radionuclide concentrations in surface and groundwaters which are down the hydrologic gradient from sites of past underground nuclear tests was continued for the NTS and six other sites located elsewhere in Nevada, Colorado, New Mexico, and Mississippi. Naturally occurring radionuclides, such as uranium isotopes and radium-226, were detected in samples collected at most locations at levels which were comparable to concentrations measured for previous years. Tritium was measured in all surface water samples at levels less than 2.5×10^{-6} μCi/ml, a concentration considered from past experience to be the highest one would expect from atmospheric fallout. Except for samples collected at wells known to be contaminated by the injection of high concentrations of radioactivity for tracer studies, no radioactivity related to past underground tests or to the contaminated wells was identified.

MONITORING DATA COLLECTION, ANALYSIS, AND EVALUATION

The major portion of the Off-Site Radiological Safety Program for the NTS consisted of continuously-operated dosimetry and air sampling networks and scheduled collections of milk and water samples at locations surrounding the NTS. Before each nuclear test, mobile monitors were positioned in the off-site areas most likely to be exposed to a possible release of radioactive material. These monitors, equipped with radiation survey instruments, rate recorders, thermoluminescent dosimeters, portable air samplers, and supplies for collecting environmental samples, were prepared to conduct a monitoring program directed from the NTS Control Point via two-way radio communications. In addition, for each event at the NTS, a U.S. Air Force aircraft with two Reynolds Electrical and Engineering Company monitors equipped with portable radiation survey instruments was airborne near surface ground zero to detect and track any radioactive effluent. Two EMSL-LV cloud sampling and tracking aircraft were also available to obtain in-cloud samples, assess total cloud volume, and provide long-range tracking in the event of a release of airborne radioactivity.

During this report period, only underground nuclear detonations were conducted. All detonations were contained. However, during re-entry drilling operations, occasional low level releases of airborne radioactivity, primarily radioxenon, did occur. According to information provided by the Nevada Operations Office, ERDA, the following quantities of radionuclides were released into the atmosphere during CY 1975:

Radionuclide	Quantity Released (Ci)
^{133}Xe	19.6
^{133m}Xe	0.3
^{3}H	2.2
Total	22.1

Continuous low-level releases of ^{3}H and ^{85}Kr occur on the NTS. Tritium is released primarily from the Sedan crater and by evaporation from ponds formed by drainage of water from tunnel test areas in the Rainier Mesa. Krypton-85 slowly seeps to the surface from underground test areas. The quantities of radioactivity from seepage are not quantitated, but are detected at on-site sampling locations.

Contained within the following sections of this report are descriptions for each surveillance network and interpretations of the analytical results which are summarized (maximum, minimum, and average concentrations) in tables. Where appropriate, the average values in the tables are compared to the applicable Concentration Guides (CG's) listed in Appendix A.

For "grab" type samples, radionuclide concentrations were extrapolated to the appropriate collection date. Concentrations determined over a period of time were extrapolated to the midpoint of the collection period. Concentration averages were calculated assuming that each concentration less than the minimum detectable concentration (MDC) was equal to the MDC.

All radiological analyses referred to within the text are briefly described in Table 3 and listed with the minimum detectable concentrations (MDC's). To assure validity of the data, analytical personnel routinely calibrate equipment, split selected samples (except for the Air Surveillance Network) for replicate analyses, and analyze spiked samples prepared by the Quality Assurance Branch, EMSL-LV, on a bi-monthly basis. All quality assurance checks for the year identified no problems which would affect the results reported here.

For the purpose of routinely assessing the total error (sampling replication error plus analytical/counting errors) associated with the collection and analysis of the different types of network samples, plans were made during this report period to initiate a duplicate sampling program for all sample types during CY 1976. The program was initiated in some of the networks near the end of this report period; but the data generated are not sufficient to be included in this report. Information on the total error associated with the different sample types will allow more complete analysis of variance in sample results and develop greater confidence in identifying results which are higher than normal.

AIR SURVEILLANCE NETWORK

The Air Surveillance Network, operated by the EMSL-LV, consisted of 48 active and 73 standby sampling stations located in 21 Western States (Figure 8). Samples of airborne particulates were collected continuously at each active station on 10-cm-diameter, glass-fiber filters at a flow rate of about 350 m^3 of air per day. The filters were collected three times per week, resulting in 48- or 72-hour samples from each active station. Activated charcoal cartridges directly behind the glass-fiber filters were used regularly for the collection of gaseous radioiodines at 21 stations near the NTS. Charcoal cartridges could have been added to all other stations, if necessary, by a telephone request to station operators. All air samples (filters and cartridges) were mailed to the EMSL-LV for analysis. Special retrieval could have been arranged at selected locations in the event a release of radioactivity was believed to have occurred.

From gamma spectrometry results, no radionuclides were identified on any filters or charcoal cartridges during this report period. Normally, radionuclides from the atmospheric testing of nuclear devices by the People's Republic of China are detected by the ASN; however, no tests were conducted during CY 1975 and apparently the atmospheric concentrations from previous tests were below the minimum detectable concentration for gamma spectrometry analyses.

NOBLE GAS AND TRITIUM SURVEILLANCE NETWORK

The Noble Gas and Tritium Surveillance Network, which was first established in March and April 1972, was operated to monitor the airborne levels of radiokrypton, radioxenon, and tritium (^{3}H) in the forms of tritiated hydrogen (HT), tritiated water (HTO), and tritiated methane (CH_3T). Originally, the Network consisted of four on-NTS and six off-NTS stations. For the purpose of ensuring that the sampling locations on or near the NTS are situated at population centers, a station was added at Indian Springs, Nevada, on April 1, 1975, and starting at the beginning of the year, the stations at Desert Rock and Gate 700 were moved to Mercury and Area 51, respectively (Figure 9).

The equipment used in this Network is composed of two separate systems, a compressor-type air sampler and a molecular sieve sampler. The compressor-type equipment continuously samples air over a 7-day period and stores it in two pressure tanks. The tanks together hold approximately 2 m^3 of air at atmospheric pressure. They are replaced weekly and returned to the EMSL-LV where the tank contents are separated and analyzed for ^{85}Kr, radioxenons, and CH_3T by gas chromatography and liquid-scintillation counting techniques (Table 3). The molecular sieve equipment samples air through a filter to remove particulates and then through a series of molecular sieve columns. Approximately 5 m^3 of air are passed through each sampler over a 7-day sampling period. From the HTO absorbed on the first molecular sieve column, the concentration of ^{3}H in μCi/ml of recovered moisture and in μCi/ml of sampled air is determined by liquid-scintillation counting techniques. The ^{3}H, passing through the first column as free hydrogen (HT), is oxidized and collected on the last molecular sieve column. From the concentration of ^{3}H for the moisture recovered from the last column, the ^{3}H (in μCi/ml of sampled air) as HT is determined.

Table 4 summarizes the results of this Network by listing the maximum, minimum, and average concentrations for ^{85}Kr, total Xe or ^{133}Xe, ^{3}H as CH_3T, ^{3}H as HTO, and ^{3}H as HT. The annual average concentrations for each station were calculated over the time period sampled assuming that all values less than MDC were equal to the MDC. All concentrations of ^{85}Kr, Xe or ^{133}Xe, ^{3}H as CH_3T, ^{3}H as HTO, and ^{3}H as HT are expressed in the same unit, μCi/ml of air. Since the ^{3}H concentration in air may vary by factors of 15-20 while the concentration in atmospheric water varies by factors up to about 7, the ^{3}H concentration in μCi/ml of atmospheric moisture is also given in the table as a more reliable indicator in cases when background concentrations of HTO are exceeded.

As shown by Table 4, the average ^{85}Kr concentrations for the year were nearly the same for all stations, ranging from 1.7×10^{-11} μCi/ml to 2.0×10^{-11} μCi/ml, with an overall average of 1.81×10^{-11} μCi/ml. This compares with overall averages of 1.60×10^{-11} μCi/ml in 1972, the first year of network operation, and 1.76×10^{-11} μCi/ml in 1974. The ambient concentration is increasing world-wide, primarily as a result of nuclear reactor operations. The maximum concentrations for all stations ranged from 2.3×10^{-11} μCi/ml to 3.8×10^{-11} μCi/ml. Based upon a review of all past ^{85}Kr data, those concentrations equal to or greater than 2.5×10^{-11} μCi/ml were considered to be above ambient background concentrations and attributable to some outside source or to anomalous variations. The sampling locations and dates for all concentrations above this level during CY 1975 are as follows:

Location	Collection Period Start	Stop	^{85}Kr Concentration (10^{-11} µCi/ml)
Death Valley Jct., California	06/17	06/24	2.7
Beatty, Nevada	12/09	12/16	2.5
Diablo, Nevada	12/10	12/17	2.5
Indian Springs, Nevada	06/02	06/09	2.7
	12/08	12/15	2.8
	12/15	12/22	3.0
Las Vegas, Nevada	04/02	04/09	2.6
	12/10	12/17	2.9
	12/17	12/24	3.0
NTS, Nevada (Mercury)	05/19	05/27	2.6
	12/08	12/15	3.4
NTS, Nevada (Area 51)	05/05	05/12	2.5
	06/02	06/09	2.5
NTS, Nevada (BJY)	03/03	03/10	2.5
	03/10	03/17	3.4
	12/08	12/15	3.8
NTS, Nevada (Area 12)	12/15	12/22	2.6
	12/08	12/15	2.7

As shown by these data, higher than normal ^{85}Kr concentrations for the sampling stations at Beatty, Diablo, Indian Springs, Las Vegas, Mercury, BJY, and Area 12 occurred during the period December 8-24. The highest of the concentrations, occurring at the NTS, were at BJY (3.8×10^{-11} µCi/ml) and Mercury (3.4×10^{-11} µCi/ml). These concentrations, and the 3.4×10^{-11} µCi/ml sample from March 10-17 at BJY, are attributed to current testing operations or seepage from the ground around the sites of past underground nuclear detonations. The highest concentration averages, either on-NTS or off-NTS, were less than 0.01 percent of the Concentration Guides for on- and off-site exposures (see Appendix A). Since all the other higher than normal ^{85}Kr concentrations in the above table occurred at different times during the year, they do not appear to be associated with NTS operations.

The concentrations of ^{3}H as HTO were at background levels at all locations except for the off-NTS stations at Beatty and Diablo and at the on-NTS stations at Area 51, BJY, and Area 12. Concentrations of ^{3}H as HT were above normal background levels only occasionally at the on-NTS station at Area 12. The concentrations of ^{3}H as CH_3T at all locations were less than the MDC. The higher than normal concentrations of ^{3}H as HT and HTO were probably the result of seepage from the ground near the sites of past tests, such as the Sedan cratering test and the Area 12 tunnel tests. The total of the average ^{3}H concentrations (HTO+HT+CH_3T) for either of the off-NTS locations identified with above background concentrations was less than 0.01 percent of the Concentration Guide for ^{3}H in air.

Concentrations of radioxenon greater than the MDC were detected at all Network locations during the year except for Death Valley Junction, Beatty,

and Tonopah. Since all off-NTS concentrations occurred in November at the same time that on-NTS concentrations were measured, they were attributable to NTS operations. The maximum concentration of radioxenon, identified as ^{133}Xe, was 3.1×10^{-11} μCi/ml at the on-NTS station at BJY. In the off-NTS area, the highest concentration was 2.5×10^{-11} μCi/ml at Diablo. At any of the off-NTS locations, the ^{133}Xe concentrations, when averaged over the total sampling times for the year, were less than 0.01 percent of the Concentration Guide for this nuclide.

DOSIMETRY NETWORK

The Dosimetry Network during 1975 consisted of 69 locations surrounding the Nevada Test Site which were monitored continuously with thermoluminescent dosimeters (TLD's). The locations of these stations, shown in Figure 10, are all within a 270-km radius of the center of the NTS and include both inhabited and uninhabited locations. Each Dosimetry Network station was routinely equipped with three Harshaw Model 2271-G2 (TLD-200) dosimeters which replaced the EG&G TL-12 dosimeters previously used. These dosimeters were exchanged on a quarterly basis. Within the general area covered by the dosimetry stations, 25 cooperating off-site residents each wore a dosimeter which was exchanged at the same time as the station dosimeters.

The 2271-G2 dosimeters consist of two small "chips" of dysprosium-activated calcium fluoride, designated TLD-200 by Harshaw, mounted within a window of Teflon plastic and attached to an aluminum card. The card is 4.4 by 3.2 cm and is about the size of the standard personnel dosimetry film packet. An energy compensation shield of about 1.2-mm-thick cadmium metal is placed over the chips and the whole card is sealed in an opaque plastic container. These dosimeters have no source of self-exposure and exhibit both sensitivity and precision superior to dosimeter types previously used by the EMSL-LV.

The smallest exposure in excess of background radiation which may be determined from these dosimeter readings depends primarily on variations in the natural background at the particular station location. Experience has shown these variations to be significant from one monitoring period to another and greater than the precision of the dosimeters themselves. Typically, however, the smallest net exposure observable for a 90-day monitoring period would be 5-15 mR in excess of background. The term "background," as used in this context, refers to naturally occurring radioactivity plus a contribution from residual man-made fission products.

After appropriate corrections were made for background exposure accumulated during shipment between the Laboratory and the monitoring location, the dosimeter readings for each station were averaged. This average value for each monitoring period and station was compared to values from the past 3 years to determine if the new value was within the range of previous background values for that station. Any values significantly greater than previous values would have led to calculations of net exposure, while values significantly less than previous values would have been examined to determine possible reader or handling errors producing invalid data. The results from each of the personnel dosimeters were compared to the background value of the nearest station to determine if a net exposure had occurred.

Table 5 lists the maximum, minimum, and average dose equivalent rate (mrem/y) measured at each station in the network during 1975. All doses are due to environmental background radiation. As noted in the summary of environmental radiation doses below, the average environmental background dose for all stations for 1975 is significantly lower than in previous years. This is believed to be due to three factors: the lesser response to low energy photons of the new 2271-G2 dosimeters relative to the older TL-12 dosimeters used previously, the unusually low levels of world-wide radiation fallout observed during 1975, and the continuing decay of old fallout from atmospheric testing at NTS. Each of these factors, while small in themselves, has had an effect which in summary is significant.

	Environmental Radiation Dose (mrem/y)		
Year	Maximum	Minimum	Average
1975	130	44	90
1974	160	62	114
1973	180	80	123
1972	200	84	144
1971	303	102	163

Independent measurements of the photon energy response to the 2271-G2 dosimeters (with the cadmium shield) and the TL-12 dosimeters reveal a relatively decreased sensitivity of the new dosimeters to photons less than 80 keV. In a year long side-by-side comparison, the 2271-G2 dosimeters showed a small, consistently lower average dose than did the TL-12. This is to be expected, since a significant fraction of the photon spectrum comprising environmental background is due to scattered photons of relatively low energy. Since the data from 1971 through 1974 were obtained with the older dosimeters, this effect tends to depress the apparent average for 1975. Although a small difference has been observed between the two TLD types, it is not known yet which measurement is a truer measure of background exposure dose. Both types give a similar response for net exposures above background. A more thorough investigation of the background response of the TLD's will be conducted by making comparisons to field measurements obtained with a pressurized ionization chamber.

During 1975 the Air Surveillance Network reported unusually low levels of radioactivity in air attributable to world-wide fallout from previous atmospheric tests. While it is difficult to quantify the external gamma-ray dose from this source, its decrease during 1975 undoubtedly contributed to the lower overall average dose measured by the Dosimetry Network, just as the occurrence of fallout from nuclear tests by the People's Republic of China in 1973 and 1974 tended to raise the network average in those years.

Probably the most significant effect in decreasing the average dose measured by the Dosimetry Network is the decay of old fallout from atmospheric testing at NTS. Figure 10 clearly shows that most network stations are concentrated in areas which received fallout from these tests, particularly to the north and northeast of NTS, and thus the network average is significantly affected by changes at those stations. As was noted in the previous summary of

environmental radiation doses, the average annual dose for the Dosimetry Network has steadily decreased over the last 4 years by an average of nearly 20 mrem per year.

It is difficult to make comparisons of Dosimetry Network data with other dose estimates, as these are usually population dose estimates, weighted by geographic location and population. For example, one report (ORP/CSD 7201, 1972) estimated the population doses for Nevada, California, and Utah to be 125, 90, and 155 mrem/y per person, respectively. The average doses for the Dosimetry Network stations in these States are 90, 80, and 72 mrem/y, and it is felt that this discrepancy is the result of locating the network stations by criteria other than population density. A study conducted by the Lawrence Livermore Laboratory (LLL) in March-June 1971 (Lindeken et al., 1972) may be more applicable for comparison. In this study, TLD's were placed at 107 weather stations around the United States for roughly 3 months. Several of these locations were close to Dosimetry Network stations and thus a direct comparison is possible. The locations monitored and the dose estimates are as follows:

Total Ionizing Radiation Dose at Selected Locations

Location	Annual Dose Equivalent (mrem/y) (LLL,1971)	(EPA,1971)	(EPA,1975)
Las Vegas, Nevada	57.8	110	52
Ely, Nevada	109	150*	91
Elko, Nevada	110	180	(not monitored)
Bishop, California	174	150	88

*1970 value; 1971 value invalid due to check source left in place.

Although an annual exposure based on a 3-month exposure dose measurement is not directly comparable to a measured 1-year exposure, the results show the large variation in exposure rates that occur in the NTS environs. Considerable variations may occur in different parts of the same city, as shown by the Las Vegas results in Table 5.

The function of the Dosimetry Network is to monitor for radiation exposures due to releases of radioactivity from the NTS. It is necessary to establish an accurate baseline for each monitoring station so that net exposure doses can be determined. This important function is served by the Dosimetry Network. The ability to measure the true background exposure rate or the average population exposure to background radiation is an added benefit derived from the use of TLD's and is of secondary importance.

A network of 30 stationary gamma exposure rate recorders placed at selected air sampling locations was used to document gamma exposure rates at fixed locations (Figure 8). These recorders use a 2.5- by 30.5-cm constant-current ionization chamber detector filled with methane, and operate on either 110 V a.c. or on a self-contained battery pack. They have a range of 0.004 mR/h to

40 mR/h with an accuracy of about ±10 percent. During this report period, no increase in exposure rates attributable to NTS operations was detected by the network of gamma rate recorders.

MILK SURVEILLANCE NETWORK

Milk is only one of the sources of dietary intake of environmental radioactivity. However, it is a very convenient indicator of the general population's intake of biologically significant radionuclide contaminants. For this reason it is monitored on a routine basis. Few of the fission product radionuclides become incorporated into the milk due to the selective metabolism of the cow. However, those that are incorporated are very important from a radiological health standpoint. The amount transferred to milk is a very sensitive measure of their concentrations in the environment. The six most common fission product radionuclides which can occur in milk are ^{3}H, $^{89,90}Sr$, ^{131}I, ^{137}Cs, and ^{140}Ba. A seventh radionuclide, ^{40}K, also occurs in milk at a reasonably constant concentration of about 1.2×10^{-6} μCi/ml. Since this is a naturally occurring radionuclide, it was not included in the analytical results summarized in this section.

The milk surveillance networks operated by the EMSL-LV were the routine Milk Surveillance Network (MSN) and the Standby Milk Surveillance Network (SMSN). The MSN, during 1975 (Figure 11), consisted of 24 different locations where 3.8-litre milk samples were collected from family cows, commercial pasteurized milk producers, Grade A raw milk intended for pasteurization, and Grade A raw milk for local consumption. In the event of a release of activity from the NTS, intensive sampling would have been conducted in the affected area within a 480-km radius of CP-1, NTS, to assess the radionuclide concentrations in milk, the radiation doses that could result from the ingestion of the milk, and the need for protective action. Samples are collected from milk suppliers and producers beyond 480 km within the SMSN.

During 1975, 87 milk samples were collected from the MSN on a quarterly collection schedule. Usually milk could not be obtained at all locations at any one collection time. Cows not lactating, no one home, or no milk on the day that field personnel arrived at the ranch were some of the reasons why some of the samples were not collected. During the year, milk sampling points also changed as dairies were closed, cows were sold, or cows were otherwise unavailable for regular milkings.

The SMSN consisted of about 175 Grade A milk processing plants in all States west of the Mississippi River. Managers of these facilities could be requested by telephone to collect raw milk samples representing milk sheds supplying milk to the plants. Since there were no releases of radioactivity from the NTS or other test locations, this network was not activated except to request one sample from each location to check the readiness and reliability of the network. Each sample was analyzed for ^{3}H and $^{89,90}Sr$ for the purpose of comparing the results with the results of the MSN.

Each MSN milk sample was analyzed for gamma-emitters and $^{89,90}Sr$. Samples collected at six locations from the MSN were also analyzed for ^{3}H. Table 3

lists the general analytical procedures and detection limits for these analyses.

The analytical results of milk samples collected from the MSN during 1975 are summarized in Table 6. The maximum, minimum, and average concentrations of the ^{137}Cs, $^{89,90}Sr$, and ^{3}H in samples collected during the year are shown for each sampling location. Although ^{137}Cs and ^{90}Sr were observed in the samples, the concentrations of these radionuclides were similar to levels found in samples collected for the SMSN. Therefore, they were attributed to world-wide fallout and not to NTS operations.

Shown below are the maximum, minimum, and average concentrations of ^{3}H, ^{90}Sr, and ^{137}Cs in the area surrounding the NTS and other areas of the Western United States. As indicated by this table, the concentrations of these radionuclides for both the MSN and the SMSN are commensurate.

Network	Radionuclide	No. of Samples	Concentration (10^{-9} µCi/ml) C_{Max}	C_{Min}	C_{Avg}
MSN	^{137}Cs	86	18	<3	<6
	^{90}Sr	87	8.7	<0.6	<3
	^{3}H	24	1000	<200	<400
SMSN	^{137}Cs	124	20	<3	<7
	^{90}Sr	33	9.2	<1	<4
	^{3}H	36	4100	<200	<700

WATER SURVEILLANCE NETWORK

Beginning January 1, 1975, the routine Water Surveillance Network (WSN) was discontinued. Ten locations (Figure 13) near the NTS were selected from the WSN, added to the Long-Term Hydrological Monitoring Program for the NTS, and sampled on an annual basis.

LONG-TERM HYDROLOGICAL MONITORING PROGRAM

During this reporting period, EMSL-LV personnel continued the collection and analysis of water samples from wells, springs, and spring-fed surface water sources which are down the hydrologic gradient of the groundwater at the NTS and at off-NTS sites of underground nuclear detonations to monitor for any migration of test-related radionuclides through the movement of groundwater. The water samples were collected from well heads or spring discharge points wherever possible. If pumps were not available, an electrical-mechanical water sampler capable of collecting 3-litre samples at depths to 1800 m was used.

Nevada Test Site

For the NTS, attempts were made to sample 12 stations monthly and 17 stations semi-annually (Figures 12 and 13). Additionally, samples were also collected annually from 10 locations selected from the discontinued WSN. Not all stations could be sampled with the desired frequency because of inclement weather conditions and inoperative pumps.

For each sampled location, samples of raw water, filtered water, and filtered and acidified water were collected. The raw water samples were analyzed for ^{3}H. Portions of the filtered and acidified samples were given radiochemical analyses by the criteria summarized in Table 7. Table 3 summarizes the analytical techniques used. Each filter was also analyzed by gamma spectrometry.

Tables 8, 9, and 10 list the analytical results for all samples collected and analyzed during this reporting period. As in the past, ^{3}H was detected in NTS Wells C and C-1 due to tracer experiments conducted prior to the commencement of this surveillance program. All ^{3}H concentrations were below 0.01 percent of the Concentration Guide for an occupationally-exposed person.

The ^{226}Ra and $^{234,235,238}U$ detected in most of the water samples occur naturally in groundwater. The concentrations of these radionuclides for this reporting period were similar to the concentrations reported for previous years.

Tables 8, 9, and 10 show concentrations of ^{90}Sr, ^{238}Pu, and ^{239}Pu which were above their respective MDC's. These concentrations, with a two-sigma counting error and percentage of the appropriate Concentration Guide, are as follows:

Location	Radionuclide	Concentration (10^{-9} µCi/ml)	% of Conc. Guide
Well A	^{238}Pu	0.092 ± 0.024	<0.01
	^{239}Pu	0.031 ± 0.022	<0.01
Crystal Spring	^{90}Sr	1.1 ± 1.0	0.37
Well C	^{90}Sr	2.6 ± 1.4	<0.01

Since these concentrations are either below or near the three-sigma counting error of each measurement, the concentrations are considered to be due to statistical error.

Due to the absence of information on background levels of ^{3}H in deep wells, the ^{3}H concentrations measured by the program can only be compared to previous determinations. Such a comparison for each location indicated that there are no significant increases in concentrations which could be the result of ^{3}H migration from the sites of underground nuclear detonations.

Other Test Sites

The annual collection and radiological analysis of water samples were continued for this program at all off-NTS sites of underground nuclear detonations except for Project Cannikin on Amchitka Island, Alaska, and Project Rio Blanco near Meeker, Colorado. The latter two sites are the responsibility of other agencies. The project sites at which samples were collected are Project Gnome near Carlsbad, New Mexico; Project Faultless in Central Nevada; Project Shoal near Fallon, Nevada; Project Gasbuggy in Rio Arriba County, New Mexico; Project Rulison near Rifle, Colorado; and Project Dribble at Tatum Dome, Mississippi. Figures 14 through 20 identify the sampling locations, and Table 2 lists additional information on the location of each site and tests performed at these locations.

A contaminated well, Well HT-2M, at the Project Dribble site was plugged from total depth to surface in July 1975. No contaminated fluid was released to the environment during the plugging operation. As a result of the plugging operation, the sample collection at all other wells at Project Dribble will be quarterly for 1 year from July 1975, semi-annually for the second year, and annually thereafter unless the analytical results of samples indicate more frequent sampling is necessary.

All samples were analyzed using the same criteria (Table 7) as for samples from the NTS Programs. The analytical results of all water samples collected during CY 1975 are summarized in Table 11.

The only sample results showing radioactivity concentrations significantly above background levels were for USGS Wells Nos. 4 and 8 near Malaga, New Mexico. As mentioned in previous reports, these wells, which are fenced, posted, and locked to prevent their use by unauthorized personnel, were contaminated by the injection of high concentrations of radioactivity for a radioactive tracer study. All surface water samples had ^{3}H concentrations below 2.5×10^{-6} µCi/ml, a level considered from past experience to be the highest one would expect from atmospheric fallout. All ^{3}H concentrations in well samples were similar to concentrations measured during previous years.

Several samples had concentrations of ^{90}Sr and ^{239}Pu above their respective MDC. The locations, concentrations with two-sigma counting errors, and percentages of the Concentration Guides for these samples are as follows:

Location	Radionuclide	Concentration (10^{-9} µCi/ml)	% of Conc. Guide
Malaga, New Mexico USGS Well No. 1	^{90}Sr	1.3 ± 0.9	0.4
Malaga, New Mexico USGS Well No. 8	^{239}Pu	0.047 ± 0.040	<0.01
Malaga, New Mexico PHS Well No. 6	^{239}Pu	0.024 ± 0.023	<0.01
Baxterville, Mississippi Well HT-1	^{239}Pu	0.048 ± 0.019	<0.01
Blanco, New Mexico San Juan River	^{90}Sr	1.9 ± 1.1	0.6

All of the preceding concentrations are less or only slightly greater than their respective three-sigma counting errors; therefore, all the concentrations are considered to be the result of statistical error and not necessarily true indications of above background measurements.

WHOLE-BODY COUNTING

During 1975, the measurements of body burdens of radioactivity in selected off-site residents were continued. The whole-body counting facility was described previously (NERC-LV-539-31, 1974).

One hundred and eleven individuals from 14 locations were examined. These locations were Pahrump, Springdale, Beatty, Moapa, Caliente, Pioche, Nyala, Diablo, Goldfield, Lathrop Wells, Ely, Tonopah, Twin Springs, and Spring Meadows Farms, Nevada. When possible, all members of a family are included.

The minimum detectable concentrations for ^{137}Cs by whole-body counting was 5×10^{-9} µCi/g for a body weight of 70 kg and a 40-minute count. Each individual was also given a complete hematological examination and a thyroid profile. A urine sample was collected from each individual for ^{3}H analysis and composite urine samples from each family were analyzed for $^{238,239}Pu$.

From the results of whole-body counting, the fission product ^{137}Cs was detected above the detection limit in 82 individuals. The maximum, minimum, and average concentrations for this radionuclide were 4.3×10^{-8}, 5.0×10^{-9}, and 1.4×10^{-8} µCi/g body weight, respectively.

These concentrations are comparable to those found by the Los Alamos Scientific Laboratory (LASL), Albuquerque, New Mexico. According to LASL personnel (Smale and Umbarger, 1976), the average body burden of ^{137}Cs measured in workers at that Laboratory was 1 nCi. Based upon the 70-kg body weight of a standard man, this is equivalent to 1.4×10^{-8} µCi/g.

In regard to the hematological examinations and thyroid profiles, no abnormal results were observed which could be attributed to past or present NTS testing operations. The concentrations of ^{238}Pu and ^{239}Pu in all urine samples were $<3 \times 10^{-10}$ µCi/ml and $<1 \times 10^{-10}$ µCi/ml, respectively. Concentrations of ^{3}H in urine samples were observed above the MDC of the measurement; however, the levels observed—average of 0.4×10^{-9} µCi/ml with a range of 0.2×10^{-9} to 1.5×10^{-9} µCi/ml—were within the range of background concentrations normally observed in surface waters or atmospheric moisture.

DOSE ASSESSMENT

The only radionuclides ascribed to NTS operations detected in off-NTS areas were ^{133}Xe (at Beatty, Diablo, Hiko, Indian Springs, and Las Vegas), ^{3}H (at Beatty and Diablo), and ^{85}Kr (at Beatty, Diablo, Indian Springs, and Las Vegas) in air samples. From the analytical results of samples collected at these locations and the dose calculations described in Appendix B, the whole-body gamma dose equivalents (D.E.) to off-NTS residents and the 80-km dose commitment in man-rem were calculated. The results, shown below, indicate that the D.E.'s at these locations were 2.1 μrem or less, which is

Location	Total Whole-Body Dose (μrem)	Percent of Radiation Protection Standard	Population	Dose Commitment Within 80 km (man-rem)
Beatty	0.15	0.00009	500	0.000075
Diablo	2.1	0.002	5	0*
Hiko	0.97	0.0006	52	0*
Indian Springs	0.34	0.0002	1670	0.00057
Las Vegas	0.32	0.0002	194,000	0*
			Total	0.00065

*Diablo, Hiko, and Las Vegas are beyond 80 km. The dose commitments for these locations are 0.000011 man-rem, 0.000050 man-rem, and 0.062 man-rem, respectively.

0.002 percent of the Radiation Protection Standard of 170 mrem/y (Appendix A) or 0.04-0.07 percent of the dose one could receive from cosmic radiation (3-5 mrem) during a round-trip flight between Washington, D.C. and the West Coast at 11,000 m above mean sea level (ERDA, 1973).

The dose commitment, which is the product of the estimated D.E. at a given location and the exposed population, was determined as a gross measurement of potential biological damage from radiation exposure, assuming that the calculated D.E. was the average dose to the population and that the relationship between dose and effects is linear. Although the maximum dose commitment occurred at Las Vegas, the dose commitment within 80 km of NTS is reported as required by the ERDA Manual, Chapter 0513. For comparison, the dose commitment at Las Vegas from 1 year's exposure to natural background radiation (about 50 mrem/y, Table 5), would be 9700 man-rem.

Since the critical organ for persons exposed to ^{85}Kr is the skin of the total body, the D.E.'s calculated from the ^{85}Kr concentrations were excluded from the whole-body gamma D.E. estimates and the 80-km, man-rem dose estimates. The skin D.E.'s for the four off-NTS locations, Beatty, Diablo, Indian Springs, and Las Vegas, were all $<3\times10^{-4}$ percent of the Radiation Protection Standard of 0.5 rem/y for a suitable sample of the exposed population.

In the derivation of the Concentration Guide for ^{85}Kr listed in the ERDA Manual, Chapter 0524, the exposure to airborne ^{85}Kr is assumed to result in a whole-body gamma dose equivalent instead of a total body skin D.E. If one applies this assumption to the previous D.E. estimates for Beatty, Diablo, Indian Springs, and Las Vegas (locations where above background ^{85}Kr concentrations were detected), the 80-km dose commitment estimate would be increased to 0.0022 man-rem, a factor of 3.4 times the first estimate. The dose commitments at Diablo, Hiko, and Las Vegas (beyond 80-km of NTS) would also be increased to 0.000037 man-rem, 0.00017 man-rem, and 0.21 man-rem, respectively.

REFERENCES

"Effluent and Environmental Monitoring and Reporting." U.S. Energy Research and Development Administration Manual, Chapter 0513. U.S. Energy Research and Development Administration. Washington, D.C. March 20, 1974.

Houghton, J. G., C. M. Sakamoto, R. O. Gifford, Nevada's Weather and Climate. Special Publication 2. Nevada Bureau of Mines and Geology, Mackay School of Mines, University of Nevada-Reno. Reno, Nevada. pp 69-74. 1975.

Quiring, Ralph E., "Climatological Data, Nevada Test Site, Nuclear Rocket Development Station (NRDS)." ERLTM-ARL-7. ESSA Research Laboratories. August 1968.

Eckel, E. B., ed. Nevada Test Site. Memoir 110. The Geological Society of America, Inc. Boulder, Colorado. 1968.

"Preliminary Draft Environmental Statement, Nevada Test Site FY-78 and Beyond." WASH- Draft Copy. U.S. Energy Research and Development Administration. March 1975.

"1973 Population and 1972 Per Capita Income Estimates for Counties and Incorporated Places in Nevada." Population and Estimates and Projections. Series P-25, No. 573. U.S. Department of Commerce, Bureau of the Census. Washington, D.C. May 1975.

"Estimates of Population of Arizona and Utah Counties, July 1, 1973, and July 1, 1974." Information provided by Mr. Donald Starsinic, U.S. Department of Commerce, Bureau of the Census. Reno, Nevada. February 1976.

"Estimates of Population of California Counties, January 1, 1974, and January 1, 1975." Information provided by Mr. Donald Starsinic, U.S. Department of Commerce, Bureau of the Census. Reno, Nevada. February 1976.

"Estimates of Ionizing Radiation Doses in the United States, 1960-2000." ORP/CSD 7201. U.S. Environmental Protection Agency. Rockville, Maryland. August 1972.

Lindeken, C. L., et al. "Geographical Variations in Environmental Radiation Background in the United States." The Natural Radiation Environment II. CONF-720805-P1. U.S. Energy Research and Development Administration. Houston, Texas. pp 317-332. August 1972.

"Environmental Monitoring Report for the Nevada Test Site and Other Test Areas Used for Underground Nuclear Detonation, January through December 1973." NERC-LV-539-31. U.S. Environmental Protection Agency. Las Vegas, Nevada. May 1974.

Smale, R. S., and C. J. Umbarger, "Discussion with Mr. D. M. Wood, Environmental Monitoring and Support Laboratory-Las Vegas (EMSL-LV), U.S. Environmental Protection Agency, during visit to EMSL-LV." H-1 Health Physics Section, Los Alamos Scientific Laboratory. Albuquerque, New Mexico. February 6, 1976.

"Estimated Average Annual Whole-Body Radiation Doses in U.S. (1973) and Comparative Information on Annual Radiation Doses." Office of Information Services, U.S. Energy Research and Development Administration, Washington, D.C. 20545. 1973.

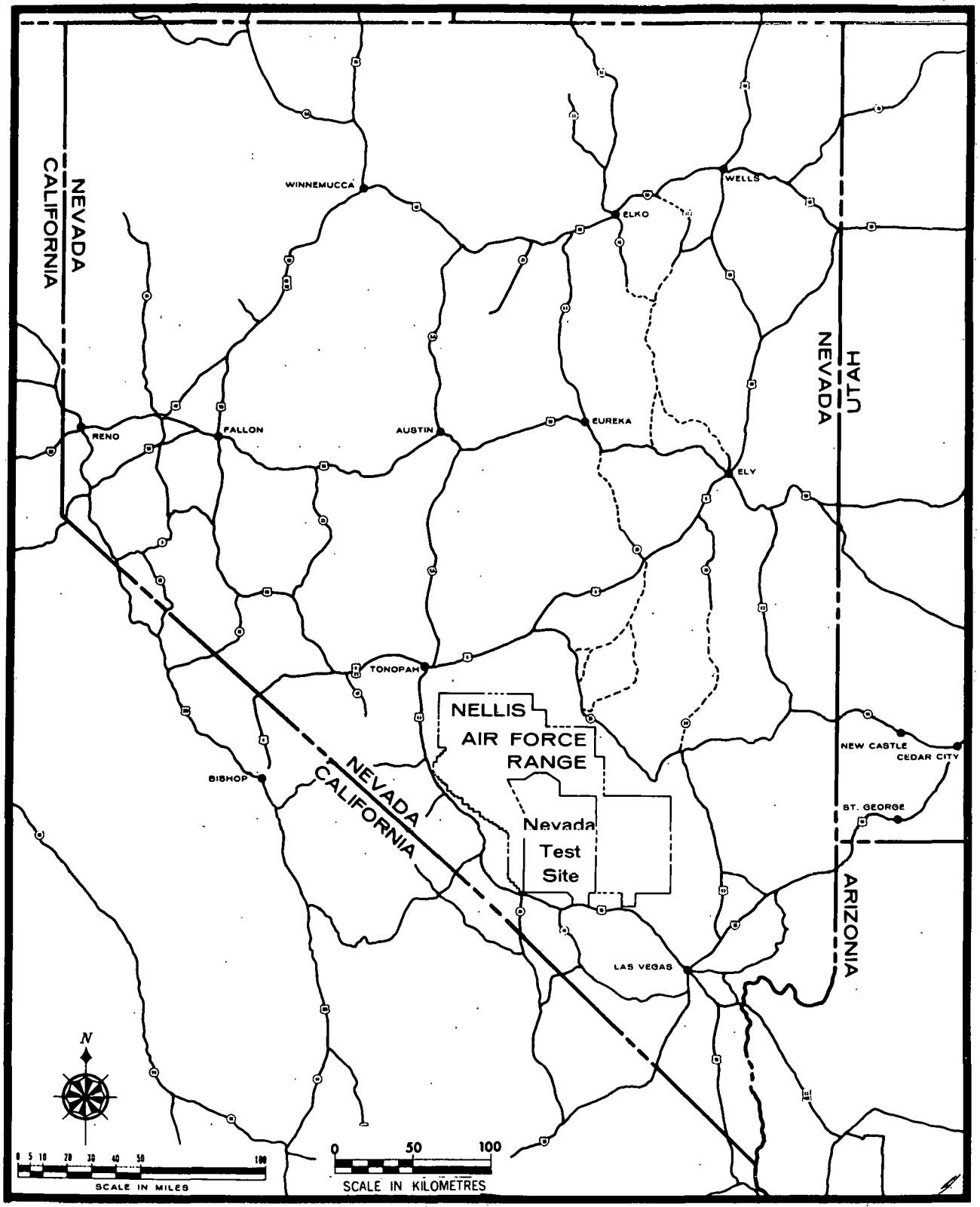

Figure 1. Nevada Test Site Location

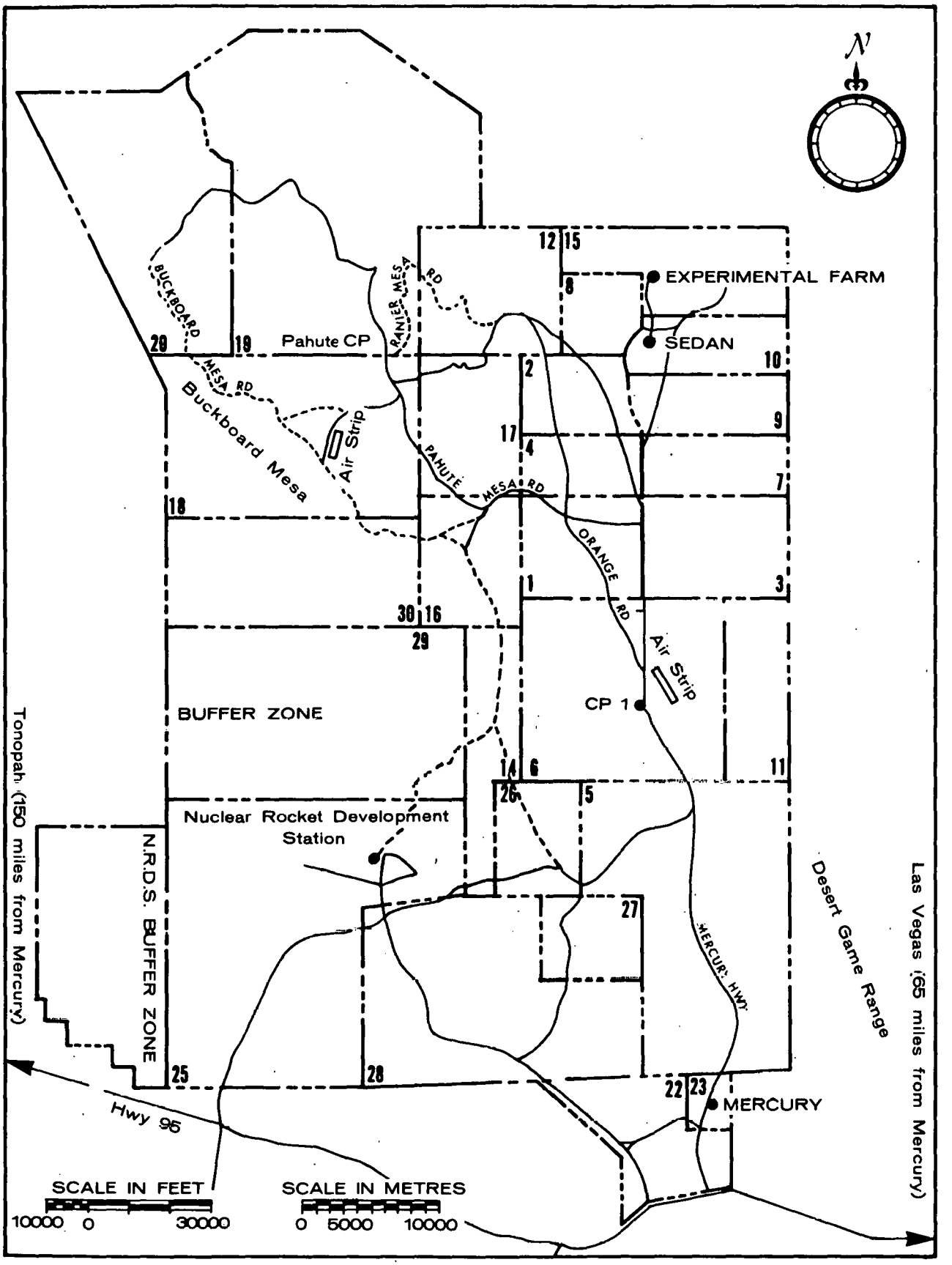

Figure 2. Nevada Test Site Road and Facility Map

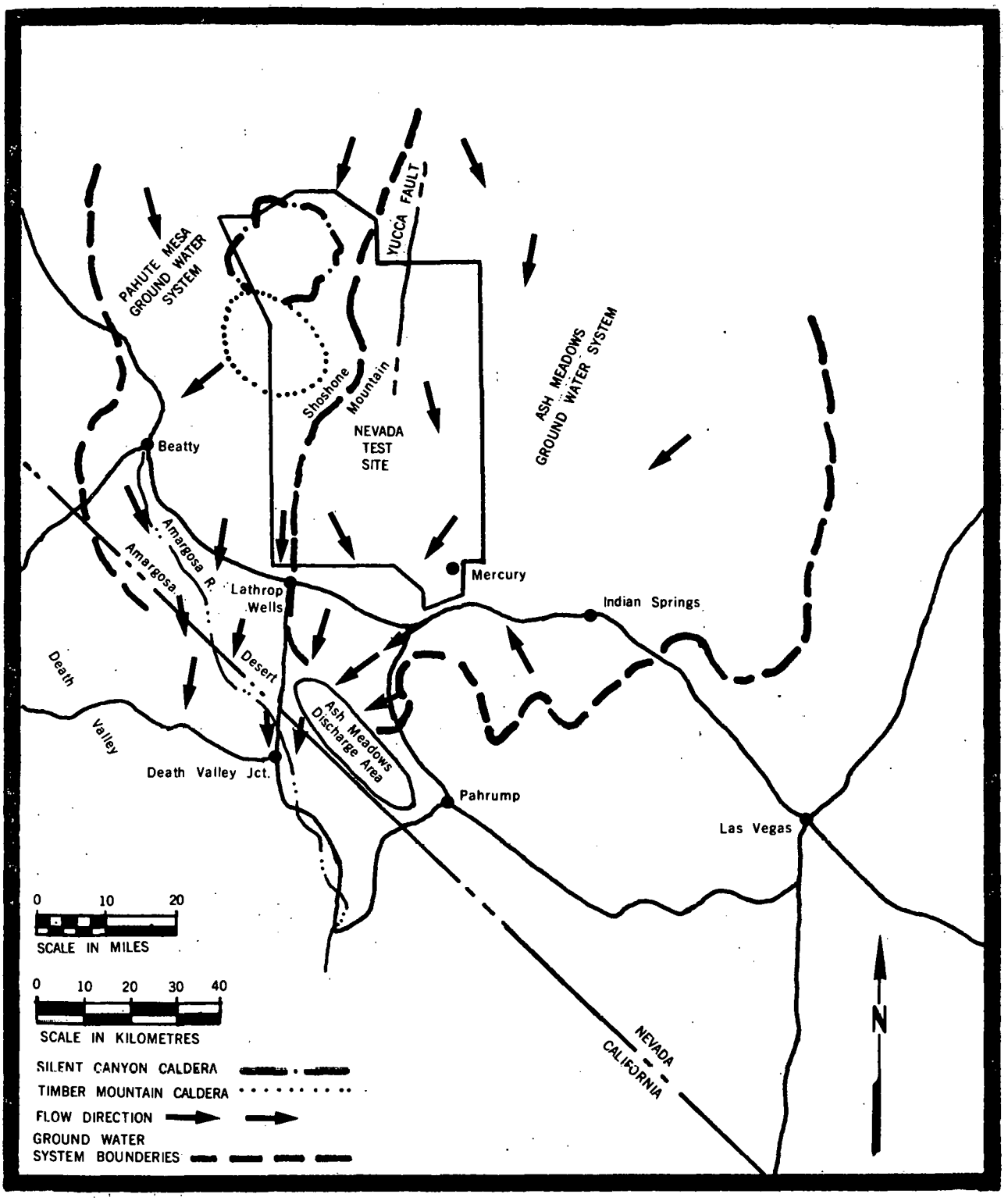

Figure 3. Groundwater Flow Systems - Nevada Test Site

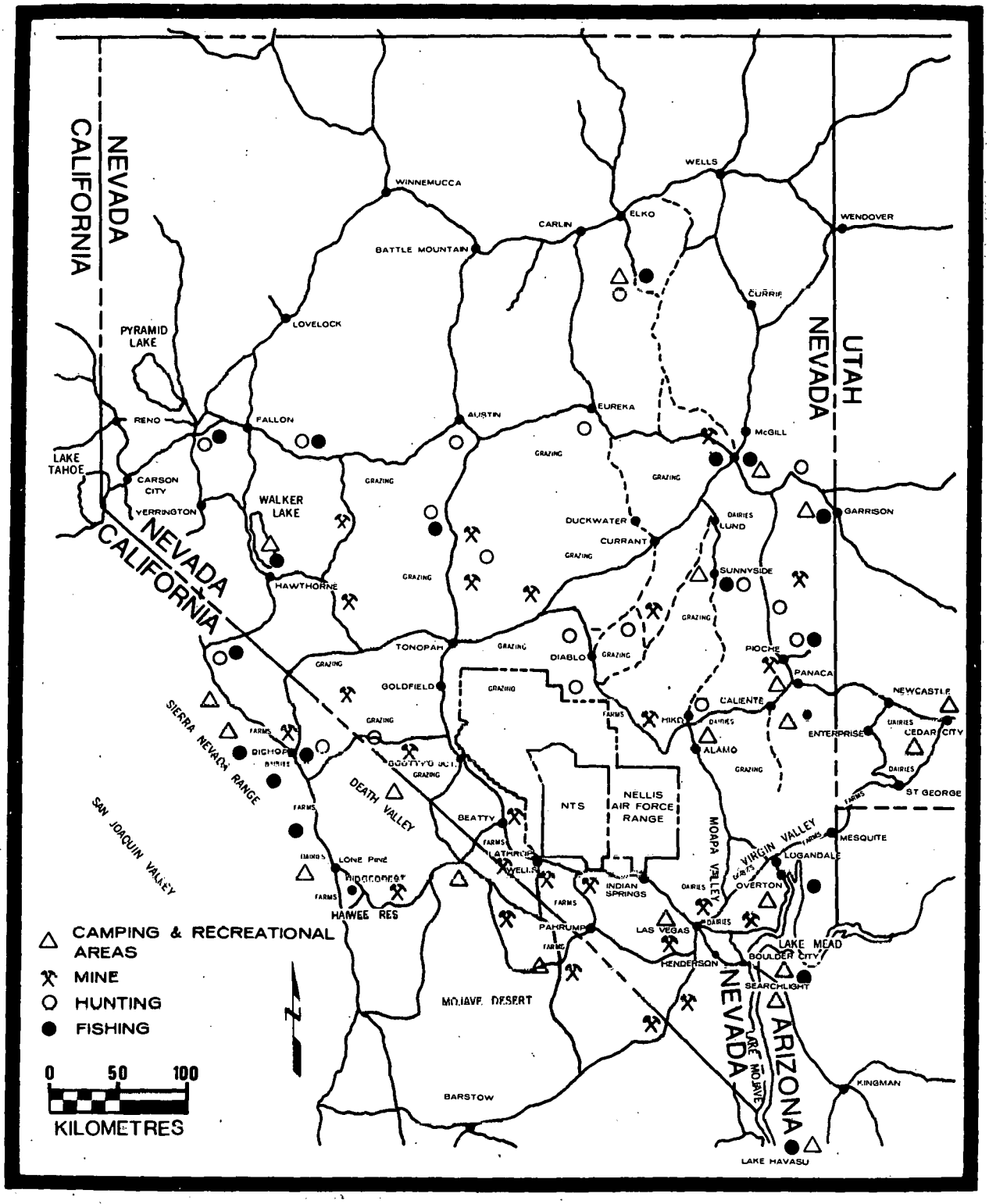

Figure 4. General Land Use, Nevada Test Site Vicinity

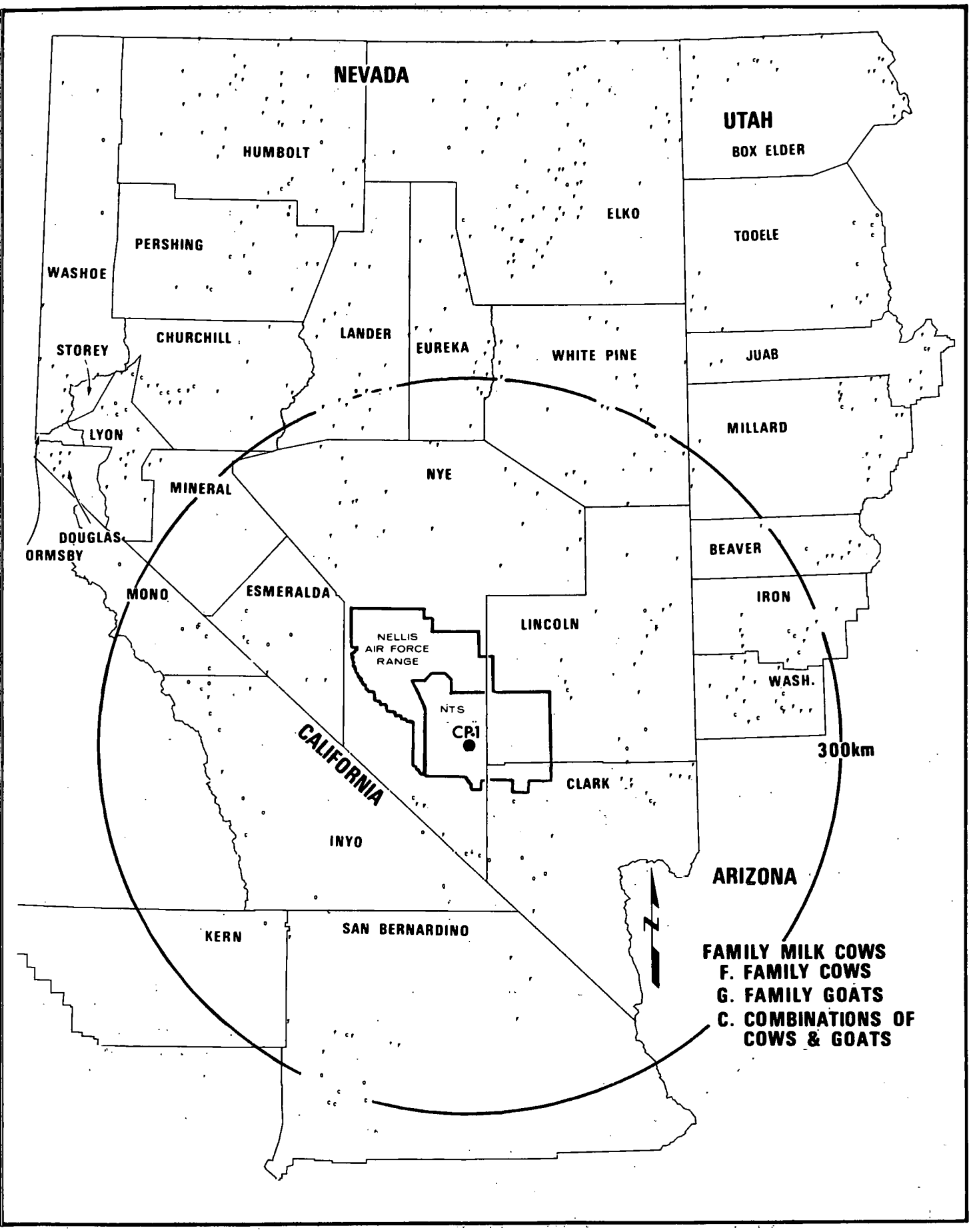

Figure 5. Location of Family Milk Cows and Goats

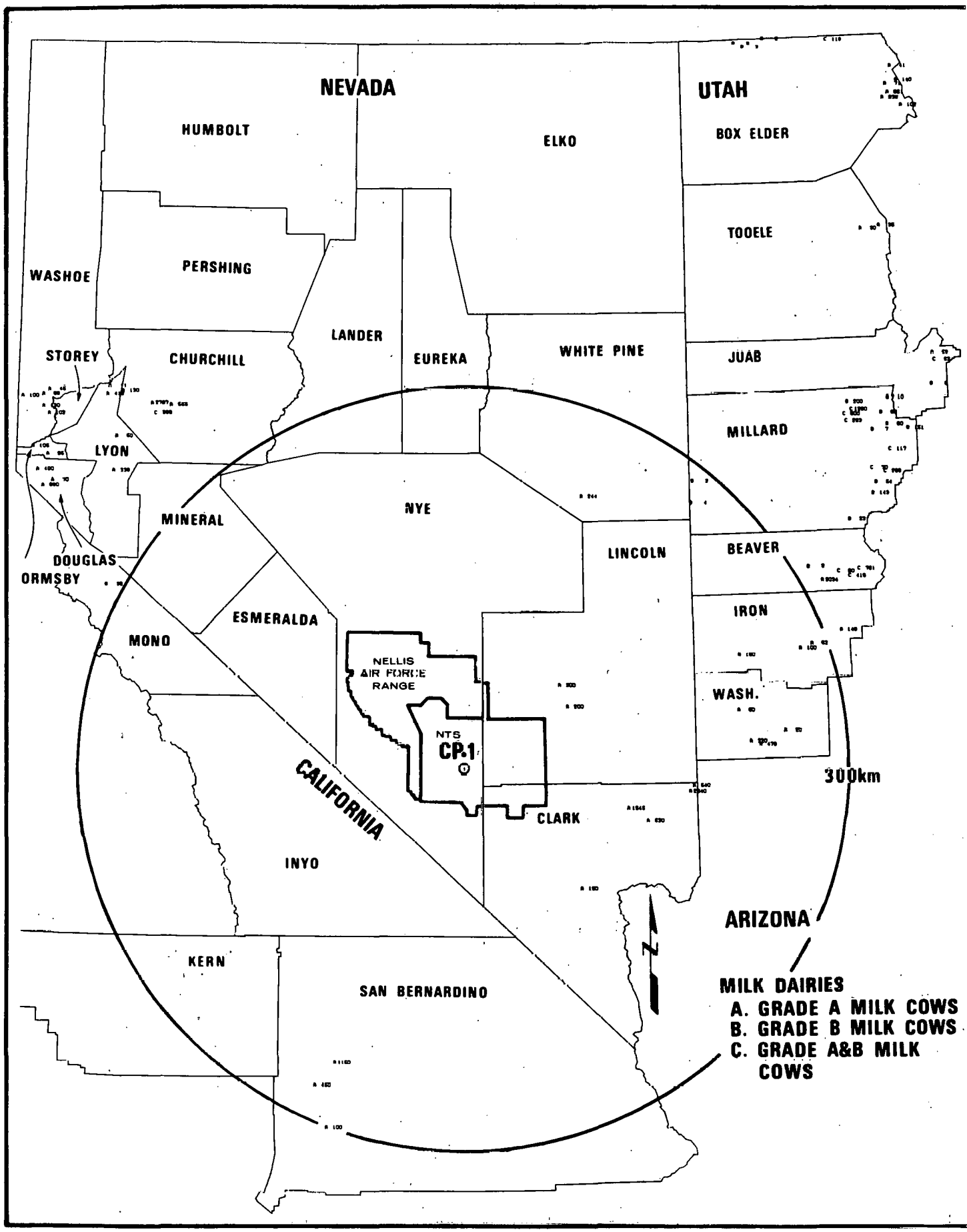

Figure 6. Location of Dairy Cows

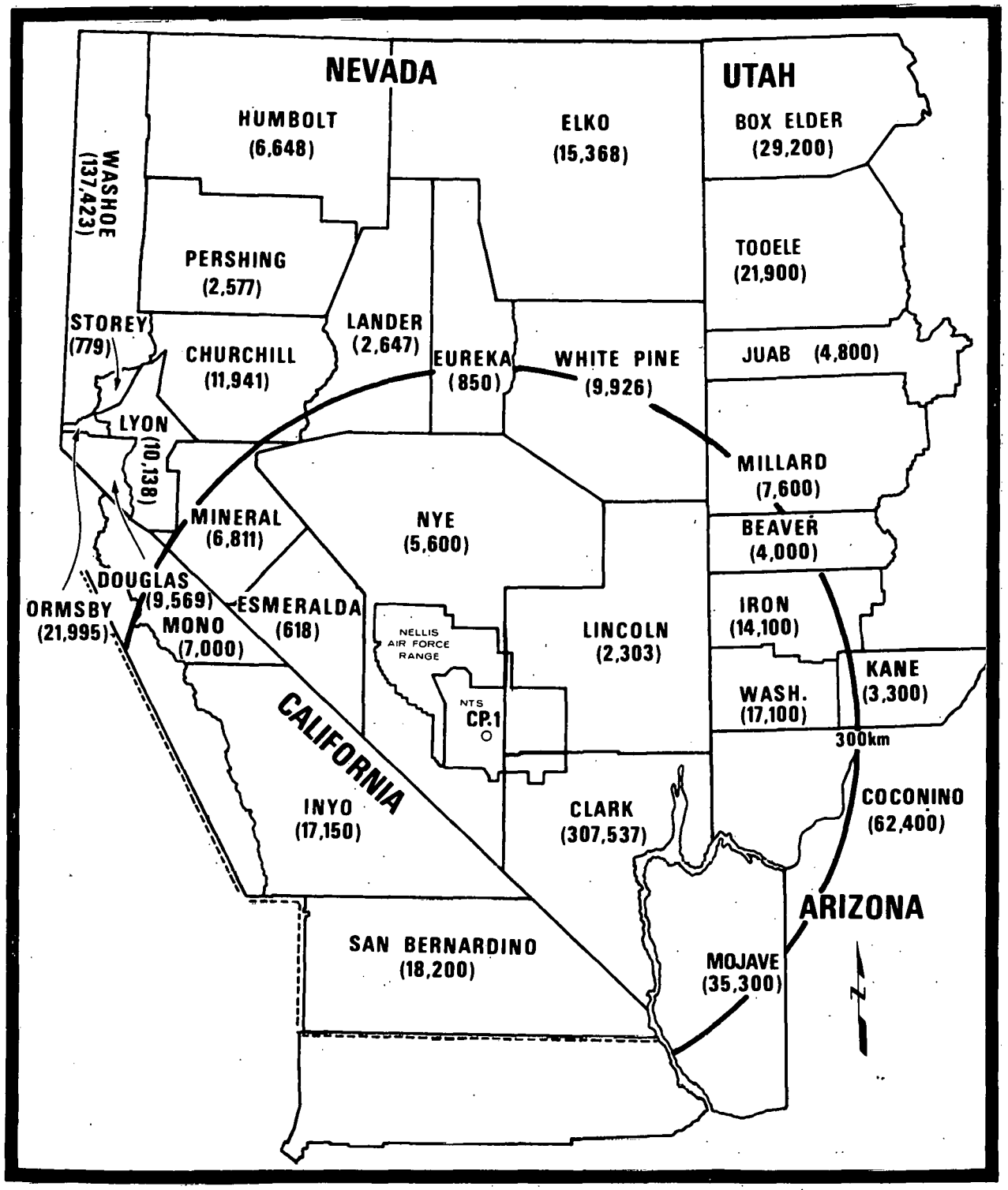

Figure 7. Population of Arizona, California, Nevada, and Utah Counties Near the Nevada Test Site

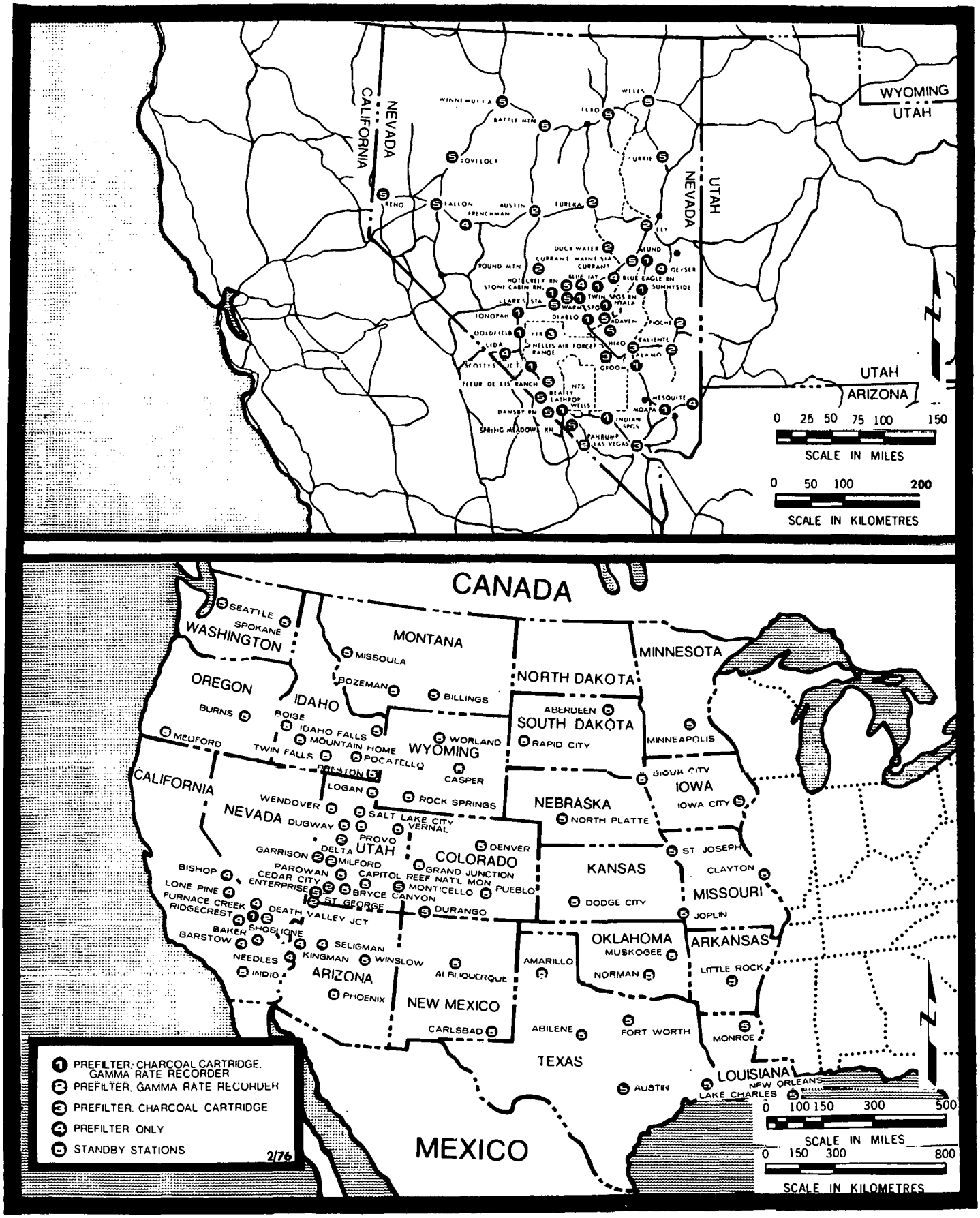

Figure 8. Air Surveillance Network

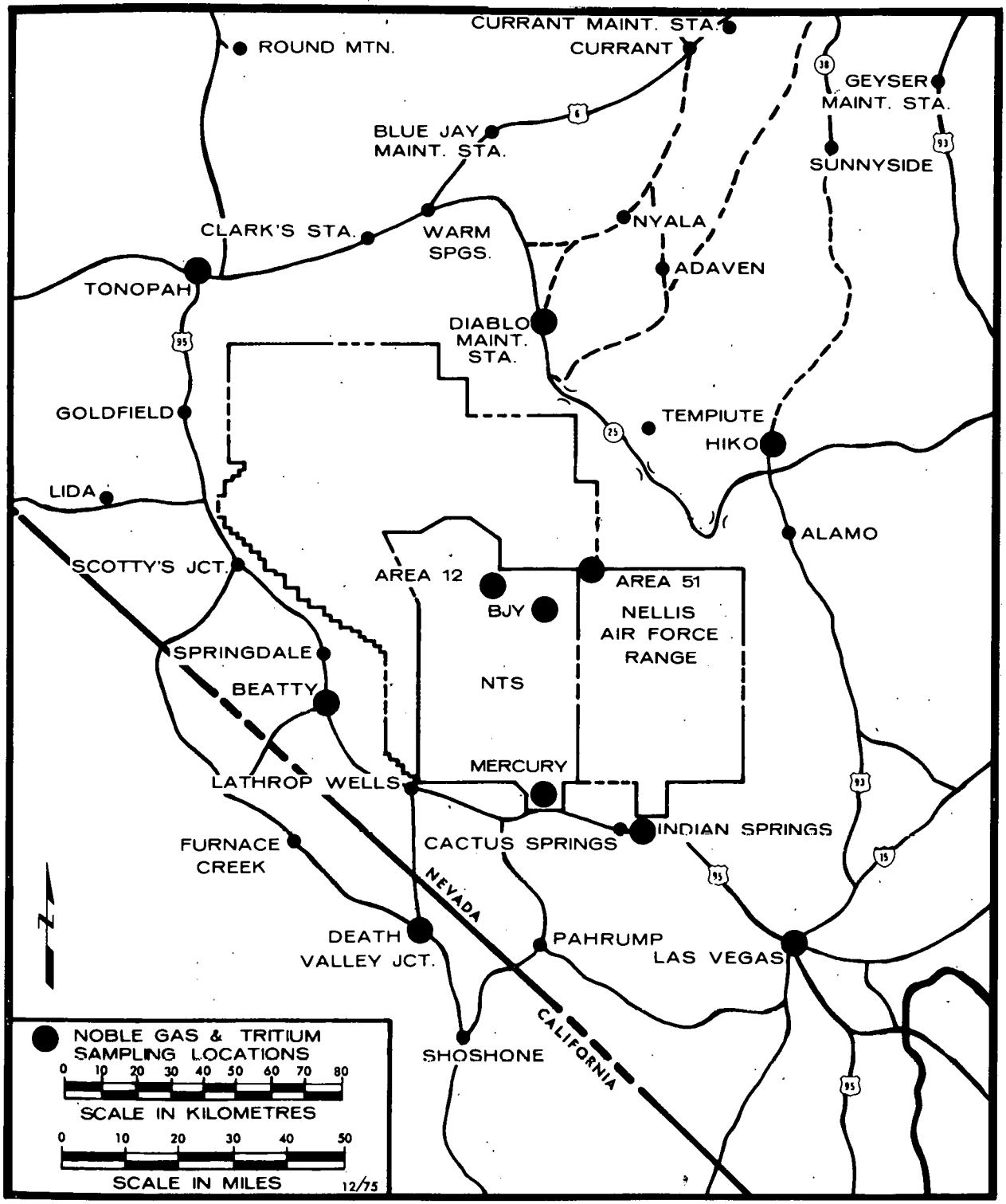

Figure 9. Noble Gas and Tritium Surveillance Network

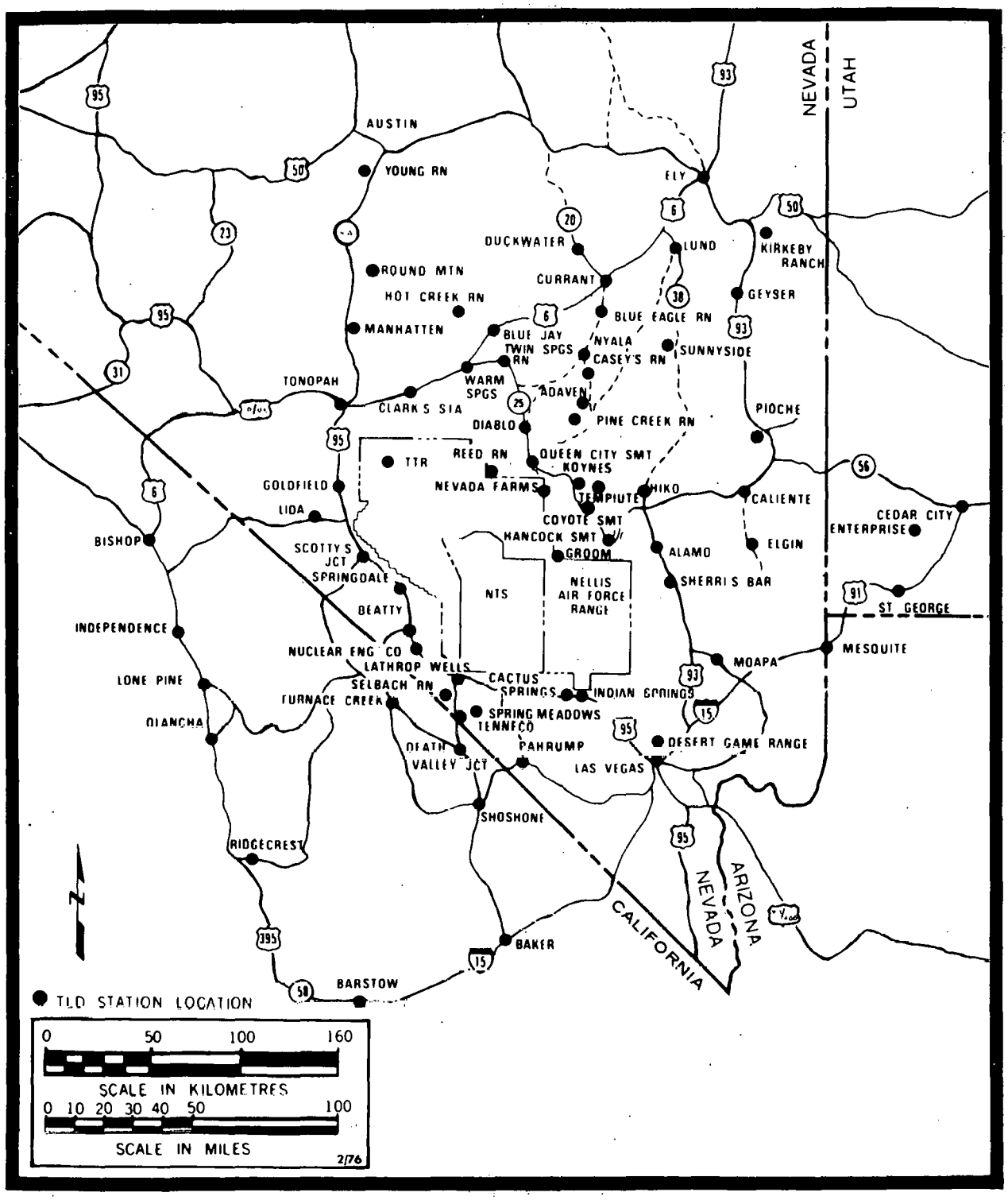

Figure 10. Dosimetry Network

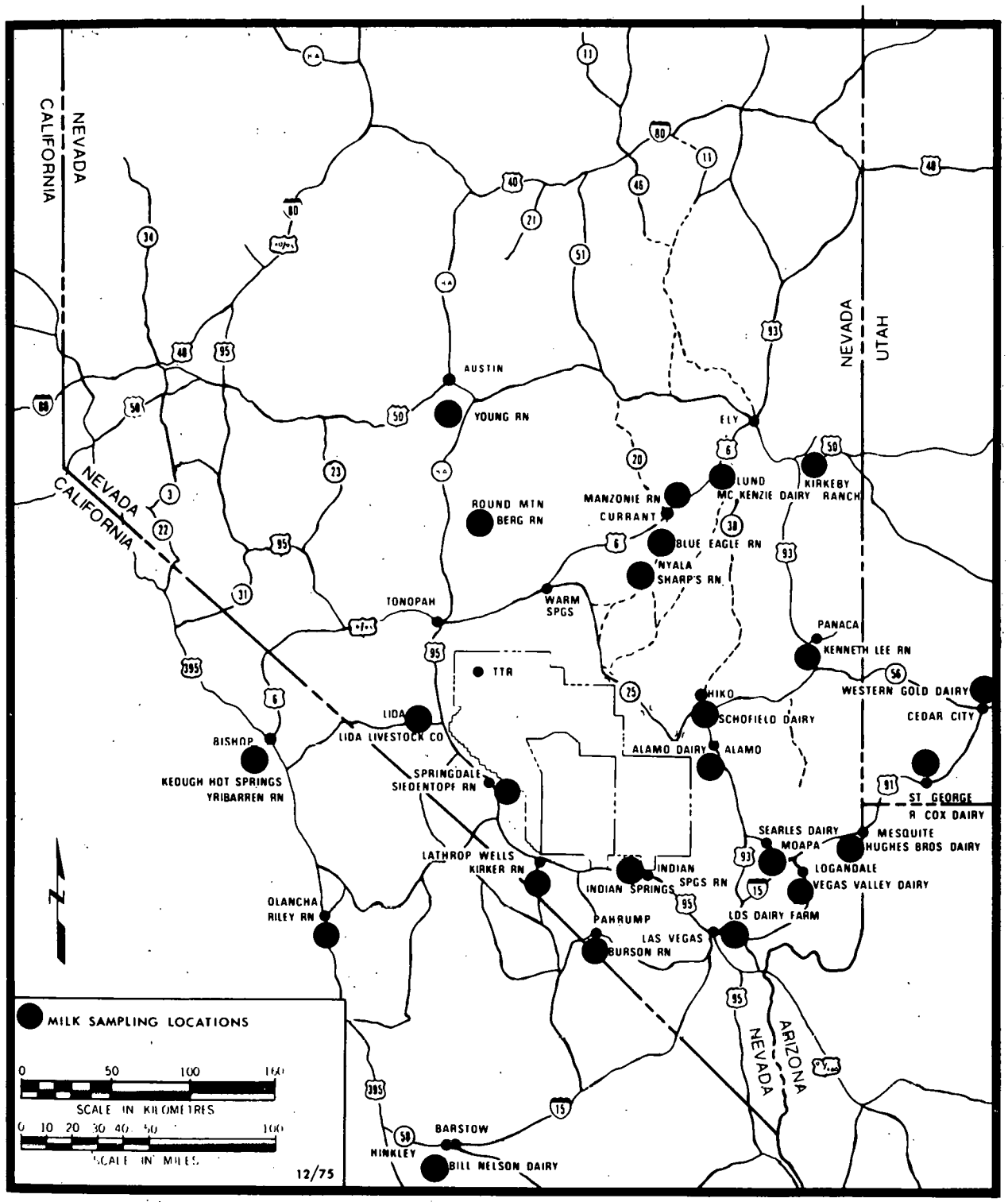

Figure 11. Milk Surveillance Network

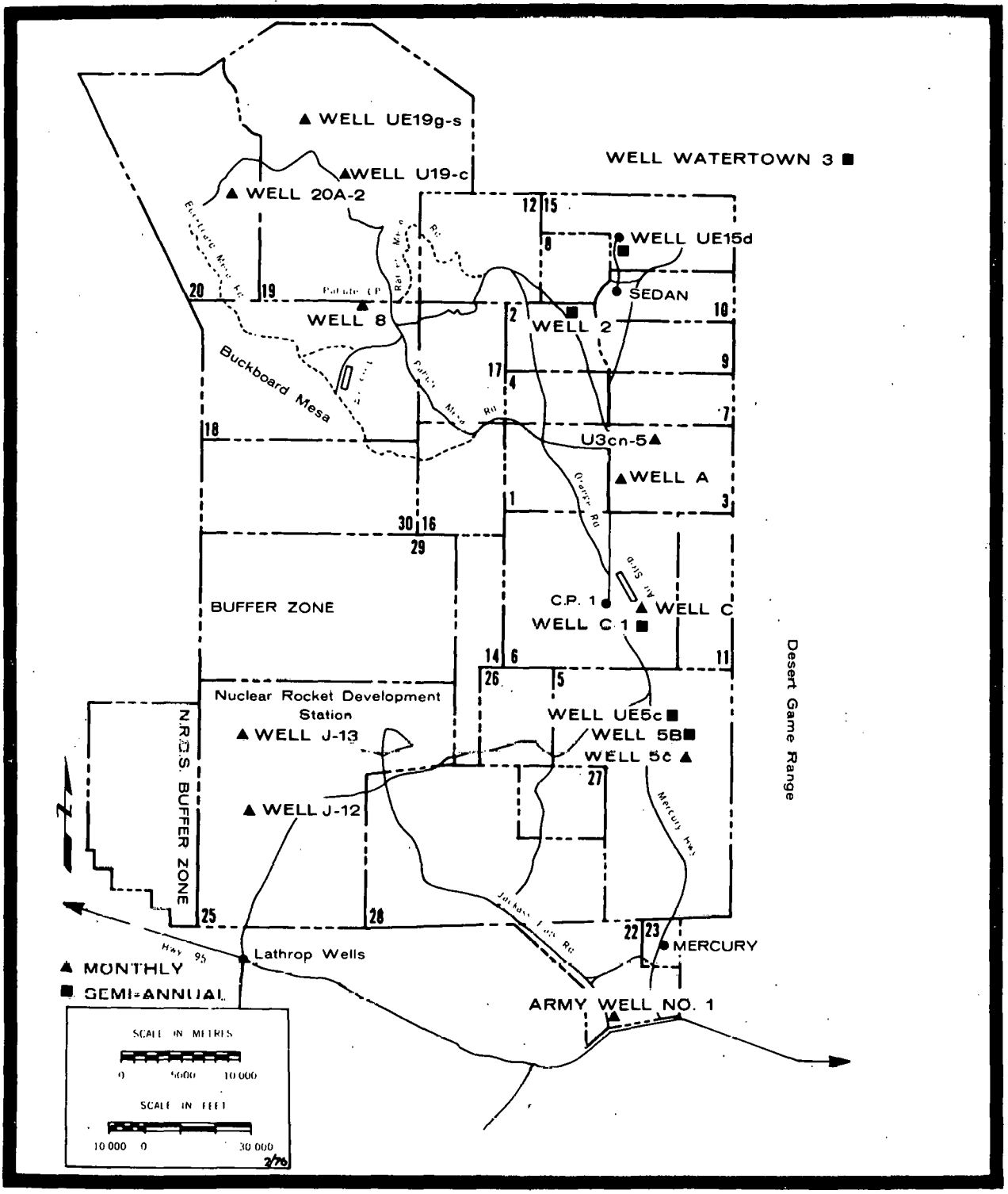

Figure 12. On-Site Long-Term Hydrological Monitoring Program, Nevada Test Site

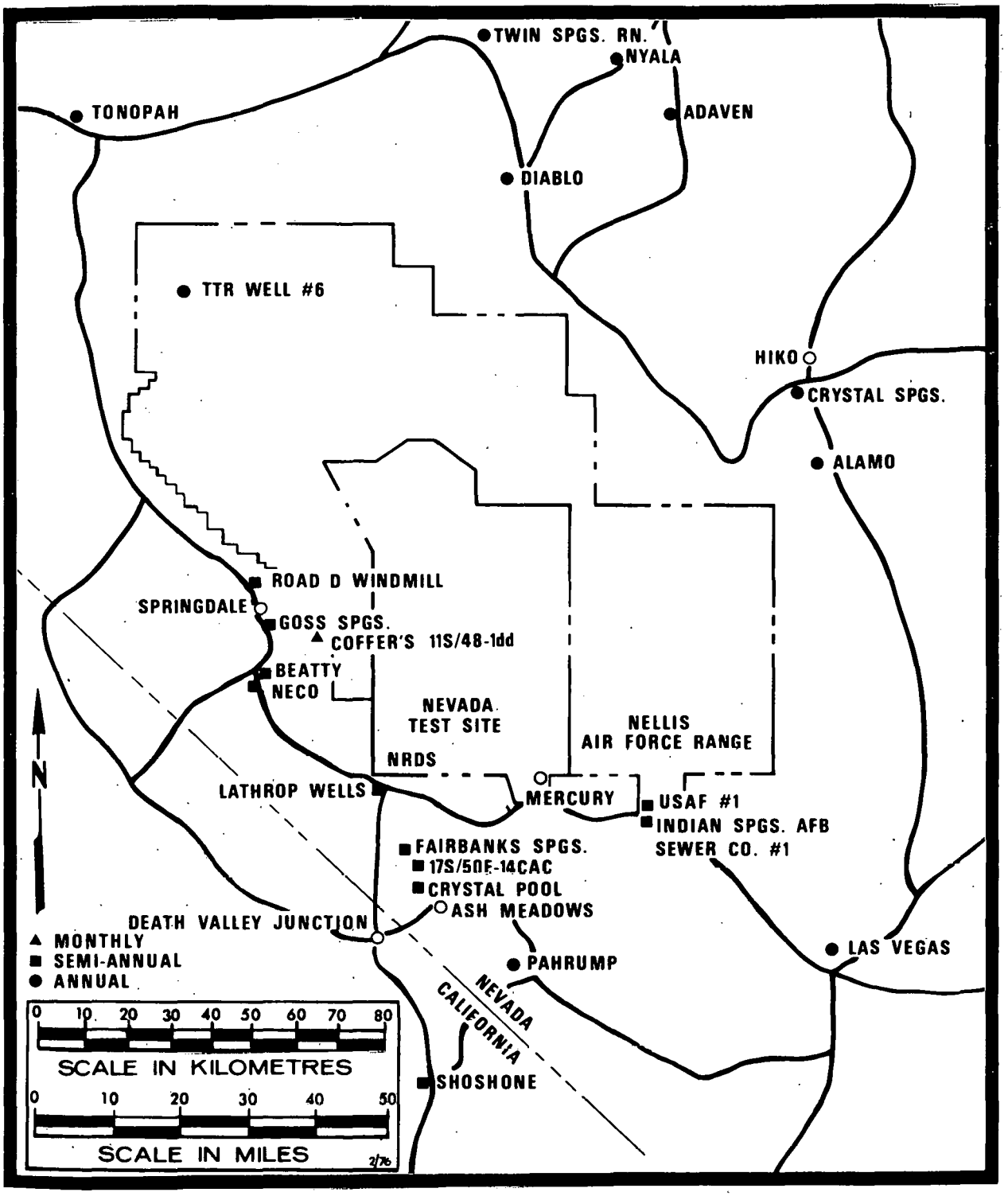

Figure 13. Off-Site Long-Term Hydrological Monitoring Program, Nevada Test Site

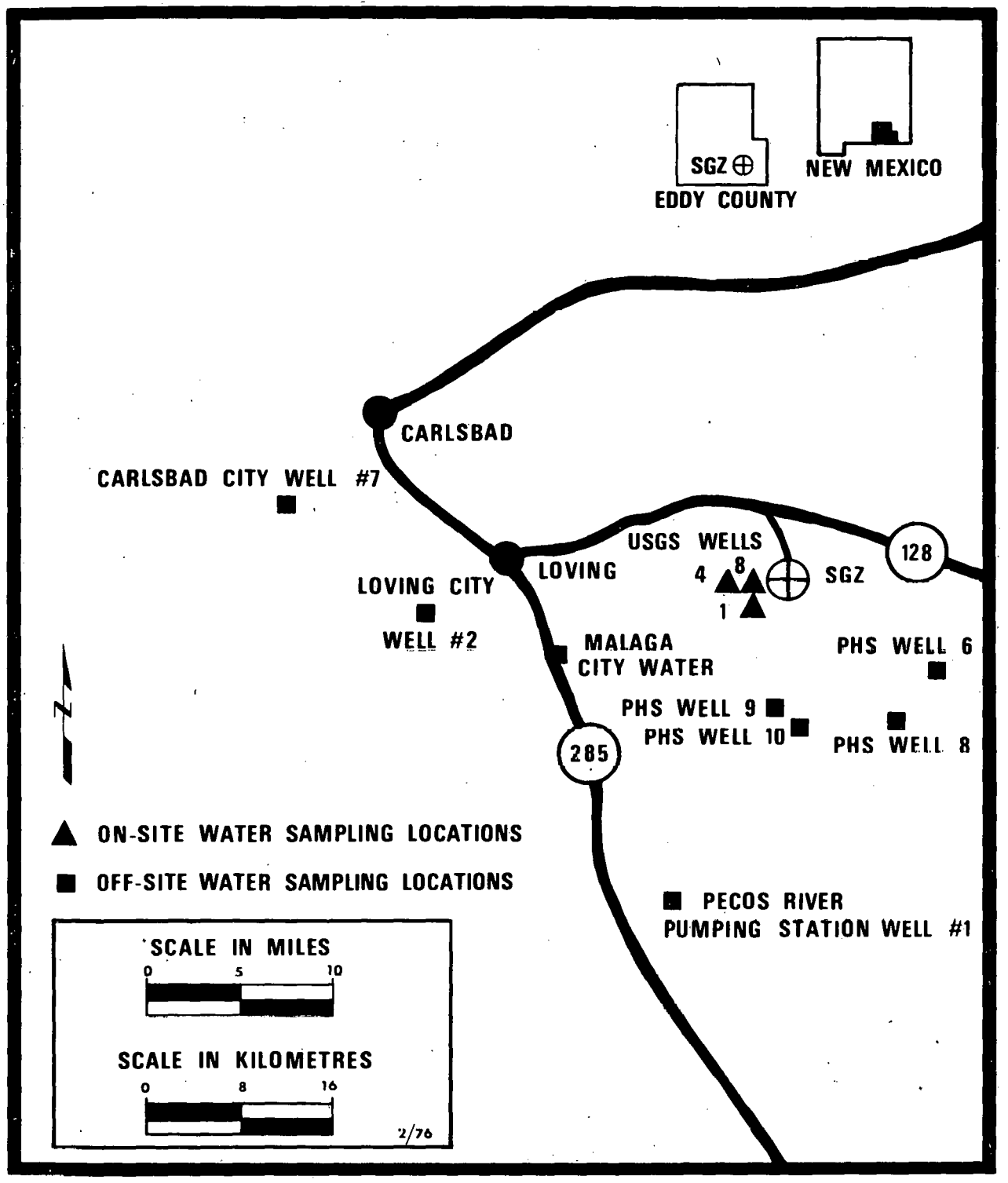

Figure 14. Long-Term Hydrological Monitoring Locations, Carlsbad, New Mexico, Project Gnome/Coach

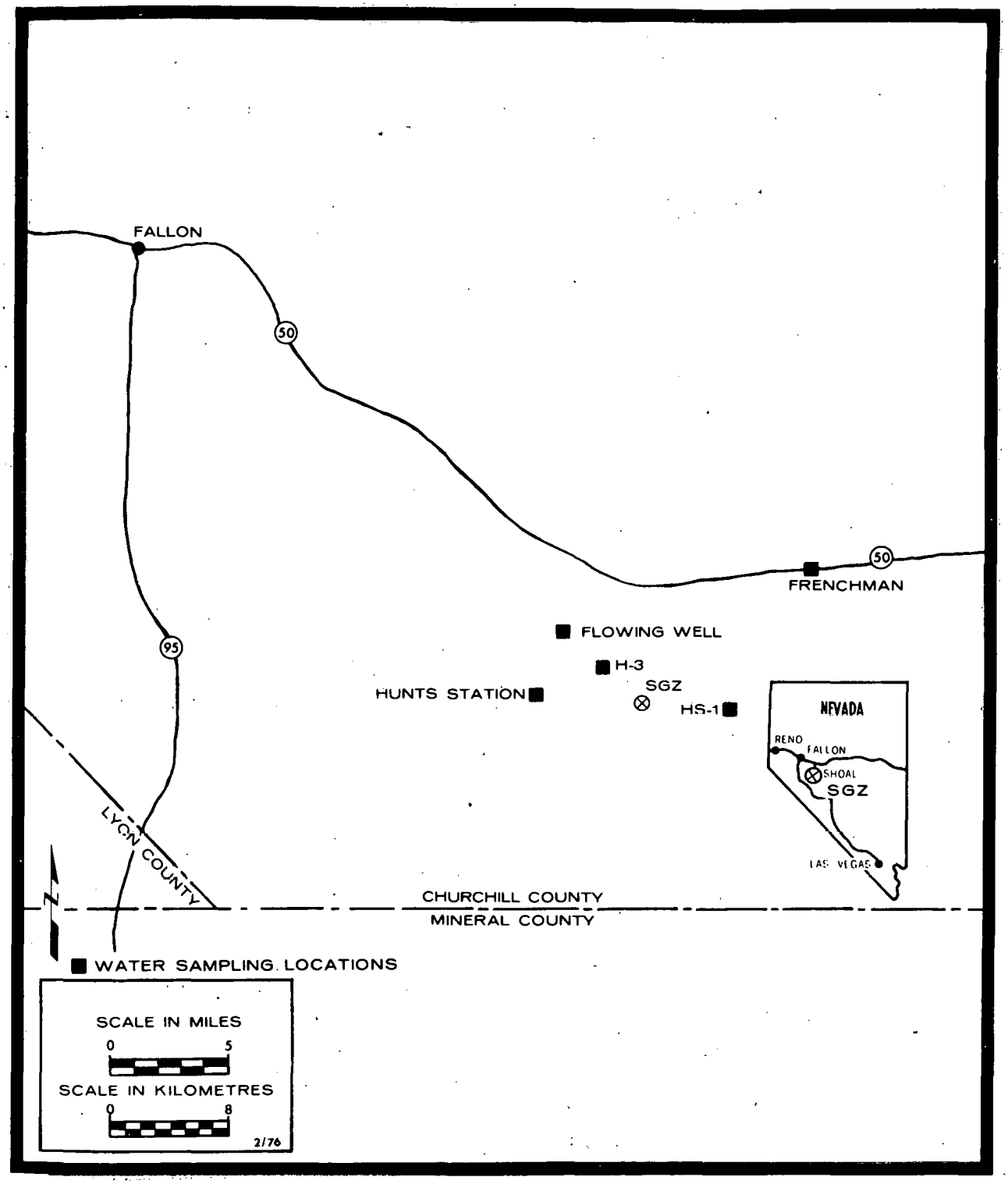

Figure 15. Long-Term Hydrological Monitoring Locations, Fallon, Nevada, Project Shoal

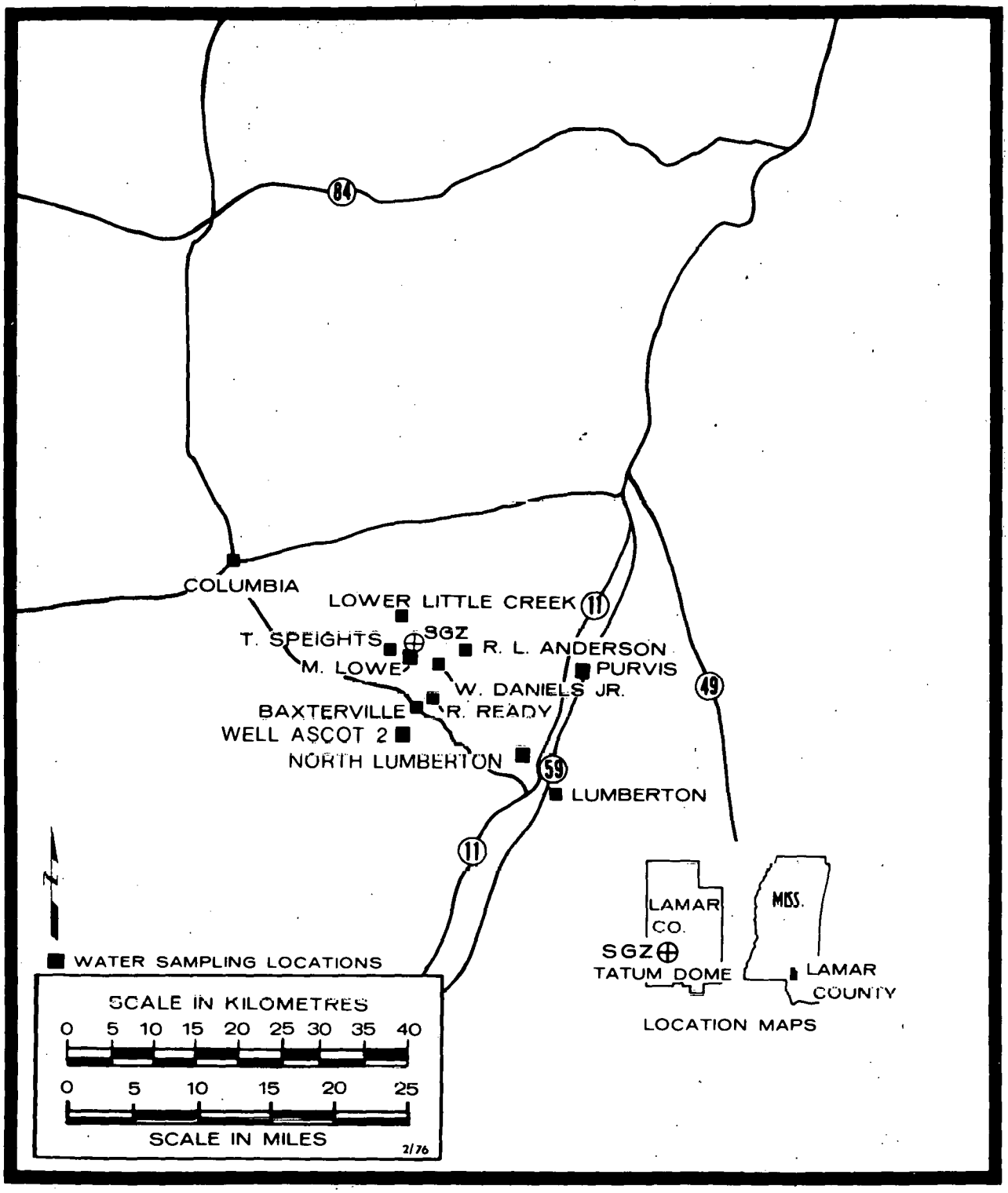

Figure 16. Long-Term Hydrological Monitoring Locations, Project Dribble/Miracle Play (Vicinity of Tatum Salt Dome, Mississippi)

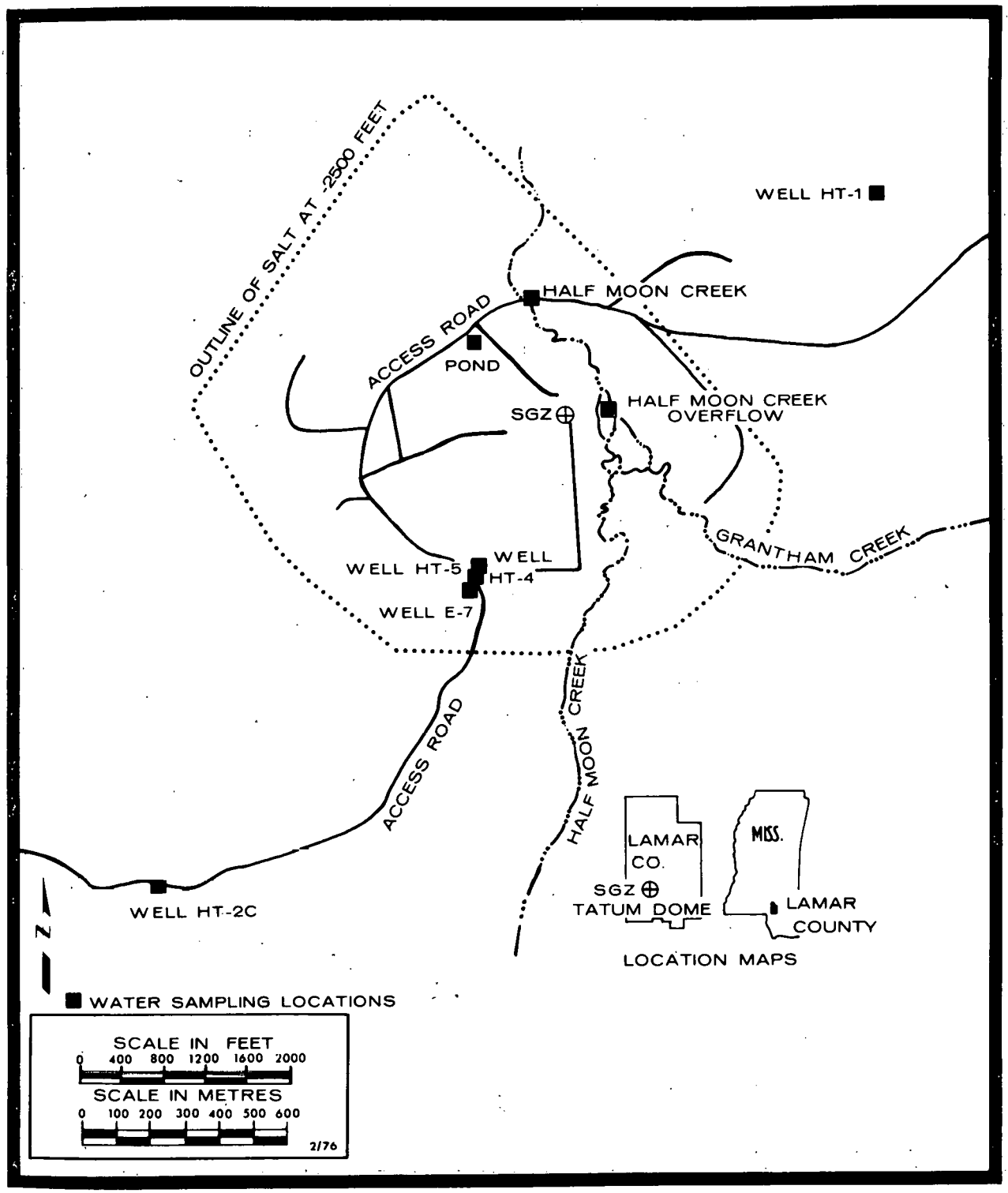

Figure 17. Long-Term Hydrological Monitoring Locations, Project Dribble/Miracle Play (Tatum Salt Dome, Mississippi)

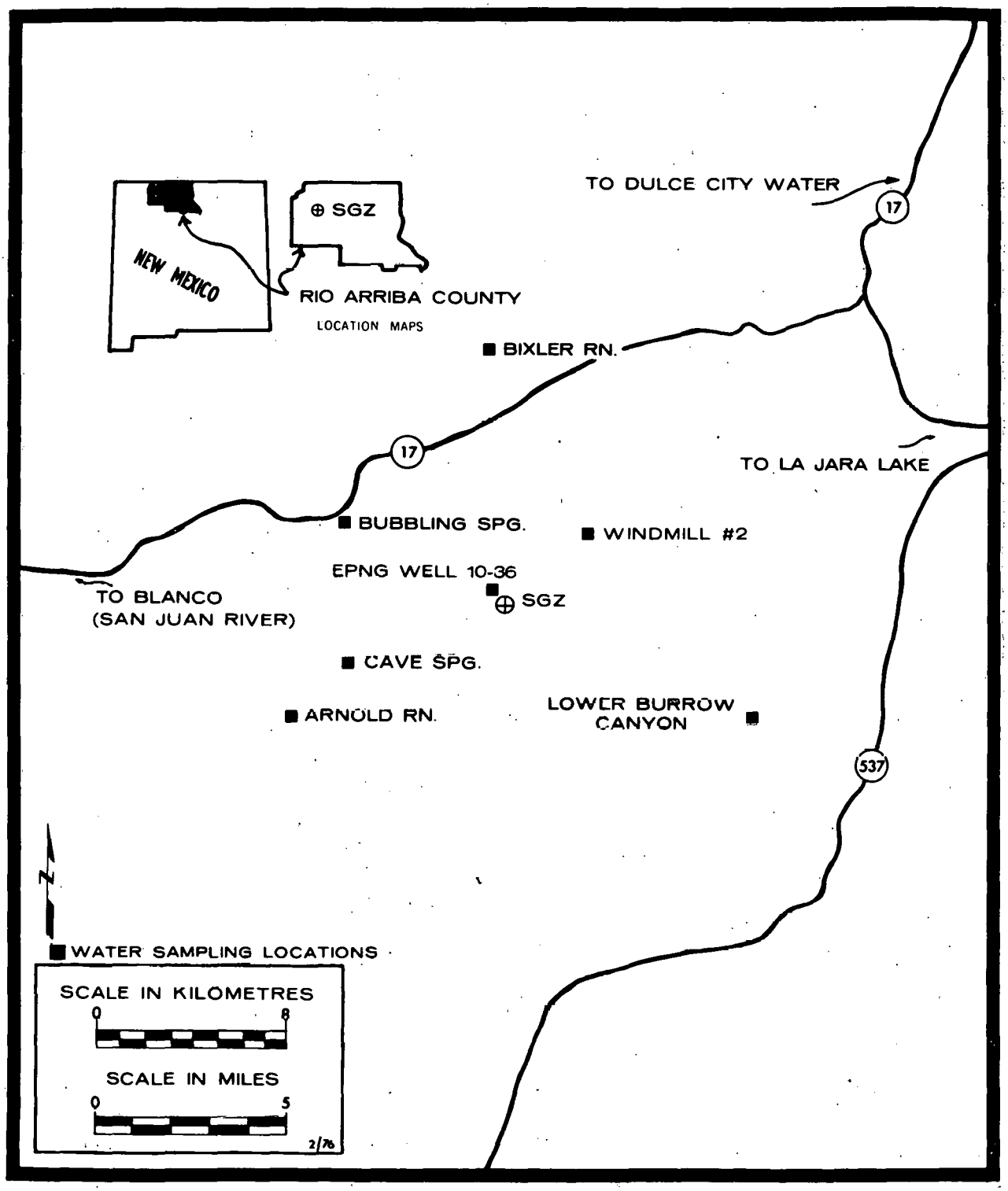

Figure 18. Long-Term Hydrological Monitoring Locations, Rio Arriba County, New Mexico, Project Gasbuggy

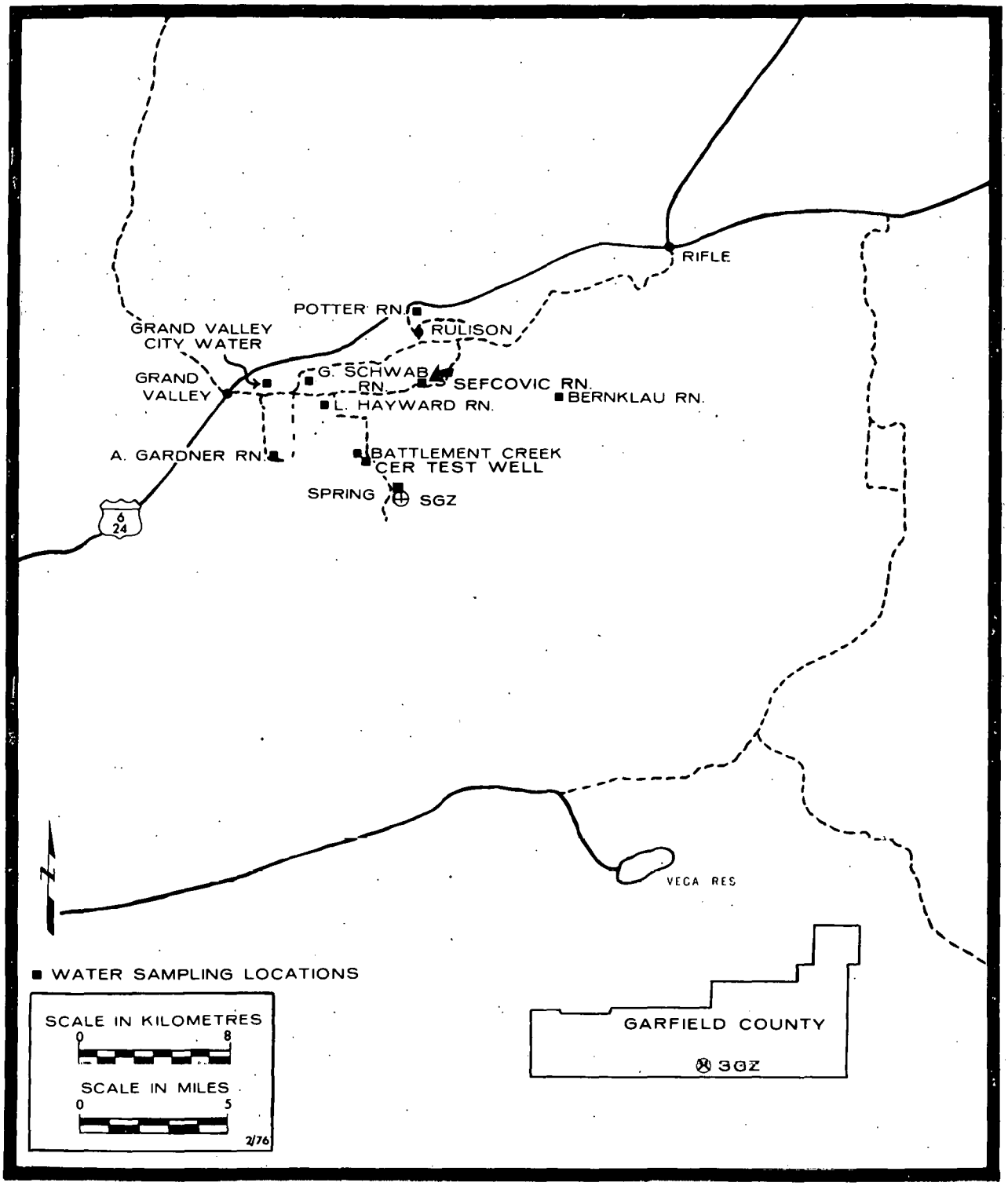

Figure 19. Long-Term Hydrological Monitoring Locations, Rulison, Colorado, Project Rulison

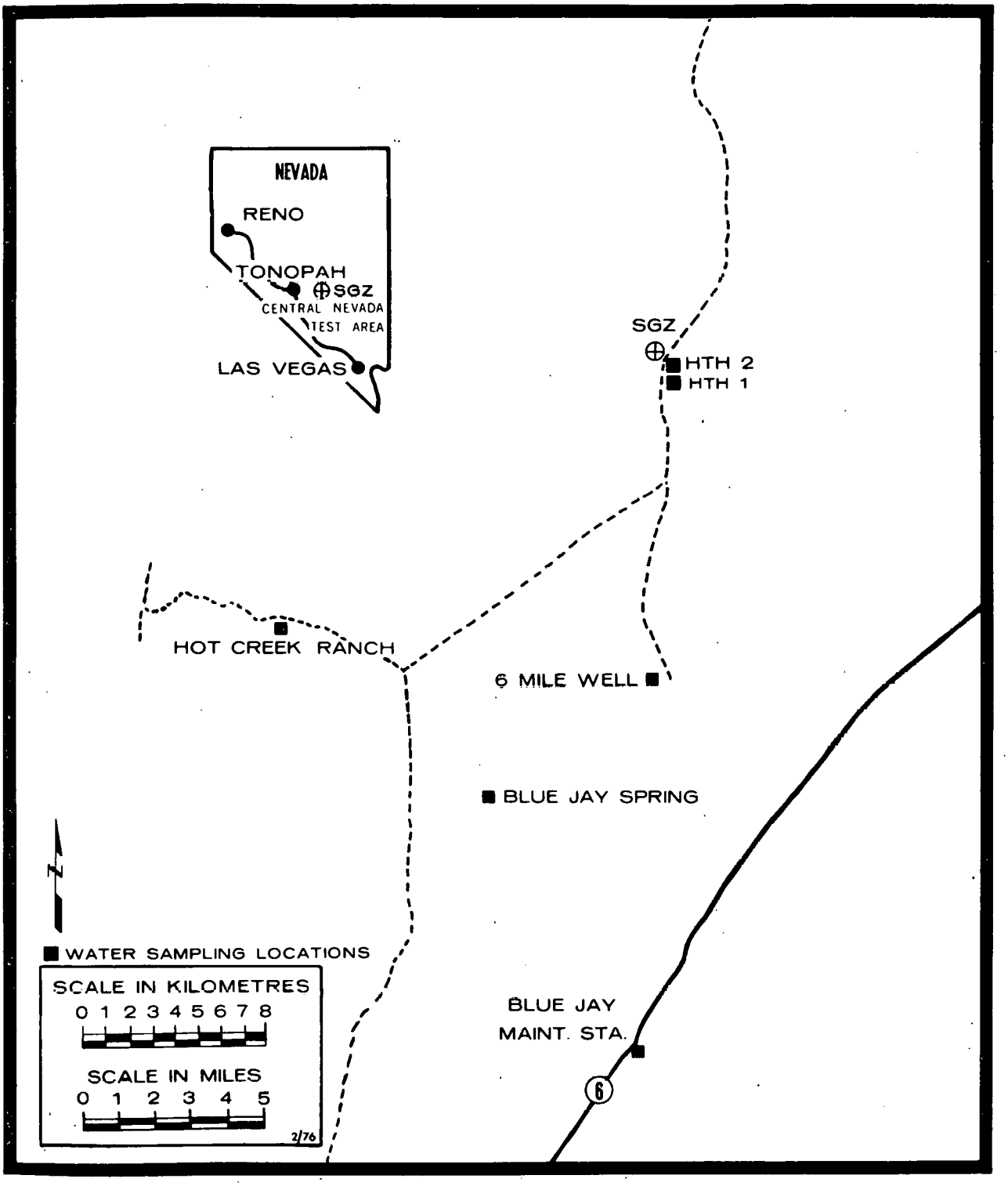

Figure 20. Long-Term Hydrological Monitoring Locations Central Nevada Test Area, Faultless Event

Table 2. Underground Testing Conducted Off the Nevada Test Site

Name of Test, Operation or Project	Date	Location	Yield[d] (kt)	Depth m (ft)	Purpose of the Event[d,e]
Project Gnome/ Coach[a]	12/10/61	48 km (30 mi) SE of Carlsbad, N.M.	3.1[f]	360 (1184)	Multi-purpose experiment.
Project Shoal[b]	10/26/63	45 km (28 mi) SE of Fallon, Nev.	12	366 (1200)	Nuclear test detection research experiment
Project Dribble[b] (Salmon Event)	10/22/64	34 km (21 mi) SW of Hattiesburg, Miss.	5.3	823 (2700)	Nuclear test detection research experiment.
Operation Long Shot[b]	10/29/65	Amchitka Island, Alaska	∿80	716 (2350)	DOD nuclear test detection experiment.
Project Dribble[b] (Sterling Event)	12/03/66	34 km (21 mi) SW of Hattiesburg, Miss.	0.38	823 (2700)	Nuclear test detection research experiment.
Project Gasbuggy[a]	12/10/67	88 km (55 mi) E of Farmington, N.M.	29	1292 (4240)	Joint Government-Industry gas stimulation experiment.
Faultless Event[c]	01/19/68	Central Nevada Test Area 96 km (60 mi) E of Tonopah, Nev.	200-1000	914 (3000)	Calibration test.
Project Miracle Play (Diode Tube)[b]	02/02/69	34 km (21 mi) SW of Hattiesburg, Miss.	Non-nuclear explosion	823 (2700)	Detonated in Salmon/Sterling cavity. Seismic studies.
Project Rulison[a]	09/10/69	19 km (12 mi) SW of Rifle, Colorado	40	2568 (8425)	Gas stimulation experiment.
Operation Milrow[c]	10/02/69	Amchitka Island, Alaska	∿1000	1219 (4000)	Calibration test.
Project Miracle Play (Humid Water)[b]	04/19/70	34 km (21 mi) SW of Hattiesburg, Miss.	Non-nuclear explosion	823 (2700)	Detonated in Salmon/Sterling cavity. Seismic studies.

Table 2. (continued)

Name of Test, Operation or Project	Date	Location	Yield[d] (kt)	Depth m (ft)	Purpose of the Event[d,e]
Operation Cannikin[c]	11/06/71	Amchitka Island, Alaska	<5000	1829 (6000)	Test of warhead for Spartan missle.
Project Rio Blanco[a]	05/17/73	48 km (30 mi) SW of Meeker, Colorado	3x30	1780 to 2040 (5840 to 6690)	Gas stimulation experiment.

[a] Plowshare Events

[b] Vela Uniform Events

[c] Weapons Tests

[d] Information from "Revised Nuclear Test Statistics," distributed on September 20, 1974, by David G. Jackson, Director, Office of Information Services, U.S. Atomic Energy Commission, Las Vegas, Nevada.

[e] News release AL-62-50, AEC Albuquerque Operations Office, Albuquerque, New Mexico. December 1, 1961

[f] "The Effects of Nuclear Weapons" Rev. Ed. 1964.

Table 3. Summary of Analytical Procedures

Type of Analysis	Analytical Equipment	Counting Period (Min)	Analytical Procedures	Sample Size (Litre)	Detection Limit[b]
Gamma Spectroscopy[a]	Gamma spectrometer with 10-cm-thick by 10-cm-diameter NaI (Tl-activated) crystal with input to 200 channels (0-2 MeV) of 400-channel, pulse-height analyzer.	100 min for milk, water, Long-Term Hydro. suspended solids and air filters; 10 min for air charcoal cartridges.	Radionuclide concentrations quantitated from gamma spectrometer data by computer using a least squares technique.	0.4-3.5 for routine milk and water samples; 700-1050m^3 for air filter samples; 7.3 litre for Long-Term Hydro. Water suspended solids.	For routine milk and water generally $\simeq 1x10^{-8}$ µCi/ml for most common fallout radionuclides in a simple spectrum. For air filters, $\simeq 3x10^{-14}$ µCi/ml. For Long-Term Hydro. suspended solids, $\simeq 3.0x10^{-9}$ µCi/ml.
$^{89-90}Sr$[c]	Low-background thin-window, gas-flow proportional counter with a 5.7-cm diameter window (80 µg/cm^2).	50	Chemical separation by ion exchange. Separated sample counted successively; activity calculated by simultaneous equations.	1.0	$^{89}Sr \simeq 2x10^{-9}$µCi/ml $^{90}Sr \simeq 1x10^{-9}$µCi/ml
^{3}H[c]	Automatic liquid scintillation counter with output printer.	200	Sample prepared by distillation.	0.005	$\simeq 2x10^{-7}$ µCi/ml
^{3}H Enrichment (Long-Term Hydrological Samples)[c]	Automatic scintillation counter with output printer.	200	Sample concentrated by electrolysis followed by distillation.	0.25	$\simeq 6x10^{-9}$ µCi/ml
$^{238,239}Pu$ ^{234,235}, ^{238}U[c]	Alpha spectrometer with 45 mm^2, 300-µm depletion depth silicon surface barrier detectors operated in vacuum chambers.	1000 - 1400	Sample is digested with acid, separated by ion exchange, electroplated on stainless steel planchet and counted by alpha spectrometer.	1	$^{238}Pu \simeq 4x10^{-11}$ µCi/ml ^{239}Pu, ^{234}U, ^{235}U $^{238}U \simeq 2x10^{-11}$ µCi/ml

Table 3. (continued)

Type of Analysis	Analytical Equipment	Counting Period (Min)	Analytical Procedures	Sample Size (Litre)	Detection Limit[b]
^{226}Ra[c]	Single channel analyzer coupled to P.M. tube detector.	30	Precipitated with Ba, converted to chloride. Stored for 30 days for ^{222}Ra ^{226}Ra to equilibrate. Radon gas pumped into scintillation cell for alpha scintillation counting.	1.5	$\approx 1 \times 10^{-10}$ μCi/ml
Gross alpha Gross beta in liquid samples[c]	Low-background thin-window, gas-flow proportional counter with a 5.7-cm-diameter window (80 μg/cm^2).	50	Sample evaporated; residue counted.	0.2	$\alpha \approx 3 \times 10^{-9}$ μCi/ml $\beta \approx 2 \times 10^{-9}$ μCi/ml
Gross beta on air filters[a]	Low-level end window, gas flow proportional counter with a 12.7-cm-diameter window (100 mg/cm^2).	20	Filters counted upon receipt and at 5 and 12 days after collection; last two counts used to extrapolate concentration to mid-collection time assuming $T^{-1.2}$ decay or using experimentally derived decay.	10-cm diameter glass fiber filter; sample collected from 700-1050m^3.	$\approx 3 \times 10^{-14}$ μCi/ml

Table 3. (continued)

Type of Analysis	Analytical Equipment	Counting Period (Min)	Analytical Procedures	Sample Size (Litre)	Detection Limit[b]
^{85}Kr Xe CH_3T[c]	Automatic liquid scintillation counter with output printer.	200	Physical separation by gas chromatography; dissolved in toluene "cocktail" for counting.	400-1000	$^{85}Kr = 2x10^{-12}$ µCi/ml Xe = $2x10^{-12}$ µCi/ml $CH_3T = 2x10^{-12}$ µCi/ml

[a] Lem, P. N. and Snelling, R. N. "Southwestern Radiological Health Laboratory Data Analysis and Procedures Manual," SWRHL-21. Southwestern Radiological Health Laboratory, U.S. Environmental Protection Agency, Las Vegas, NV. March 1971

[b] The detection limit for all samples is defined as that radioactivity which equals the 2-sigma counting error.

[c] Johns, F. B. "Handbook of Radiochemical Analytical Methods," EPA 680/4-75-001. U.S. Environmental Protection Agency, NERC-LV, Las Vegas, NV. February 1975.

Table 4. 1975 Summary of Analytical Results for the Noble Gas and Tritium Surveillance Network

Sampling Location	No. Days Sampled	Radio-nuclide	Radioactivity Concentrations Units	C_{Max}	C_{Min}	C_{Avg}	% of Conc. Guide*
Death Valley Jct., CA	340.2	^{85}Kr	$10^{-12}\mu Ci/ml$ air	27	11	17	0.02
	340.2	Total Xe	$10^{-12}\mu Ci/ml$ air	< 7	< 4	< 5	<0.01
	326.0	^{3}H as HTO	$10^{-6}\mu Ci/ml$ H_2O	0.97	< 0.2	< 0.4	<0.01
	340.2	^{3}H as CH_3T	$10^{-12}\mu Ci/ml$ air	< 3	< 2	< 2	
	318.9	^{3}H as HTO	$10^{-12}\mu Ci/ml$ air	6.1	< 0.4	< 2	<0.01
	326.0	^{3}H as HT	$10^{-12}\mu Ci/ml$ air	9.4	< 0.4	< 3	
Beatty, NV	368.4	^{85}Kr	$10^{-12}\mu Ci/ml$ air	25	11	19	0.02
	368.4	Total Xe	$10^{-12}\mu Ci/ml$ air	< 7	< 4	< 5	<0.01
	348.4	^{3}H as HTO	$10^{-6}\mu Ci/ml$ H_2O	2.2	< 0.2	< 0.5	<0.01
	368.4	^{3}H as CH_3T	$10^{-12}\mu Ci/ml$ air	< 3	< 2	< 2	
	348.4	^{3}H as HTO	$10^{-12}\mu Ci/ml$ air	8.4	< 0.5	< 3	<0.01
	341.5	^{3}H as HT	$10^{-12}\mu Ci/ml$ air	9.3	< 0.4	< 3	
Diablo, NV	346.2	^{85}Kr	$10^{-12}\mu Ci/ml$ air	29	11	18	0.02
	346.3	^{133}Xe	$10^{-12}\mu Ci/ml$ air	25	< 4	< 6	<0.01
	347.4	^{3}H as HTO	$10^{-6}\mu Ci/ml$ H_2O	2.4	< 0.2	< 0.5	<0.01
	346.2	^{3}H as CH_3T	$10^{-12}\mu Ci/ml$ air	< 3	< 2	< 2	
	347.4	^{3}H as HTO	$10^{-12}\mu Ci/ml$ air	22	< 0.2	< 3	<0.01
	347.4	^{3}H as HT	$10^{-12}\mu Ci/ml$ air	8.2	< 0.4	< 2	
Hiko, NV	346.5	^{85}Kr	$10^{-12}\mu Ci/ml$ air	23	10	17	0.02
	353.4	^{133}Xe	$10^{-12}\mu Ci/ml$ air	20	< 4	< 5	<0.01
	313.6	^{3}H as HTO	$10^{-6}\mu Ci/ml$ H_2O	1.4	< 0.2	< 0.4	<0.01
	353.4	^{3}H as CH_3T	$10^{-12}\mu Ci/ml$ air	< 3	< 2	< 2	
	313.6	^{3}H as HTO	$10^{-12}\mu Ci/ml$ air	11	< 0.4	< 2	<0.01
	313.6	^{3}H as HT	$10^{-12}\mu Ci/ml$ air	6.7	< 0.3	< 2	

Table 4. (continued)

Sampling Location	No. Days Sampled	Radionuclide	Radioactivity Concentration Units	C_{Max}	C_{Min}	C_{Avg}	% of Conc. Guide*
Indian Springs, NV **	252.7	^{85}Kr	$10^{-12}\mu Ci/ml$ air	30	9	20	0.02
	259.7	^{133}Xe	$10^{-12}\mu Ci/ml$ air	12	< 4	< 5	<0.01
	259.7	^{3}H as HTO	$10^{-6}\mu Ci/ml$ H_2O	1.4	< 0.2	< 0.4	<0.01
	259.7	^{3}H as CH_3T	$10^{-12}\mu Ci/ml$ air	< 3	< 2	< 2	
	259.7	^{3}H as HTO	$10^{-12}\mu Ci/ml$ air	7.5	< 0.2	< 3	<0.01
	259.7	^{3}H as HT	$10^{-12}\mu Ci/ml$ air	6	0.42	2.5	
Las Vegas, NV-NV00	361.4	^{85}Kr	$10^{-12}\mu Ci/ml$ air	30	9.6	18	0.02
	361.5	^{133}Xe	$10^{-12}\mu Ci/ml$ air	11	< 4	< 5	<0.01
	354.6	^{3}H as HTO	$10^{-6}\mu Ci/ml$ H_2O	1.2	< 0.2	< 0.4	<0.01
	361.4	^{3}H as CH_3T	$10^{-12}\mu Ci/ml$ air	< 3	< 2	< 2	
	354.6	^{3}H as HTO	$10^{-12}\mu Ci/ml$ air	4.4	< 0.4	< 2	<0.01
	354.6	^{3}H as HT	$10^{-12}\mu Ci/ml$ air	4.7	< 0.3	< 1	
NTS, NV Bldg. 790	343.2	^{85}Kr	$10^{-12}\mu Ci/ml$ air	34	8.2	18	0.02
	349.3	^{133}Xe	$10^{-12}\mu Ci/ml$ air	13	< 4	< 5	<0.01
	341.3	^{3}H as HTO	$10^{-6}\mu Ci/ml$ H_2O	1.4	< 0.2	< 0.5	<0.01
	349.3	^{3}H as CH_3T	$10^{-12}\mu Ci/ml$ air	< 3	< 2	< 3	
	341.3	^{3}H as HTO	$10^{-12}\mu Ci/ml$ air	6.3	< 0.4	< 2	<0.01
	341.3	^{3}H as HT	$10^{-12}\mu Ci/ml$ air	5.4	0.23	< 2	
NTS, NV Area 51	328.3	^{85}Kr	$10^{-12}\mu Ci/ml$ air	25	12	18	0.02
	328.3	^{133}Xe	$10^{-12}\mu Ci/ml$ air	12	< 4	< 5	<0.01
	342.2	^{3}H as HTO	$10^{-6}\mu Ci/ml$ H_2O	7.3	< 0.2	< 0.6	<0.01
	321.3	^{3}H as CH_3T	$10^{-12}\mu Ci/ml$ air	< 3	< 2	< 2	
	342.2	^{3}H as HTO	$10^{-12}\mu Ci/ml$ air	20	< 0.2	< 3	<0.01
	342.2	^{3}H as HT	$10^{-12}\mu Ci/ml$ air	4.5	< 0.2	< 2	

Table 4. (continued)

Sampling Location	No. Days Sampled	Radio-nuclide	Radioactivity Concentration Units	C_{Max}	C_{Min}	C_{Avg}	% of Conc. Guide*
NTS, NV BJY	363.4	^{85}Kr	$10^{-12}\mu Ci/ml$ air	38	9.8	19	0.02
	363.4	^{133}Xe	$10^{-12}\mu Ci/ml$ air	31	< 4	< 6	<0.01
	363.4	^{3}H as HTO	$10^{-6}\mu Ci/ml$ H_2O	3.6	< 0.3	< 2	<0.01
	363.4	^{3}H as CH_3T	$10^{-12}\mu Ci/ml$ air	< 3	< 2	< 2	
	363.4	^{3}H as HTO	$10^{-12}\mu Ci/ml$ air	20	< 1	< 7	<0.01
	363.4	^{3}H as HT	$10^{-12}\mu Ci/ml$ air	9.2	< 0.4	< 1	
NTS, NV Area 12	335.2	^{85}Kr	$10^{-12}\mu Ci/ml$ air	27	12	18	0.02
	335.2	^{133}Xe	$10^{-12}\mu Ci/ml$ air	13	< 4	< 5	<0.01
	363.2	^{3}H as HTO	$10^{-6}\mu Ci/ml$ H_2O	58	0.25	6	<0.01
	342.2	^{3}H as CH_3T	$10^{-12}\mu Ci/ml$ air	< 3	< 2	< 2	
	363.2	^{3}H as HTO	$10^{-12}\mu Ci/ml$ air	210	0.71	25	<0.01
	363.2	^{3}H as HT	$10^{-12}\mu Ci/ml$ air	25	< 0.2	< 2	
Tonopah, NV	355.4	^{85}Kr	$10^{-12}\mu Ci/ml$ air	24	10	17	0.02
	361.3	Total Xe	$10^{-12}\mu Ci/ml$ air	< 9	< 4	< 5	<0.01
	368.3	^{3}H as HTO	$10^{-6}\mu Ci/ml$ H_2O	1.3	< 0.2	< 0.4	<0.01
	361.3	^{3}H as CH_3T	$10^{-12}\mu Ci/ml$ air	< 3	< 2	< 2	
	368.3	^{3}H as HTO	$10^{-12}\mu Ci/ml$ air	5.6	< 0.4	< 2	<0.01
	368.3	^{3}H as HT	$10^{-12}\mu Ci/ml$ air	4.2	< 0.2	< 2	

* Concentration Guides used for NTS stations are those applicable to exposures to radiation workers. Those used for off-NTS stations are for exposure to a suitable sample of the population in an uncontrolled area. See Appendix A for Concentration Guides.

**Although the Indian Springs station was installed for only 9 months of the year (April-December), the concentration average over the 9 months was assumed to be representative of levels at that location for the entire year.

Table 5. 1975 Summary of Radiation Doses for the Dosimetry Network

Station Location	Measurement Period	Dose Equivalent Rate (mrem/d) Max.	Min.	Avg.	Annual Adjusted Dose Equivalent* (mrem/y)
Adaven, NV	1/08/75 - 1/21/76	0.36	0.32	0.34	120
Alamo, NV	1/06/75 - 1/13/76	0.25	0.23	0.24	88
Baker, CA	1/06/75 - 1/12/76	0.22	0.19	0.21	77
Barstow, CA	1/06/75 - 1/12/76	0.25	0.23	0.25	91
Beatty, NV	1/14/75 - 1/20/76	0.31	0.26	0.28	100
Bishop, CA	1/08/75 - 1/14/76	0.24	0.21	0.24	88
Blue Eagle Rch., NV	1/07/75 - 1/22/76	0.17	0.15	0.16	58
Blue Jay, NV	1/08/75 - 1/21/76	0.33	0.27	0.31	110
Cactus Springs, NV	1/13/75 - 1/19/76	0.17	0.14	0.16	58
Caliente, NV	1/08/75 - 1/14/76	0.28	0.26	0.27	99
Casey's Ranch, NV	1/07/75 - 1/21/76	0.21	0.16	0.19	69
Cedar City, UT	1/13/75 - 1/21/76	0.23	0.18	0.19	69
Clark Station, NV	1/08/75 - 1/21/76	0.31	0.29	0.30	110
Coyote Summit, NV	1/06/75 - 1/20/76	0.33	0.28	0.31	110
Currant, NV	1/07/75 - 1/22/76	0.25	0.23	0.23	84
Death Valley Jct., CA	1/15/75 - 1/15/76	0.22	0.20	0.21	77
Desert Game Range, NV	1/13/75 - 1/19/76	0.16	0.12	0.13	48
Desert Oasis, NV	1/13/75 - 1/19/76	0.18	0.14	0.16	58
Diablo Maint. Sta., NV	1/09/75 - 1/20/76	0.38	0.30	0.33	120
Duckwater, NV	1/07/75 - 1/22/76	0.29	0.23	0.27	99
Elgin, NV	1/08/75 - 1/14/76	0.30	0.28	0.27	110
Ely, NV	1/06/75 - 1/20/76	0.27	0.23	0.25	91
Enterprise, UT	1/15/75 - 1/21/76	0.30	0.23	0.24	88
Furnace Creek, CA	1/08/75 - 1/15/76	0.19	0.17	0.18	66
Geyser Maint. Sta., NV	1/06/75 - 1/20/76	0.26	0.23	0.24	88
Goldfield, NV	1/13/75 - 1/20/76	0.26	0.23	0.24	88
Groom Lake, NV	1/06/75 - 1/20/76	0.19	0.18	0.18	66

Table 5. (continued)

Station Location	Measurement Period	Dose Equivalent Rate (mrem/d) Max.	Min.	Avg.	Annual Adjusted Dose Equivalent* (mrem/y)
Hancock Summit, NV	1/06/75 - 1/20/76	0.40	0.33	0.35	130
Hiko, NV	1/06/75 - 1/13/76	0.23	0.18	0.20	73
Hot Creek Ranch, NV	1/08/75 - 1/21/76	0.25	0.21	0.20	84
Independence, CA	1/07/75 - 1/14/76	0.26	0.23	0.24	88
Indian Springs, NV	1/13/75 - 1/19/76	0.18	0.16	0.18	66
Kirkeby Ranch, NV	1/06/75 - 1/20/76	0.21	0.19	0.20	73
Koynes, NV	1/09/75 - 1/20/76	0.25	0.22	0.24	88
Las Vegas (McCarran), NV	1/10/75 - 1/08/76	0.13	0.11	0.12	44
Las Vegas (Placak), NV	1/10/75 - 1/08/76	0.14	0.12	0.13	48
Las Vegas (USDI), NV	1/10/75 - 1/08/76	0.17	0.15	0.16	58
Lathrop Wells, NV	1/15/75 - 1/20/76	0.27	0.23	0.24	88
Lida, NV	1/13/75 - 1/19/76	0.29	0.26	0.27	99
Lone Pine, CA	1/07/75 - 1/13/76	0.24	0.23	0.23	84
Lund, NV	1/08/75 - 1/21/76	0.22	0.21	0.21	77
Manhattan, NV	1/14/75 - 1/21/76	0.37	0.28	0.31	110
Mesquite, NV	1/13/75 - 1/19/76	0.21	0.15	0.17	62
Nevada Farms, NV	1/06/75 - 1/20/76	0.33	0.27	0.29	110
Nuclear Eng. Co., NV	1/15/75 - 1/20/76	0.37	0.30	0.34	120
Nyala, NV	1/07/75 - 1/21/76	0.24	0.19	0.22	80
Olancha, CA	1/07/75 - 1/13/76	0.24	0.20	0.22	80
Pahrump, NV	1/16/75 - 1/22/76	0.19	0.17	0.18	66
Pine Creek Ranch, NV	1/08/75 - 1/21/76	0.32	0.29	0.30	110
Pioche, NV	1/07/75 - 1/14/76	0.32	0.28	0.29	106
Queen City Summit, NV	1/06/75 - 1/20/76	0.36	0.30	0.34	120
Reed Ranch, NV	1/06/75 - 1/20/76	0.31	0.25	0.28	102
Ridgecrest, CA	1/07/75 - 1/13/76	0.22	0.18	0.20	73
Round Mountain, NV	1/14/75 - 1/21/76	0.32	0.26	0.29	106

Table 5. (continued)

Station Location	Measurement Period	Dose Equivalent Rate (mrem/d) Max.	Min.	Avg.	Annual Adjusted Dose Equivalent* (mrem/y)
Scotty's Junction, NV	1/10/75 - 1/19/76	0.31	0.27	0.29	106
Selbach Ranch, NV	1/16/75 - 1/21/76	0.30	0.26	0.27	99
Sherri's Bar, NV	1/06/75 - 1/13/76	0.19	0.15	0.18	66
Shoshone, CA	1/15/75 - 1/15/76	0.27	0.25	0.26	95
Spring Meadows, NV	1/16/75 - 1/21/76	0.18	0.13	0.15	55
Springdale, NV	1/14/75 - 1/21/76	0.32	0.28	0.30	110
St. George, UT	1/13/75 - 1/22/76	0.20	0.15	0.16	58
Sunnyside, NV	1/08/75 - 1/21/76	0.25	0.18	0.22	80
Tempiute, NV	1/06/75 - 1/20/76	0.31	0.27	0.28	100
Tenneco, NV	1/16/75 - 1/21/76	0.29	0.24	0.25	91
Tonopah Test Range, NV	1/09/75 - 1/20/76	0.28	0.24	0.26	95
Tonopah, NV	1/09/75 - 1/20/76	0.31	0.25	0.28	100
Twin Springs Ranch, NV	1/08/75 - 1/21/76	0.31	0.25	0.28	102
Warm Springs, NV	1/08/75 - 1/21/76	0.32	0.25	0.27	99
Young's Ranch, NV	1/14/75 - 1/21/76	0.26	0.21	0.23	84

* Annual adjusted dose equivalent is average dose equivalent rate (mrem/d) times 365 d.

Table 6. 1975 Summary of Analytical Results for the Milk Surveillance Network

Sampling Location	Sample Type[a]	No. of Samples	Radio-nuclide	Radioactivity Conc. (10^{-9} µCi/ml) C_{Max}	C_{Min}	C_{Avg}
Bishop, CA Sierra Creamery	11	1	^{137}Cs	<4	<4	<4
		1	^{89}Sr	<3	<3	<3
		1	^{90}Sr	4.3	4.3	4.3
Hinkley, CA Bill Nelson Dairy	12	4	^{137}Cs	<6	<4	<5
		4	^{89}Sr	<4	<1	<2
		4	^{90}Sr	4.9	<1	<3
Keough Hot Spgs., CA[b] Yribarren Ranch	13	2	^{137}Cs	<5	<4	<5
		2	^{89}Sr	<2	<1	<2
		2	^{90}Sr	2.2	<2	<2
Olancha, CA Hunter Ranch	13	1	^{137}Cs	<4	<4	<4
		1	^{89}Sr	<4	<4	<4
		1	^{90}Sr	4.0	4.0	4.0
Olancha, CA[c] Riley Ranch	13	2	^{137}Cs	<5	<4	<5
		2	^{89}Sr	<2	<2	<2
		2	^{90}Sr	2.7	2.0	2.4
Alamo, NV Alamo Dairy	12	4	^{137}Cs	<8	<4	<5
		4	^{89}Sr	<4	<1	<2
		4	^{90}Sr	4.5	<1	<3
Austin, NV Young's Ranch	13	4	^{137}Cs	<7	<3	<6
		4	^{89}Sr	<3	<2	<2
		4	^{90}Sr	5.3	2.0	2.9
		4	^{3}H	1000	350	590

Table 6. (continued)

Sampling Location	Sample Type[a]	No. of Samples	Radio-nuclide	Radioactivity Conc. (10^{-9} µCi/ml) C_{Max}	C_{Min}	C_{Avg}
Currant, NV Blue Eagle Ranch	13	4	^{137}Cs	18	<4	<10
		4	^{89}Sr	<5	<2	<3
		4	^{90}Sr	5.2	<1	<3
Currant, NV Manzonie Ranch	13	4	^{137}Cs	<8	<3	<5
		4	^{89}Sr	<4	<2	<2
		4	^{90}Sr	2.4	<1	<2
Hiko, NV Schofield Dairy	12	4	^{137}Cs	<8	<4	<5
		4	^{89}Sr	<4	<1	<2
		4	^{90}Sr	2.4	<1	<2
		4	^{3}H	450	<300	<400
Las Vegas, NV LDS Dairy Farms	12	4	^{137}Cs	5	<3	<4
		4	^{89}Sr	<3	<1	<2
		4	^{90}Sr	3.8	<0.9	<2
		4	^{3}H	740	<300	<400
Lathrop Wells, NV Kirker Ranch	13	3	^{137}Cs	<5	<4	<5
		3	^{89}Sr	<2	<1	<2
		3	^{90}Sr	1.5	<0.7	<2
Lida, NV Lida Livestock Company	13	4	^{137}Cs	<5	<3	<4
		4	^{89}Sr	<3	<1	<2
		4	^{90}Sr	3.8	<2	<2
Logandale, NV Vegas Valley Dairy	12	4	^{137}Cs	<7	<4	<5
		4	^{89}Sr	<3	<1	<2
		4	^{90}Sr	4.5	<0.8	<3

Table 6. (continued)

Sampling Location	Sample Type[a]	No. of Samples	Radio-nuclide	Radioactivity Conc. (10^{-9} µCi/ml) C_{Max}	C_{Min}	C_{Avg}
Lund, NV McKenzie Dairy	12	4	^{137}Cs	<7	<4	<5
		4	^{89}Sr	<4	<2	<2
		4	^{90}Sr	2.9	1.4	2.0
		4	^{3}H	490	<300	<400
Mesquite, NV Hughes Bros. Dairy	12	4	^{137}Cs	<7	<4	<5
		4	^{89}Sr	<3	<1	<2
		4	^{90}Sr	3.9	<2	<3
		4	^{3}H	360	<300	<300
Moapa, NV Searles Dairy	12	4	^{137}Cs	<8	<4	<6
		4	^{89}Sr	<3	<2	<2
		4	^{90}Sr	5.7	1.3	2.7
Nyala, NV Sharp's Ranch	13	4	^{137}Cs	<6	<4	<5
		4	^{89}Sr	<2	<1	<2
		4	^{90}Sr	4.2	<0.1	<2
		4	^{3}H	700	<300	<400
Pahrump, NV Burson Ranch	13	4	^{137}Cs	<7	<4	<5
		4	^{89}Sr	<3	<2	<2
		4	^{90}Sr	2.2	<1	<2
Panaca, NV Kenneth Lee Ranch	13	3	^{137}Cs	<6	<4	<5
		3	^{89}Sr	<4	<2	<2
		3	^{90}Sr	5.1	1.5	2.8
Round Mountain, NV Berg Ranch	13	4	^{137}Cs	<10	<4	<7
		4	^{89}Sr	<4	<2	<2
		4	^{90}Sr	8.7	2.8	4.7

Table 6. (continued)

Sampling Location	Sample Type[a]	No. of Samples	Radio-nuclide	Radioactivity Conc. (10^{-9} µCi/ml) C_{Max}	C_{Min}	C_{Avg}
Shoshone, NV Kirkeby Ranch	13	4	^{137}Cs	<4	<4	<4
		4	^{89}Sr	<3	<1	<2
		4	^{90}Sr	5.5	<0.9	<3
Springdale, NV Siedentopf Ranch	13	4	^{137}Cs	<7	<4	<5
		4	^{89}Sr	<4	<2	<2
		4	^{90}Sr	<2	<1	<2
Cedar City, UT Western Gold Dairy	12	3	^{137}Cs	<9	<4	<6
		3	^{89}Sr	<3	<2	<2
		3	^{90}Sr	4.5	1.2	2.5
St. George, UT R. Cox Dairy	12	4	^{137}Cs	<5	<3	<4
		4	^{89}Sr	<3	<1	<2
		4	^{90}Sr	4.5	<1	<2

[a] 11 = Pasteurized Milk
12 = Raw Milk from Grade A Producer(s)
13 = Raw Milk from family cow(s)

[b] New sampling location; the Sierra Creamery closed.

[c] New sampling location; replaces the Hunter Ranch

Table 7. Analytical Criteria for Long-Term Hydrological Monitoring Program Samples

	Monthly Samples	Semi-Annual Samples	Annual Samples
Gross alpha	All samples	All samples	All samples
Gross beta	All samples	All samples	All samples
Gamma scan	All samples	All samples	All samples
^{3}H[a]	All samples	All samples	All samples
$^{89,90}Sr$	Jan. and July samples. Any other sample if gross beta exceeds 1 x 10^{-8} µCi/ml.	Jan. sample only. July sample if gross beta exceeds 1 x 10^{-8} µCi/ml.	All samples collected at locations for the first time within CY75. Subsequent samples if gross beta exceeds 1 x 10^{-8} µCi/ml.
^{226}Ra	Any sample if gross alpha exceeds 3 x 10^{-9} µCi/ml.	Any sample if gross alpha exceeds 3 x 10^{-9} µCi/ml.	Any sample if gross alpha exceeds 3 x 10^{-9} µCi/ml.
U	Jan. and July samples in CY75.	Jan. sample only in CY75.	Only samples collected at locations for the first time during CY75.
$^{238,239}Pu$	Jan. and July samples in CY75.	Jan. sample only in CY75.	Only samples collected at locations for the first time during CY75.

[a] Starting in January 1975, all samples were first analyzed by the conventional technique (MDC$\sim$2 x 10^{-7} µCi/ml) as a screening method to determine if a sample should be analyzed by the enrichment technique (MDC$\sim$6 x 10^{-9} µCi/ml).

Table 8. 1975 Summary of Analytical Results for the NTS Monthly Long-Term Hydrological Monitoring Program

Sampling Location	No. Samples Collected[a]	No. Samples Analyzed	Radio-nuclide	Radioactivity Conc. 10^{-9} µCi/ml C_{Max}	C_{Min}	C_{Avg}	% of Conc. Guide
NTS	11	11	^{3}H	<10	<6	<8	<0.01
Well 20 A-2		2	^{89}Sr	<2	<2	<2	<0.01
		2	^{90}Sr	<2	<1	<1	<0.01
		11	^{226}Ra	0.32	0.031	0.12	0.03
		2	^{234}U	4.1	3.8	4.0	<0.01
		2	^{235}U	0.049	0.023	0.036	<0.01
		2	^{238}U	0.99	0.98	0.99	<0.01
		2	^{238}Pu	<0.04	<0.03	<0.04	<0.01
		2	^{239}Pu	<0.04	<0.04	<0.04	<0.01
NTS	10	10	^{3}H	<9	<6	<8	<0.01
Well 8		2	^{89}Sr	<2	<2	<2	<0.01
		2	^{90}Sr	<10	<2	<6	<0.05
		2	^{234}U	0.52	0.35	0.44	<0.01
		2	^{235}U	<0.04	<0.02	<0.03	<0.01
		2	^{238}U	0.13	<0.07	<0.1	<0.01
		2	^{238}Pu	<0.03	<0.02	<0.03	<0.01
		2	^{239}Pu	<0.03	<0.02	<0.03	<0.01
NTS	6	6	^{3}H	<9	<6	<8	<0.01
Well J-12		1	^{89}Sr	<2	<2	<2	<0.01
		1	^{90}Sr	<1	<1	<1	<0.01
		1	^{226}Ra	0.27	0.27	0.27	<0.07
		1	^{234}U	1.1	1.1	1.1	<0.01
		1	^{235}U	<0.01	<0.01	<0.01	<0.01
		1	^{238}U	0.18	0.18	0.18	<0.01
		1	^{238}Pu	<0.06	<0.06	<0.06	<0.01
		1	^{239}Pu	<0.04	<0.04	<0.04	<0.01
NTS	5	4[b]	^{3}H	10	<7	<9	<0.01
Well U3CN-5		5	^{89}Sr	<2	<2	<2	<0.01
		5	^{90}Sr	<2	<0.8	<0.9	<0.01
		5	^{226}Ra	2.4	0.78	1.8	0.5
		2	^{234}U	1.7	0.39	1.0	<0.01
		2	^{235}U	0.02	<0.02	<0.02	<0.01
		2	^{238}U	0.37	0.11	0.24	<0.01
		2	^{238}Pu	<0.06	<0.05	<0.05	<0.01
		2	^{239}Pu	<0.05	<0.03	<0.04	<0.01

Table 8. (continued)

Sampling Location	No. Samples Collected[a]	No. Samples Analyzed	Radio-nuclide	Radioactivity Conc. 10^{-9} µCi/ml C_{Max}	C_{Min}	C_{Avg}	% of Conc. Guide
NTS	5	5	^{3}H	8	<7	<8	<0.01
Well J-13		1	^{89}Sr	<2	<2	<2	<0.01
		1	^{90}Sr	<0.9	<0.9	<0.9	<0.01
		1	^{226}Ra	0.067	0.067	0.067	0.017
		1	^{234}U	1.7	1.7	1.7	<0.01
		1	^{235}U	<0.02	<0.02	<0.02	<0.01
		1	^{238}U	0.22	0.22	0.22	<0.01
		1	^{238}Pu	<0.03	<0.03	<0.03	<0.01
		1	^{239}Pu	<0.04	<0.04	<0.04	<0.01
NTS	10	10	^{3}H	18	<6	<9	<0.01
Well UE 19g-s		2	^{89}Sr	<2	<2	<2	<0.01
		2	^{90}Sr	<2	<0.9	<1	<0.01
		10	^{226}Ra	0.3	0.056	0.14	0.035
		2	^{234}U	14	9.1	12	<0.01
		2	^{235}U	0.16	0.089	0.12	<0.01
		2	^{238}U	4	2.2	3.1	<0.01
		2	^{238}Pu	<0.03	<0.03	<0.03	<0.01
		2	^{239}Pu	<0.07	<0.02	<0.05	<0.01
Beatty, NV	9	9	^{3}H	14	<6	<8	<0.01
Well 11S/48-1dd		2	^{89}Sr	<2	<2	<2	<0.01
		2	^{90}Sr	<1	<0.9	<1	<0.01
		8	^{226}Ra	0.32	0.056	0.17	0.043
		2	^{234}U	9	9	9	<0.01
		2	^{235}U	0.080	0.081	0.085	<0.01
		2	^{238}U	1.8	1.7	1.8	<0.01
		2	^{238}Pu	<0.04	<0.02	<0.03	<0.01
		2	^{239}Pu	<0.03	<0.03	<0.03	<0.01
NTS	1	1	^{3}H	<10	<10	<10	<0.01
Well U 19-c							

Table 8. (continued)

Sampling Location	No. Samples Collected[a]	No. Samples Analyzed	Radionuclide	Radioactivity Conc. 10^{-9} µCi/ml C_{Max}	C_{Min}	C_{Avg}	% of Conc. Guide
NTS	11	10[b]	^{3}H	<10	<7	<8	<0.01
Well A		4	^{89}Sr	<2	<1	<2	<0.01
		4	^{90}Sr	<0.9	<0.8	<0.9	<0.01
		11	^{226}Ra	0.50	0.017	0.13	0.03
		2	^{234}U	5.4	5.1	5.3	<0.01
		2	^{235}U	0.067	0.048	0.058	<0.01
		2	^{238}U	1.7	1.5	1.6	<0.01
		2	^{238}Pu	0.092	<0.04	<0.07	<0.01
		2	^{239}Pu	0.031	<0.03	<0.03	<0.01
NTS	11	11	^{3}H	150	40	90	<0.01
Well C		10	^{89}Sr	<3	<1	<2	<0.01
		10	^{90}Sr	3	<1	<1	<0.01
		12	^{226}Ra	1.3	0.062	0.83	0.2
		2	^{234}U	9.2	8.7	9	<0.01
		2	^{235}U	0.10	0.099	0.01	<0.01
		2	^{238}U	2.6	2.4	2.5	<0.01
		2	^{238}Pu	<0.05	<0.03	<0.04	<0.01
		2	^{239}Pu	<0.08	<0.03	<0.05	<0.01
NTS	11	11	^{3}H	15	<6	<9	<0.01
Well 5C		3	^{89}Sr	<3	<1	<2	<0.01
		3	^{90}Sr	<1	<0.9	<1	<0.01
		11	^{226}Ra	0.29	0.061	0.14	0.035
		2	^{234}U	5.4	2.4	3.9	<0.01
		2	^{235}U	0.093	<0.08	<0.09	<0.01
		2	^{238}U	2.7	1.2	2	<0.01
		2	^{238}Pu	<0.05	<0.04	<0.04	<0.01
		2	^{239}Pu	<0.05	<0.04	<0.04	<0.01
NTS	9	8[b]	^{3}H	18	<7	<10	< 0.01
Well Army No. 1		3	^{89}Sr	<1	<1	<1	<0.01
		3	^{90}Sr	<2	<1	<2	<0.02
		8	^{226}Ra	0.59	0.0094	0.30	0.075
		2	^{234}U	2.4	2.4	2.4	<0.01
		2	^{235}U	0.031	<0.02	<0.03	<0.01
		2	^{238}U	0.78	0.72	0.75	<0.01
		2	^{238}Pu	<0.03	<0.03	<0.03	<0.01
		2	^{239}Pu	<0.06	<0.02	<0.04	<0.01

[a] Samples could not be collected every month due to weather conditions or inoperative pumps.

[b] Sample lost in analysis.

Table 9. 1975 Summary of Analytical Results

for the NTS Semi-Annual Long-Term Hydrological Monitoring Program

Sampling Location	Date	Sample Type[a]	Radio-nuclide	Radioactivity Conc. (10^{-9} µCi/ml)	% of Conc. Guide[b]
NTS Well UE 15d	1/15	23	^{3}H	<7	<0.01
			^{89}Sr	<2	<0.01
			^{90}Sr	<2	<0.01
			^{226}Ra	1.5	0.4
			^{234}U	4.7	<0.01
			^{235}U	0.026	<0.01
			^{238}U	1.2	<0.01
			^{238}Pu	<0.05	<0.01
			^{239}Pu	<0.04	<0.01
NTS Well UE 15d	7/08	23	^{3}H	<7	<0.01
			^{89}Sr	<1	<0.01
			^{90}Sr	<0.9	<0.01
NTS Well 2	1/14	23	^{3}H	<9	<0.01
			^{89}Sr	<1	<0.01
			^{90}Sr	<0.08	<0.01
			^{226}Ra	0.21	0.05
			^{234}U	1.7	<0.01
			^{235}U	<0.01	<0.01
			^{238}U	0.34	<0.01
			^{238}Pu	<0.04	<0.01
			^{239}Pu	<0.04	<0.01
NTS Well 2	7/08	23	^{3}H	8.3	<0.01
NTS Well C-1	1/14	23	^{3}H	70	<0.01
			^{89}Sr	<1	<0.01
			^{90}Sr	<0.8	<0.01
			^{226}Ra	0.067	0.02
			^{234}U	7.7	<0.01
			^{235}U	0.23	<0.01
			^{238}U	2	<0.01
			^{238}Pu	<0.04	<0.01
			^{239}Pu	<0.03	<0.01

Table 9. (continued)

Sampling Location	Date	Sample Type[a]	Radio-nuclide	Radioactivity Conc. (10^{-9} µCi/ml)	% of Conc. Guide[b]
NTS Well C-1	7/08	23	^{3}H	51	<0.01
			^{89}Sr	<1	<0.01
			^{90}Sr	<1	<0.01
NTS Well UE 5c	1/14[c]	23	^{3}H	<8	<0.01
			^{89}Sr	<1	<0.01
			^{90}Sr	<0.9	<0.01
			^{226}Ra	0.36	0.09
			^{234}U	3.4	<0.01
			^{235}U	0.056	<0.01
			^{238}U	1.6	<0.01
			^{238}Pu	<0.03	<0.01
			^{239}Pu	<0.01	<0.01
NTS Well 5B	1/15	23	^{3}H	<8	<0.01
			^{89}Sr	<3	<0.01
			^{90}Sr	<2	<0.01
			^{226}Ra	0.10	0.03
			^{234}U	2.7	<0.01
			^{235}U	0.091	<0.01
			^{238}U	1.8	<0.01
			^{238}Pu	<0.06	<0.01
			^{239}Pu	<0.04	<0.01
NTS Well 5B	7/09	23	^{3}H	10	<0.01
			^{89}Sr	<1	<0.01
			^{90}Sr	<0.9	<0.01
NTS Watertown No. 3	1/14	23	^{3}H	<8	<0.01
			^{89}Sr	<1	<0.01
			^{90}Sr	<0.9	<0.01
			^{234}U	1.4	<0.01
			^{235}U	0.024	<0.01
			^{238}U	0.52	<0.01
			^{238}Pu	<0.04	<0.01
			^{239}Pu	<0.04	<0.01

Table 9. (continued)

Sampling Location	Date	Sample Type[a]	Radionuclide	Radioactivity Conc. (10^{-9} µCi/ml)	% of Conc.[b] Guide
NTS Watertown No. 3	7/08	23	^{3}H	<7	<0.01
Ash Meadows, NV Crystal Pool	1/22	27	^{3}H	<8	<0.01
			^{89}Sr	<2	<0.07
			^{90}Sr	<1	<0.3
			^{226}Ra	0.22	0.7
			^{234}U	11	0.04
			^{235}U	0.23	<0.01
			^{238}U	4.5	0.01
			^{238}Pu	<0.04	<0.01
			^{239}Pu	<0.04	<0.01
Ash Meadows, NV Crystal Pool	7/15	27	^{3}H	<8	<0.01
			^{89}Sr	<1	<0.03
			^{90}Sr	<0.9	<0.3
Ash Meadows, NV Well 17S/50E-14CAC	1/22	23	^{3}H	<8	<0.01
			^{89}Sr	<2	<0.07
			^{90}Sr	<2	<0.4
			^{226}Ra	0.089	0.3
			^{234}U	2.4	<0.01
			^{235}U	0.033	<0.01
			^{238}U	0.89	<0.01
			^{238}Pu	<0.03	<0.01
			^{239}Pu	<0.04	<0.01
Ash Meadows, NV Well 17S/50E-14CAC	7/15	23	^{3}H	11	<0.01
			^{226}Ra	0.47	2
Ash Meadows, NV Fairbanks Springs	1/22	27	^{3}H	<9	<0.01
			^{89}Sr	<2	<0.07
			^{90}Sr	<1	<0.3
			^{226}Ra	0.44	2
			^{234}U	2.2	<0.01
			^{235}U	0.029	<0.01
			^{238}U	0.89	<0.01
			^{238}Pu	<0.03	<0.01
			^{239}Pu	<0.03	<0.01

Table 9. (continued)

Sampling Location	Date	Sample Type[a]	Radionuclide	Radioactivity Conc. (10^{-9} µCi/ml)	% of Conc. Guide[b]
Ash Meadows, NV Fairbanks Springs	7/15	27	^{3}H	<8	<0.01
Beatty, NV City Supply	1/21	23	^{3}H	17	<0.01
			^{89}Sr	<2	<0.07
			^{90}Sr	<1	<0.3
			^{226}Ra	0.16	0.5
			^{234}U	8.2	0.3
			^{235}U	0.18	<0.01
			^{238}U	2.6	<0.01
			^{238}Pu	<0.04	<0.01
			^{239}Pu	<0.02	<0.01
Beatty, NV City Supply	7/15	23	^{3}H	<7	<0.01
			^{89}Sr	<2	<0.05
			^{90}Sr	<0.8	<0.3
			^{226}Ra	0.13	0.43
Beatty, NV Nuclear Engineering Co.	1/21	23	^{3}H	<7	<0.01
			^{89}Sr	<2	<0.07
			^{90}Sr	<1	<0.3
			^{226}Ra	0.078	0.3
			^{234}U	6.1	0.02
			^{235}U	0.95	<0.01
			^{238}U	2.3	<0.01
			^{238}Pu	<0.04	<0.01
			^{239}Pu	<0.03	<0.01
Beatty, NV Nuclear Engineering Co.	7/14	23	^{3}H	<8	<0.01
			^{226}Ra	0.033	0.1
Indian Springs, NV USAF No. 1	1/23	23	^{3}H	11	<0.01
			^{89}Sr	<7	<0.2
			^{90}Sr	<1	<0.3
			^{226}Ra	0.22	0.7
			^{234}U	4.2	0.01
			^{235}U	0.034	<0.01
			^{238}U	0.75	<0.01
			^{238}Pu	<0.04	<0.01
			^{239}Pu	<0.04	<0.01

Table 9. (continued)

Sampling Location	Date	Sample Type[a]	Radio-nuclide	Radioactivity Conc. (10^{-9} µCi/ml)	% of Conc. Guide[b]
Indian Springs, NV USAF No. 1	7/14	23	^{3}H	35	<0.01
			^{226}Ra	0.23	0.8
Indian Springs, NV Sewer Co. Inc. Well No. 1	1/23	23	^{3}H	<7	<0.01
			^{89}Sr	<2	<0.07
			^{90}Sr	<1	<0.3
			^{226}Ra	0.095	0.32
			^{234}U	3.4	0.01
			^{235}U	0.021	<0.01
			^{238}U	0.73	<0.01
			^{238}Pu	<0.04	<0.01
			^{239}Pu	<0.02	<0.01
Indian Springs, NV Sewer Co. Inc. Well No. 1	7/14	23	^{3}H	<40	<0.01
			^{226}Ra	0.072	0.2
Lathrop Wells, NV City Supply	1/22	23	^{3}H	<8	<0.01
			^{89}Sr	<1	<0.03
			^{90}Sr	<1	<0.3
			^{234}U	1.1	<0.01
			^{235}U	<0.01	<0.01
			^{238}U	0.44	<0.01
			^{238}Pu	<0.03	<0.01
			^{239}Pu	<0.03	<0.01
Lathrop Wells, NV City Supply	7/14	23	^{3}H	<7	<0.01
			^{226}Ra	4.6	15
Springdale, NV Goss Springs	1/21	27	^{3}H	<8	<0.01
			^{89}Sr	<2	<0.07
			^{90}Sr	<1	<0.3
			^{226}Ra	0.15	0.5
			^{234}U	3.6	0.01
			^{235}U	0.057	<0.01
			^{238}U	1.1	<0.01
			^{238}Pu	<0.03	<0.01
			^{239}Pu	<0.03	<0.01

Table 9. (continued)

Sampling Location	Date	Sample Type[a]	Radionuclide	Radioactivity Conc. (10^{-9} µCi/ml)	% of Conc. Guide[b]
Springdale, NV Goss Springs	7/14	27	^{3}H	<7	<0.01
Springdale, NV Road D Windmill	1/21	23	^{3}H	<6	<0.01
			^{89}Sr	<2	<0.07
			^{90}Sr	<2	<0.4
			^{234}U	1.9	<0.01
			^{235}U	0.062	<0.01
			^{238}U	1.1	<0.01
			^{238}Pu	<0.04	<0.01
			^{239}Pu	<0.03	<0.01
Springdale, NV Road D Windmill	7/14	23	^{3}H	<7	<0.01
Shoshone, CA Shoshone Spring	1/22	27	^{3}H	<8	<0.01
			^{89}Sr	<1	<0.03
			^{90}Sr	<1	<0.3
			^{226}Ra	0.17	0.6
			^{234}U	3.3	0.01
			^{235}U	0.041	<0.01
			^{238}U	1.2	<0.01
			^{238}Pu	<0.05	<0.01
			^{239}Pu	<0.06	<0.01
Shoshone, CA Shoshone Spring	7/15	27	^{3}H	<8	<0.01
			^{89}Sr	<1	<0.03
			^{90}Sr	<0.9	<0.3

[a] 23 - Well
27 - Spring

[b] All on-NTS percentages are for radiation workers. All off-NTS percentages are for an individual in an uncontrolled area.

[c] Only one sample was collected during the year due to an inoperative pump.

Table 10. 1975 Summary of Analytical Results for the NTS Annual Long Term Hydrological Monitoring Program

Sampling Location	Date	Sample Type[a]	Radio-nuclide	Radioactivity Conc. (10^{-9} µCi/ml)	% of Conc. Guide
Hiko, NV Crystal Springs	8/25	27	^{3}H	300	0.01
			^{89}Sr	<2	<0.06
			^{90}Sr	1.1	0.4
			^{226}Ra	0.79	2.6
			^{234}U	4.3	0.01
			^{235}U	0.059	<0.01
			^{238}U	1.3	<0.01
			^{238}Pu	<0.03	<0.01
			^{239}Pu	<0.04	<0.01
Alamo, NV City Supply	8/25	23	^{3}H	17	<0.01
			^{89}Sr	<2	<0.05
			^{90}Sr	<1	<0.3
			^{234}U	3.6	0.01
			^{235}U	0.016	<0.01
			^{238}U	1.8	<0.01
			^{238}Pu	<0.03	<0.01
			^{239}Pu	<0.02	<0.01
Warm Springs, NV Twin Springs Ranch	8/25	27	^{3}H	<8	<0.01
			^{89}Sr	<2	<0.05
			^{90}Sr	<0.9	<0.3
			^{226}Ra	0.22	0.7
			^{234}U	4.6	0.02
			^{235}U	0.087	<0.01
			^{238}U	1.8	<0.01
			^{238}Pu	<0.04	<0.01
			^{239}Pu	<0.03	<0.01
Diablo, NV Highway Maint. Station	8/25	23	^{3}H	10	<0.01
			^{89}Sr	<2	<0.05
			^{90}Sr	<1	<0.3
			^{234}U	1.7	<0.01
			^{235}U	0.034	<0.01
			^{238}U	0.78	<0.01
			^{238}Pu	<0.04	<0.01
			^{239}Pu	<0.04	<0.01

Table 10. (continued)

Sampling Location	Date	Sample Type[a]	Radionuclide	Radioactivity Conc. (10^{-9} µCi/ml)	% of Conc. Guide
Nyala, NV	9/03	23	^{3}H	22	<0.01
Sharp Ranch			^{89}Sr	<1	<0.04
			^{90}Sr	<2	<0.7
			^{234}U	1.9	<0.01
			^{235}U	0.02	<0.01
			^{238}U	0.6	<0.01
			^{238}Pu	<0.03	<0.01
			^{239}Pu	<0.03	<0.01
Adaven, NV	8/26	27	^{3}H	130	<0.01
Adaven Spring			^{89}Sr	<2	<0.06
			^{90}Sr	<1	<0.4
			^{226}Ra	<0.05	<0.2
			^{234}U	3.3	0.01
			^{235}U	0.087	<0.01
			^{238}U	1.2	<0.01
			^{238}Pu	<0.03	<0.01
			^{239}Pu	<0.02	<0.01
Pahrump, NV	8/27	23	^{3}H	16	<0.01
Calvada Well No. 3			^{89}Sr	<2	<0.05
			^{90}Sr	<1	<0.3
			^{226}Ra	0.31	1.0
			^{234}U	6.9	0.02
			^{235}U	0.15	<0.01
			^{238}U	2.2	<0.01
			^{238}Pu	<0.03	<0.01
			^{239}Pu	<0.02	<0.01
Tonopah, NV	8/27	23	^{3}H	10	<0.01
City Supply			^{89}Sr	<2	<0.06
			^{90}Sr	<1	<0.4
			^{234}U	2.9	<0.01
			^{235}U	0.088	<0.01
			^{238}U	1.1	<0.01
			^{238}Pu	<0.05	<0.01
			^{239}Pu	<0.03	<0.01

Table 10. (continued)

Sampling Location	Date	Sample Type[a]	Radio-nuclide	Radioactivity Conc. (10^{-9} µCi/ml)	% of Conc. Guide
Clark Station, NV	8/27	23	^{3}H	12	<0.01
Tonopah Test Range			^{89}Sr	<2	<0.06
Well No. 6			^{90}Sr	<1	<0.4
			^{234}U	3.4	0.01
			^{235}U	0.062	<0.01
			^{238}U	1.9	<0.01
			^{238}Pu	<0.03	<0.01
			^{239}Pu	<0.02	<0.01
Las Vegas, NV	8/27	23	^{3}H	16	<0.01
Well No. 28			^{89}Sr	<2	<0.07
			^{90}Sr	<2	<0.5
			^{234}U	2.1	<0.01
			^{235}U	0.032	<0.01
			^{238}U	0.61	<0.01
			^{238}Pu	<0.03	<0.01
			^{239}Pu	<0.04	<0.01

[a] 23 - Well
27 - Spring

Table 11. 1975 Summary of Analytical Results

for the Off-NTS Long-Term Hydrological Monitoring Program

Sampling Location	Date	Sample Type[c]	Depth (Metres[a])	Radio-nuclide	Radioactivity Conc. (10^{-9} µCi/ml)	% of Conc. Guide
				PROJECT GNOME		
Malaga, NM USGS Well No. 1	3/23	23	161	^{3}H	<8	<0.01
				^{89}Sr	<2	<0.07
				^{90}Sr	1.3	0.4
				^{226}Ra	6	20
				^{234}U	5.5	0.02
				^{235}U	0.055	<0.01
				^{238}U	1.8	<0.01
				^{238}Pu	<0.6	<0.01
				^{239}Pu	<2	<0.04
Malaga, NM USGS Well No. 4	3/23	23	148	^{3}H	960,000	30
				^{89}Sr	<1,800	<60
				^{90}Sr	11,000	4000
				^{226}Ra	0.13	0.4
				^{234}U	2.9	<0.01
				^{235}U	0.055	<0.01
				^{238}U	0.74	<0.01
				^{238}Pu	<0.6	<0.01
				^{239}Pu	<2	<0.05
Malaga, NM USGS Well No. 8	3/23	23	144	^{3}H	1,200,000	40
				^{89}Sr	<900	<30
				^{90}Sr	11,000	4000
				^{137}Cs	<20	<0.1
				^{226}Ra	1.6	5
				^{234}U	2.7	<0.01
				^{235}U	<0.1	<0.01
				^{238}U	0.88	<0.01
				^{238}Pu	<0.05	<0.01
				^{239}Pu	0.047	<0.01
Malaga, NM PHS Well No. 6	3/22	23		^{3}H	<200	<0.01
				^{89}Sr	<2	0.05
				^{90}Sr	<0.9	<0.3
				^{234}U	1.2	<0.01
				^{235}U	0.045	<0.01
				^{238}U	0.99	<0.01
				^{238}Pu	<0.04	<0.01
				^{239}Pu	0.024	<0.01

Table 11. (continued)

Sampling Location	Date	Sample Type[c]	Depth (Metres[a])	Radio-nuclide	Radioactivity Conc. (10^{-9} µCi/ml)	% of Conc. Guide
Malaga, NM PHS Well No. 8	3/22	23		^{3}H	<8	<0.01
				^{89}Sr	<3	<0.09
				^{90}Sr	<0.9	<0.3
				^{234}U	3.9	0.01
				^{235}U	0.092	<0.01
				^{238}U	1.8	<0.01
				^{238}Pu	<0.5	<0.01
				^{239}Pu	<0.9	<0.02
Malaga, NM PHS Well No. 9	3/22	23		^{3}H	<8	<0.01
				^{89}Sr	<3	<0.1
				^{90}Sr	<0.9	<0.3
				^{234}U	1.4	<0.01
				^{235}U	0.046	<0.01
				^{238}U	0.62	<0.01
				^{238}Pu	<0.03	<0.01
				^{239}Pu	<0.04	<0.01
Malaga, NM PHS Well No. 10	3/22	23		^{3}H	<8	<0.01
				^{89}Sr	<2	<0.07
				^{90}Sr	<0.7	<0.2
				^{234}U	9.6	0.03
				^{235}U	0.079	<0.01
				^{238}U	1.5	<0.01
				^{238}Pu	<0.6	<0.01
				^{239}Pu	<1	<0.02
Malaga, NM[b] City Water	3/21	23		^{3}H	<7	<0.01
				^{89}Sr	<2	<0.06
				^{90}Sr	<0.9	<0.3
				^{234}U	0.04	<0.01
				^{235}U	<0.01	<0.01
				^{238}U	0.056	<0.01
				^{238}Pu	<0.04	<0.01
				^{239}Pu	<0.04	<0.01

Table 11. (continued)

Sampling Location	Date	Sample Type[c]	Depth (Metres[a])	Radio-nuclide	Radioactivity Conc. (10^{-9} µCi/ml)	% of Conc. Guide
Malaga, NM	3/21	23		^{3}H	<9	<0.01
Pecos River				^{89}Sr	<2	<0.05
Pumping Station				^{90}Sr	<0.8	<0.3
Well No. 1				^{234}U	4.2	0.01
				^{235}U	0.054	<0.01
				^{238}U	1.3	<0.01
				^{238}Pu	<0.04	<0.01
				^{239}Pu	<0.05	<0.01
Loving, NM	3/21	23		^{3}H	<8	<0.01
City Well No. 2				^{89}Sr	<2	<0.05
				^{90}Sr	<0.9	<0.3
				^{234}U	1.8	<0.01
				^{235}U	0.032	<0.01
				^{238}U	0.63	<0.01
				^{238}Pu	<0.05	<0.01
				^{239}Pu	<0.03	<0.01
Carlsbad, NM	3/21	23		^{3}H	<8	<0.01
City Well No. 7				^{89}Sr	<1	<0.05
				^{90}Sr	<0.7	<0.2
				^{234}U	0.65	<0.01
				^{235}U	<0.01	<0.01
				^{238}U	0.3	<0.01
				^{238}Pu	<0.04	<0.01
				^{239}Pu	<0.03	<0.01
PROJECT SHOAL						
Frenchman, NV	2/21	23		^{3}H	<10	<0.01
Well H-3				^{89}Sr	<6	<0.2
				^{90}Sr	<4	<2
				^{234}U	0.8	<0.01
				^{235}U	0.022	<0.01
				^{238}U	0.66	<0.01
				^{238}Pu	<0.03	<0.01
				^{239}Pu	<0.04	<0.01

Table 11. (continued)

Sampling Location	Date	Sample Type[c]	Radionuclide	Radioactivity Conc. (10^{-9} µCi/ml)	% of Conc. Guide
Frenchman, NV Flowing Well	2/20	23	^{3}H	<9	<0.01
			^{89}Sr	<5	<0.2
			^{90}Sr	<4	<1
			^{226}Ra	0.26	0.9
			^{234}U	0.36	<0.01
			^{235}U	<0.02	<0.01
			^{238}U	0.23	<0.01
			^{238}Pu	<0.2	<0.01
			^{239}Pu	<0.09	<0.01
Frenchman, NV Hunts Station	2/20	23	^{3}H	<8	<0.01
			^{89}Sr	<6	<0.2
			^{90}Sr	<4	<1
			^{234}U	0.73	<0.01
			^{235}U	0.035	<0.01
			^{238}U	0.41	<0.01
			^{238}Pu	<0.05	<0.01
			^{239}Pu	<0.02	<0.01
Frenchman, NV Frenchman Station	2/19	23	^{3}H	<7	<0.01
			^{89}Sr	<6	<0.2
			^{90}Sr	<4	<1
			^{226}Ra	0.17	0.6
			^{234}U	23	0.08
			^{235}U	0.55	<0.01
			^{238}U	11	0.03
			^{238}Pu	<0.05	<0.01
			^{239}Pu	<0.05	<0.01
Frenchman, NV Well HS-1	2/19	23	^{3}H	<7	<0.01
			^{89}Sr	<6	<0.2
			^{90}Sr	<4	<2
			^{226}Ra	0.067	0.2
			^{234}U	3.3	0.01
			^{235}U	0.098	<0.01
			^{238}U	2.2	<0.01
			^{238}Pu	<0.04	<0.01
			^{239}Pu	<0.02	<0.01

Table 11. (continued)

Sampling Location	Date	Sample Type[c]	Depth (Metres[a])	Radio-nuclide	Radioactivity Conc. (10^{-9} µCi/ml)	% of Conc. Guide
			PROJECT DRIBBLE			
Baxterville, MS City Supply	7/18	23		^{3}H	38	<0.01
				^{89}Sr	<1	<0.05
				^{90}Sr	<0.9	<0.3
				^{234}U	0.034	<0.01
				^{235}U	<0.01	<0.01
				^{238}U	<0.03	<0.01
				^{238}Pu	<0.03	<0.01
				^{239}Pu	<0.02	<0.01
	10/17	23		^{3}H	93	<0.01
Baxterville, MS Lower Little Creek	7/21	22		^{3}H	110	<0.01
				^{89}Sr	<2	<0.06
				^{90}Sr	<1	<0.3
				^{234}U	0.032	<0.01
				^{235}U	<0.009	<0.01
				^{238}U	0.03	<0.01
				^{238}Pu	<0.03	<0.01
				^{239}Pu	<0.04	<0.01
	10/19	22		^{3}H	130	<0.01
Baxterville, MS Well HT-1	7/03	23	399	^{3}H	<6	<0.01
	7/20	23	358	^{3}H	8.6	<0.01
				^{89}Sr	<2	<0.05
				^{90}Sr	<1	<0.4
				^{226}Ra	15	0.5
				^{234}U	17	0.06
				^{235}U	1.1	<0.01
				^{238}U	29	0.07
				^{238}Pu	<0.03	<0.01
				^{239}Pu	0.048	<0.01
	10/15	23	389	^{3}H	74	<0.01

Table 11. (continued)

Sampling Location	Date	Sample Type[c]	Depth (Metres[a])	Radio-nuclide	Radioactivity Conc. (10^{-9} µCi/ml)	% of Conc. Guide
Baxterville, MS Well HT-2c	7/03	23	108	^{3}H	15	<0.01
	7/20	23	108	^{3}H	29	<0.01
				^{89}Sr	<2	<0.05
				^{90}Sr	<1	<0.3
				^{234}U	0.045	<0.01
				^{235}U	<0.009	<0.01
				^{238}U	0.025	<0.01
				^{238}Pu	<0.03	<0.01
				^{239}Pu	<0.02	<0.01
	10/18	23	108	^{3}H	35	<0.01
Baxterville, MS Well HT-4	7/02	23	122	^{3}H	16	<0.01
	7/20	23	122	^{3}H	9.3	<0.01
				^{89}Sr	<2	<0.05
				^{90}Sr	<1	<0.3
				^{234}U	0.032	<0.01
				^{235}U	<0.01	<0.01
				^{238}U	<0.01	<0.01
				^{238}Pu	<0.04	<0.01
				^{239}Pu	<0.02	<0.01
	10/18	23	122	^{3}H	20	<0.01
Baxterville, MS Well HT-5	7/02	23	183	^{3}H	8.3	<0.01
	7/20	23	183	^{3}H	24	<0.01
				^{89}Sr	<2	<0.06
				^{90}Sr	<1	<0.4
				^{234}U	0.027	<0.01
				^{235}U	0.02	<0.01
				^{238}U	<0.03	<0.01
				^{238}Pu	<0.04	<0.01
				^{239}Pu	<0.03	<0.01
	10/18	23	183	^{3}H	12	<0.01

Table 11. (continued)

Sampling Location	Date	Sample Type[c]	Depth (Metres[a])	Radio-nuclide	Radioactivity Conc. (10^{-9} µCi/ml)	% of Conc. Guide
Baxterville, MS Well E-7	7/03	23	282	^{3}H	<7	<0.01
	7/20	23	282	^{3}H	<8	<0.01
				^{89}Sr	<1	<0.04
				^{90}Sr	<0.9	<0.3
				^{234}U	<0.02	<0.01
				^{235}U	<0.01	<0.01
				^{238}U	0.017	<0.01
				^{238}Pu	<0.03	<0.01
				^{239}Pu	<0.02	<0.01
	10/18	23	282	^{3}H	<7	<0.01
Baxterville, MS Well Ascot No. 2	7/19	23	638	^{3}H	18	<0.01
				^{89}Sr	<2	<0.05
				^{90}Sr	<0.8	<0.3
				^{234}U	0.026	<0.01
				^{235}U	<0.01	<0.01
				^{238}U	0.017	<0.01
				^{238}Pu	<0.03	<0.01
				^{239}Pu	<0.02	<0.01
	10/15	23	651	^{3}H	20	<0.01
				^{89}Sr	<3	<0.1
				^{90}Sr	<2	<0.5
Baxterville, MS Half Moon Creek	7/01	22		^{3}H	90	<0.01
	7/19	22		^{3}H	67	0.01
				^{89}Sr	<2	<0.05
				^{90}Sr	<1	<0.3
				^{234}U	<0.02	<0.01
				^{235}U	<0.01	<0.01
				^{238}U	<0.02	<0.01
				^{238}Pu	<0.04	<0.01
				^{239}Pu	<0.04	<0.01
	10/19	22		^{3}H	64	<0.01

Table 11. (continued)

Sampling Location	Date	Sample Type[c]	Depth (Metres[a])	Radio-nuclide	Radioactivity Conc. (10^{-9} µCi/ml)	% of Conc. Guide
Baxterville, MS Half Moon Creek Overflow	7/02	22		^{3}H	480	0.02
	7/19	22		^{3}H	2200	0.07
				^{89}Sr	<2	<0.05
				^{90}Sr	<2	<0.4
				^{234}U	<0.02	<0.01
				^{235}U	<0.01	<0.01
				^{238}U	<0.02	<0.01
				^{238}Pu	<0.04	<0.01
				^{239}Pu	<0.02	<0.01
	10/19	22		^{3}H	380	0.01
Baxterville, MS T. Speights Residence	7/01	23		^{3}H	110	<0.01
	7/18	23		^{3}H	48	<0.01
				^{89}Sr	<2	<0.06
				^{90}Sr	<1	<0.4
				^{234}U	0.048	<0.01
				^{235}U	<0.01	<0.01
				^{238}U	0.036	<0.01
				^{238}Pu	<0.02	<0.01
				^{239}Pu	<0.03	<0.01
	10/20	23		^{3}H	96	<0.01
Baxterville, MS R. L. Anderson Residence	7/01	23		^{3}H	58	<0.01
	7/21	23		^{3}H	93	<0.01
				^{89}Sr	<2	<0.06
				^{90}Sr	<1	<0.4
				^{226}Ra	0.53	2
				^{234}U	0.044	<0.01
				^{235}U	<0.01	<0.01
				^{238}U	<0.01	<0.01
				^{238}Pu	<0.03	<0.01
				^{239}Pu	<0.02	<0.01
	10/20	23		^{3}H	74	<0.01

Table 11. (continued)

Sampling Location	Date	Sample Type[c]	Depth (Metres[a])	Radio-nuclide	Radioactivity Conc. (10^{-9} µCi/ml)	% of Conc. Guide
Baxterville, MS Mark Lowe Residence	7/22	23		^{3}H	220	<0.01
				^{89}Sr	<2	<0.05
				^{90}Sr	<0.8	<0.3
				^{234}U	<0.01	<0.01
				^{235}U	<0.007	<0.01
				^{238}U	0.012	<0.01
				^{238}Pu	<0.04	<0.01
				^{239}Pu	<0.03	<0.01
	10/17	23		^{3}H	160	<0.01
Baxterville, MS R. Ready Residence	7/22	23		^{3}H	64	<0.01
				^{89}Sr	<2	<0.05
				^{90}Sr	<1	<0.3
				^{234}U	0.034	<0.01
				^{235}U	<0.02	<0.01
				^{238}U	<0.03	<0.01
				^{238}Pu	<0.01	<0.01
				^{239}Pu	<0.01	<0.01
	10/20	23		^{3}H	64	<0.01
Baxterville, MS W. Daniels, Jr. Residence	7/01	23		^{3}H	130	<0.01
	7/22	23		^{3}H	80	<0.01
				^{89}Sr	<2	<0.06
				^{90}Sr	<1	<0.3
				^{234}U	0.029	<0.01
				^{235}U	<0.01	<0.01
				^{238}U	0.031	<0.01
				^{238}Pu	<0.04	<0.01
				^{239}Pu	<0.03	<0.01
	10/17	23		^{3}H	80	<0.01
Lumberton, MS City Supply Well No. 2	7/21	23		^{3}H	<7	<0.01
				^{89}Sr	<2	<0.06
				^{90}Sr	<1	<0.4
				^{234}U	<0.02	<0.01
				^{235}U	<0.02	<0.01
				^{238}U	<0.02	<0.01
				^{238}Pu	<0.04	<0.01
				^{239}Pu	<0.03	<0.01

Table 11. (continued)

Sampling Location	Date	Sample Type[c]	Depth (Metres[a])	Radio-nuclide	Radioactivity Conc. (10^{-9} µCi/ml)	% of Conc. Guide
Lumberton, MS City Supply Well No. 2 (continued)	10/20	23		^{3}H	<6	<0.01
Purvis, MS City Supply	7/18	23		^{3}H	<8	<0.01
				^{89}Sr	<1	<0.04
				^{90}Sr	<0.9	<0.3
				^{234}U	<0.02	<0.01
				^{235}U	<0.008	<0.01
				^{238}U	<0.01	<0.01
				^{238}Pu	<0.03	<0.01
				^{239}Pu	<0.02	<0.01
	10/17	23		^{3}H	14	<0.01
Columbia, MS City Supply	7/22	23		^{3}H	Lost Sample	
				^{89}Sr	<1	<0.05
				^{90}Sr	<0.9	<0.3
				^{234}U	0.027	<0.01
				^{235}U	<0.007	<0.01
				^{238}U	0.029	<0.01
				^{238}Pu	<0.04	<0.01
				^{239}Pu	<0.04	<0.01
	10/17	23		^{3}H	35	<0.01
Lumberton, MS North Lumberton City Supply	7/21	23		^{3}H	<7	<0.01
				^{89}Sr	<2	<0.05
				^{90}Sr	<1	<0.3
				^{234}U	<0.02	<0.01
				^{235}U	<0.01	<0.01
				^{238}U	0.018	<0.01
				^{238}Pu	<0.03	<0.01
				^{239}Pu	<0.02	<0.01
	10/17	23		^{3}H	<7	<0.01
Baxterville, MS Pond W of GZ	7/02	21		^{3}H	Lost Sample	

Table 11. (continued)

Sampling Location	Date	Sample Type[c]	Depth (Metres[a])	Radio-nuclide	Radioactivity Conc. (10^{-9} µCi/ml)	% of Conc. Guide
Baxterville, MS Pond W of GZ (continued)	7/22	21		^{3}H	120	<0.01
				^{89}Sr	<1	<0.05
				^{90}Sr	<0.8	<0.3
				^{234}U	0.023	<0.01
				^{235}U	<0.01	<0.01
				^{238}U	0.019	<0.01
				^{238}Pu	<0.04	<0.01
				^{239}Pu	<0.03	<0.01
	10/19	21		^{3}H	61	<0.01
PROJECT GASBUGGY						
Gobernador, NM Arnold Ranch	5/25	27		^{3}H	<10	<0.01
				^{89}Sr	<2	<0.07
				^{90}Sr	<0.9	<0.3
				^{234}U	2.3	<0.01
				^{235}U	0.052	<0.01
				^{238}U	1.0	<0.01
				^{238}Pu	<0.2	<0.01
				^{239}Pu	<0.1	<0.01
Gobernador, NM Lower Burro Canyon	5/25	23		^{3}H	<8	<0.01
				^{89}Sr	<2	<0.07
				^{90}Sr	<1	<0.3
				^{234}U	0.12	<0.01
				^{235}U	<0.01	<0.01
				^{238}U	<0.01	<0.01
				^{238}Pu	<0.1	<0.01
				^{239}Pu	<0.06	<0.01
Gobernador, NM Fred Bixler Ranch	5/24	23		^{3}H	13	<0.01
				^{89}Sr	<2	<0.06
				^{90}Sr	<0.9	<0.3
				^{234}U	0.27	<0.01
				^{235}U	<0.02	<0.01
				^{238}U	0.055	<0.01
				^{238}Pu	<0.04	<0.01
				^{239}Pu	<0.03	<0.01

Table 11. (continued)

Sampling Location	Date	Sample Type[c]	Depth (Metres[a])	Radio-nuclide	Radioactivity Conc. (10^{-9} µCi/ml)	% of Conc. Guide
Blanco, NM San Juan River	5/26	22		^{3}H	510	0.02
				^{89}Sr	<2	<0.08
				^{90}Sr	1.9	0.6
				^{234}U	0.50	0.02
				^{235}U	0.018	<0.01
				^{238}U	0.30	<0.01
				^{238}Pu	<0.03	<0.01
				^{239}Pu	<0.04	<0.01
Gobernador, NM Cave Springs	5/25	27		^{3}H	9.3	<0.01
				^{89}Sr	<1	<0.04
				^{90}Sr	<0.9	<0.3
				^{226}Ra	0.16	0.5
				^{234}U	3.1	0.01
				^{235}U	0.13	<0.01
				^{238}U	2.0	<0.01
				^{238}Pu	<0.03	<0.01
				^{239}Pu	<0.05	<0.01
Gobernador, NM Windmill No. 2	5/24	23		^{3}H	8	<0.01
				^{89}Sr	<2	<0.06
				^{90}Sr	<0.9	<0.3
				^{234}U	0.38	<0.01
				^{235}U	<0.009	<0.01
				^{238}U	0.14	<0.01
				^{238}Pu	<0.2	<0.01
				^{239}Pu	<0.2	<0.01
Gobernador, NM Bubbling Springs	5/24	27		^{3}H	<10	<0.01
				^{89}Sr	<2	<0.06
				^{90}Sr	<0.9	<0.3
				^{226}Ra	0.75	0.3
				^{234}U	3.1	0.01
				^{235}U	0.065	<0.01
				^{238}U	1.6	<0.01
				^{238}Pu	<0.03	<0.01
				^{239}Pu	<0.02	<0.01

Table 11. (continued)

Sampling Location	Date	Sample Type[c]	Depth (Metres[a])	Radio-nuclide	Radioactivity Conc. (10^{-9} µCi/ml)	% of Conc. Guide
Dulce, NM City Water	5/24	21		^{3}H	260	<0.01
				^{89}Sr	<1	<0.04
				^{90}Sr	<0.8	<0.3
				^{234}U	0.28	<0.01
				^{235}U	<0.01	<0.01
				^{238}U	0.15	<0.01
				^{238}Pu	<0.03	<0.01
				^{239}Pu	<0.02	<0.01
Dulce, NM La Jara Lake	5/24	21		^{3}H	280	<0.01
				^{89}Sr	<2	<0.06
				^{90}Sr	<0.9	<0.3
				^{234}U	0.91	<0.01
				^{235}U	0.03	<0.01
				^{238}U	0.59	<0.01
				^{238}Pu	<0.09	<0.01
				^{239}Pu	<0.05	<0.01
Gobernador, NM EPNG Well 10-36	5/26	23	1097	^{3}H	13	<0.01
				^{89}Sr	<0.9	<0.03
				^{90}Sr	<0.8	<0.3
				^{226}Ra	0.25	0.8
				^{234}U	0.042	<0.01
				^{235}U	<0.007	<0.01
				^{238}U	0.027	<0.01
				^{238}Pu	<2	<0.05
				^{239}Pu	<6	<0.1
PROJECT RULISON						
Rulison, CO Lee L. Hayward Ranch	5/21	23		^{3}H	350	0.01
				^{89}Sr	<2	<0.06
				^{90}Sr	<0.8	<0.3
				^{226}Ra	<0.05	<0.2
				^{234}U	8.1	0.03
				^{235}U	0.14	<0.01
				^{238}U	3.9	<0.01
				^{238}Pu	<0.04	<0.01
				^{239}Pu	<0.03	<0.01

Table 11. (continued)

Sampling Location	Date	Sample Type[c]	Depth (Metres[a])	Radio-nuclide	Radioactivity Conc. (10^{-9} µCi/ml)	% of Conc. Guide
Rulison, CO	5/22	23		^{3}H	380	0.01
Glen Schwab				^{89}Sr	<2	<0.08
Ranch				^{90}Sr	<1	<0.4
				^{226}Ra	0.13	0.4
				^{234}U	12	0.04
				^{235}U	0.25	<0.01
				^{238}U	6	0.02
				^{238}Pu	<0.03	<0.01
				^{239}Pu	<0.02	<0.01
Grand Valley, CO	5/21	23		^{3}H	510	0.02
Albert Gardner				^{89}Sr	<2	<0.07
Ranch				^{90}Sr	<1	<0.3
				^{234}U	2.4	<0.01
				^{235}U	0.056	<0.01
				^{238}U	1.1	<0.01
				^{238}Pu	<0.03	<0.01
				^{239}Pu	<0.02	<0.01
Grand Valley, CO	5/22	27		^{3}H	130	<0.01
City Water				^{89}Sr	<2	<0.07
Supply				^{90}Sr	<1	<0.3
				^{234}U	2.5	<0.01
				^{235}U	0.059	<0.01
				^{238}U	0.92	<0.01
				^{238}Pu	<0.03	<0.01
				^{239}Pu	<0.04	<0.01
Grand Valley, CO	5/21	27		^{3}H	480	0.02
Spring 300 Yds.				^{89}Sr	<2	<0.05
NW of GZ				^{90}Sr	<0.9	<0.3
				^{234}U	1.3	<0.01
				^{235}U	0.037	<0.01
				^{238}U	0.66	<0.01
				^{238}Pu	<0.03	<0.01
				^{239}Pu	<0.04	<0.01

Table 11. (continued)

Sampling Location	Date	Sample Type[c]	Depth (Metres[a])	Radio-nuclide	Radioactivity Conc. (10^{-9} µCi/ml)	% of Conc. Guide
Rulison, CO Felix Sefcovic Ranch	5/22	23		^{3}H	580	0.02
				^{89}Sr	<2	<0.06
				^{90}Sr	<0.8	<0.3
				^{234}U	0.49	<0.01
				^{235}U	0.017	<0.01
				^{238}U	0.26	<0.01
				^{238}Pu	<0.04	<0.01
				^{239}Pu	<0.03	<0.01
Anvil Points, CO Bernklau Ranch	5/21	27		^{3}H	510	0.02
				^{89}Sr	<1	<0.04
				^{90}Sr	<0.8	<0.3
				^{234}U	2.4	<0.01
				^{235}U	0.039	<0.01
				^{238}U	1.0	<0.01
				^{238}Pu	<0.03	<0.01
				^{239}Pu	<0.02	<0.01
Grand Valley, CO Battlement Creek	5/21	22		^{3}H	300	0.01
				^{89}Sr	<2	<0.05
				^{90}Sr	<1	<0.4
				^{234}U	0.36	<0.01
				^{235}U	0.024	<0.01
				^{238}U	0.18	<0.01
				^{238}Pu	<0.02	<0.01
				^{239}Pu	<0.02	<0.01
Grand Valley, CO CER Well	5/22	23	13.6	^{3}H	540	0.02
				^{89}Sr	<2	<0.07
				^{90}Sr	<1	<0.3
				^{234}U	0.24	<0.01
				^{235}U	<0.009	<0.01
				^{238}U	0.18	<0.01
				^{238}Pu	<0.04	<0.01
				^{239}Pu	<0.02	<0.01
Rulison, CO Potter Ranch	5/21	27		^{3}H	420	0.01
				^{89}Sr	<2	<0.07
				^{90}Sr	<1	<0.3
				^{226}Ra	0.089	0.3
				^{234}U	4.7	0.02
				^{235}U	0.13	<0.01
				^{238}U	3.1	<0.01
				^{238}Pu	<0.04	<0.01
				^{239}Pu	<0.02	<0.01

Table 11. (continued)

Sampling Location	Date	Sample Type[c]	Depth (Metres[a])	Radio-nuclide	Radioactivity Conc. (10^{-9} µCi/ml)	% of Conc. Guide
			FAULTLESS EVENT			
Blue Jay, NV Highway Maint. Station	3/11	23		^{3}H	<8	<0.01
				^{89}Sr	<2	<0.07
				^{90}Sr	<1	<0.4
				^{234}U	3.3	0.01
				^{235}U	0.07	<0.01
				^{238}U	1.3	<0.01
				^{238}Pu	<0.03	<0.01
				^{239}Pu	<0.04	<0.01
Warm Springs, NV Hot Creek Ranch	3/11	27		^{3}H	26	<0.01
				^{89}Sr	<2	<0.07
				^{90}Sr	<1	<0.4
				^{234}U	1.8	<0.01
				^{235}U	0.035	<0.01
				^{238}U	1.1	<0.01
				^{238}Pu	<0.02	<0.01
				^{239}Pu	<0.02	<0.01
Blue Jay, NV Blue Jay Spring	3/11	27		^{3}H	11	<0.01
				^{89}Sr	<1	<0.03
				^{90}Sr	<1	<0.3
				^{234}U	3.9	0.01
				^{235}U	0.073	<0.01
				^{238}U	2.1	<0.01
				^{238}Pu	<0.03	<0.01
				^{239}Pu	<0.05	<0.01
Blue Jay, NV Sixmile Well	3/11	23		^{3}H	<8	<0.01
				^{89}Sr	<2	<0.05
				^{90}Sr	<0.9	<0.3
				^{234}U	1.9	<0.01
				^{235}U	0.019	<0.01
				^{238}U	0.74	<0.01
				^{238}Pu	<0.02	<0.01
				^{239}Pu	<0.02	<0.01

Table 11. (continued)

Sampling Location	Date	Sample Type[c]	Depth (Metres[a])	Radio-nuclide	Radioactivity Conc. (10^{-9} µCi/ml)	% of Conc. Guide
Well HTH-1	3/12	23	259	^{3}H	<7	<0.01
				^{89}Sr	<2	<0.08
				^{90}Sr	<1	<0.4
				^{234}U	1.7	<0.01
				^{235}U	0.059	<0.01
				^{238}U	1.0	<0.01
				^{238}Pu	<0.05	<0.01
				^{239}Pu	<0.03	<0.01
	8/14	23	259	^{3}H	<7	<0.01
Well HTH-2	3/12	23	184	^{3}H	<8	<0.01
				^{89}Sr	<2	<0.05
				^{90}Sr	<0.7	<0.2
				^{234}U	2.5	<0.01
				^{235}U	<0.02	<0.01
				^{238}U	0.75	<0.01
				^{238}Pu	<0.04	<0.01
				^{239}Pu	<0.03	<0.01
	8/14	23	184	^{3}H	<8	<0.01

[a] If depth not shown, water was collected at surface.

[b] Sample collected from tap in Malaga. Water originates from Loving City Well No. 2.

[c] 21 - Pond, Lake, Reservoir, Stock Tank, Stock Pond
22 - Stream, River, Creek
23 - Well
27 - Spring

APPENDIX A. RADIATION PROTECTION STANDARDS FOR EXTERNAL AND INTERNAL EXPOSURE*

ANNUAL DOSE COMMITMENT

Type of Exposure	Dose Limit to Critical Individuals in Uncontrolled Area at Points of Maximum Probable Exposure (rem)	Dose Limit to Suitable Sample of the Exposed Population in an Uncontrolled Area (rem)
Whole Body, gonads or bone marrow	0.5	0.17
Other organs	1.5	0.5

CONCENTRATION GUIDES (CG's)

Network or Program	Sampling Medium	Radionuclide	CG (μCi/ml)	Basis of Exposure
Air Surveillance Network	air	^{7}Be	1.1×10^{-8}	Suitable sample of the exposed population in uncontrolled area.
		^{95}Zr	3.3×10^{-10}	
		^{103}Ru	1.0×10^{-9}	
		^{106}Ru	6.7×10^{-11}	
		^{140}Ba	3.3×10^{-10}	
		^{141}Ce	1.7×10^{-9}	
		^{144}Ce	6.7×10^{-11}	
Noble Gas and Tritium Surveillance Network, On-NTS	air	^{85}Kr	1.0×10^{-5}	Individual in controlled area.
		^{3}H	5.0×10^{-6}	
		^{133}Xe	1.0×10^{-5}	
Noble Gas and Tritium Surveillance Network, Off-NTS	air	^{85}Kr	1.0×10^{-7}	Suitable sample of the exposed population in uncontrolled area.
		^{3}H	6.7×10^{-8}	
		^{133}Xe	1.0×10^{-7}	
Water Surveillance Network	water	^{3}H	1.0×10^{-3}	Suitable sample of the exposed population in an uncontrolled area.
		^{89}Sr	1.0×10^{-6}	
		^{90}Sr	1.0×10^{-7}	
		^{238}Pu	1.7×10^{-6}	
		^{239}Pu	1.7×10^{-6}	
		^{226}Ra	1.0×10^{-8}	

*"Radiation Protection Standards," ERDA Manual, Chapter 0524.

CONCENTRATION GUIDES (CG's) continued

Network or program	Sampling Medium	Radio-nuclide	CG (μCi/ml)	Basis of Exposure
Long-Term Hydrological Program	water	^{3}H	3.0×10^{-3}	Individual in uncontrolled area.
		^{89}Sr	3.0×10^{-6}	
		^{90}Sr	3.0×10^{-7}	
		^{238}Pu	5.0×10^{-6}	
		^{239}Pu	5.0×10^{-6}	
		^{234}U	3.0×10^{-5}	
		^{235}U	3.0×10^{-5}	
		^{238}U	4.0×10^{-5}	
		^{226}Ra	3.0×10^{-8}	
		^{137}Cs	2.0×10^{-5}	
		^{3}H	1.0×10^{-1}	Individual in controlled area.
		^{89}Sr	3.0×10^{-4}	
		^{90}Sr	1.0×10^{-5}	
		^{238}Pu	1.0×10^{-4}	
		^{239}Pu	1.0×10^{-4}	
		^{234}U	9.0×10^{-4}	
		^{235}U	8.0×10^{-4}	
		^{238}U	1.0×10^{-3}	
		^{226}Ra	4.0×10^{-7}	

APPENDIX B. DOSE ASSESSMENT CALCULATIONS

METHOD

The radionuclides detected in off-NTS air samples and attributed to NTS operations were ^{133}Xe, ^{85}Kr, and ^{3}H. Based upon the time-integrated concentrations of ^{133}Xe and ^{3}H at each location where the nuclide(s) were detected, whole-body dose estimates were calculated from the following equations.

D.E. = $0.25\ E\psi$*, where D.E. is the whole-body dose equivalent resulting from exposure to airborne ^{133}Xe, rem;

E is the effective energy of the radiations released per disintegration of ^{133}Xe, 0.19 MeV/dis;

ψ is the time-integrated concentration of ^{133}Xe, $Ci \cdot sec/m^3$.

D.E. = $0.47\ E\chi$**, where D.E. is the whole-body dose equivalent resulting from exposure to airborne ^{3}H, rem;

E is the effective energy released per disintegration of ^{3}H, 0.010 MeV/ dis;

χ is the time-integrated concentration of ^{3}H in air, $\mu Ci \cdot d/m^3$.

The 80-km, man-rem dose was calculated from the product of these dose equivalents and the population at each sampling location.

Since the gamma radiation per disintegration of ^{85}Kr is negligible (0.514 MeV, 0.41 percent abundance) the major hazard from this nuclide is beta radiation to the skin of the total body. Skin dose equivalents were calculated from the time-integrated concentration of ^{85}Kr at each sampling location where ^{85}Kr was detected and the same equation for ^{133}Xe, except an effective energy of 0.24 MeV/dis was used instead of the 0.19 MeV/dis which was for ^{133}Xe.

---

* "Meteorology and Atomic Energy," U.S. Atomic Energy Commission, Division of Technical Information, Oak Ridge, Tennessee. p 339. July 1968

** Based upon the assumptions of "Report of Committee IV on Evaluation of Radiation Doses to Body Tissues from Internal Contamination Due to Occupational Exposures." Recommendation of the International Committee on Radiological Protection, ICRP Publication 10. Pergamon Press, New York. pp 29-30. 1968

RESULTS

The results of the whole-body dose calculations are summarized, as follows:

Location	Radio-nuclide	Time-Integrated Concentration ($\mu Ci\text{-}s/m^3$)	Whole-Body Dose (μrem)	Population	Dose Commitment Within 80 km (man-rem)
Beatty	^{3}H	2.7	0.15	500	0.000075
Diablo	^{3}H	8.6	0.46	5	0*
	^{133}Xe	34	1.6		0*
Hiko	^{133}Xe	20	0.97	52	0.000570*
Indian Springs	^{133}Xe	7.2	0.34	1670	0.00057
Las Vegas	^{133}Xe	6.6	0.32	194,000	0*
				Total	0.00065

* Diablo, Hiko, and Las Vegas are beyond 80 km. Dose commitments at these locations were calculated as 0.000010 man-rem, 0.000050 man-rem, and 0.062 man-rem, respectively.

Although the total body skin dose equivalents calculated from the ^{85}Kr concentrations are not appropriate for inclusion with the 80-km dose commitment estimates, the results of this calculation are summarized as follows for comparison to the Radiation Protection Standard of 0.5 rem/y for exposures to the skin at a suitable sample of the population.

Location	Time-Integrated Concentration of ^{85}Kr ($\mu Ci\text{-}s/m^3$)	Total Body Skin Dose (μrem)	Percent of Radiation Protection Standard
Beatty	4.8	0.29	$6x10^{-5}$
Diablo	12	0.72	$1x10^{-4}$
Indian Springs	15	0.87	$2x10^{-4}$
Las Vegas	15	0.90	$2x10^{-4}$

If one used the conservative assumption of the ERDA Manual, Chapter 0524, that exposure to airborne ^{85}Kr results in a whole-body gamma exposure, the doses at Beatty, Diablo, Indian Springs, and Las Vegas would be increased by the doses above. This would result in a 80-km dose commitment of 0.0022 man-rem, a factor of 3.4 times the first estimate, and dose commitments at Diablo and Las Vegas of 0.000014 man-rem and 0.22 man-rem, respectively.

APPENDIX C. LIST OF ABBREVIATIONS AND SYMBOLS

µrem	Micro-roentgen-equivalent-man.
µCi/g	Microcurie per gram.
µCi/ml	Microcurie per millilitre.
AEC	Atomic Energy Commission.
ASN	Air Surveillance Network.
C	Temperature in Celsius.
CG	Concentration Guide.
Ci	Curie.
cm	Centimetre.
CP-1	Control Point One.
CY	Calendar year.
D.E.	Dose Equivalent.
EMSL-LV	Environmental Monitoring and Support Laboratory-Las Vegas.
EPA	Environmental Protection Agency.
ERDA	Energy Research and Development Administration.
ERDA/NV	Energy Research and Development Administration/Nevada Operations Office.
ft	Feet.
kg	Kilogram.
kt	Kiloton.
LLL	Lawrence Livermore Laboratory
m	Metre.
MDC	Minimum detectable concentration.
mrem/y	Milli-roentgen-equivalent-man per year.
mrem/d	Milli-roentgen-equivalent-man per day.

mR	Milli-roentgen.
mR/h	Milli-roentgen per hour.
MSL	Mean sea level.
MSN	Milk Surveillance Network.
nCi	Nanocurie.
NTS	Nevada Test Site.
PHS	Public Health Service.
SMSN	Standby Milk Surveillance Network.
TLD	Thermoluminescent dosimeter.
USGS	United States Geological Society.
WSN	Water Surveillance Network.
^{3}H	Tritium or Hydrogen-3.
HT	Tritiated Hydrogen.
HTO	Tritiated Water.
CH_3T	Tritiated Methane.
Ba	Barium.
Cs	Cesium.
K	Potassium.
Kr	Krypton.
Pu	Plutonium.
Ra	Radium.
Sr	Strontium.
U	Uranium.
Xe	Xenon.

DISTRIBUTION

1 - 25 Environmental Monitoring & Research Laboratory, Las Vegas, NV
26 Mahlon E. Gates, Manager, ERDA/NV, Las Vegas, NV
27 Troy E. Wade, ERDA/NV, Las Vegas, NV
28 David G. Jackson, ERDA/NV, Las Vegas, NV
29 Paul B. Dunaway, ERDA/NV, Las Vegas, NV
30 - 31 Bruce W. Church, ERDA/NV, Las Vegas, NV (2)
32 Mary G. White, ERDA/NV, Las Vegas, NV
33 Roger Ray, ERDA/NV, Las Vegas, NV
34 Chief, NOB/DNA, ERDA/NV, Las Vegas, NV
35 - 36 Robert R. Loux, ERDA/NV, Las Vegas, NV (2)
37 A. J. Whitman, ERDA/NV, Las Vegas, NV
38 Elwood M. Douthett, ERDA/NV, Las Vegas, NV
39 Shed R. Elliott, ERDA/NV, Las Vegas, NV
40 Ernest D. Campbell, ERDA/NV, Las Vegas, NV
41 Thomas M. Humphrey, ERDA/NV, Las Vegas, NV
42 - 43 Peter K. Fitzsimmons, ERDA/NV, Las Vegas, NV (2)
44 Robert W. Newman, ERDA/NV, Las Vegas, NV
45 Harold F. Mueller, ARL/NOAA, ERDA/NV, Las Vegas, NV
46 Virgil Quinn, ARL/NOAA, ERDA/NV, Las Vegas, NV
47 - 49 Technical Library, ERDA/NV, Las Vegas, NV (3)
50 Mail and Records, ERDA/NV, Las Vegas, NV
51 R. S. Brundage, CER Geonuclear Corporation, P.O. Box 15090, Las Vegas, NV 89114
52 Leslie Estep, ERDA/SAN, San Francisco Operation Office, 1333 Broadway, Oakland, CA 94616
53 - 57 Martin B. Biles, DSSC, ERDA, Washington, D.C. (5)
58 Major General J. K. Bratton, AGMMA, ERDA, Washington, D.C.
59 A. J. Hodges, DMA, ERDA, Washington, D.C.
60 Gordon Facer, MA, ERDA, Washington, D.C.
61 Andrew J. Pressesky, RDD, ERDA, Washington, D.C.
62 James L. Liverman, BER, ERDA, Washington, D.C.
63 P. L. Randolph, El Paso Natural Gas Co., P.O. Box 1492, El Paso, TX 79978
64 Gilbert J. Ferber, ARL/NOAA, Silver Springs, MD
65 William Horton, Bureau of Environmental Health, State of Nevada 505 E. King St., Carson City, NV 89710

66 Dr. Wilson K. Talley, Assistant Administrator for Research & Development, EPA, Washington, D.C.

67 William D. Rowe, Deputy Assistant Administrator for Radiation Programs, EPA, Washington, D.C.

68 Dr. William A. Mills, Director, Division of Criteria & Standards, ORP, EPA, Washington, D.C.

69 David S. Smith, Director, Division of Technology Assessment, ORP, EPA, Washington, D.C.

70 Bernd Kahn, Chief, Radiochemistry & Nuclear Engineering, NERC, EPA, Cincinnati, OH

71- 72 Floyd L. Galpin, Director, Environmental Analysis Division, ORP, EPA, Washington, D.C. (2)

73 Dr. Gordon Everett, Director, Office of Technical Analysis, EPA, Washington, D.C.

74 Regional Administrator, EPA, Region IV, Atlanta, GA

75 Regional Radiation Representative, EPA, Region IV, Atlanta, GA

76 State of Mississippi

77 Regional Administrator, EPA, Region VI, Dallas, TX

78 Regional Radiation Representative, EPA, Region VI, Dallas, TX

79 State of New Mexico

80 Regional Administrator, EPA, Region VIII, Denver, CO

81 Regional Radiation Representative, EPA, Region VIII, Denver, CO

82 State of Colorado

83 State of Utah

84 Regional Administrator, EPA, Region IX, San Francisco, CA

85 Regional Radiation Representative, EPA, Region IX, San Francisco, CA

86 State of Arizona

87 State of California

88 State of Nevada

89 Eastern Environmental Radiation Facility, EPA, Montgomery, AL

90 Library, EPA, Washington, D.C.

91 Kenneth M. Oswald, LLL, Mercury, NV

92 Roger E. Batzel, LLL, Livermore, CA

93 James E. Carothers, LLL, Livermore, CA

94 John Hopkins, LASL, Los Alamos, NM

95 Jerome E. Dummer, LASL, Los Alamos, NM

96 Arden E. Bicker, REECo, Mercury, NV

97 A. W. Western, REECo, Mercury, NV

98 Savino W. Cavender, M.D., REECo, Mercury, NV

99 Carter D. Broyles, Sandia Laboratories, Albuquerque, NM

100 George Tucker, Sandia Laboratories, Albuquerque, NM

101 Albert E. Doles, Eberline Instrument Co., Santa Fe, NM

102 Robert H. Wilson, University of Rochester, Rochester, NY

103 Richard S. Davidson, Battelle Memorial Institute, Columbus, OH

104 J. P. Corley, Battelle Memorial Institute, Richland, WA

105 John M. Ward, President, Desert Research Institute, University of Nevada, Reno, NV

106 ERDA/HQ Library, Attn: Eugene Rippeon, ERDA, Washington, D.C.

107 - 134 Technical Information Center, Oak Ridge, TN (for public availability)

135 T. F. Cornwell, DMA, ERDA, Washington, D.C.

ENVIRONMENTAL MONITORING AND
SUPPORT LABORATORY
P.O. BOX 15027
LAS VEGAS, NEVADA 89114

POSTAGE AND FEES PAID
U.S. ENVIRONMENTAL PROTECTION AGENCY
EPA-335

B

NERC-LV-539-8

SELECTED CENSUS INFORMATION AROUND THE NEVADA TEST SITE

by
Environmental Surveillance
National Environmental Research Center

U.S. ENVIRONMENTAL PROTECTION AGENCY
Las Vegas, Nevada

February 1973

This project performed under a Memorandum of
Understanding No. AT(26-1)-539
for the
U. S. ATOMIC ENERGY COMMISSION

NERC-LV-539-8

SELECTED CENSUS INFORMATION AROUND THE NEVADA TEST SITE

by
Environmental Surveillance
National Environmental Research Center

U.S. ENVIRONMENTAL PROTECTION AGENCY
Las Vegas, Nevada

Published February 1973

This project performed under a Memorandum of
Understanding No. AT(26-1)-539
for the
U. S. ATOMIC ENERGY COMMISSION

ABSTRACT

The National Environmental Research Center-Las Vegas (NERC-LV), Environmental Protection Agency, conducts a comprehensive off-site radiological safety program in support of nuclear testing at the Nevada Test Site (NTS). To facilitate the planning and management of required surveillance and monitoring operations, and to assess potential and actual population exposures resulting from radioactive releases into the areas beyond the boundaries of the NTS, the NERC-LV collects and maintains census information in the area around the NTS.

This report summarizes this census information which includes the number and distribution of resident adults and children, family milk cows, and Grade A dairy cows located by azimuth and distance within a radius of 450 miles of Control Point 1 at approximately the center of the NTS, 36° 15' N, 116° 04' W.

TABLE OF CONTENTS

LIST OF TABLES AND FIGURE

INTRODUCTION

In accordance with a Memorandum of Understanding between the Environmental Protection Agency and the Atomic Energy Commission, the National Environmental Research Center-Las Vegas (NERC-LV) conducts a comprehensive off-site radiological safety program in support of nuclear testing at the Nevada Test Site (NTS). As part of this program, the NERC-LV collects and maintains census information in the area around the NTS to facilitate the planning and management of surveillance and monitoring operations, and to assess potential and actual population exposures resulting from radioactive releases into the areas beyond the boundaries of the NTS. Included in the information compiled are data concerning the number of resident adults and children, family milk cows, and Grade A dairy cows located in these off-site areas.

This report summarizes the number and distribution of human population and milk cow population by azimuth and distance from Control Point 1 (CP-1) located roughly at the center of the NTS, 36° 15' N, 116° 04' W. Tables 1 and 2 show the population distribution out to a distance of 450 miles from CP-1. Tables 3 and 4 list the milk cow distribution. The data are presented in 30-degree sectors at distance increments of 25 miles. Figure 1 shows the azimuth/distance distribution of census data within a radius of 200 miles of CP-1.

BACKGROUND CONSIDERATIONS

The State of Nevada has a total population of 488,738 (1970 census), of which 395,336, or 80.9%, reside in urban areas and 93,402, or 19.1% in the extensive rural areas. The Las Vegas and Reno metropolitan areas account for approximately 98% of the total urban population. The Las Vegas area is 73 miles from the NTS on an azimuth of 136° and the Reno area 271 miles on an azimuth of 311°. The rural population is widely scattered throughout the state with less than one-half the people residing in areas with a population over 1,000. The urban population increased 97.4% over the previous census while the rural population increased 10.4%. The major incorporated cities are experiencing the highest growth rate: Carson City - 15,468, up 199.6%; Henderson - 16,395, up 30.9%; Las Vegas - 125,787, up 95.3%; North Las Vegas - 36,216, up 96.6%; Reno - 72,863, up 41.6%; and Sparks - 24,187, up 45.5%.

Nevada has approximately 9,000,000 acres in farm and ranch land and an estimated 2,100 farms or ranches with an average size of 4,286 acres. Nevada farms and ranches last year produced 1,009,000 tons of crops on 491,000 acres with a total value of $30,228,000. Principal crops harvested include corn silage, 4,000 acres; all grain, 33,000 acres; cotton and seed, 2,300 acres; alfalfa seed, 22,000 acres; and all hay, 428,000 acres.

Livestock production is the most important phase of agriculture. The value of all livestock totaled $120,000,000. in 1971. Principal livestock raised are cattle and calves, approximately 600,000 beef and 26,000 milk; sheep and lambs, about 239,000 head; and hogs and pigs, about 9,400 head. Milk production is estimated at 139,000,000 pounds at a market value of $7,564,000.

Details of resident and milk cow population in the areas extending to a distance of approximately 50 miles beyond the NTS and the Nellis Air Force Range boundaries are updated continuously. Biennial detailed surveys beyond the 50-mile radius are conducted to update census information, including residents, family milk cows, and Grade "A" dairies for the entire State of Nevada and portions of Arizona, Utah, Idaho and California.

CLOSE-IN POPULATION DISTRIBUTION

The off-site area nearest the NTS is predominantly a rural area consisting of a variety of farms and ranches ranging in size from a few acres to several hundred thousand acres. Several small communities are located in the area, the largest being the Pahrump valley. This rural community has an estimated population of 1,100 and is located about 45 miles south of the NTS. The Amargosa Farm area has a population of about 200 and is located about 30 miles southwest. The Spring Meadows Farm area is a relatively new development consisting of approximately 10,000 acres with a population of somewhat more than 100. This area is about 35 miles south-southwest of the NTS. The largest town in the near off-site area is Beatty with a population of more than 500 and located about 40 miles to the west. The region north and east is primarily open range land used for cattle grazing, although not extensively. Some of the valleys in this region are also used for winter grazing by certain sheep herders from the northern part of the state. There are also 12 mining operations within 50 miles of the NTS, about five of which are operated on a regular basis.

ADJACENT STATES

The Mohave Desert of California which includes Death Valley National Monument, lies along the southwestern border of Nevada. The population in the Monument boundaries varies considerably from season to season with fewer than 200 permanent residents and tourists in the area during any given period in the summer months. However, during the winter as many as 12,000 tourists and campers can be in the area, particularly during the major holiday periods. The largest town in this general area is Barstow, located 165 miles south-southwest of the NTS with a population of over 12,000. The Owens Valley, where numerous farms, ranches and small towns are located, lies 25 to 35 miles west of Death Valley. The largest town is Bishop, located 140 miles west-northwest of the NTS with a population of about 3,000.

The extreme southwestern region of Utah is somewhat more developed than the adjacent part of Nevada. The largest town is Cedar City, with a population of approximately 9,000 and located 175 miles east-northeast of the NTS. The next largest community is St. George located 135 miles east of the NTS with a population of somewhat more than 7,000. Both communities engage in seasonal fruit and vegetable production. The area also has several small Grade "A" dairies.

The extreme northwestern region of Arizona is mostly undeveloped range land with the exception of that portion in the Lake Mead Recreation area. Several small retirement communities are found along the Colorado River, primarily at Lake Mohave and Lake Havasu. The largest town in the area is Kingman, located 175 miles southeast of the NTS with a population of about 6,000.

REFERENCES

1. U. S. Department of Commerce - Bureau of Census Publications PC (1)-A30, PHC (2)-30 and PC (VI)-30.

2. U. S. Department of Agriculture - "Nevada Agricultural Statistics 1970."

3. U. S. Department of Agriculture - Nevada Crop and Livestock Reporting Service Bulletins.

4. Nevada Bureau of Mines - Report 18 and Associated Periodic Bulletins.

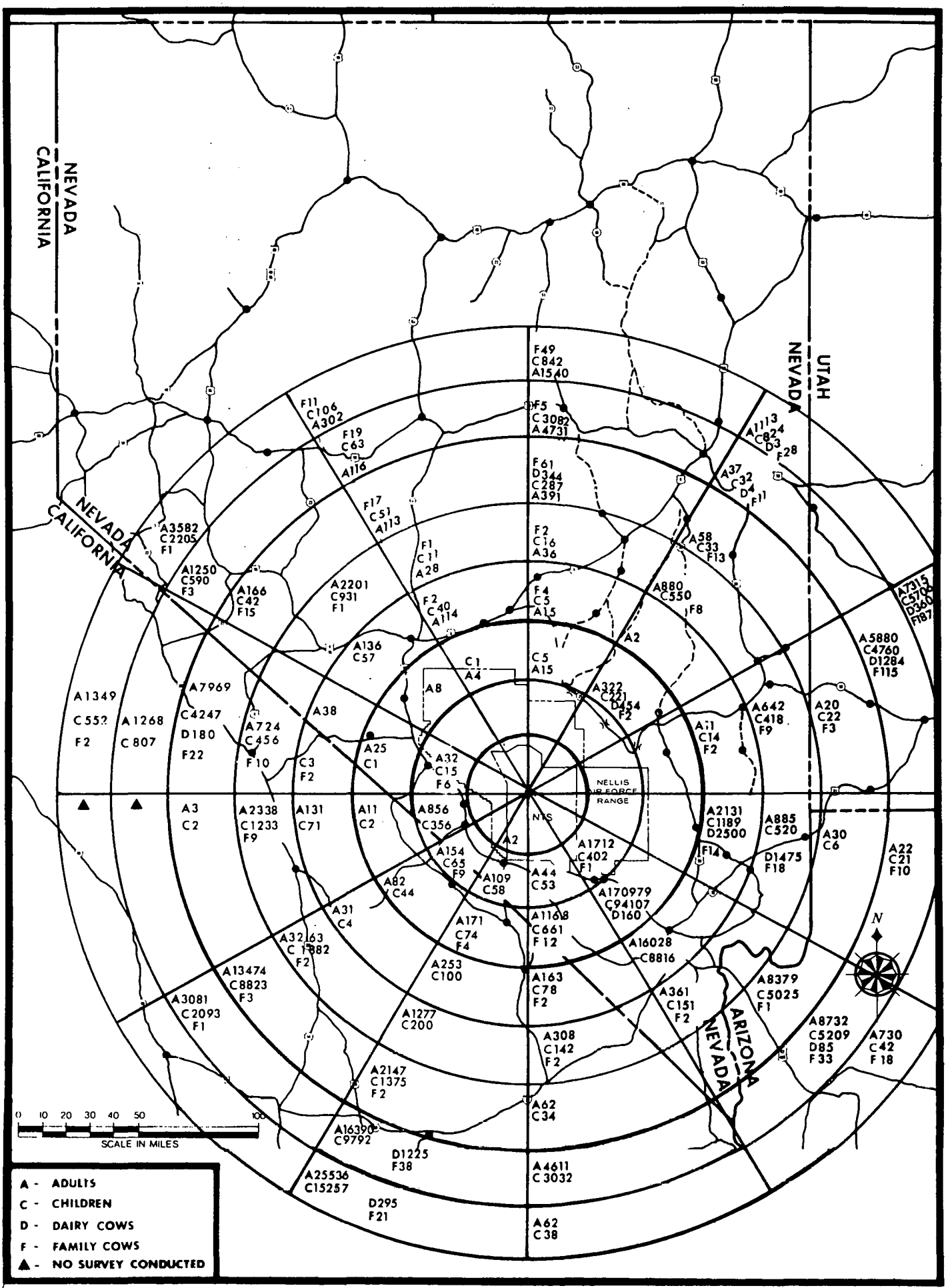

Figure 1. Population distribution by azimuth/distance.

Table 1. Number and distribution of adults by azimuth and distance from NTS/CP-1.

Distance (Miles)	AZIMUTH (Degrees) 0-29	30-59	60-89	90-119	120-149	150-179	180-209	210-239	240-269	270-299	300-329	330-359	Total
0-25	0	0	0	0	0	0	2	0	0	0	0	0	2
25-50	0	0	0	0	1,712	44	109	154	856	32	0	0	2,907
50-75	20	322	11	0	170,979	1,168	141	82	11	25	8	4	172,771
75-100	15	2	642	2,131	16,028	163	253	31	141	38	136	114	19,694
100-125	36	880	20	885	361	308	1,277	3,263	2,338	724	2,201	28	12,321
125-150	391	58	5,880	30	8,379	62	2,147	13,474	3	7,969	166	113	38,672
150-175	4,731	37	7,315	22	8,732	4,611	16,390	3,081	0	1,268	1,250	116	47,553
175-200	1,540	1,113	3,254	798	730	62	25,536	0	2	1,349	3,582	302	38,268
200-225	100	41	1,468	73	647	----	----	----	----	14	4,374	118	6,835
225-250	405	2,214	----	2,885	202	----	----	----	----	----	10,689	299	16,694
250-275	6,442	2,246	32	20,931	----	----	----	----	----	----	90,793	4,497	124,941
275-300	1,610	2,714	----	53	----	----	----	----	----	----	571	4,333	9,281
300-325	230	215	----	----	----	----	----	----	----	----	360	240	1,045
325-350	865	----	----	----	----	----	----	----	----	----	29	381	1,275
350-375	458	----	----	----	----	----	----	----	----	----	----	682	1,140
375-400	126	----	----	----	----	----	6	----	----	----	9	11	152
400-425	----	2	----	----	----	----	----	4	----	----	----	2	8
425-450	----	----	----	----	----	----	----	----	----	----	----	----	----
TOTAL	16,969	9,844	18,622	27,808	207,770	6,418	45,861	20,089	3,351	11,419	114,168	11,240	493,559

---- = Survey incomplete.

Table 2. Number and distribution of children by azimuth and distance from NTS/CP-1.

Distance (Miles)	AZIMUTH (Degrees) 0-29	30-59	60-89	90-119	120-149	150-179	180-209	210-239	240-269	270-299	300-329	330-359	Total
0-25	0	0	0	0	0	0	0	0	0	0	0	0	0
25-50	0	0	0	0	402	53	58	65	356	15	0	0	949
50-75	5	221	14	0	94,107	661	74	44	2	1	0	1	95,130
75-100	5	0	418	1,189	8,816	78	100	4	71	3	57	40	10,781
100-125	16	571	22	520	151	142	200	1,882	1,233	456	931	11	6,135
125-150	287	33	4,760	6	5,025	34	1,375	8,823	2	4,247	42	51	24,685
150-175	3,083	32	5,706	21	5,209	3,032	9,792	2,093	0	807	590	63	30,428
175-200	842	824	2,610	597	421	38	15,257	0	0	552	2,205	106	23,452
200-225	51	27	1,110	10	339	----	----	----	----	6	2,766	56	4,365
225-250	239	1,911	----	2,217	105	----	----	----	----	----	5,894	112	10,478
250-275	4,293	1,973	22	16,633	----	----	----	----	----	----	44,609	2,737	70,267
275-300	1,011	1,976	----	39	----	----	----	----	----	----	235	2,190	5,451
300-325	148	155	----	----	----	----	----	----	----	----	170	108	581
325-350	590	----	----	----	----	----	----	----	----	----	12	212	814
350-375	253	----	----	----	----	----	----	----	----	----	----	354	607
375-400	135	----	----	----	----	----	4	----	----	----	2	5	146
400-425	----	2	----	----	----	----	----	3	----	----	----	1	6
425-450	----	----	----	----	----	----	----	----	----	----	----	----	----
TOTAL	10,958	7,725	14,662	21,232	114,575	4,038	26,860	12,914	1,664	6,087	57,513	6,047	284,275

---- = Survey incomplete.

Table 3. Number and distribution of grade "A" cows by azimuth and distance from NTS/CP-1.

Distance (Miles)	AZIMUTH (Degrees) 0-29	30-59	60-89	90-119	120-149	150-179	180-209	210-239	240-269	270-299	300-329	330-359	Total
0-25	0	0	0	0	0	0	0	0	0	0	0	0	0
25-50	0	0	0	0	0	0	0	0	0	0	0	0	0
50-75	0	454	0	0	160	0	0	0	0	0	0	0	614
75-100	0	0	0	2,500	0	0	0	0	0	0	0	0	2,500
100-125	0	0	0	1,475	0	0	0	0	0	0	0	0	1,475
125-150	344	0	1,284	0	0	0	0	0	0	180	0	0	1,808
150-175	0	4	360	0	85	0	1,225	0	0	0	0	0	1,674
175-200	0	3	1,588	0	0	0	295	0	0	0	0	0	1,886
200-225	0	25	1,358	----	----	----	----	----	----	----	942	----	2,325
225-250	0	991	1,100	----	----	----	----	----	----	----	3,733	----	5,824
250-275	0	899	133	----	456	----	----	----	----	----	1,597	----	3,085
275-300	0	1,457	50	----	50	----	----	----	----	----	205	150	1,912
300-325	0	3,869	327	----	12,723	80	----	----	----	----	----	----	16,999
325-350	0	9,728	----	70	22,056	----	----	----	----	----	----	----	31,854
350-375	52	12,930	----	25	5,279	----	----	----	----	----	----	----	18,286
375-400	131	8,902	----	65	268	----	----	----	----	----	----	----	9,366
400-425	----	7,292	----	----	----	----	----	----	----	----	----	----	7,292
425-450	21	275	----	----	1,993	----	----	----	----	----	----	----	2,289
TOTAL	548	46,829	6,200	4,135	43,070	80	1,520			180	6,477	150	109,189

---- = Survey incomplete.

Table 4. Number and distribution of family cows by azimuth and distance from NTS/CP-1.

Distance (Miles)	AZIMUTH (Degrees) 0-29	30-59	60-89	90-119	120-149	150-179	180-209	210-239	240-269	270-299	300-329	330-359	Total
0-25	0	0	0	0	0	0	0	0	0	0	0	0	0
25-50	0	0	0	0	1	0	0	9	0	6	0	0	16
50-75	0	2	2	0	0	12	4	0	0	0	0	0	20
75-100	4	0	9	14	0	2	0	0	0	2	0	2	33
100-125	2	8	3	18	2	2	0	2	9	10	1	1	58
125-150	61	13	115	0	1	0	2	3	0	22	15	17	249
150-175	5	11	187	10	33	0	38	1	0	0	3	19	307
175-200	49	28	100	14	18	0	21	0	0	2	1	11	244
200-225	45	6	24	1	20	----	----	----	----	----	70	31	197
225-250	57	86	----	1	----	----	----	----	----	----	242	26	412
250-275	104	86	----	3	----	----	----	----	----	----	78	40	311
275-300	67	57	----	11	----	----	----	----	----	----	3	41	179
300-325	38	5	----	----	----	----	----	----	----	----	8	28	79
325-350	58	----	----	----	----	----	----	----	----	----	1	70	129
350-375	52	----	----	----	----	----	----	----	----	----	----	35	87
375-400	11	----	----	----	----	----	----	----	----	----	1	2	14
400-425	----	6	----	----	----	----	----	----	----	----	----	----	6
425-450	----	----	----	----	----	----	----	----	----	----	----	----	----
TOTAL	553	308	440	72	75	16	65	15	9	42	423	323	2,341

---- = Survey incomplete.


C

UCRL-51830

AN EXAMINATION OF THE GEOLOGY AND SEISMOLOGY ASSOCIATED WITH AREA 410 AT THE NEVADA TEST SITE

W. J. Hannon

H. L. McKague

May 23, 1975

Prepared for U.S. Energy Research & Development Administration under contract No. W-7405-Eng-48

LAWRENCE LIVERMORE LABORATORY
University of California/Livermore

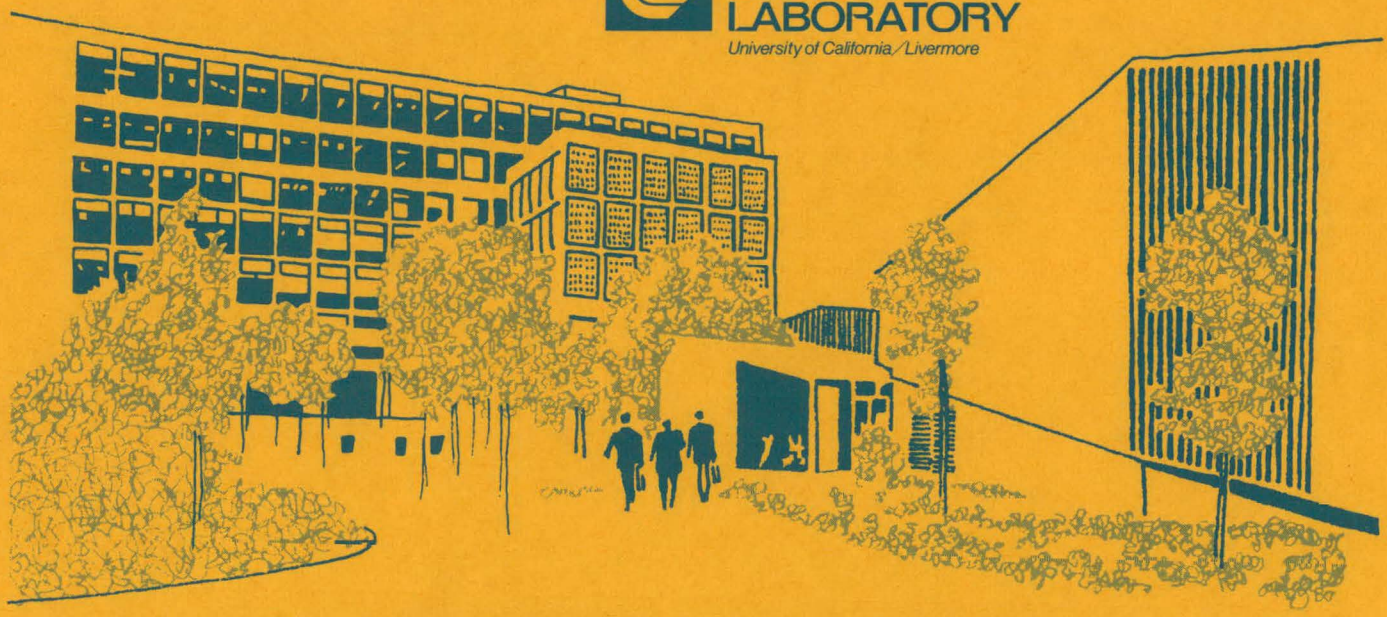

Printed in the United States of America
Available from
National Technical Information Service
U. S. Department of Commerce
5285 Port Royal Road
Springfield, Virginia 22151
Price: Printed Copy $___*; Microfiche $2.25

*Pages	NTIS Selling Price
1-50	$4.00
51-150	$5.45
151-325	$7.60
326-500	$10.60
501-1000	$13.60

Distribution Category
UC-11

LAWRENCE LIVERMORE LABORATORY
University of California/Livermore, California/94550

UCRL-51830

AN EXAMINATION OF THE GEOLOGY AND SEISMOLOGY ASSOCIATED WITH AREA 410 AT THE NEVADA TEST SITE

W. J. Hannon

H. L. McKague

MS. date: May 23, 1975

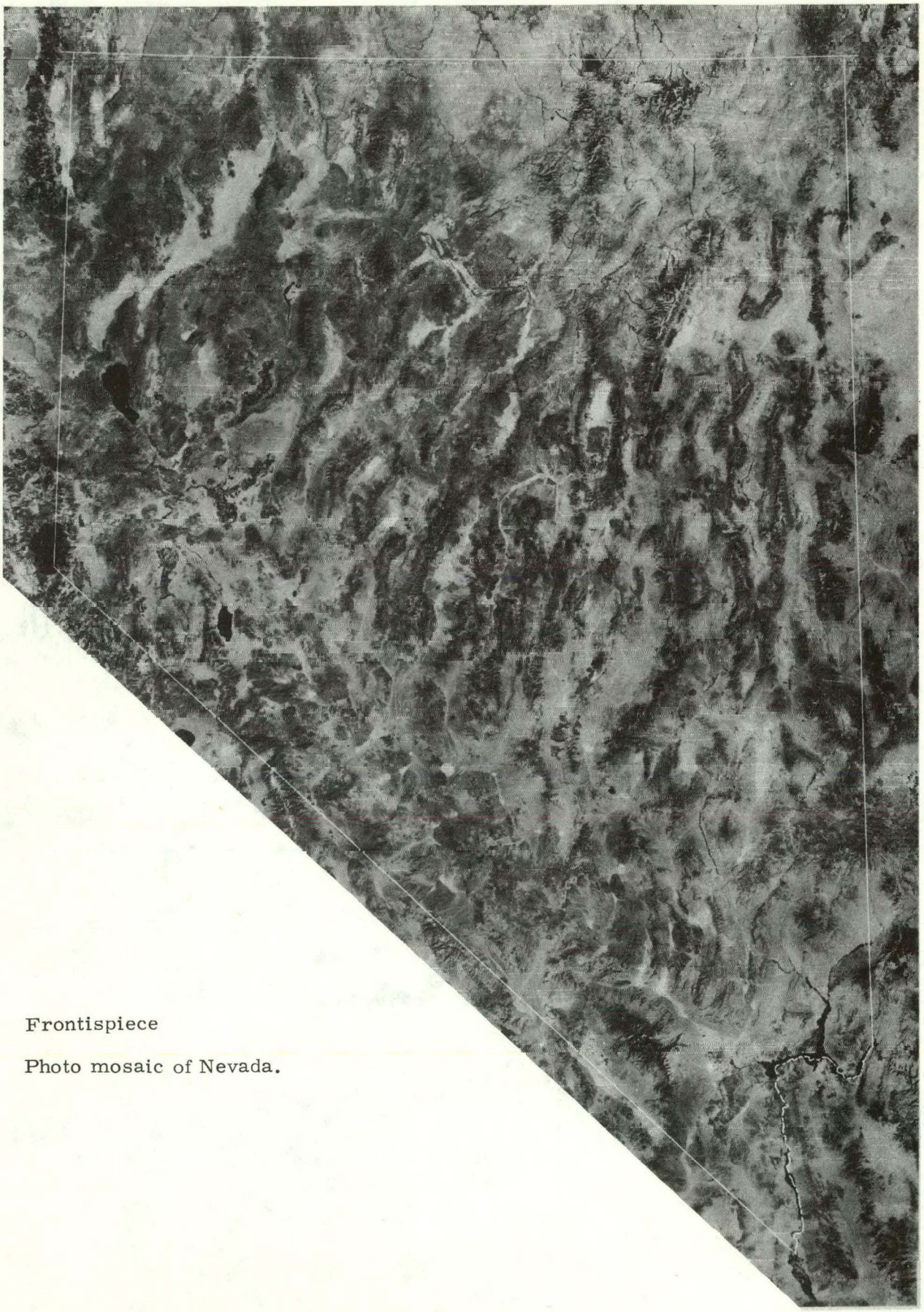

Frontispiece

Photo mosaic of Nevada.

Contents

AN EXAMINATION OF THE GEOLOGY AND SEISMOLOGY ASSOCIATED WITH AREA 410 AT THE NEVADA TEST SITE

Abstract

This report summarizes regional and local geology at the Nevada Test Site and identifies major tectonic features and active faults. Sufficient information is given to perform seismic safety analyses of present and future critical construction at the Super Kukla Site and Sites A and B in Area 410. However, examination of local minor faults and joints and soil thickness studies should be undertaken at construction time. The Cane Spring Fault is identified as the most significant geologic feature from the viewpoint of the potential seismic risk. Predictions of the peak ground acceleration (0.9 g), the response spectra for the Safe Shutdown Earthquake, and the maximum displacement across the Cane Spring Fault are made.

Introduction

ERDA has requested that LLL investigate the earthquake hazard for critical facilities at the Livermore site, Site 300, and Area 410 at the Nevada Test Site (NTS). A safety analysis is needed because facilities containing radioactive materials are located in these areas. This report examines the geology and seismicity of the Super Kukla Reactor Site and Sites A and B in Area 410.

The geological investigations consist of summaries of the regional and local geologic history, past and present tectonic features, and regional and local stratigraphy. Active faults were identified on the basis of geology, surficial expression, seismicity, and the stress state of the region. The Cane Spring Fault was identified as the most significant feature on the basis of its length and its proximity to the facilities being studied.

Once the active faults were identified, their dimensions and prior seismic history were used together with the results of previous investigations to predict acceleration levels. Two different prediction schemes were used depending on whether the nearest point on the fault was greater or less than 5 km from the building sites. In the former case, the predictions were based on the results of empirical observations of peak accelerations versus distance for a given magnitude and on studies of magnitude versus fault length. In the latter case, the prediction scheme was based upon close-in observations made during the 1966 Parkfield earthquake and the 1971 San Fernando earthquake. These were suitably scaled on the basis of estimated peak acceleration.

The results of the analysis show that the Cane Spring Fault is the primary

seismic hazard. A peak acceleration of 0.9 g is assigned to this fault and 0.2-0.5 m is estimated as the maximum displacement to be expected across the fault. The corresponding response spectra are determined.

Regional Geology

NTS is located within the south central part of the Great Basin section of the Basin and Range physiographic province (Fig. 1).[1] This province is characterized by a series of linear north to northeast trending mountain ranges (frontispiece and Fig. 2).[1] The ranges, which rise to heights of 2100 to 3100 m, are separated by intermountain basins at elevations of 900 to 1500 m.

In general, the rocks of the Basin and Range Province can be characterized as metamorphic rocks of Early Precambrian age [1640 m.y. (million years)][2]; sedimentary rocks of Late Precambrian (850 m.y.),[3] Paleozoic, and Mesozoic age; plutonic rocks of Mesozoic and Tertiary age; and volcanic and sedimentary rocks of Cenozoic age.

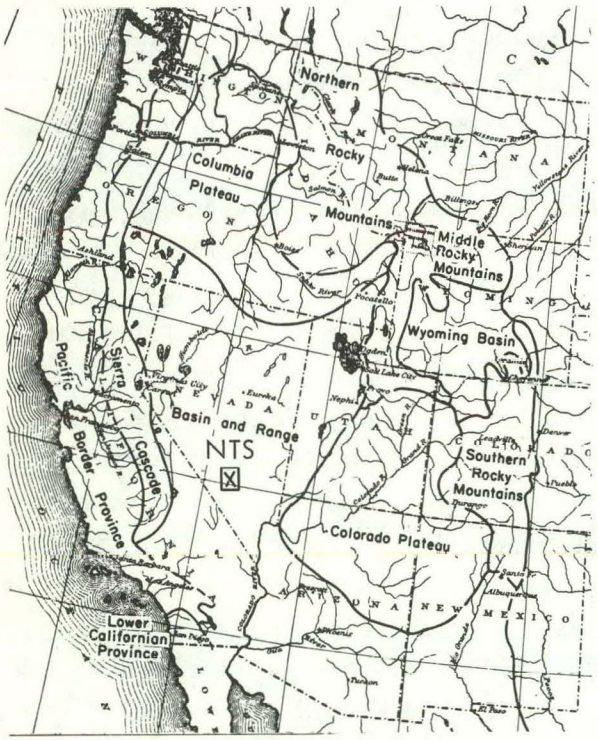

Fig. 1. Map of physiographic provinces of the Western United States.[1] (From Physiography of the United States by Charles B. Hunt. W. H. Freeman and Company. Copyright © 1967.)

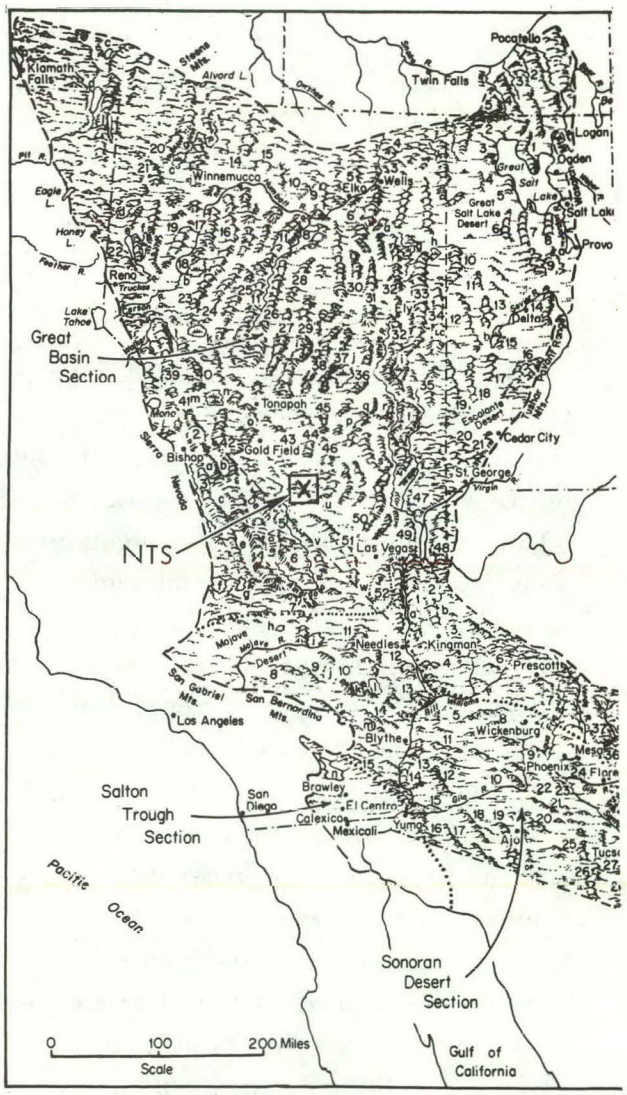

Fig. 2. Physiographic map of the Basin and Range Province.[1] (From Physiography of the United States by Charles B. Hunt. W. H. Freeman and Company. Copyright © 1967.)

The crust of the basin is relatively thin, averaging about 15 km thick. In Mesozoic time, complex thrusting and folding occurred and a number of granitic plutons were intruded. In the Tertiary period,[4] a change to extensional deformation occurred giving rise to three general groups of interrelated structures: (1) block faulting, (2) major zones of strike-slip faulting, and (3) volcano-tectonic features.[5]

GEOLOGIC HISTORY

The older Precambrian rocks are highly metamorphosed sedimentary and igneous rocks, now represented by scattered occurrences of schists, gneisses, and marbles. These rocks were involved in the Hudsonian orogeny (1640-1680 m.y.)[2] The overlying Upper Precambrian rocks are relatively unmetamorphosed sedimentary and volcanic rocks.[3] These rocks are divided into two series. The lower series ranges from 850-1250 m.y. in age. The upper series is 850 m.y. old and cannot be consistently separated from the Lower Cambrian rocks. The depositional pattern of the upper series departs from that of older rocks but is similar to the pattern of younger rocks deposited in the Cordilleran geosyncline. Stewart[3] proposes that this represents a change in tectonic setting and that these Upper Precambrian to Lower Cambrian rocks (570 to 850 m.y.) were the initial deposits in the Cordilleran geosyncline.

The rocks of Cordilleran geosyncline can most simply be divided into a eugeosynclinal group of clastic sedimentary rocks to the west of a group of miogeosynclinal, predominantly carbonate rocks. The NTS is near the thickest section of the miogeosyncline.[6] The eastern boundary of the eugeosyncline lies about 80 km west of the NTS [Figs. 3 (Ref. 7) and 4]. The miogeosynclinal sequence is largely Paleozoic rocks with some remnants of Lower Mesozoic rocks at the top.[2]

The rocks in the vicinity of the NTS may be roughly described as follows: the oldest rocks consist of a 1500-m-thick Precambrian and Lower Cambrian sequence of clastic rocks. These clastic rocks underlie a 4600-m-thick Middle Cambrian to Middle Devonian carbonate sequence. The Eleana Formation, a 2400-m-thick clastic sequence of Upper Devonian and Mississippian age rocks, overlies the lower carbonate sequence. The Eleana Formation, in turn, is overlain by an 1100-m-thick carbonate sequence of Pennsylvanian-Permian age. A stratigraphic column for the pre-Mesozoic rocks at NTS and vicinity is given in Table 1.[8, 9]

REGIONAL DEFORMATION AND VOLCANISM

The rocks of the eugeosyncline to the west were deformed by the Antler orogeny of early Mississippian time (340 m.y.). This orogeny occurred northwest of NTS and is represented at the test site by the Eleana Formation. The Antler orogeny appears to have had a minimal structural effect on the miogeosynclinal rocks in the vicinity of NTS. However, after the deposition of the upper carbonate sequence, compressional deformation occurred in the Mesozoic era (Fig. 5). According to Barnes and Poole,[10] folding was preceded, accompanied, and followed by southeastward thrusting. They propose that the

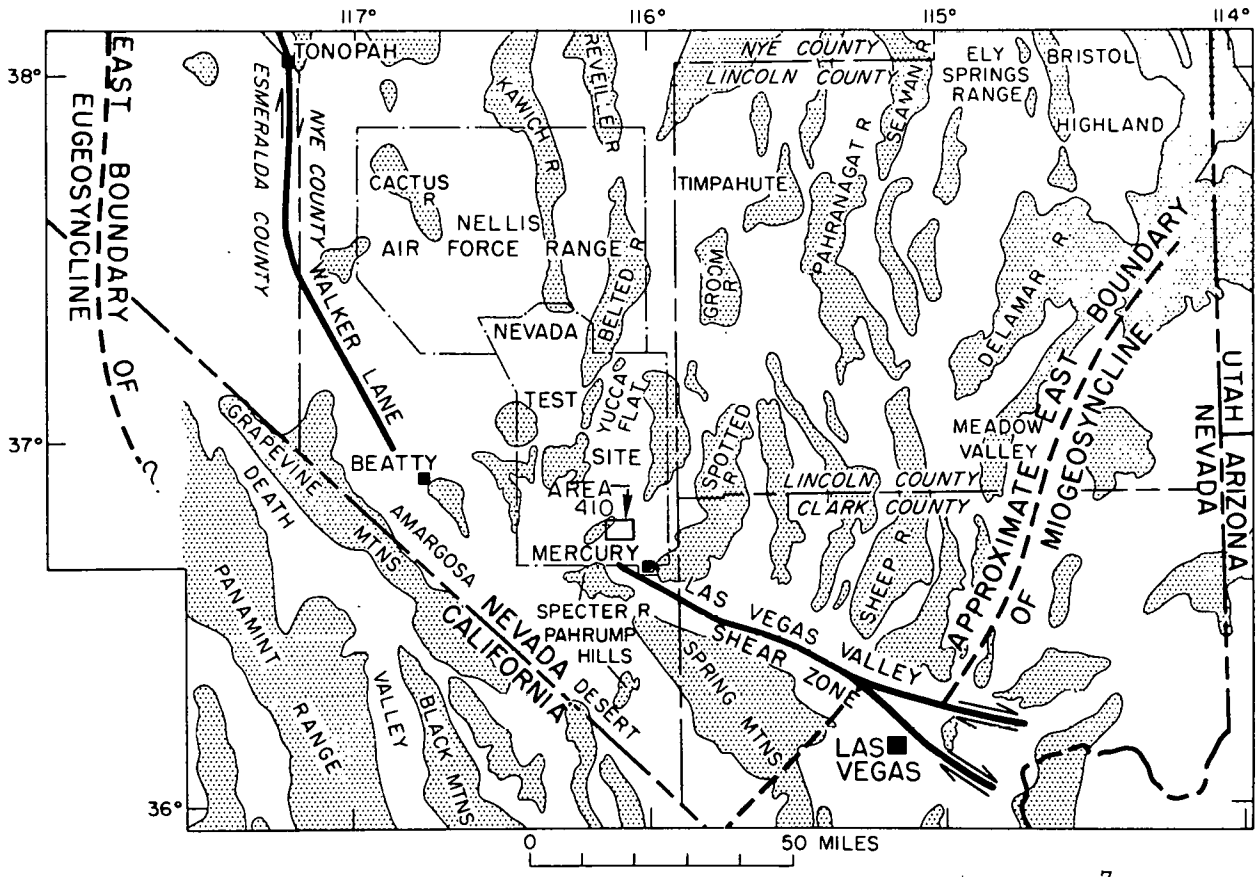

Fig. 3. Map showing extent of Cordilleran Geosyncline in vicinity of NTS.[7] (From Refs. 6 and 7. U. S. Geological Society of America.)

Table 1. Pre-Mesozoic Stratigraphic column for NTS and vicinity.

Geologic age	Geologic unit	Thickness (m)
Mississippian	Keeler Canyon Formation	65
	Red Spring Shale	120
	Perdido Formation	182
	Tin Mountain	91
Devonian	Lost Burro Formation	455
Silurian	Hidden Valley Dolomite	395
Ordvician	Ely Springs Dolomite	167
	Eureka Quartzite	100
	Pogonip Group	516
Cambrian	Nopah Formation	500
	Bonanza King Formation	1080
	Carrara Formation	405
	Zabriskie Quartzite	306
Precambrian	Wood Canyon Formation	680
	Stirling Quartzite	490
	Johnnia Formation	710
	Noonday dolomite and equivalent basinal units	330
	Kingston Peak Formation	1080
	Beck Spring Dolomite	340
	Crystal Spring Formation	1010

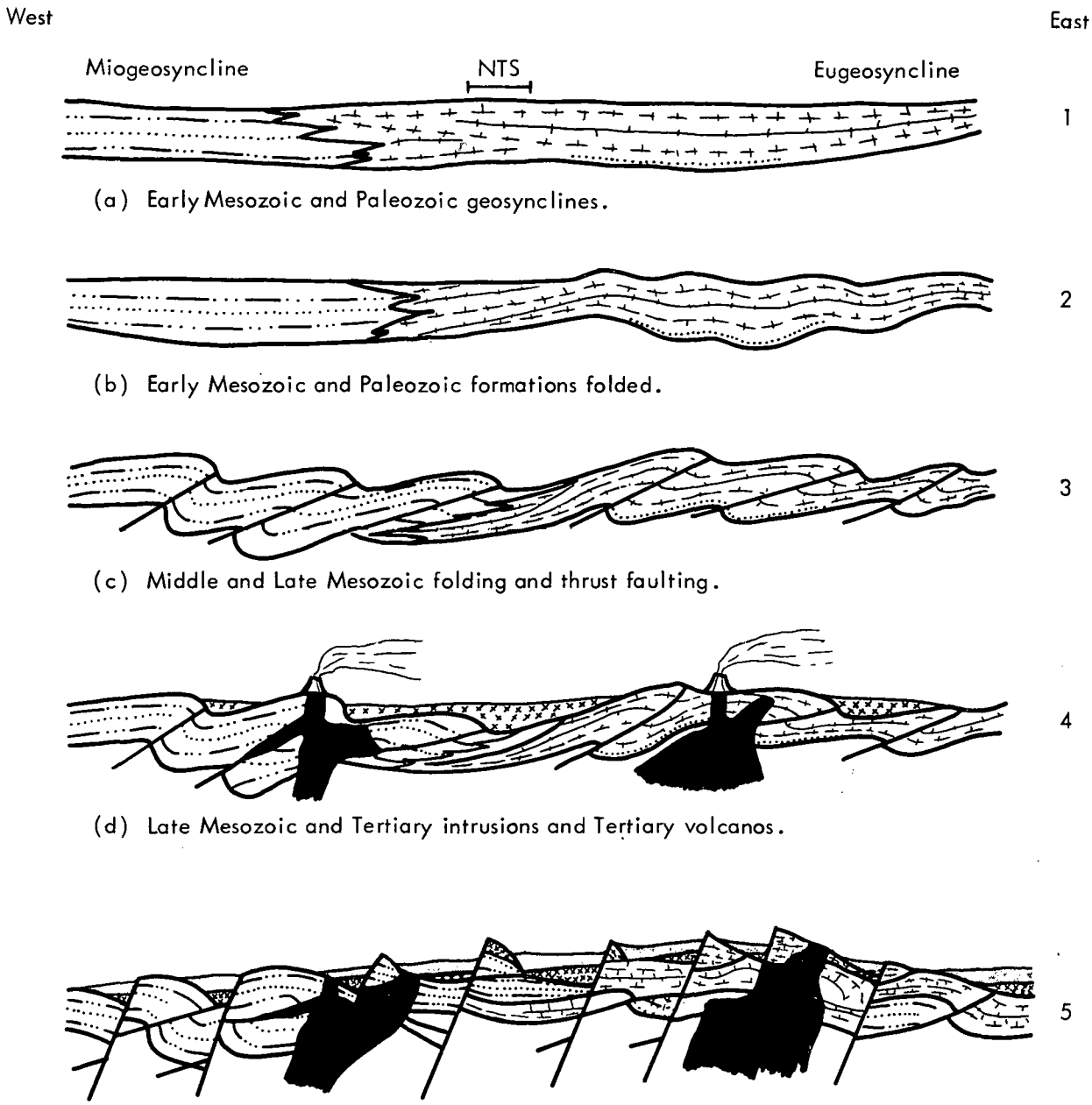

Fig. 4. Generalized evolution of structure and topograph in the vicinity of NTS.[1] (From Physiography of the United States by Charles B. Hunt. W. H. Freeman and Company. Copyright © 1967.)

root zone of the thrusts lies to the northwest of Yucca Flat.

Several episodes of Mesozoic thrusting have been recognized. Burchfield et al.[11] recognized a period of Jurassic (165 ± 4 m.y. and possibly 213 m.y.) thrust faulting in southeastern California, which they correlated with the thrusting observed at the NTS. Another episode of thrusting occurred between 75 and 90 m.y. ago in the Spring Mountains southeast of NTS.[12] King[2] notes that the Mesozoic deformation is progressively younger eastward across the foldbelt. Also, he noted that there is no clear separation between Middle Mesozoic and Late Mesozoic orogenies.

Starting approximately 26 m.y. ago,[4] the central part of the Cordillerian geosyncline was disrupted by block faulting resulting from extensional deformation. According to King,[2] major faulting occurred as recently as the early Pleistocene with minor faulting continuing today in places. It has been suggested by

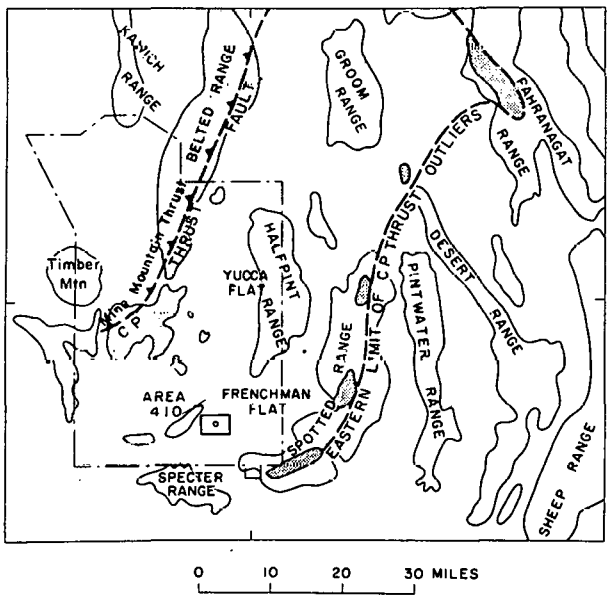

Fig. 5. Map showing Mesozoic thrust faults in NTS and vicinity.

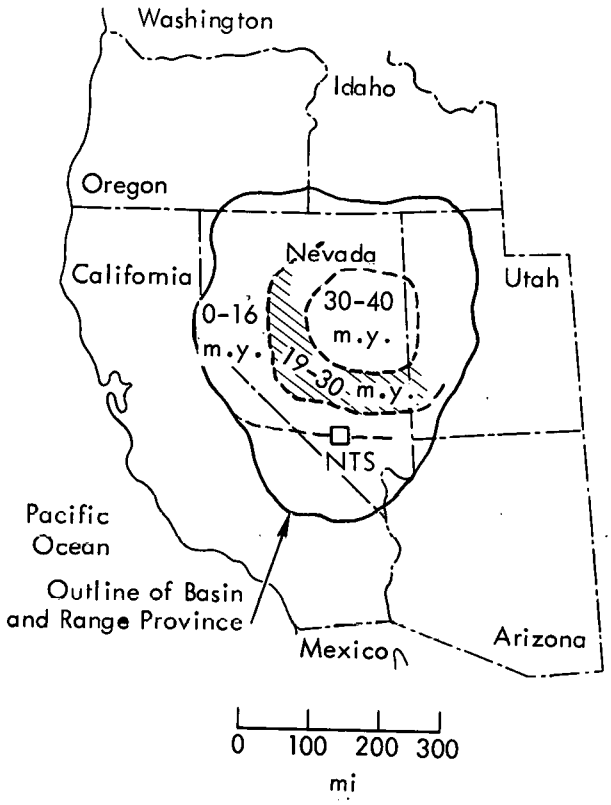

Fig. 6. Age distribution of Tertiary volcanism in Nevada.

Stewart[13] that the tensional deformation is the result of right lateral movement between the North American Plate and the Pacific Plate along the San Andreas and related faults. It is thought that the movement produces tensional fragmentation (Basin and Range structure) oblique to the trend of the plate boundaries.

An extensive period of volcanism started about 40 m.y.[14] and continued up until at least 0.25 m.y.[15] The oldest volcanic rocks occur most commonly in east central Nevada with the younger rocks occurring peripherally around the older center [Fig. 6 (Ref. 16)]. In addition, the older rocks are acidic in composition (andesite to rhyolite) while the youngest rocks are predominantly mafic (basalt). The acidic rocks are the most prevalent volcanic rocks in the vicinity of NTS.

NTS Geology

GENERAL GEOLOGY

The geology of NTS can be broadly divided into (1) a basement of compressively deformed Upper Precambrian and Paleozoic sedimentary rocks, (2) an overlying section of Tertiary and Quaternary volcanic rocks which are broken up by normal faulting, and (3) Late Tertiary and Quaternary alluvium and colluvium cut by normal faulting.

As noted before, the Precambrian and Paleozoic miogeosynclinal rocks at NTS can be divided into four groups. They are: (1) an Upper Precambrian and Lower Cambrian clastic sequence in which quartzite predominates, (2) a Middle Cambrian through Middle Devonian carbonate sequence, (3) the Devonian and Mississippian Eleana Formation composed of argillites and quartzites, and (4) a sequence of Late Paleozoic carbonates (see Table 1).

DEFORMATION AND VOLCANISM

During the Paleozoic and Mesozoic eras, these rocks were subjected to several periods of compressive deformation. At NTS, the Mesozoic deformation resulted in the formation of folds and thrust faults (Fig. 4 b, c). The major thrust faults formed were the C. P. Thrust and the associated Mine Mountain Thrust (Fig. 5).

The C. P. and Mine Mountain Thrust Faults are generally characterized by Upper Precambrian and Lower Paleozoic rocks overlying Middle and Upper Paleozoic rocks. Subsequently, the thrusts were cut by later normal faulting and have not been active in the Tertiary. (Fig. 4)

The Precambrian-Paleozoic rocks were locally intruded by Mesozoic plutonic rocks (Fig. 4d). Two small, predominantly quartz, monzonite stocks, the Gold Meadows stock and the Climax stock, are exposed in the northern part of NTS. They have an average K-Ar age of 93 ± 5 m.y.[17]

Tertiary volcanic rocks form a composite sequence over 12, 190 m thick.[17] These volcanic rocks, especially the pre-Upper Miocene formations, are irregularly distributed as a result of preexisting topographic erosion and subsequent structural deformation. The Upper Miocene tuffs of Crater Flat (13.8 ± 0.4 m.y.) are the oldest widespread units at NTS. The younger volcanic units are easier to correlate over long distances. The general stratigraphy of the volcanic rocks is given in Table 2.

The oldest volcanic rocks at NTS occur within the Oligocene (29 m.y.) Horse Springs Formation. The location of the volcanic center or centers from which this and other older tuffs originated is unknown. The tuffs and lavas on the NTS of Late Miocene and Pliocene age are from volcanic centers within and near the NTS (Fig. 7). Table 3 summarizes the data for those volcanic centers of interest. There appears to be a close relationship between volcanism and normal faulting both in time and space.[5] Carr[5] believes there is an association of eruptive centers and calderas with the intersection of right-lateral shear zones and northeast trending faults.

Table 2. Generalized stratigraphic column of Tertiary volcanic rocks at NTS.[17]

Unit	General lithology	Volcanic center
Thirsty Canyon Tuff	Peralkaline ash-flow tuffs	Black Mountain Caldera
Labyrinth Canyon Member Gold Flat Member Trail Ridge Member Spearhead Member		
Timber Mountain Tuff	Rhyolitic to quartz-latitic ash-flow tuffs	Timber Mountain Caldera
Ammonia Tanks Member Rainier Mesa Member		
Paintbrush Tuff	Rhyolitic to quartz-latitic ash-flow tuffs	Claim Canyon Caldera
Tiva Canyon Member Yucca Mountain Member Pah Canyon Member Topopah Spring Member Lavas of Scrugham Peak Quadrangle (interbedded with Paintbrush tuff)	Rhyolitic lavas	Local centers on south side Pahute Mesa
Wahmonie Formation Salyer Formation	Dacitic to rhyodacitic lavas, breccias, tuffs, and sandstones	Wahmonie Flat-Mt. Salyer
Stockade Wash Tuff	Calcalkalic rhyolitic ash-flow tuff	Silent Canyon Caldera
Tuffs and rhyolites of Area 20		
Belted Range Tuff	Peralkaline ash-flow tuffs	
Grouse Canyon Member Tub Spring Member Rhyolite lavas of Quartet Dome (interbedded with lavas and ash-flow tuffs from Silent Canyon Caldera	Rhyolitic lavas	Localized centers around Silent Canyon Caldera
Crater Flat Tuff	Low-silica rhyolitic ash-flow tuffs	Sleeping Butte Caldera in north west part of Timber Mountain Caldera Complex
Older Ash-Flow Tuffs	Rhyolitic to dacitic tuffs	North of NTS

The extension which produced the north to northeast trending normal faulting began between 14 and 17 m.y. ago[4] and is probably continuing today. At NTS, two normal fault systems are present (Fig. 8). The older set strikes northeast and northwest. This system appears to have formed during or shortly after the extrusion of the oldest tuffs. This is based on the observation that the frequencies of

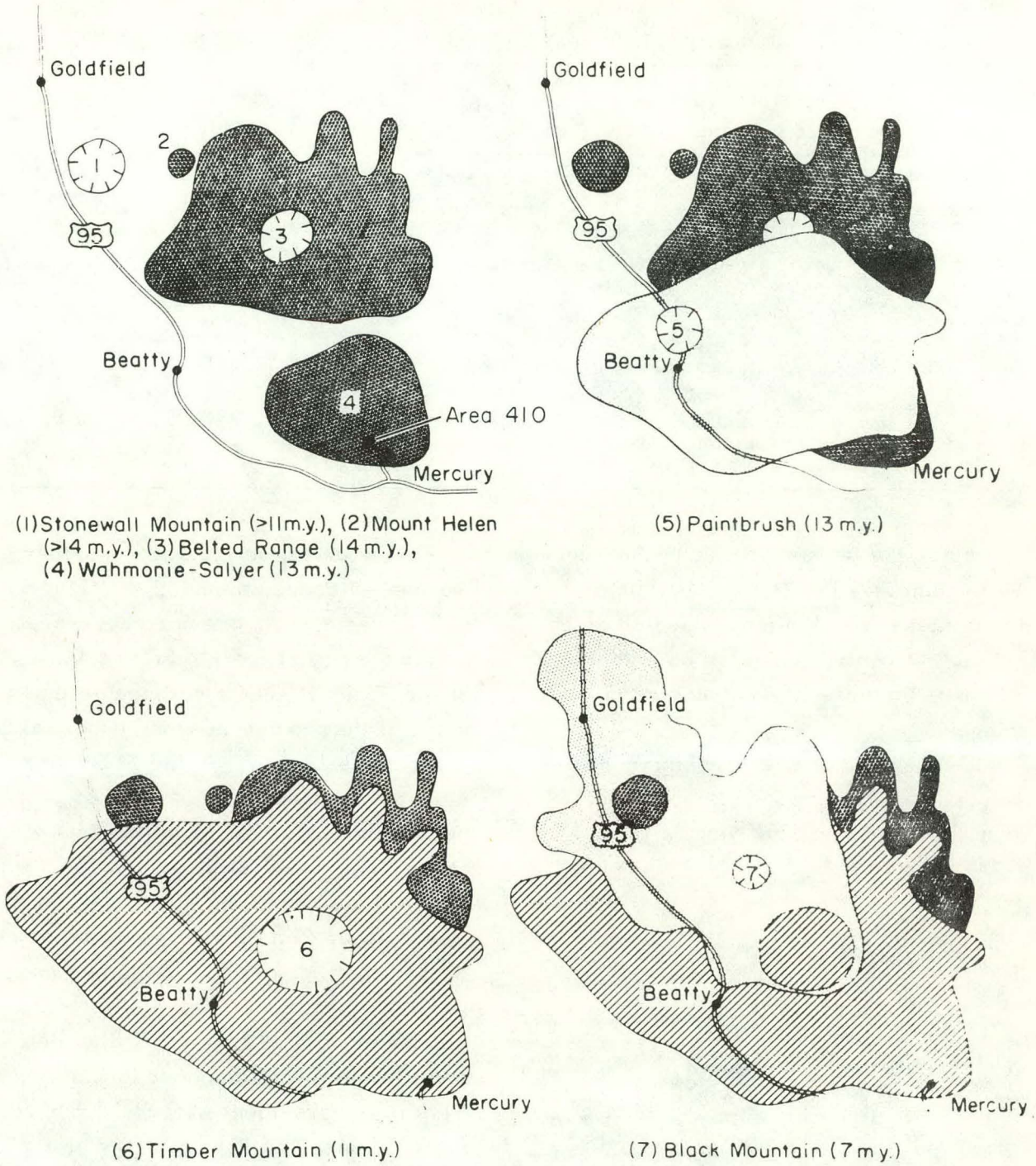

Fig. 7. Maps showing seven volcanic centers and five of the ash-flow tuff sheets that have been delimited in and adjacent to the NTS. (From Ref. 6. U. S. Geological Socicty of America.)

faulting in the older tuffs (>17 m.y.) and the pre-Tertiary rocks are similar. The older faulting appears to have ceased between 17 and 14 m.y. ago.

The younger fault set strikes north-south. This phase of faulting appears to have begun between 17 and 14 m.y. ago and is probably still continuing. For

Table 3. Summary of information for volcanic centers on and near NTS.

Volcanic center	Location	Associated lithologic unit	Age (m.y.)	Chemistry
Black Mountain	8 km west of NTS	Thirsty Canyon Tuff	7.5-6.2	Peralkaline
Timber Mountain	On western border of NTS	Timber Mountain Tuff	11.3-9.5	Calc-alkalic
Claim Canyon	35 to 40 km west of NTS in vicinity of Beatty, Nevada	Paintbrush Tuff	13.4-12.4	Calc-alkalic
Wahmonie-Salyer	6 km northwest of Area 410, NTS	Wahmonie Formation	12.5-12.9	Calc-alkalic
Silent Canyon	Beneath eastern Pahute Mesa, NTS	Belted Range Tuff	14.8-13.1	Peralkaline

example, the fault scarp along the Yucca Fault indicates its Recent Age. It is these faults with their north-south orientation that control the position and orientation of the present day basins and ranges.

The west-northwest-striking right-lateral Las Vegas Shear Zone is located just south of Mercury, Nevada (Fig. 3).

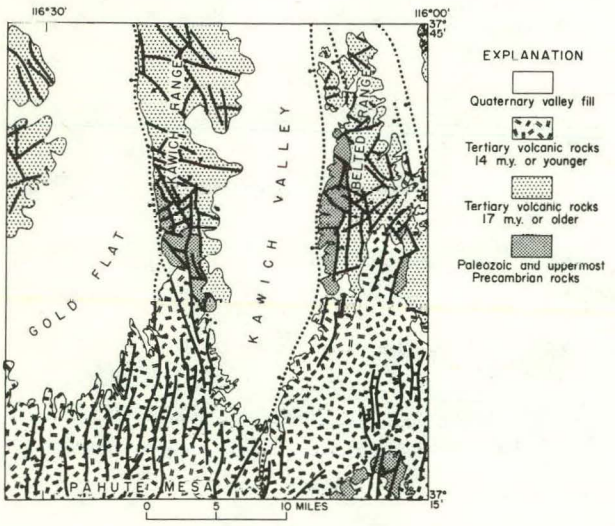

Fig. 8. Geologic map of the Belted and Kawich Ranges. (From Ref. 4. U.S. Geological Society of America publication.)

It is a major linear feature in southern Nevada. Because the north-striking ranges assume a more northeastwardly strike as they approach the Las Vegas Shear Zone, it seems reasonable that much of the movement along it has taken place since 17 m.y. In the Frenchman Mountain block east of Las Vegas, it appears that movement along the Las Vegas Shear Zone ended 11 m.y. ago.[18] Thus, much of the movement along the Las Vegas Shear Zone may have been restricted to a 6 m.y. period. Based on Longwell's[18] estimate of 67 km of lateral displacement along the zone, the displacement would be on the order of 1.1 cm/yr. This is in agreement with Stewart's estimate,[13] based on the geometry of block faulting, of 0.3 to 1.5 cm/yr. Southwest of Mercury in the Specter Range, the Las Vegas Shear Zone loses definition. Its extent and location to the northwest is unclear. Associated with the Las Vegas Shear Zone are several northeast-striking faults with left-lateral displacement ranging up to 5 Km. The Cane Spring Fault is one of these.

The final elements in the NTS geologic picture are the Late Tertiary and Quaternary alluvium- and colluvium-filled basins. Because they are structurally controlled by the north-south striking later fault systems, they must have developed and been filled with alluvium in the last 17 m.y. In some basins the alluvial fill is in excess of 1000 m thick. Several ages of alluvium have been recognized. A general stratigraphic column for alluvium-colluvium is given in Table 4. Some faults were contemporaneous with and/or postdated the younger alluvium. The Yucca Fault is an example.

GEOLOGY OF AREA 410

Area 410 is located in the southern part of NTS, near the southern boundary of the Southern Nevada Volcanic Field. The area falls within four geologic quadrangle maps. They are the Cane Spring Quadrangle,[19] the Skull Mountain Quadrangle,[20] the Camp Desert Rock Quad rangle,[21] and the Specter Range NW Quadrangle.[22] Within Area 410, the rocks are predominantly Tertiary tuffs and tuffaceous sediments and Tertiary or younger basalts, alluvium, and colluvium (Fig. 9).

Area 410 is southeast of the Wahmonie-Salyer Volcanic Center (Fig. 9). Most of the rock within this area is from that center. The older Salyer Formation occurs in the northeastern part of Area 410, while the younger Wahmonie Formations occurs over much of the remaining area. The Ammonia Tanks Formation overlies these older formations unconformably in some areas.

Cane Spring Wash and some of the hillsides are mantled with alluvium and/or colluvium of various ages. The older gravels are commonly more indurate than the younger alluvium. Alluvium and colluvium of at least four different ages have been recognized.[23] The oldest underlies the basalt of Skull Mountain. This is in turn unconformably overlain by alluvium and colluvium composed of boulders of Wahmonie lava and basalt of Skull Mountain. This alluvium is inferred by Ekren[23] to be either Late Tertiary or Very Early Quaternary. The basis for this inference is the amount of erosion this unit is assumed to have undergone. The definite Quarternary alluvium occurs in and adjacent to the present day stream channels. The colluvium consists of talus and landslipped blocks on the flanks of the hills and mountains.

The predominant structures in the area are a series of northeast-striking faults, of which the Cane Spring Fault is the longest. On the geologic map of Area 410, most of the faulting appears to be concentrated in the Salyer Formation and older units. There may be several reasons for this. They include: (1) these rocks are older and have been subjected to more tectonic activity, and (2) these lithologic units are thinner and more recognizable, thus faulting within them may be easier to recognize. The Ammonia Tanks member definitely appears to be less faulted than the underlying rocks. This means that much of the northeast faulting is pre-Ammonia Tanks and therefore occurred before 11 m.y. ago. This is in agreement with the end of movement along the Las Vegas Shear Zone as postulated by Longwell.[18] It should be noted

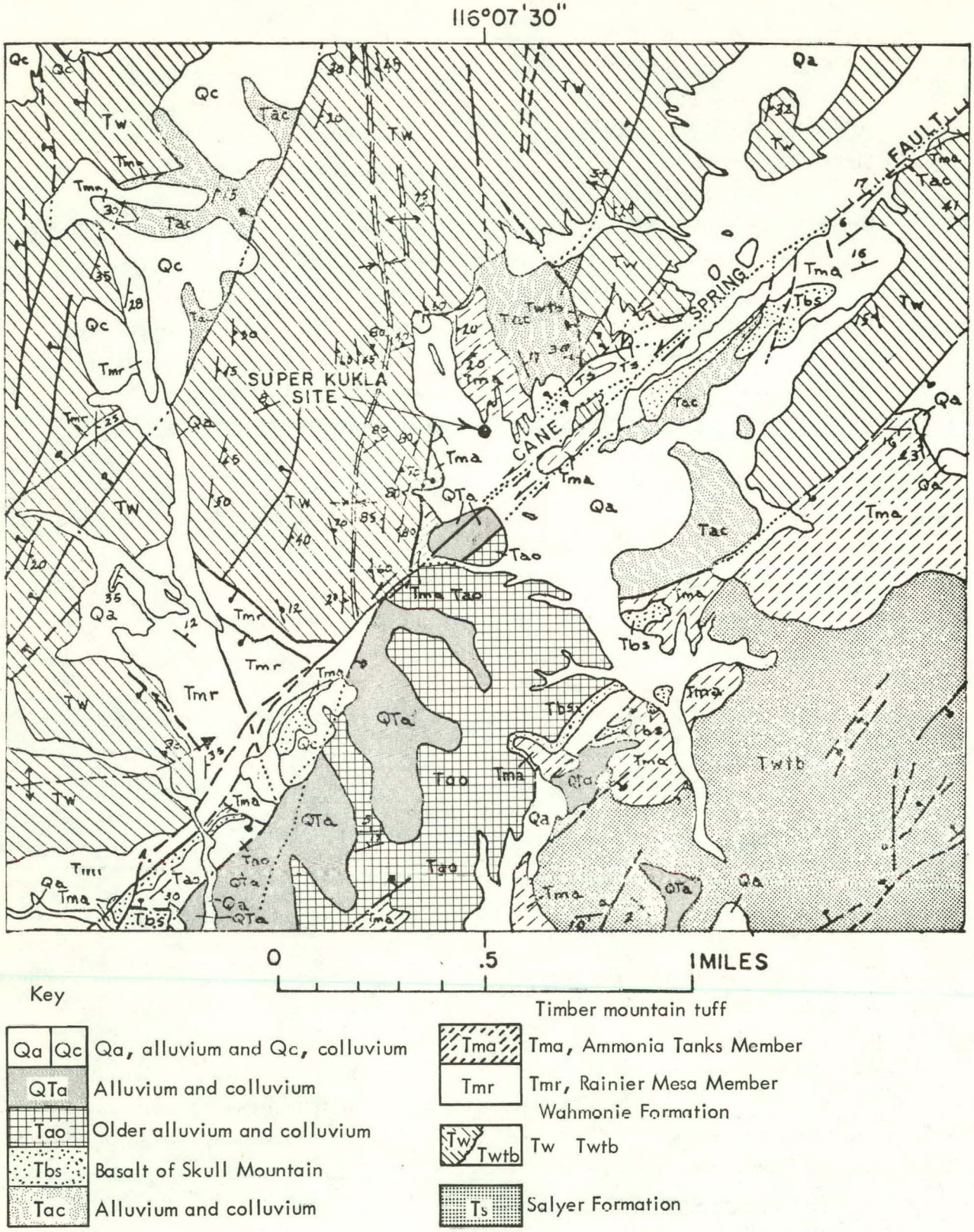

Fig. 9. Generalized geologic map of Area 410.

Table 4. Alluvium stratigraphy column in Cane Spring Quadrangle.

Geologic age	Lithology	Thickness (m)
Quaternary	Alluvium	0 - 30
	Alluvium and colluvium	0 - 150
	Older Alluvium	0 - 10
Late Tertiary or early Quaternary	Alluvium and colluvium	0 - 45
	Basalt of Skull Mountain	0 - 15
Tertiary	Alluvium and colluvium	0 - 75

that the Cane Spring Fault was active in the post-Ammonia Tanks period.

Much of the faulting on the southeast side of the Cane Spring Fault appears to have been inactive for the last 11 m.y. The Cane Spring Fault and parallel faults to the northwest offset the basalt of Skull Mountain (which is inferred to be 7 m. y. old).[23]

The age of the last movement on the Cane Spring Fault is difficult to determine. The alluvium directly overlying the basalt of Skull Mountain was offset by the Cane Spring Fault.[20] This alluvium is inferred to be Late Tertiary or very Early Quaternary. Photolineaments in alluvium parallel to the northeast extension of the Cane Spring Fault were field-checked by Ekren.[23] He could detect no displacement in either the alluvium of Cane Spring Wash or in the top few feet of underlying older alluvium.

Thus, on the basis of the displacement of sediments, we have no conclusive evidence that the fault should be considered active. However, we do have two other lines of evidence that NTS, in general, and these sites, in particular, are located in regions which are undergoing active deformation:

(1) As a result of examining a number of factors including borehole deformation, directions of crack propagation following nuclear events, seismic data, and strain measurements, Carr[5] has proposed that the NTS is undergoing extension in a N50°W - S50°E extension.

(2) Seismic evidence (Fig. 10) shows earthquake epicenters have been located as close as 5 km to the Cane Spring Fault. In addition, the Massachusetts Mountain Earthquake of August 5, 1971, occurred near the intersection of a northwest-trending structural lineament and a possible extension of the Cane Spring Fault. Although the earthquake, the fault, and the northwest-trending lineaments have an uncertain relationship, Carr[5] believes that the fault and the other features have "...been active concurrently and tend to offset one another."

Therefore, we are in the position of having a zone of significant structural weakness located in an area of active seismicity and structural deformation but of having no evidence for recent

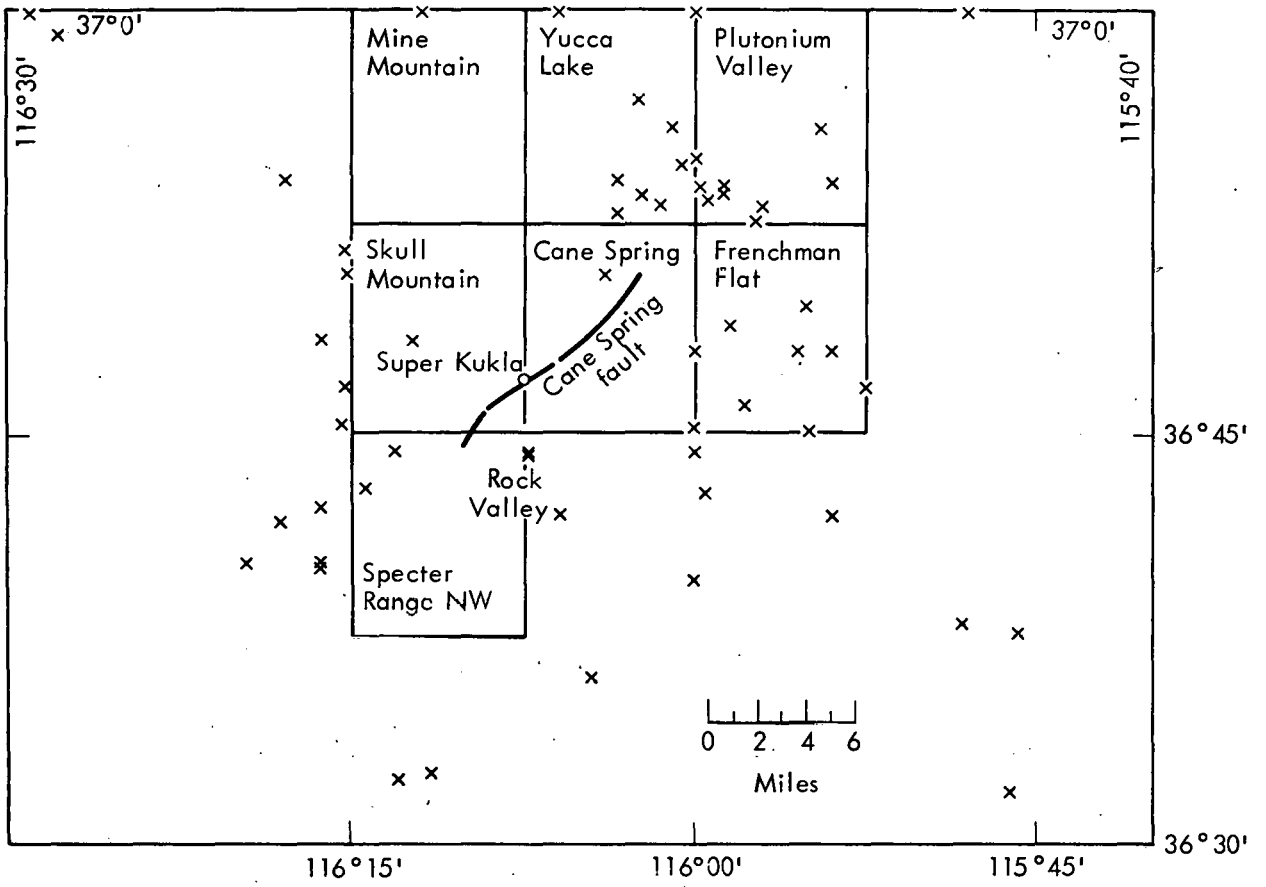

Fig. 10. Seismicity of area surrounding Super Kukla Reactor Site between 1961 and 1972.[23]

movement along the fault trace. It is our position, and that of Ekren,[23] that the continuing activity in the area together with the existing evidence of structural weakness provide sufficient evidence that the Cane Spring Fault should be considered active for seismic safety analysis purposes.

GEOLOGY OF SPECIFIC BUILDING SITES IN THE AREAS OF INTEREST

At the time of this study, there were a number of buildings of interest in the three areas. These included buildings 5100, 5120, 5130, 5140, 5310, 5318, 5319, 5320, 5325, 5400, and 5410 (Fig. 11). Our investigations of these buildings indicated that their foundations rest on either bedrock or shallow soil layers whose thickness is less than a small fraction of a wavelength for the frequencies of interest.

In general, there are numerous small faults throughout Area 410. The larger of these are shown on Fig. 11. Many small faults, which can not be adequately shown on Fig. 11, are present throughout the area. Such faults commonly have less than a meter of displacement and can be traced only for a few tens of meters.

As new buildings are considered in the area, the specific building sites will

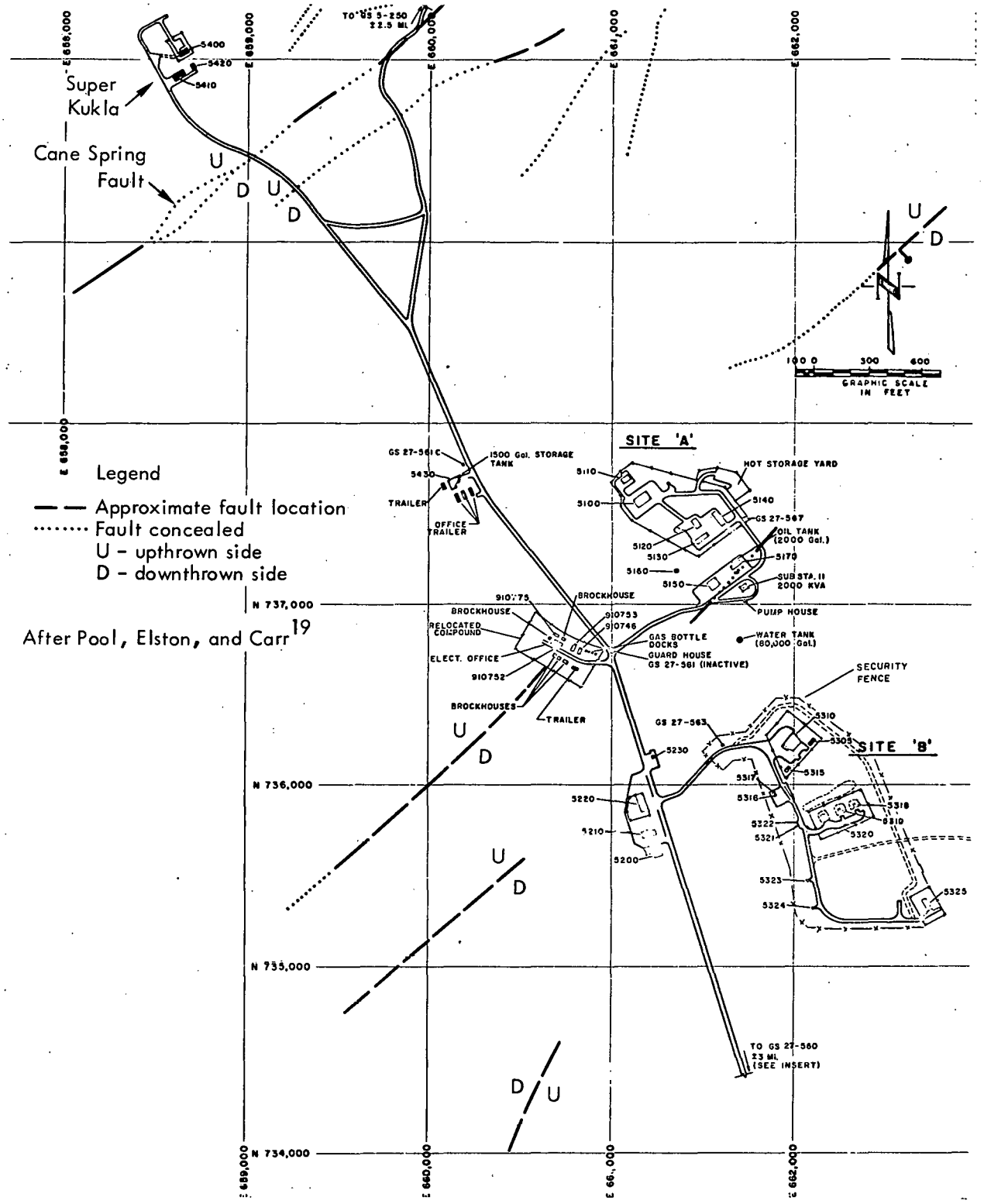

Fig. 11. Distribution of faults in vicinity of Super Kukla, Site A, and Site B.

have to be examined for the presence of these minor faults. Also the soil thickness will have to be examined. With the exceptions of these two localized features, this report should provide sufficient information for the seismic safety analysis of the proposed construction.

Regional Seismicity

The previous sections described the geologic history of NTS in general and Area 410 in particular. In the following sections, we use this information together with information about the seismicity during historic times to estimate the Safe Shutdown Earthquake (SSE), i.e., the earthquake producing the maximum vibratory accelerations at the site.[24] The characteristics of this SSE can then be used in evaluating the response of buildings at the Super Kukla Site and areas A and B (Fig. 11).

In Table 5, we list the earthquakes of magnitude 6 or greater that have occurred within historic time at distances less than about 320 km from NTS. Table 6 gives additional smaller earthquakes in the magnitude range 4.0 to 6.0 which occurred in the area 36°-37°N by 115°-116°W. These data were drawn from the articles by Slemmons et al.,[25] Ryall et al.,[26] and Gumper and Scholz[27] for the years prior to 1960 and from the work of Landers[28] for subsequent years. From these tables and from the curves of maximum acceleration versus distance from the causative fault given in Schnabel and Seed,[29] we can conclude that, except for the motion generated by the Owens Valley earthquake of 1872, Area 410 has not been subjected to peak ground accelerations in excess of 0.05 g in historic times from earthquakes within a radius of 320 km. (The Owen's

Table 5. Historic earthquakes occurring within 320 km of NTS having magnitudes ≥ 6.0.

Date	Latitude	Longitude	Magnitude	Approximate distance (km)	Descriptive name
03/26/1872	36.8	118.2	8.3	160	Owen's Valley
11/10/16	35.5	116.0	6.1	140	So. Nevada
09/18/27	37.5	118.8	6.0	255	Long Valley
12/21/32	38.8	118.0	7.2	280	Cedar Mtn.
01/30/34	38.3	118.4	6.3	270	Excelsior Mtn.
03/15/46	35.7	118.0	6.3	210	Walker Pass
04/10/47	35.0	116.3	6.4	200	Manix
12/04/48	33.9	116.3	6.5	320	Desert Hot Springs
07/23/52	35.3	118.6	6.1	280	Kern Co.
07/29/52	35.3	118.8	6.1	290	Kern Co.
08/16/66	37.4	114.2	6.1	180	So. Nevada

Table 6. Historic earthquakes occurring within the area 36°-37°N by 115°-116°W and having magnitudes in the range 4.0-6.0.

Date	Latitude	Longitude	Magnitude	Approximate distance (km)
11/10/16	36.2	116.0	—	70
03/28/34	37.3	116.6	4.5	70
03/30/34	37.7	115.3	4.9	120
03/30/34	37.7	115.3	4.0	120
03/31/34	37.7	115.3	4.0	120
04/10/36	37.1	115.6	4.0	60
06/10/36	36.6	115.5	—	60
07/28/36	37.6	115.8	4.0	90
07/28/36	37.6	115.8	—	90
07/28/36	37.6	115.8	4.5	90
07/28/36	37.6	115.8	4.0	90
11/21/39	36.5	115.0	4.0	100
03/10/40	37.5	115.0	5.0	130
03/11/40	37.0	115.0	4.5	100
04/07/40	37.0	115.0	4.5	100
05/09/40	36.2	116.2	—	70
10/12/40	37.5	115.0	—	130
06/06/41	37.1	115.8	4.0	40
09/29/54	37.5	115.8	4.4	80
03/17/55	36.2	115.2	—	100
01/28/59	36.8	116.2	4.0	10
03/27/61	36.6	116.3	4.4	30
05/07/67	37.0	115.0	4.7	100
01/06/69	37.3	116.5	4.5	70
08/10/70	37.2	115.9	4.1	50
08/05/71	36.9	116.0	4.3	15[a]
02/19/73	36.8	115.9	4.5	20[b]

[a] Massachusetts Mountain.
[b] Ranger Mountain (Frenchman Flat).

Valley earthquake could have generated peak accelerations of 0.1 g.)

Nuclear explosions are the other source of significant ground motion during historic times. Using the prediction equations given in the manual published by the Environmental Research Corporation,[30] we calculated the maximum ground acceleration from past events to be 0.04 g. We shall see that all of these historic sources are much less than the motions predicted from the SSE generated for the Cane Spring Fault.

Characterization of the Seismic Source and the Properties of the Ground Motion

In the previous section, we have considered the events occurring in historic time and have, in a sense, established a lower bound for peak acceleration of 0.1 g. To estimate the upper bound required by the definition of the SSE, we shall assume that the maximum earthquake will occur along an existing fault. This is reasonable in the sense that these zones of weakness are likely sites for new earthquakes. Furthermore, it allows us to correlate observed parameters with prior empirical studies to establish a consistent prediction process. The uncertainties are large. However, we do not see any reasonable alternative, consistent with the reactor siting guidelines.

THE METHOD USED

Wight[31] describes a process which uses the observed fault length and previous studies to estimate the maximum earthquake. Although there are a number of uncertainties, his approach provides a systematic method of addressing the problem. A brief description of the process follows. Given the total fault length, the length of rupture is estimated at one-half the observed fault length following Albee and Smith.[32] Then the works of Lieberman and Pomeroy[33] and Housner[34] relating the rupture length and the magnitude of the earthquake are used to estimate the magnitude of the SSE (see Fig. 12 which is a modified version of Wight's[31] Fig. 11). Once the magnitude of the SSE is known, the results of Schnabel and Seed[35] are used to estimate the maximum acceleration as a function of distance for a given magnitude (Fig. 13) for distances greater than 5 km.*

For distances less than 5 km a different approach is used. Some of the difficulties involved in making predictions at these short distances are discussed in Boore and Page[36] and Boore.[37] In general, we shall use an approach based on the maximum accelerations observed at similar sites.

*Although the exact value used is somewhat arbitrary, the value chosen is consistent with the lower limit of the distance for standard acceleration versus distance curves. (For an example, see Ref. 32.)

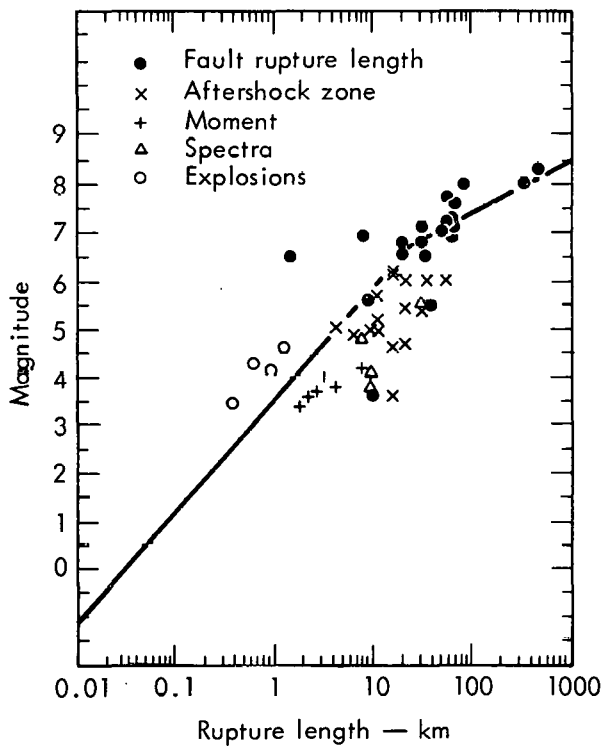

Fig. 12. Earthquake magnitude as a function of rupture length along the fault. Data is from Ref. 33 and the curve from Ref. 34.

The other quantity which we want to generate is the time history of the SSE. It can be derived from the ground motion recorded at a comparable site or from the spectra scaled from those provided in Ref. 38 if the distances are greater than 5 km. Both procedures are mentioned in Wight's report. In the event that the latter approach is used, there are standard procedures[39] for generating a synthetic seismogram having the specified response spectrum.

Finally, some attempt must be made to correct for the effect of soil if that is present. One approach for doing this is that used by Seed and Idriss.[40,41] Wight goes into more detail about the various methods used. Since soil effects are negligible in the present case, we suggest that the interested reader check Wight's work and his references.

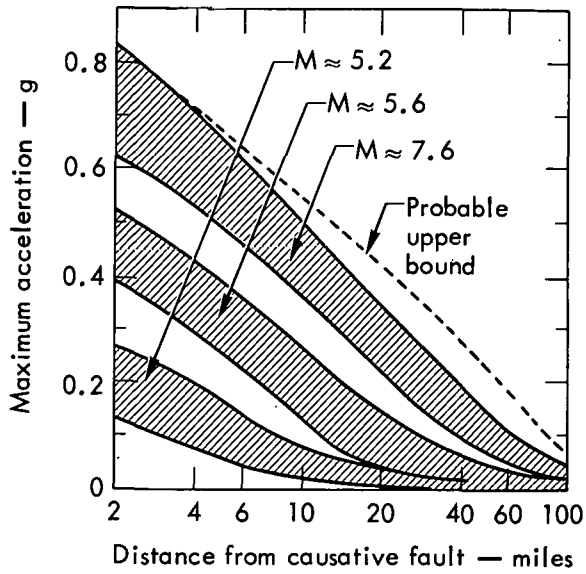

Fig. 13. Maximum acceleration as a function of distance for given magnitudes.[35]

HISTORICAL OBSERVATIONS OF LARGE ACCELERATIONS

Since we are interested in predicting the properties of the SSE, which, by definition, is concerned with the maximum vibratory acceleration, it is worthwhile to specifically examine some of the larger accelerations that have been observed in the western U.S. Wight does this in his report to some extent, but the importance of the subject makes a repetition worthwhile. In general, the value of the observed peak acceleration has risen as the number of strong motion instruments has increased. Prior to 1966, the highest ground accelerations (0.3 g) had been recorded during the El Centro, California, earthquake of May 18, 1946, and the Olympia, Washington, earthquake of April 13, 1949.

In 1966, a magnitude 5.5 earthquake occurred on the San Andreas Fault near Parkfield, California. It was accompanied by surface breakage along approximately 32 km of the fault. A number of seismic stations had been emplaced in a line across the fault at the time of the earthquake. Properties of selected stations in this array are given in Table 7 using data from Cloud and Perez.[42] The immediate consequence of the N65E measurement at Station 2 was to raise the maximum observed peak acceleration to 0.5 g. In addition, the missing record from the instrument N25W took on added importance both because of the possibility that it might have recorded even larger accelerations and because the peak acceleration should be determined from the vector sum of the two horizontal

Table 7. Selected station and acceleration data for the Parkfield earthquake.

Station name	Distance to fault (km)	Foundation	Orientation	Peak acceleration (g)
Temblor	6.4	Alluvium	N65W	0.27
			vertical	0.16
			S25W	0.40
2	0.1	Alluvium	N65E	0.50
			vertical	0.35
			N25W	Missing
5	5.3	Alluvium	N85E	0.46
			vertical	0.18
			N5W	0.40

components.* An initial investigation by Housner and Trifunac[43] using a seismoscope record from Station 2 indicated that the acceleration on the component oriented N25W was stronger than the 0.5 g recorded on the component oriented N65E. This was consistent with the fact that the fault exhibits right lateral strike slip motion along a trend N25° - 40°W which is nearly parallel to the direction of motion measured by the N25°W accelerometer. Later, Trifunac and Hudson[44] were able to reconstruct the missing component using a seismoscope record from the same area. The reconstruction indicated that the missing component was 25-30 % higher than the one which had been recorded. The combined components indicate a peak acceleration of 0.7 to 0.8 g rather than the 0.5-g maximum which is usually cited from the examination of the N65°E record. Although Station 2 was located on alluvium, there are indications[42] that soil amplification effects are negligible in the period range of interest.

Further support to these values of high ground acceleration was provided by the record made by the accelerometer at Pacoima Dam during the San Fernando, California earthquake (magnitude 6.6) of February 9, 1971. The recording site was about 4 km from the surface rupture associated with motion on the Tujunga Thrust Fault. The surface rupture is about 15 km in length and the dam is located at about the center of the rupture. The topography is quite rugged and the accelerometer was located on a rocky spine extending out into the valley containing the Pocoima Dam.[44] During the earthquake, several cycles of acceleration in the range 0.6 - 0.7 g were observed early in the record and one peak of 1.25 g was observed on each component later in the record (see Fig. 14).[44] From the vector sum of the components, we conclude that the site was subjected to peak accelerations similar to 1 g early in the disturbance and as high as 1.6 g later. Several explanations of these high accelerations have been put forward. These involve

*However, note that it seems to be customary practice to use merely the largest component of acceleration which has been recorded, not the vector sum which represents the true maximum acceleration. The main reasons for this appear to be related to matters of convenience and have little or no technical justification.

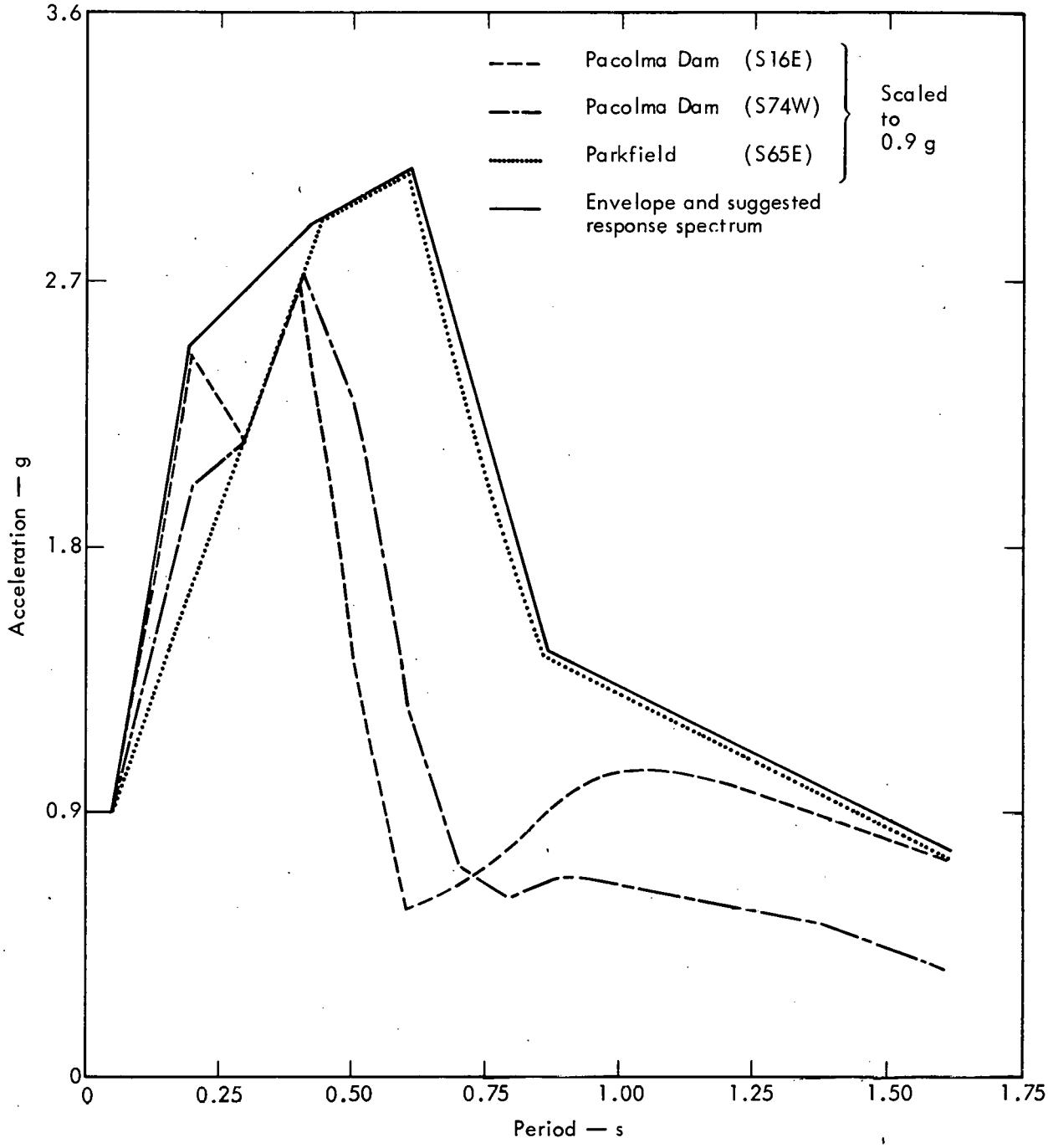

Fig. 14. Scaled and suggested horizontal response spectra for Area 410 seismic safety analysis.

effects due to a combination of localized rupture effects and low attenuation in the hard rock material at the site[45] and site topography.[46-48] Two of the latter articles, Refs. 46 and 48, are based on numerical modeling of the area around the dam. They obtain reductions in peak acceleration from 1.25 g to 0.73 and 0.40 g, respectivcly, as a result of filtering and correction for the topography. The other article[41] used measurements made at the damsite and surrounding areas for eight

aftershocks to compute empirical topographic corrections. These gave reductions in the peak g-levels of the components from 1.25 to 0.89 g or 0.76 g depending on the component. Because of the uncertainties in the numerical modeling involved in the other two studies, we tend to give greater weight to this empirical investigation. We use an average reduction factor of 0.65 to correct for the topographic amplification of the vector sum. This gives a corrected peak vector acceleration of 1.0 g.

In addition to the observational evidence, a number of "order of magnitude" calculations[49, 50] indicate that there is no theoretical reason why peak accelerations greater than 1 g cannot occur. Furthermore, a number of references[24, 36, 37, 51] indicate that the behavior of the near fault region (2-5 km) cannot be described by an extrapolation of curves based on data from distances greater than 5 km. Also, these references indicate that there is only a rough correlation of peak acceleration with either magnitude or geology in the fault region. These conclusions are in agreement with the intuitive feeling that the peak close-in effects should depend on such things as the shear strength of the material, the stress drop, the attenuation, and the nature of the fracture zone. Further, we expect the effects of fault geometry to be important at short distances.

In summary, we have the following observational evidence regarding the ground motion at sites less than 5 km from the fault zone:

- Single peaks as high as 1.6 g have been recorded in the vector ground accelerations in areas with large topographic relief. Even after applying an empirical correction factor of 0.65 on the basis of observations made by Mickey, Perez, and Cloud,[47] we have a corrected, vector ground acceleration with a peak of 1.0 g.
- Vector ground accelerations with single peaks near 0.8 g have been observed in less rugged areas.
- The component peak acceleration at short distances is only roughly correlated with the magnitude of the earthquake.
- Predictions for distances less than 5 km cannot be made on the basis of curves constructed from measurements made at larger distances.

THE SAFE SHUTDOWN EARTHQUAKE

Recognizing the many uncertainties inherent in the process, we can now use the prediction process outlined in the preceding sections and the cited references to obtain an estimate of the peak accelerations and the safe shutdown earthquake for Area 410 at NTS. In Table 8, we list the various faults which have been identified out to a distance of 320 km and give various observed and derived properties.[52-55] As previously discussed, we have considered all of the faults in the immediate area to be active. Since all of the buildings of interest are within less than 2 km of each other, we have used a single distance to the faults for all of the buildings. In general, the magnitudes were computed by the method described previously. The Owens Valley, the Cane Spring, and the Massachusetts Mountain - Cane Spring Complex values are exceptions to this. For the Owen's Valley result, we used the historically observed magnitude of 8.3

Table 8. Observed and derived properties of major faults within 320 km of Area 410 at NTS.

Fault	Distance to fault (km)	Length of fault (km)	Maximum rupture length (km)	Past displacement (km)	Magnitude[a]	Peak acceleration (g)[b]	Remarks
Cane Spring	0.2	16-18	8-9	1.6-4.8	5.8	0.9[c]	One of a series of left-lateral in echelon faults associated with Las Vegas Shear Zone.[20]
Massachusetts Mountain	9.0	1.6-3	0.8-4	1.6	5.3	0.2	A series of NE and NW striking faults. Possible extension of the Cane Spring Fault. Massachusetts Mountain earthquake (mag 4.3) occurred 8/5/71 near junction with Cane Spring.
Massachusetts Mountain plus Cane Spring	0.2	18-26	9-13	1.6-4.8	6.1	0.9[c]	This gives an estimate of the combined system.[5]
Yucca	14	24-32	12-16	0.2	6.5	0.4	A right laterial fault with some vertical displacement.[5]
Las Vegas	16	130	65	64	7.0	0.5	Major regional feature with right lateral slip.[5, 15]
Furnace Creek-Death Valley	64	300	150	80	7.5	0.2	Recent movement on some associated faults.[8, 52]
Garlock	130	240	120	20	7.4	0.05	Active slip movement during recent times.[53, 54]
Owens Valley	160	180	90		8.3[d]	0.1	Large earthquake associated with fault in 1872.
White Wolf	260	70	35	3 (vertical)	7.2	<0.05	Reverse fault. Recent earthquake activity.[53]
San Andreas	310	960	480	105-560	8.2	<0.05	Ref. 55.

[a]Estimated from Fig. 12 and the maximum rupture length unless otherwise noted.

[b]Estimated from Fig. 13, the magnitude and the distance unless otherwise noted.

[c]Estimated from Pacoima Dam and Parkfield spectra suitably scaled.

[d]Historic maximum.

associated with the 1872 earthquake and calculated the acceleration from Fig. 13.

We can expect that the ground motion appropriate for sites near the Cane Spring Fault and the Massachusetts Mountain – Cane Spring Complex Fault could be as great as that experienced at sites near the San Fernando and Parkfield earthquakes. These had corrected peak vector accelerations of 1.0 g and 0.8 g, respectively. However, the earthquake magnitude for the Cane Spring Fault (5.8-6.1) is intermediate to those of the San Fernando (magnitude 6.6) and Parkfield (magnitude 5.5) earthquakes. Therefore, we choose the intermediate value of 0.9 g as being appropriate for the peak acceleration to be associated with the SSE occurring on these faults.

Finally, we are left with the problem of determining the response spectra to be used for the SSE. In general, the effect of attenuation suggests that two different response spectra be generated. One, for close-in earthquakes of moderate size, would be rich in high-frequency components. The other, for very large, distant earthquakes, would be relatively rich in low-frequency components. However, in the present case, the effects of the large earthquakes at distance are secondary to those of the projected magnitude 5.8-6.1 earthquake on the Cane Spring – Massachusetts Mountain Faults. Therefore, we will use the spectra developed for these faults with proper scaling as described below.

In Fig. 14, we give the horizontal response spectrum estimated for Area 410. The response spectrum is the envelope of the two components of the Pacoima Dam records (Fig. 15), the San Fernando earthquake, and the N65°E component of the Station 2 record for the Parkfield earthquake (Fig. 16), all scaled to 0.9 g. Data were obtained from Refs. 56 and 31, respectively.

Although the spectrum is reasonable in view of the accepted engineering practice [compare, for example, a curve (not shown) constructed for 0.7 g by the methods of Refs. 38 and 57], we believe that present practice places undue emphasis on the zero period value in the spectrum. At one point we considered scaling on the basis of the average of the highest of four peak accelerations. This approach has the merit of reducing the emphasis placed on a single peak (see Ref. 35, for some comments on the dependence of spectra on single peaks). It gave spectra which were about 10% higher and gave closer agreement between the Parkfield and Pacoima Dam spectra. However, since we consider 10% variation to be within the uncertainty of the present curve, since the present curve corresponds to accepted practice, and since we are not in a position to justify a new approach at this time (although we believe a new approach should be developed), we present the results of Fig. 14.

To obtain an estimate of the response spectrum for the vertical displacement, we suggest the procedure relating the horizontal and vertical spectra given in Ref. 38. In general, the suggested vertical response spectra values are two-thirds those of the horizontal spectra for periods greater than 4 s; for periods less than 0.3 s, they are the same; and for periods between 0.3 and 4 s, the ratio varies from two-thirds to one.

The values for the Operating Basis Earthquake are strictly speaking the

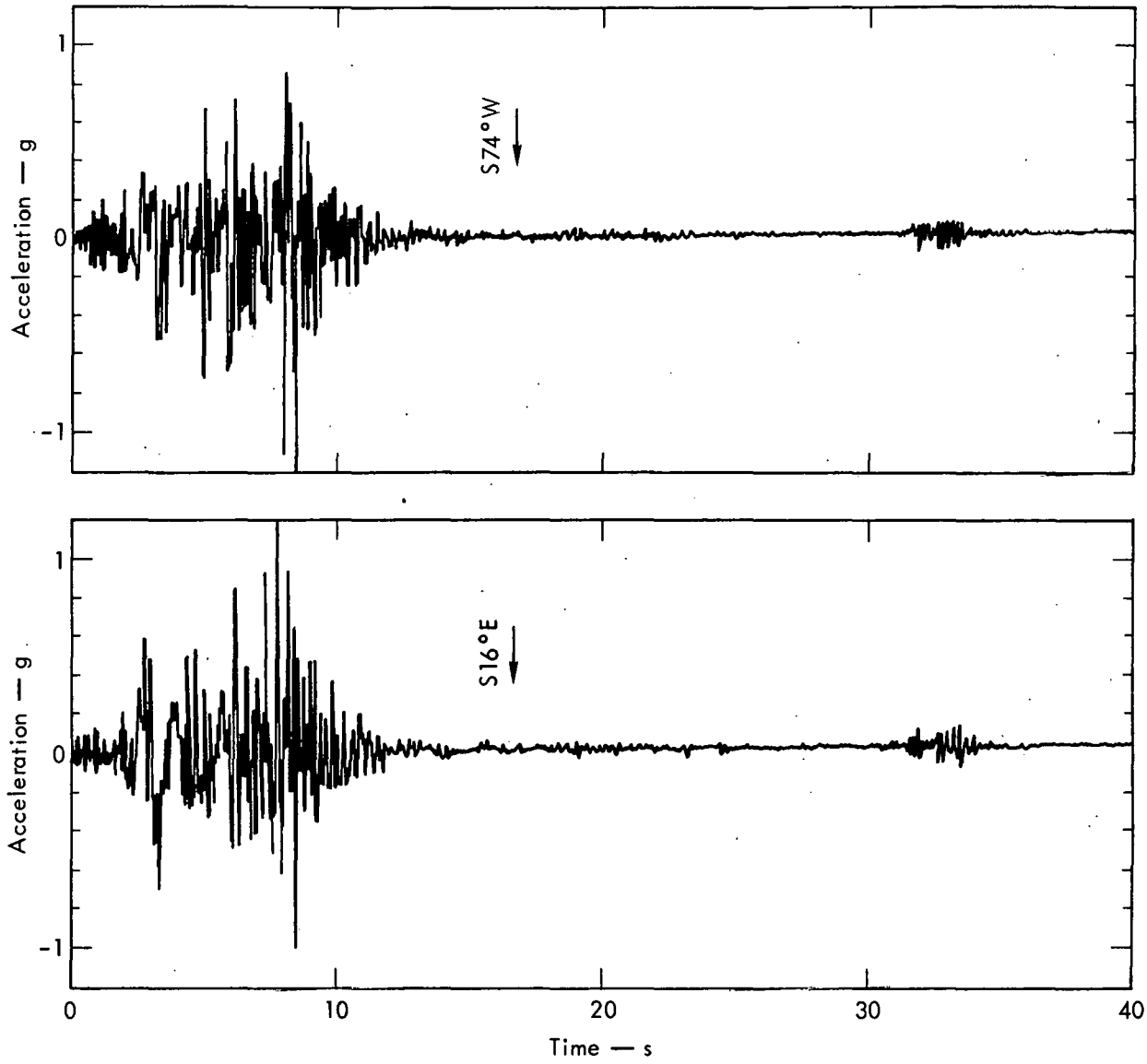

Fig. 15. Plot of accelerograms recorded at the strong motion site adjacent to Pacoima Dam.[44]

province of the design engineer. We note that common practice is to use an Operating Basis Earthquake corresponding to one-half the SSE.

In general, spectra determined in this way should be corrected for soil amplification. However, since the buildings in question are sited on bedrock or, at most, one to two meters (less than a small fraction of a wavelength) of alluvium, there is no need to correct the soil layer for the

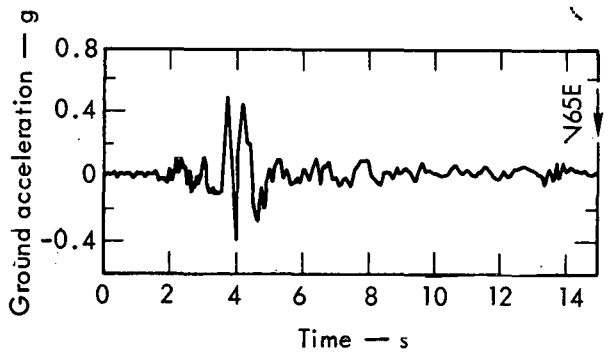

Fig. 16. Plot of accelerogram recorded at strong motion Site No. 2 for the Parkfield earthquake.

purpose of determination of the seismic motion. However, the presence of such a layer of alluvium is of possible importance in the interaction of the soil and the foundation.

Finally, we consider the relative displacements to which the buildings might be subjected by faulting. The Cane Spring Fault is an obvious zone of weakness in the earth's crust and the whole area must be considered to be subject to significant tectonic stress and to be in a zone of continuing seismic activity.[5,6] Faulting associated with this zone of weakness could occur anywhere along a broad zone including the region occupied by the buildings of interest. Using the results of Chinnery,[58] we find a relative displacement of 0.2-0.5 m (at the $+1\sigma$ level) across the fault trace for an earthquake of magnitude 5.8-6.1. This is less than the 1-2 m value considered reasonable by Ekren.[23] The corresponding vertical displacement is estimated to be about one-third of the horizontal displacement.[22]

Summary

In response to the ERDA request that critical buildings in Area 410 at NTS be evaluated in a safety analysis report, we conducted a geological and seismological investigation of the area. We considered those factors necessary to meet the requirements of Sec. 2.5 of the ERDA standard guidelines.[24]

In particular, we reviewed the regional and local geology at the site, identified potential seismic sources, estimated the peak acceleration and SSE characteristics appropriate for the bedrock and shallow alluvium locations of the buildings, and estimated the peak relative displacement. Because of the size and proximity of the Cane Spring Fault, we arrived at a prediction of a peak acceleration of 0.9 g for the site. The corresponding response spectrum for the SSE is given in Fig. 14. The primary bases for these conclusions were the requirement that maximum values were to be predicted and the fact that values of peak acceleration of this size have, in fact, been observed. The response spectrum was determined from the envelope of records from the San Fernando and Parkfield earthquakes, suitably scaled. Finally, a maximum relative displacement across the Cane Spring Fault of 0.2 to 0.5 m was estimated as being appropriate for the site on the basis of a magnitude 5.8-6.1 earthquake.

Acknowledgments

We thank Larry Wight of LLL for his many useful discussions and his calculations of some of the response spectra. Without his knowledge and assistance, our work would have been considerably more difficult. Our thanks also to R. D. McArthur (LLL-N) for spot checking some field relationships in Area 410 and for

discussing some aspects of Area 410 geology. We also thank William Quinlivan, Frank Byers, Jr., and E. B. Ekren of the Special Projects Branch, U. S. Geologic Survey, for reviewing the geologic portion of this report.

References

1. C. B. Hunt, Physiography of the United States (W. H. Freeman and Co., San Francisco, Cal., 1967).
2. P. B. King, The Tectonics of North America – A Discussion to Accompany the Tectonic Map of North America, Scale 1:5,000,000, U. S. Geological Survey, Washington, D. C., Professional Paper 628 (1969).
3. J. H. Stewart, Geol. Soc. Am. Bull. 83, 1345 (1972).
4. E. B. Ekren, C. L. Rogers, R. E. Anderson, and P. O. Orkild, "Age of Basin and Range Faults in Nevada Test Site and Nellis Air Force Range Nevada," in Nevada Test Site, Memoir 110, E. G. Eckel, Ed. (Geological Society of America, Boulder, Colo., 1968), pp. 247-250.
5. W. J. Carr, Summary of Tectonic and Structural Evidence for Stress Orientation at the Nevada Test Site, U. S. Geological Survey, Washington, D. C., Rept. USGS-474-181 (1974).
6. E. B. Ekren, "Geologic Setting of Nevada Test Site and Nellis Air Force Range," in Nevada Test Site, Memoir 110, E. B. Eckel, Ed., (Geological Society of America, Boulder, Colo., 1968), pp. 11-19.
7. J. Gilluly, Volcanism, Tectonism, and Plutonism in the Western United States (Geological Society of America, Boulder, Colo., 1965), Spec. Paper 80.
8. L. A. Wright, B. W. Troxel, E. G. Williams, M. T. Roberts, and P. E. Diehl, "Precambrian Sedimentary Environments of the Death Valley Region, Eastern California," in Guidebook: Death Valley Region, California and Nevada (Death Valley Publishing Co., Shoshone, Cal., 1974).
9. M. W. Reynolds, "Geology of the Grapevine Mountains, Death Valley, California: A Summary," in Guidebook: Death Valley Region, California and Nevada (Death Valley Publishing Co., Shoshone, Cal., 1974).
10. H. Barnes and F. G. Poole, "Regional Thrust-Fault System in Nevada Test Site and Vicinity," in Nevada Test Site, Memoir 110, E. B. Eckel, Ed. (Geological Society of America, Boulder, Colo., 1968) pp. 233-238.
11. B. D. Burchfield, P. J. Pelton, and J. Sutter, Geol. Soc. Am. Bull. 81, 211 (1970).
12. R. J. Fleck, Geol. Soc. Am. Bull. 81, 2807 (1970).
13. J. H. Stewart, Geol. Soc. Am. Bull. 82, 1019 (1971).
14. R. L. Armstrong, E. B. Ekren, E. H. McKee, and D. C. Noble, Am. Jour. Sci. 267, 478 (1969).
15. M. L. Silberman and E. H. McKee, Isochron/West, No. 4, 7 (1972).
16. E. H. McKee, Geol. Soc. Am. Bull. 82, 3497 (1971).
17. R. F. Marvin, F. M. Byers, Sr., H. H. Mehnert, P. P. Orkild, and T. W. Stern, Geol. Soc. Am. Bull. 81, 2657 (1970).
18. C. R. Longwell, Geol. Soc. Am. Bull., 85, 985 (1974).

19. F. G. Poole, D. P. Elston, and W. J. Carr, Geologic Map of the Cane Spring Quadrangle, Nye County Nevada, U.S. Geol. Survey Geol. Quad. Map GQ 455 (1965).
20. E. B. Ekren and K. A. Sargent, Geologic Map of Skull Mountain Quadrangle, Nye County Nevada, U. S. Geol. Survey Geol. Quad. Map GQ-387 (1965).
21. E. N. Hinrichs, Geologic Map of the Camp Desert Rock Quadrangle, Nye County Nevada, U. S. Geol. Survey Geol. Quad. Map GQ-726 (1968).
22. K. A. Sargent and J. H. Stewart, Geologic Map of the Specter Range NW Quadrangle, U. S. Geol. Survey Geol. Quad. Map GQ 884 (1971).
23. E. B. Ekren, Geologic Examination of the Super Kukla Reactor Site, Nevada Test Site, U. S. Geol. Survey, Washington, D. C., Rept. USGS 474-161 (1972).
24. USAEC Regulatory Staff, Standard Format and Content of Safety Analysis Reports for Nuclear Power Plants, Rev. 1, (October 1972) pp. 2.5-7.
25. D. B. Slemmons, A. E. Jones, and J. I. Gimlett, Bull. Seis. Soc. Am. 55, 519 (1965).
26. A. Ryall, D. B. Slemmons, and L. D. Gedney, Bull. Seis. Soc. Am. 56, 1105 (1966).
27. F. J. Gumper and C. Scholz, Bull. Seism. Soc. Am. 61, 1413 (1971).
28. J. F. Landers, "Seismological Notes," a regular feature, in Bull. Seism. Soc. Am. (1961-1974).
29. P. B. Schnabel and H. B. Seed, Bull. Seism. Soc. Am. 63, 501 (1973).
30. Environmental Research Corporation, Prediction of Ground Motion Characteristics of Underground Nuclear Detonations, U. S. ERDA, Nevada Operations Office, Las Vegas, Rept. NVO-1163-29 (1974).
31. L. H. Wight, A Geological and Seismological Investigation of the Lawrence Livermore Laboratory Site, Lawrence Livermore Laboratory, UCRL-51592, Rev. 1 (1974).
32. A. L. Albee and J. L. Smith, "Earthquake Characteristics and Fault Activity in Southern California," in Engineering Geology in Southern California (L. A. Section, Assoc. of Engrg. Geologists), R. Lung and R. Proctor, Eds. (1966), pp. 9-34.
33. R. C. Lieberman and P. W. Pomeroy, Bull. Seism. Soc. Am. 60, 879 (1970).
34. G. W. Housner, "Engineering Estimates of Ground Shaking and Maximum Earthquake Magnitude," in Proc. 4th World Conf. Earthquake Engrg. (Editorial Universitaria, Santiago, Chile, 1969), pp. 1-13.
35. P. B. Schnabel and H. B. Seed, Bull. Seis. Soc. Am. 63, 501 (1973).
36. D. M. Boore and R. A. Page, Accelerations Near Faulting in Moderate-sized Earthquakes, U. S. Geological Survey open file report.
37. D. M. Boore, "Empirical and Theoretical Study of Near Fault Propagation in Proc. 5th World Conf. Earthquake Engrg. (Ministry Public Works, Rome, Italy, 1973), No. 301a.
38. Design Response Spectra for Seismic Design of Nuclear Power Plants, USAEC Regulatory Guide 1.60 (USAEC, Washington, D. C., 1973).

39. G. W. Housner and P. C. Jennings, ASCE J. Engrg., Mech. Div. 90 (EMI), 113 (1964).
40. H. B. Seed and I. M. Idriss, J. Soil Mech., Found. Div., ASCE 95(SM5), 1199 (1969).
41. H. B. Seed and I. M. Idriss, Soil Moduli and Damping Factors for Dynamic Response, University of California, Berkeley, Rept. EERC-70-10 (1970).
42. W. K. Cloud, and V. Perez, Bull. Seism. Soc. Am. 57, 1179 (1967).
43. G. W. Housner and M. D. Trifunac, Bull. Seism. Soc. Am. 57, 1193 (1967).
44. M. D. Trifunac and D. E. Hudson, Bull. Seism. Soc. Am. 61, 1393 (1971).
45. B. A. Bolt, Bull. Seism. Soc. Am. 62, 1053 (1972).
46. D. M. Boore, Bull. Seism. Soc. Am. 63, 1603 (1973).
47. W. V. Mickey, V. Perez, and W. K. Cloud, "Amplification Studies of the Pacoima Dam from Aftershocks of the San Fernando Earthquake," in Proc. 5th World Conf. Earthquake Engrg.(Ministry of Public Works, Rome, Italy,1973), No. 86.
48. R. B. Reimer, R. W. Clough, and J. M. Raphael, "Evaluation of the Pacoima Dam Accelerogram," in Proc. 5th World Conf. Earthquake Engrg. (Ministry of Public Works, Rome, Italy 1973), No. 293.
49. J. N. Brune, J. Geophys. Res. 75, 4997 (1970).
50. Y. Ida, Bull. Seism. Soc. Am. 63, 959 (1973).
51. N. C. Donovan, "A Statistical Evaluation of Strong Motion Data Including the February 9, 1971 San Fernando Earthquake," in Proc. 5th World Conf. Earthquake Engrg. (Ministry of Public Works, Rome, Italy, 1973) No. 155.
52. L. A. Wright, and B. W. Troxel, Geol. Soc. Am. Bull. 78, 933 (1967).
53. J. P. Buwalda, "Geology of the Tehachapi Mountains, California," in Geology of Southern California, Bulletin 170, R. H. Jahns, Ed. (California Division of Mines, Sacramento, Cal., 1954).
54. D. F. Hewett, "General Geology of the Mojave Desert Region, California," in Geology of Southern California, Bulletin 170, R. H. Jahns, Ed. (California Division of Mines, Sacramento, Cal., 1954).
55. L. F. Noble, "The San Andreas Fault Zone from Soledad Pass to Cajon Pass, California," in Geology of Southern California, R. H. Jahns, Ed. (California Division of Mines, Sacramento, Cal., 1954).
56. P. C. Jennings, Ed., Engineering Features of the San Fernando Earthquake, February 9, 1971, Earthquake Engineering Research Laboratory, California Institute of Technology, Pasadena, Cal., Rept. 71-02 (1971).
57. John Blume and Associates, Recommendations for Shape of Earthquake Response Spectra, USAEC, Rept. WASH-1254 (1973).
58. M. A. Chinnery, Bull. Seism. Soc. Am. 59, 1969 (1969).

MBB/jd/la

Technical Information Department
LAWRENCE LIVERMORE LABORATORY
University of California | Livermore, California | 94550


D

UCRL-52074

DIFFUSION CLIMATOLOGY FOR HYPOTHETICAL ACCIDENTS IN AREA 410 OF THE NEVADA TEST SITE

Kendall R. Peterson

May 20, 1976

Prepared for U.S. Energy Research & Development Administration under contract No. W-7405-Eng-48

LAWRENCE LIVERMORE LABORATORY
University of California/Livermore

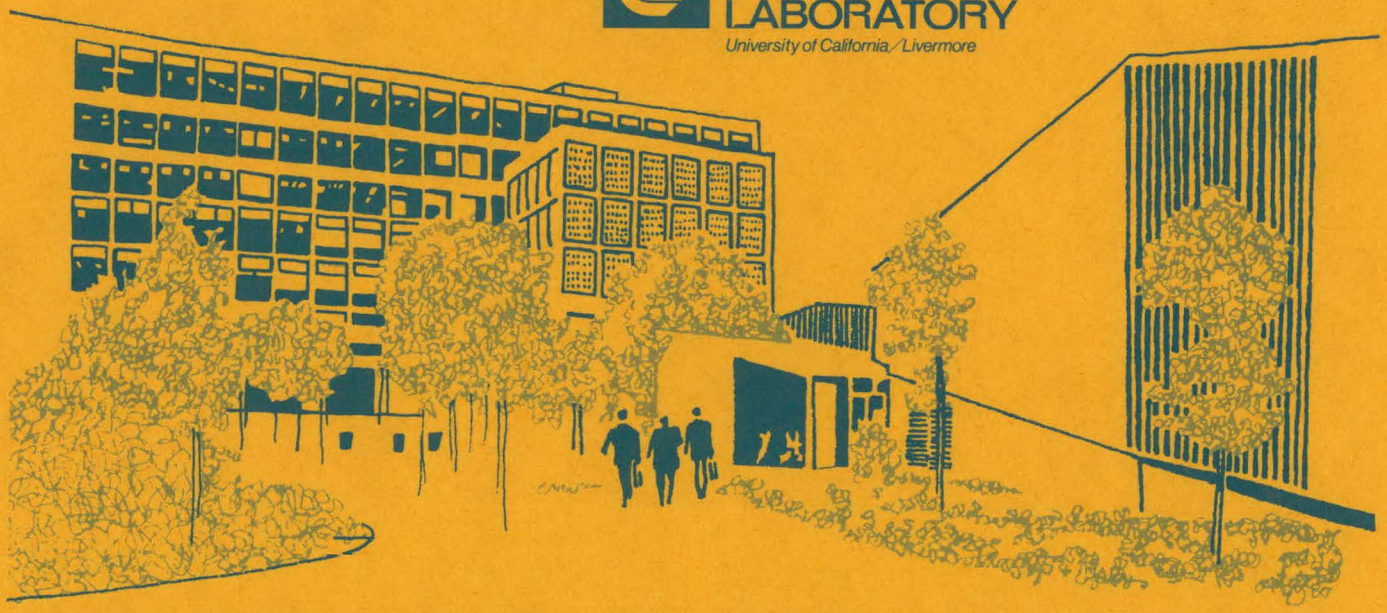

Printed in the United States of America
Available from
National Technical Information Service
U.S. Department of Commerce
5285 Port Royal Road
Springfield, VA 22161
Price: Printed Copy $; Microfiche $2.25

Page Range	Domestic Price	Page Range	Domestic Price
001–025	$ 3.50	326–350	10.00
026–050	4.00	351–375	10.50
051–075	4.50	376–400	10.75
076–100	5.00	401–425	11.00
101–125	5.25	426–450	11.75
126–150	5.50	451–475	12.00
151–175	6.00	476–500	12.50
176–200	7.50	501–525	12.75
201–225	7.75	526–550	13.00
226–250	8.00	551–575	13.50
251–275	9.00	576–600	13.75
276–300	9.25	601–up	*
301–325	9.75		

*Add $2.50 for each additional 100 page increment from 601 to 1,000 pages: add $4.50 for each additional 100 page increment over 1,000 pages.

Distribution Category
UC-11

LAWRENCE LIVERMORE LABORATORY
University of California/Livermore, California/94550

UCRL-52074

DIFFUSION CLIMATOLOGY FOR HYPOTHETICAL ACCIDENTS IN AREA 410 OF THE NEVADA TEST SITE

Kendall R. Peterson

May 20, 1976

THIS PAGE

WAS INTENTIONALLY

LEFT BLANK

Contents

DIFFUSION CLIMATOLOGY FOR HYPOTHETICAL ACCIDENTS IN AREA 410 OF THE NEVADA TEST SITE

Abstract

The regional climate around the Nevada Test Site (NTS) is described. Then the specific climate of the NTS and Lawrence Livermore Laboratory's Area 410 is described, based mainly on observations of winds at 10 m above ground made during 1968 near the Super Kukla reactor. Emphasis is placed on the wind direction and speed and the atmospheric stability in Area 410. Included are estimates of the fastest winds expected in tornadoes and severe thunderstorms.

Three accident scenarios in Area 410 are covered: dispersal of 1 kg of Pu-239 from explosion of 68 kg (150 pounds) of high explosives, release of gross fission products from a 10^{19} fissions accident resulting from inadvertant formation of a critical mass, and accidental detonation of a 100-ton fission primary.

An Instantaneous Point Source (IPS) code was developed at Lawrence Livermore Laboratory and is explained. The IPS code estimates concentrations in the surface air of radioactive particles that have negligible settling rates (have a radius less than 5 μm). For each accident, this code calculated and plotted contour maps that show the estimated exposures of the area to radioactive particles from the explosion. The code calculated two types of exposure maps: one based on arithmetically averaged, integrated exposures and the other based on exposure limits that would be exceeded 5% of the time.

Introduction

This report describes the climatology of the Nevada Test Site and gives normalized, integrated estimates of surface air concentrations of the small particles (less than 5-μm radius) that might be released to the atmosphere by the three more probable accident senarios at Area 410, Nevada Test Site. This area, staffed by LLL personnel, contains the Laboratory's assembly buildings for nuclear devices that are developed in Livermore and sent to Area 410 prior to testing.

This document is an adaptation of a memorandum prepared by the author for use in formulating the meteorological portion of a Safety

Analysis Report (SAR) on Area 410. The purpose of this document is twofold: (1) to be included as an appendix to the SAR, and (2) to serve as an informative document to atmospheric-diffusion meteorologists and others who may not wish to receive the entire SAR.

Regional Meteorology Around the Nevada Test Site

GENERAL CLIMATE

NTS is located in the southern Nevada desert. This region is one of the most arid in the entire United States. Figure 1 shows the average annual rainfall for NTS and surrounding areas. Figure 2[1] shows the average monthly precipitation for selected areas near NTS. The 1962 to 1971 monthly averages and extremes of precipitation for Yucca Flat at NTS, 18 km NE of Area 410, are shown in Fig. 3. The annual surface-water evaporation rate is many times greater than the rainfall in the region. No large bodies of surface water exist over the entire region, with the exception of Lake Mead, a man-made reservoir.

In the winter, the primary cause of the arid nature of the region is the so-called "rain shadow" caused by the Sierra Nevada Mountains, which make the eastward-moving Pacific storms lose their moisture on the upwind, western slopes. Low-pressure centers generally approach from the southwest to northwest, usually passing to the north of NTS. On the average, a storm system passes about once every 7 to 10 days during the winter.

In the summer, Pacific storms do not affect southern Nevada, but moisture sometimes comes from the Gulf of Mexico or the Gulf of California. This moisture falls primarily in isolated convective storms, which can be intense over a few square kilometres. There may be large variations in precipitation within the storm's area.

The extent of summer showers over southern Nevada depends primarily on the penetration of the south winds. Thus, precipitation tends to diminish to the north. On rare occasions, tropical storms occurring off the west coast of Mexico in late summer and fall will move northward, bringing heavy and widespread precipitation to southern Nevada.

SEVERE WEATHER

Thunderstorms and dust devils are common occurrences at the Nevada Test Site. Tornadoes have never been observed at NTS, but a few have occurred within 250 km. McDonald,

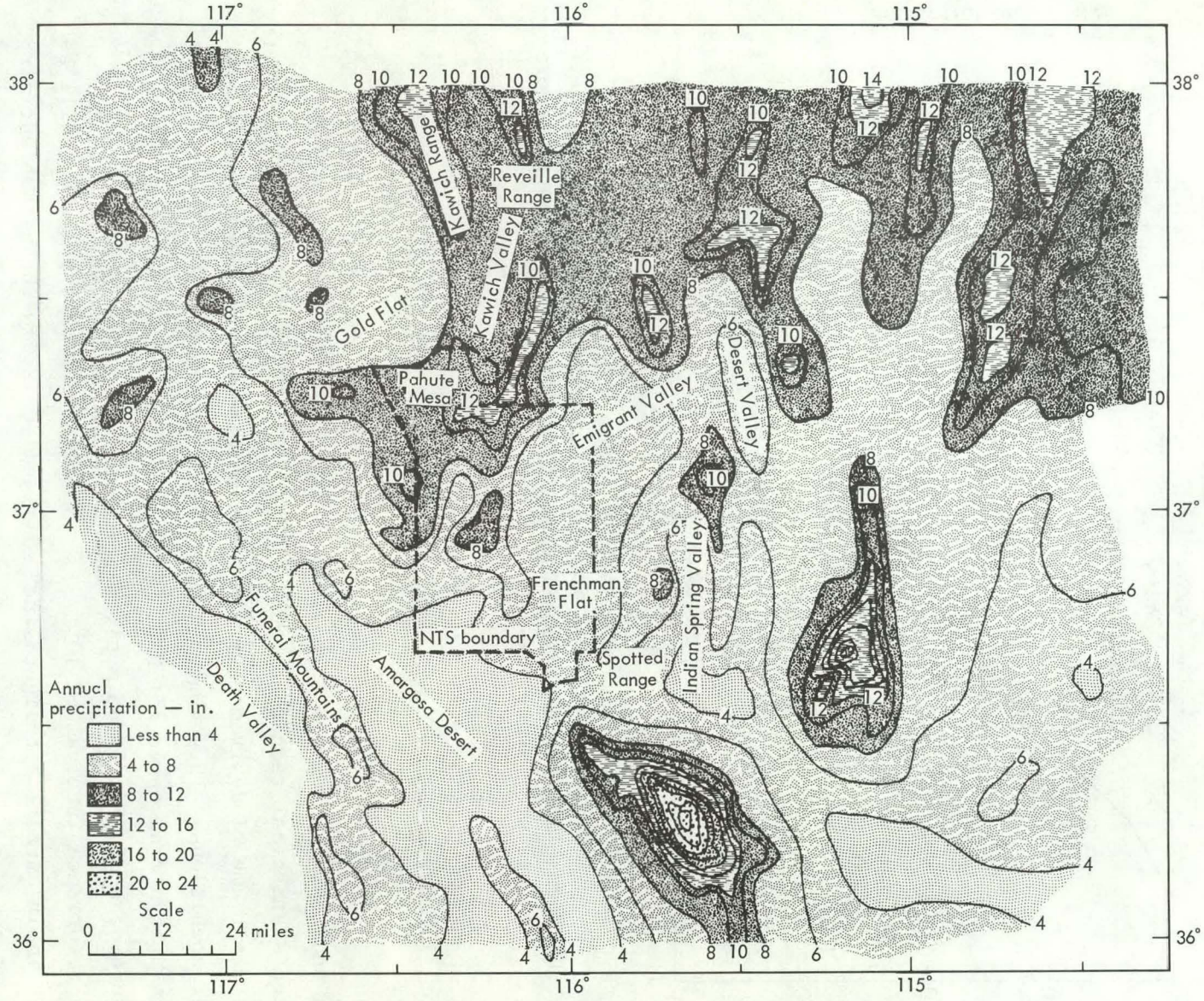

Fig. 1. Mean annual precipitation of Nevada Test Site and vicinity. Based on a map by Ralph F. Quiring, Air Resources Laboratory, Las Vegas, Nevada (1965).

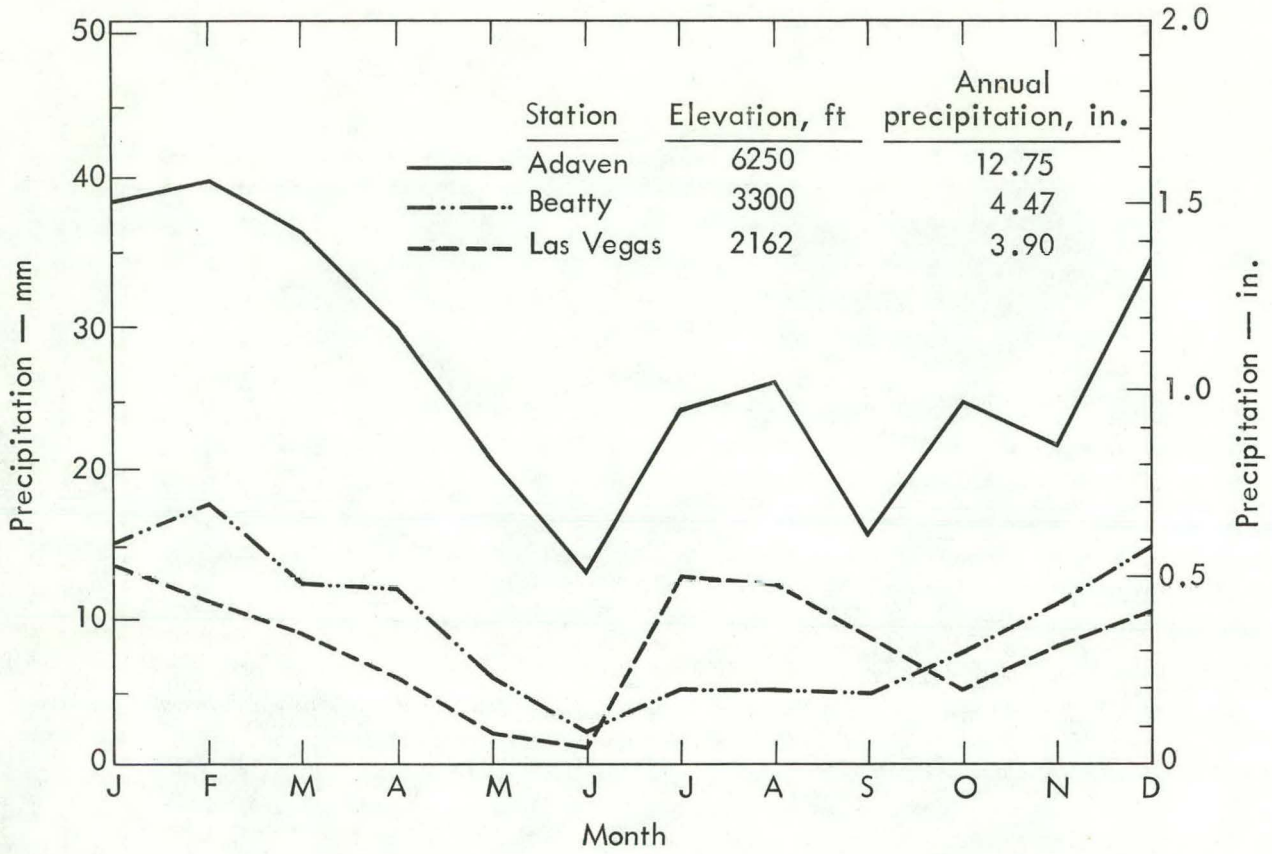

Fig. 2. Normal monthly precipitation in millimetres and inches at several points near NTS (1931-1960).

Minor, and Mehta[2] have used commonly accepted statistical techniques to estimate extreme winds from severe weather conditions. They suggest a maximum-design wind speed for NTS from tornadoes of 28 m/s (63 mph), with a recurrence interval of 10^6 years. Their extreme "straight line" design wind speed -- occurring in other meteorological phenomena, such as thunderstorms -- is 94 m/s (210 mph) for the same recurrence interval.

AIR-POLLUTION POTENTIAL AT NTS

A study of atmospheric stability conditions in the region indicates conditions are stable very rarely (less than 5% of the time, on an annual basis). Therefore, any locally generated pollution will be readily mixed with the ambient air, resulting in lower pollutant concentrations at the site's boundary than would occur in most other locations within the United States.

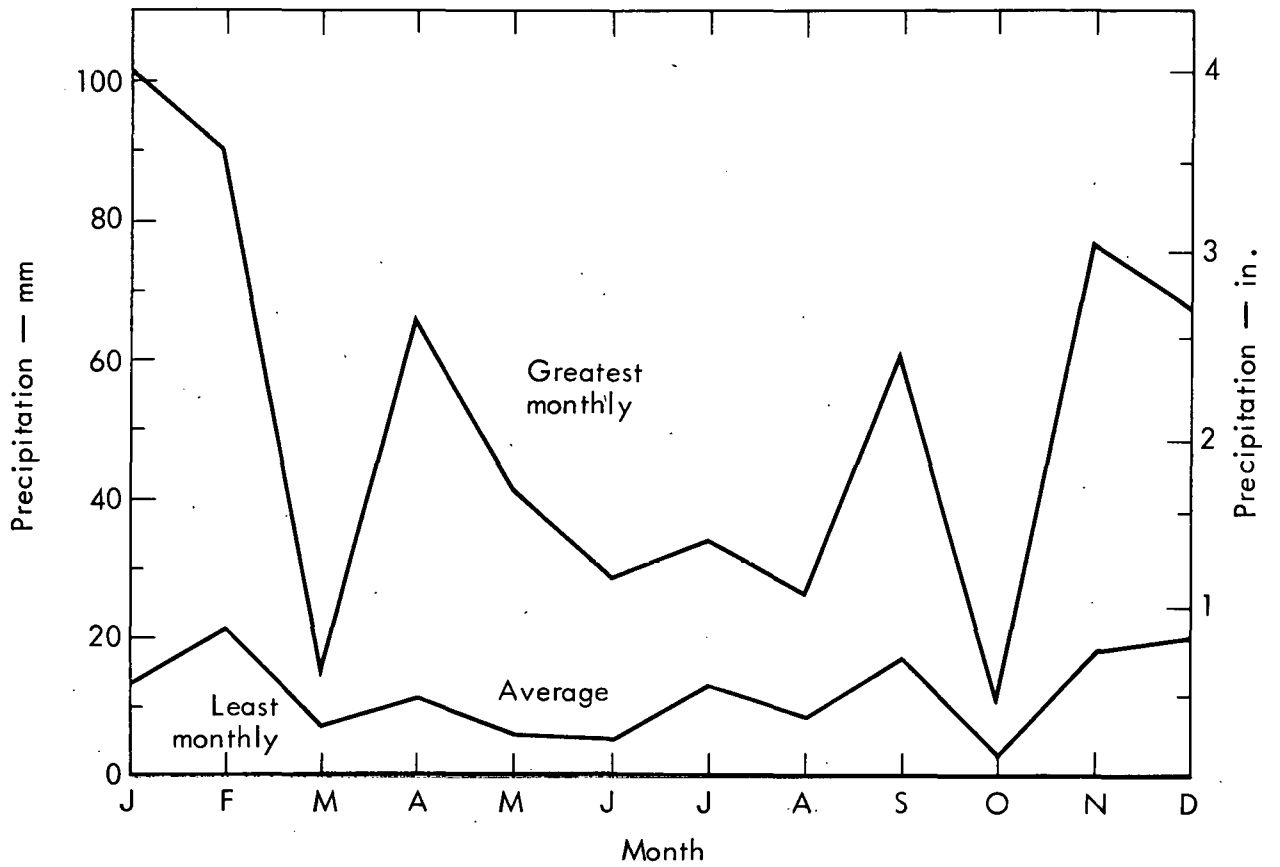

Fig. 3. Precipitation at Yucca Flat in NTS, 1962-71. Least monthly precipitation was less than 0.51 mm (0.02 in.) for all months.

Local Meteorology of the Nevada Test Site and Area 410

STATION SUMMARY

The climate of Area 410 is essentially the same as that of surrounding regions. Table 1 gives the weather summary for the years 1962 through 1971 for the Yucca Weather Station at NTS. Figure 3 shows the average, greatest, and least monthly precipitation at Yucca Flat during the same 10-year period. Yucca is the only continuously manned weather station that has been in operation at NTS for 10 years. The data reported in Table 1 are fairly typical of NTS averages, although differences arise due to local topography.

The only significant difference between the weather at Area 410 and that of surrounding area is the greater rainfall due to elevation.

Table 1. Climatological summary (1962-1971) of Yucca Flat, Nevada — Nevada Test Site (latitude 36°57'N, longitude 116°03'W, elevation 3,924 ft). Data from National Climatic Center, Asheville, North Carolina.

	Jan	Feb	Mar	Apr	May	Jun	Jul	Aug	Sep	Oct	Nov	Dec	Ann.
Temperature, °F													
Averages													
Daily maximum	52.1	56.7	60.9	67.8	78.9	87.6	96.1	95.0	86.4	76.1	61.8	50.7	72.5
Daily minimum	20.8	25.8	27.7	34.4	43.5	49.9	57.0	58.1	46.7	36.9	27.6	19.9	37.4
Monthly	36.5	41.3	44.3	51.1	61.2	68.8	76.6	76.6	66.5	56.5	44.7	35.3	54.9
Extremes										+			
Highest	73	77	87	89	97	107	107	107	105	94	82	70	Aug
(yr)	(1971)	(1963)	(1966)	(1962)	(1967)	(1970)	(1967)	(1970)	(1971)	(1964)	(1962)	(1964)	1970# 107
Lowest	-2	5	9	13	25	29	40	39	25	12	13	-14	Dec
(yr)	(1970)	(1971) #	(1969)	(1966)	(1967)	(1971) #	(1964) #	(1968)	(1971)	(1971)	(1966)	(1967)	1967 -14
Degree days (base 65°)													
Heating	877	662	634	411	147	35	0	1	51	266	602	914	4600
Cooling	0	0	0	1	38	154	366	368	103	9	0	0	1039
Precipitation, in.													
Average	.53	.84	.29	.45	.24	.21	.52	.34	.68	.13	.71	.79	5.73
Greatest monthly	4.02	3.55	.60	2.57	1.62	1.13	1.34	1.04	2.38	.45	3.02	2.66	4.02
(yr)	(1969)	(1969)	(1969)	(1965)	(1971)	(1969)	(1966)	(1965)	(1969)	(1969)	(1965)	(1965)	Jan 1969
Least monthly	T	T	.02	T	T	T	0	0	0	0	0	T	0
(yr)	(1971) #	(1967) #	(1966)	(1962)	(1970) #	(1971)	(1963)	(1962)	(1968) #	(1967) #	(1962)	(1969) #	Sep 1968#
Greatest daily	1.25	1.16	.38	1.08	.86	.45	.77	.35	2.13	.42	1.10	1.31	2.13
(yr)	(1969)	(1969)	(1969)	(1965)	(1971)	(1969)	(1969)	(1971) #	(1969)	(1969)	(1970)	(1965)	Sep 1969

Table 1, continued.

	Jan	Feb	Mar	Apr	May	Jun	Jul	Aug	Sep	Oct	Nov	Dec	Ann.
Snow													
Average	0.9	1.9	2.0	0.7	0	0	0	0	0	0	0.5	2.3	8.3
Greatest monthly	4.3	17.4	7.5	3.0	T	0	0	0	0	T	4.8	9.9	17.4
(yr)	(1962)	(1969)	(1969)	(1964)	(1964)					(1971)	(1964)	(1971)	Feb 1969
Greatest daily	4.3	6.2	4.5	3.0	T	0	0	0	0	T	2.3	7.4	7.4
(yr)	(1962)	(1969)	(1969)	(1964)	(1964)					(1971)	(1964)	(1971)	Dec 1971
Relative humidity, %													
Hour (Pacific Standard Time)													
04	67	67	58	52	46	39	40	44	43	46	61	68	53
10	49	45	31	27	22	19	20	23	21	24	39	50	31
16	35	32	23	21	17	14	15	16	17	19	31	41	23
22	60	56	44	38	31	26	28	30	32	36	52	64	41
Wind, mph[a]													
Average speed	6.6	6.9	8.4	9.1	8.3	7.9	7.5	6.7	7.0	6.8	6.1	6.6	7.4
Peak speed	58	52	55	60+	60+	60+	55	60+	52	60	51	53	60+
(yr)	(1965)	(1967)	(1971)	(1970) #	(1967)	(1967)	(1971)	(1968)	(1970)	(1971)	(1970)	(1970)	Apr 1970#
Resultant, Dir/Sp													
23-02 PST	233/ 0.7	275/ 1.1	240/ 1.8	250/ 2.2	260/ 1.5	272/ 1.9	278/ 0.9	222/ 1.5	281/ 1.3	286/ 1.3	234/ 1.2	288/ 1.9	—
11-14 PST	135/ 2.6	118/ 2.7	186/ 4.5	198/ 5.1	179/ 7.2	185/ 8.2	185/ 12.0	182/ 12.0	163/ 6.4	138/ 3.7	152/ 4.1	109/ 1.0	—
Station pressure, in.													
Averages	26.10	26.05	25.99	25.96	25.94	25.92	26.00	26.00	26.00	26.06	26.08	26.07	26.01
Highest	26.54	26.42	26.43	26.39	26.39	26.20	26.19	26.22	26.36	26.40	26.58	26.59	26.59
Lowest	25.42	25.56	25.48	25.50	25.47	25.56	25.68	25.71	25.56	25.52	25.64	25.49	25.42
Average sky cover, sunrise to sunset[b]	4.9	5.0	4.8	4.5	4.3	3.0	3.0	3.0	2.1	2.9	4.8	4.6	3.9

Table 1, continued.

	Jan	Feb	Mar	Apr	May	Jun	Jul	Aug	Sep	Oct	Nov	Dec	Ann.
Average number of days													
Sunrise to sunset													
Clear	13	11	12	13	14	19	19	20	22	20	13	14	190
Partly cloudy	8	8	9	9	11	7	9	8	6	7	7	8	97
Cloudy	10	9	10	8	6	4	3	3	2	4	10	9	78
Precipitation													
.01 inch or more	2	3	3	3	2	2	3	3	2	1	3	3	30
.10 inch or more	1	2	1	1	1	1	2	1	1	1	2	1	14
.50 inch or more	*	*	0	*	*	0	*	0	1	0	*	1	3
1.00 inch or more	*	*	0	*	0	0	0	0	*	0	*	*	1
1.0 inch or more of snow	*	1	1	*	0	0	0	0	0	0	*	1	3
Thunderstorms	*	0	1	1	1	2	4	4	2	*	*	*	14
Temperature													
Maximum													
90°F or more	0	0	0	0	4	14	29	27	11	2	0	0	87
32°F or less	1	*	0	0	0	0	0	0	0	0	0	1	2
Minimum													
32°F or less	29	23	24	12	2	*	0	0	1	9	23	29	152
0°F or less	*	0	0	0	0	0	0	0	0	0	0	1	1

* One or more occurrences during the period of record but average less than 0.5 day.

Most recent of multiple occurrences.

+ Peak speed exceeded the upper limit of the analog recorder.

T Trace, an amount too small to measure.

(a) Average and peak speed are for the period starting with December 1964. The direction and magnitude of the resultant wind are from a summary covering the period December 1964 through May 1969.

(b) Sky cover is expressed in the range from 0 for no clouds to 10 when the sky is completely covered with clouds. Clear, partly cloudy and cloudy are defined as average daytime cloudiness of 0-3, 4-7 and 8-10 tenths, respectively.

Figure 4[2] shows the way in which rainfall increases with elevation for the region around NTS. Data collected from stations at NTS agree quite closely with the plot of average behavior shown in Fig. 4. Figure 5[3] shows the predicted rainfall for storms of return periods varying from 1.1 to 1000 years. These curves are based on extreme value theory; the data represent average behavior for the NTS area.

WINDS

Table 2[3] is a summary of wind data collected at Area 410 during 1964-1968. The recording equipment was unable to measure speeds in excess of 27 m/s (60 mph). However, it should be noted that only two observations of winds greater than 17 m/s (39 mph) were observed. Table 3[2] shows the maximum wind velocities to be expected in the area of NTS.

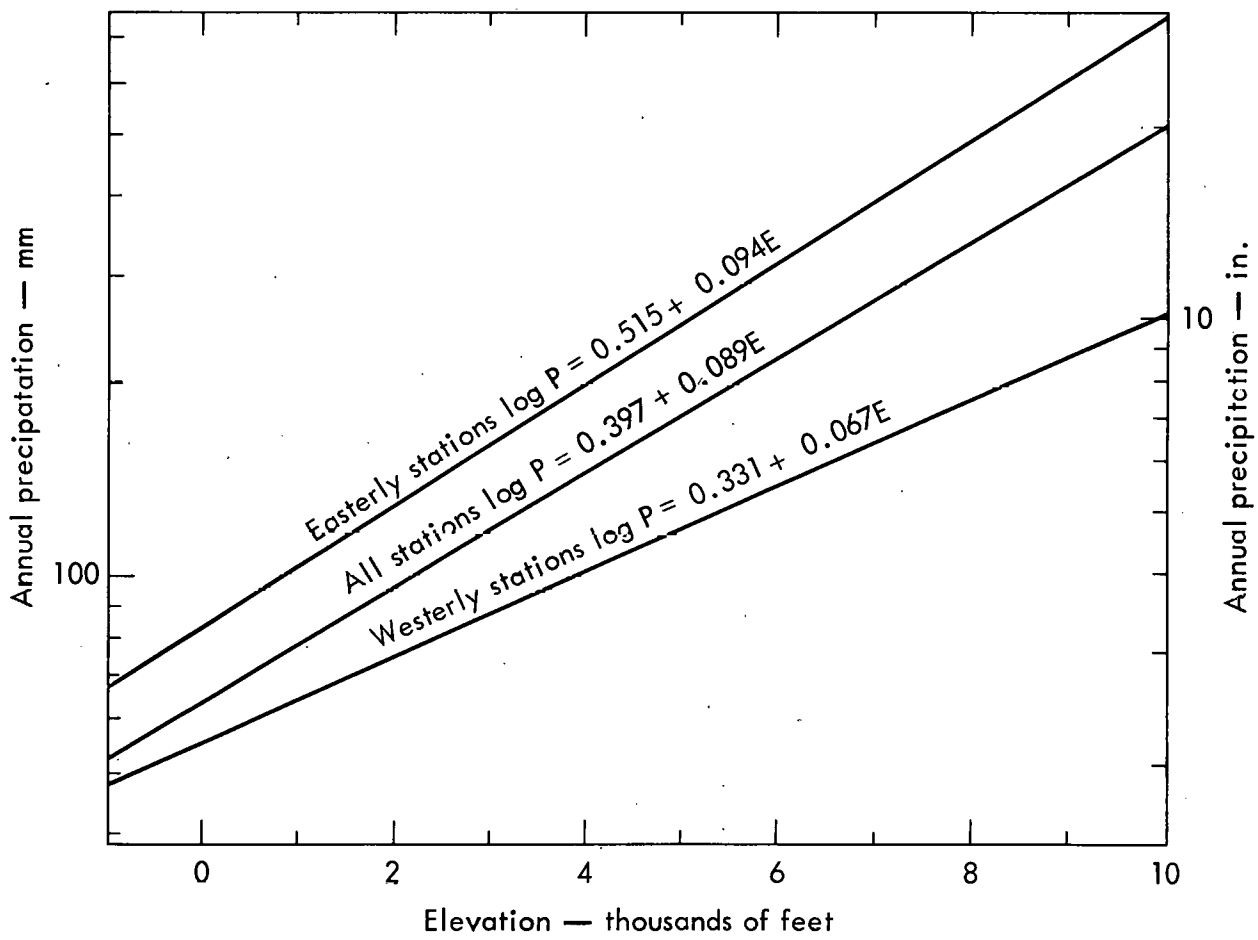

Fig. 4. Log-linear relationship between normal annual precipitation and elevation in southern Nevada (1931-1960).

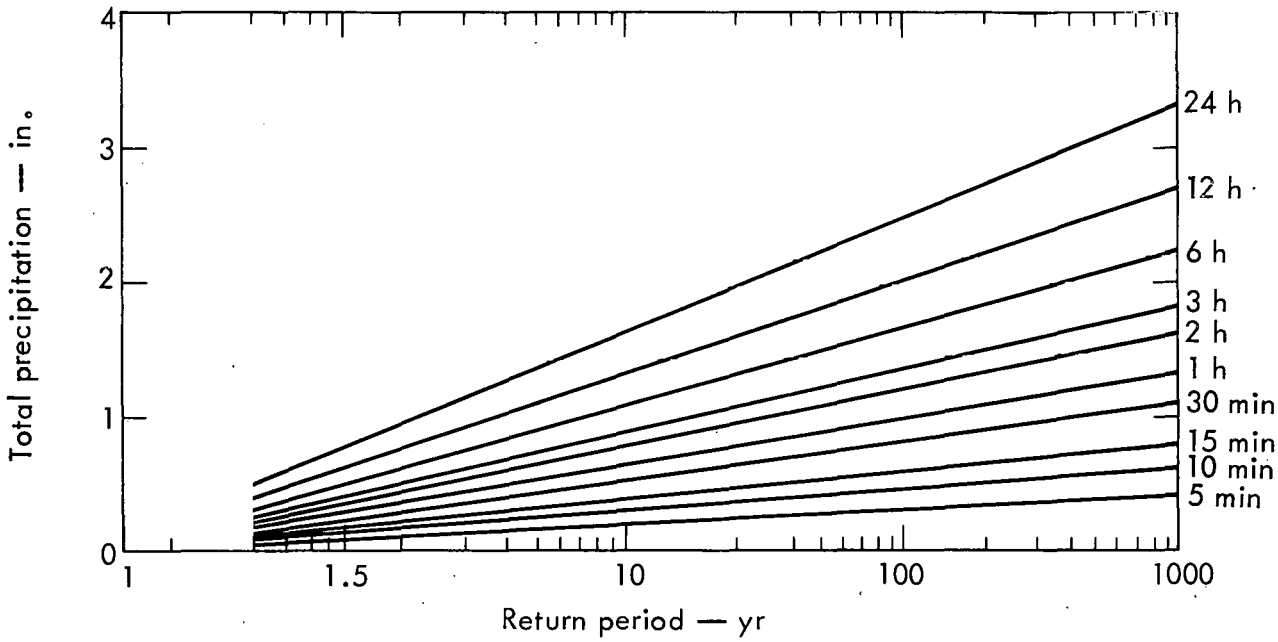

Fig. 5. Probability of precipitation lasting from 5 min to 24 h at NTS.

Table 2. Breakdown of wind-speed observations for Area 410, 1964-68 at 9.1 m above ground. Data from Ref. 3.

Speed range		Percent of observations
m/s	mph	
0.5- 2.0	1- 4	16.0
2.1- 4.2	5- 9	44.5
4.3- 6.5	10-14	24.8
6.6- 8.7	15-19	9.3
8.8-13.2	20-29	4.1
13.3-17.7	30-39	0.4
17.8-22.1	40-49	<0.01[a]
≥22.2	≥50	<0.01[b]

[a]Three observations.

[b]One observation.

Table 3. Extreme winds expected at NTS at 9.1 m (30 ft) above surface.

Return period, yr	Fastest[a]		Gust	
	mph	m/sec	mph	m/s
2	48	21	62	28
5	55	25	72	32
10	61	27	79	35
50	75	34	97	43
100	82	37	107	48

[a]Approximately 1-min average wind.

Wind directions and speeds, as well as stability categories were averaged over half-hour intervals for the entire period from January through December, 1968. The measurements were taken near the Super Kukla reactor building at 10 m above the ground. To study seasonal effects, these data were divided into winter (October through February) and summer (March through September) seasons.*

The percentage frequencies of wind directions and average speeds are given in Table 4. In general, the strongest winds blow toward the north through east; the weakest winds blow toward the west through north. The winter and summer winds are remarkably similar in speed and average about 4 m/s for all directions. The frequencies vary more with direction than do the speeds. The annual frequencies show a double maximum -- in the directions toward north through east and toward south through west. The seasonal frequencies show a single maximum -- in the directions toward south through west for winter, and toward north through east for summer.

*This breakdown of seasons was based on the afternoon resultant wind speeds shown in Table 1.

ATMOSPHERIC STABILITY

Atmospheric stability was estimated from the wind-direction traces made during 1968. The method outlined by Slade[4] was used to determine these (Pasquill-Gifford) stabilities. A description of these stability categories is given in Table 5. Table 6 shows the annual percentage frequencies and those for both seasons. The outstanding feature of this table is the relatively

Table 4. Frequencies and average speeds vs direction for winds in Area 410, 1968 data.

Direction toward which wind blows	Annual		Winter		Summer	
	Frequency, %	Av Speed, m/s	Frequency, %	Av Speed, m/s	Frequency, %	Av Speed, m/s
N	9.7	5.07	6.0	4.58	12.3	5.24
NNE	12.4	4.90	6.0	4.76	16.9	4.94
NE	8.9	4.25	5.4	4.90	11.4	4.03
ENE	10.3	3.76	6.9	5.16	12.7	3.22
E	5.7	3.11	3.3	3.96	7.3	2.84
ESE	3.6	3.28	2.9	3.72	4.1	3.07
SE	2.9	2.95	3.1	3.55	2.8	2.50
SSE	4.6	3.43	5.5	3.96	4.0	2.91
S	9.2	4.11	10.4	3.97	8.3	4.23
SSW	11.2	3.78	15.2	3.54	8.4	4.09
SW	10.5	3.61	18.0	3.83	5.2	3.08
WSW	5.0	4.15	10.3	4.46	1.3	2.40
W	0.8	5.10	2.0	5.14	0.1	1.90
WNW	0.4	2.64	0.4	2.50	0.4	2.73
NW	1.5	2.77	1.6	2.98	1.5	2.61
NNW	3.3	3.27	3.2	3.44	3.3	3.15
All directions	100.0	3.99	100.0	4.11	100.0	3.91

low frequency of stable conditions (E and F).* There appears to be no significant seasonal variation. Finally, the unstable categories (A, B and C) account for about three-fourths of all observations. This is a desirable feature since an unstable atmosphere will mix and dilute effluents more rapidly than at a site where neutral (D) and stable (E and F) categories predominate.

Tabular wind roses, classed by stability category, wind direction, and wind-speed range are given in Tables 7, 8, and 9 for annual, winter, and summer periods,

*Other researchers, e.g., J. B. Knox (in a personal communication), have noted a tendency for a systematic bias, favoring more unstable categories, when the $\Delta\theta$-method is used with strip charts of wind direction.

respectively. Note that the total of directional and wind-speed frequencies for a given stability category is the percentage of time that particular stability occurred; these totals agree with the values

Table 5. Description of atmospheric stability categories (Pasquill-Gifford).

Category	Degree of stability	Angular spread of wind direction (30-min period)	Description
A	Extremely unstable	150°	Rapid mixing; usually occurs on hot afternoons.
B	Moderately unstable	120°	Moderate mixing; usually occurs on warm days.
C	Slightly unstable	90°	Usually occurs in daytime.
D	Neutral stability	60°	Occurs day or night, often during overcast skies.
E	Slightly stable	30°	Slow dilution; can occur day or night.
F	Moderately stable	15°	Very slow dilution; occurs at night with clear skies.

Table 6. Percentage frequency of stability categories at Area 410.

	Frequency, %		
Stability category	Annual	Winter (Oct-Feb)	Summer (Mar-Sept)
A	27.5	29.6	26.1
B	17.1	15.6	18.2
C	26.9	28.2	26.3
D	23.7	21.8	25.2
E	4.3	4.4	4.2
F	0.3	0.6	0.2

Table 7. Annual frequencies of winds.

Direction toward which the wind blows	Frequency, %							
	For winds having speeds (in m/s) of:						Totals by direction	Av speed
	0.5-2.0	2.1-3.5	3.6-5.5	5.6-9.0	9.1-12.0	>12		
				Stability Category A				
N	0.47	0.98	0.61	0.17	0.0	0.0	2.23	3.30
NNE	0.34	0.88	1.24	0.53	0.02	0.0	3.01	4.19
NE	0.48	0.67	0.84	0.26	0.0	0.0	2.25	3.64
ENE	0.44	0.41	0.57	0.47	0.14	0.01	2.04	4.58
E	0.35	0.53	0.38	0.15	0.0	0.0	1.41	3.37
ESE	0.51	0.33	0.39	0.14	0.0	0.0	1.37	3.18
SE	0.74	0.35	0.31	0.16	0.0	0.0	1.56	2.87
SSE	0.55	0.32	0.44	0.13	0.03	0.0	1.47	3.30
S	0.71	0.31	0.40	0.36	0.02	0.0	1.80	3.56
SSW	0.50	0.75	0.73	0.60	0.01	0.0	2.59	4.07
SW	0.38	1.0	0.88	0.70	0.09	0.01	3.06	4.41
WSW	0.25	0.99	0.94	0.53	0.16	0.05	2.81	4.75
W	0.02	0.19	0.33	0.19	0.06	0.0	0.78	5.19
WNW	0.02	0.02	0.0	0.0	0.0	0.0	0.04	2.03
NW	0.07	0.09	0.07	0.0	0.0	0.0	0.23	2.86
NNW	0.25	0.49	0.12	0.03	0.0	0.0	0.89	2.75
Total	6.08	8.19	8.25	4.42	0.53	0.07	27.54	3.88

Table 7, continued.

				Stability Category B				
N	0.20	0.53	0.74	0.67	0.03	0.0	2.17	4.75
NNE	0.29	0.47	1.37	1.06	0.02	0.01	3.22	4.97
NE	0.12	0.28	0.49	0.39	0.01	0.0	1.29	4.74
ENE	0.17	0.23	0.10	0.07	0.0	0.01	0.58	3.40
E	0.12	0.07	0.10	0.09	0.0	0.0	0.38	3.84
ESE	0.23	0.09	0.05	0.09	0.0	0.0	0.46	3.10
SE	0.24	0.03	0.06	0.02	0.01	0.0	0.36	2.52
SSE	0.11	0.12	0.16	0.10	0.02	0.0	0.51	4.20
S	0.62	0.35	0.32	0.31	0.02	0.0	1.62	3.51
SSW	0.87	0.80	0.62	0.72	0.02	0.0	3.03	3.83
SW	0.31	0.60	0.47	0.32	0.0	0.0	0.10	3.17
WSW	0.01	0.06	0.03	0.0	0.0	0.0	0.0	0.0
NW	0.11	0.25	0.10	0.01	0.0	0.0	0.47	2.91
NNW	0.34	0.51	0.28	0.12	0.0	0.0	1.25	3.20
Total	3.74	4.39	4.89	3.97	0.13	0.02	17.14	4.08
				Stability Category C				
N	0.19	0.49	0.93	0.94	0.22	0.06	3.73	6.19
NNE	0.21	0.76	1.14	1.74	0.17	0.06	4.08	5.63
NE	0.18	0.64	0.95	0.59	0.07	0.03	2.46	4.81
ENE	0.34	1.11	0.65	0.26	0.06	0.04	2.46	3.91
E	0.19	0.30	0.26	0.07	0.0	0.0	0.82	3.38

Table 7, continued.

ESE	0.19	0.21	0.14	0.06	0.01	0.0	0.61	3.29
SE	0.23	0.05	0.13	0.05	0.02	0.0	0.48	3.32
SSE	0.44	0.17	0.24	0.11	0.02	0.0	0.98	3.20
S	0.52	0.52	0.82	0.60	0.09	0.0	2.55	4.38
SSW	0.93	0.87	0.75	0.55	0.15	0.0	3.25	3.88
SW	0.98	1.20	0.77	0.35	0.05	0.0	3.35	3.33
WSW	0.14	0.24	0.10	0.09	0.0	0.0	0.57	3.44
W	0.0	0.0	0.0	0.0	0.0	0.0	0.0	0.0
WNW	0.03	0.06	0.0	0.0	0.0	0.0	0.09	2.28
NW	0.22	0.23	0.10	0.01	0.0	0.0	0.56	2.58
NNW	0.19	0.28	0.25	0.18	0.02	0.0	0.92	4.00
Total	4.88	7.13	7.23	6.60	0.88	0.19	26.91	4.43
			Stability Category D					
N	0.04	0.11	0.32	0.66	0.24	0.02	1.39	6.81
NNE	0.14	0.47	0.64	0.58	0.10	0.11	2.04	5.56
NE	0.26	1.01	0.90	0.54	0.07	0.03	2.81	4.41
ENE	0.64	2.48	1.31	0.35	0.01	0.04	4.83	3.51
E	0.53	1.04	0.25	0.13	0.05	0.0	2.00	3.09
ESE	0.14	0.32	0.24	0.13	0.03	0.0	0.86	3.99
SE	0.11	0.12	0.11	0.06	0.0	0.0	0.40	3.53
SSE	0.36	0.36	0.35	0.18	0.01	0.0	1.26	3.55
S	0.24	0.55	0.83	0.85	0.09	0.0	2.56	4.99

Table 7, continued.

SSW	0.58	0.51	0.22	0.43	0.06	0.0	1.80	3.85
SW	0.65	0.77	0.25	0.19	0.05	0.01	1.92	3.21
WSW	0.21	0.57	0.20	0.21	0.0	0.01	1.20	3.71
W	0.0	0.01	0.0	0.0	0.0	0.0	0.01	2.80
WNW	0.06	0.06	0.05	0.03	0.0	0.0	0.20	3.45
NW	0.07	0.11	0.03	0.04	0.0	0.0	0.25	3.30
NNW	0.04	0.03	0.05	0.09	0.0	0.0	0.21	4.85
Total	4.07	8.52	5.75	4.47	0.71	0.22	23.74	4.15
			Stability Category E					
N	0.01	0.0	0.02	0.02	0.0	0.0	0.05	4.99
NNE	0.0	0.03	0.0	0.0	0.0	0.0	0.03	2.80
NE	0.01	0.02	0.05	0.0	0.01	0.0	0.09	4.46
ENE	0.09	0.30	0.01	0.01	0.0	0.0	0.31	2.55
E	0.20	0.71	0.11	0.03	0.0	0.0	1.05	2.82
ESE	0.01	0.19	0.04	0.03	0.0	0.0	0.27	3.50
SE	0.03	0.02	0.05	0.01	0.0	0.0	0.11	3.58
SSE	0.02	0.14	0.14	0.06	0.0	0.0	0.36	4.14
S	0.12	0.18	0.25	0.11	0.0	0.0	0.66	3.93
SSW	0.10	0.19	0.05	0.17	0.0	0.0	0.51	4.17
SW	0.11	0.12	0.07	0.09	0.0	0.01	0.40	4.00
WSW	0.03	0.13	0.09	0.09	0.0	0.0	0.34	4.32
W	0.01	0.0	0.0	0.0	0.0	0.0	0.01	1.25

Table 7, continued.

WNW	0.03	0.01	0.0	0.0	0.0	0.0	0.04	1.64
NW	0.01	0.0	0.02	0.0	0.0	0.0	0.03	3.45
NNW	0.0	0.02	0.0	0.0	0.0	0.0	0.02	2.80
Total	0.78	1.96	0.90	0.62	0.01	0.01	4.28	3.58
			Stability Category F					
N	0.01	0.0	0.01	0.0	0.0	0.0	0.02	2.90
NNE	0.0	0.0	0.0	0.01	0.0	0.0	0.01	7.30
NE	0.01	0.01	0.0	0.0	0.0	0.0	0.02	2.03
ENE	0.0	0.01	0.01	0.0	0.03	0.0	0.05	7.80
E	0.0	0.01	0.0	0.0	0.0	0.0	0.01	2.80
ESE	0.0	0.02	0.0	0.0	0.0	0.0	0.02	2.80
SE	0.0	0.0	0.0	0.0	0.0	0.0	0.0	0.0
SSE	0.01	0.0	0.0	0.01	0.01	0.0	0.03	6.37
S	0.0	0.0	0.0	0.02	0.0	0.0	0.02	7.30
SSW	0.02	0.01	0.0	0.01	0.0	0.0	0.04	3.15
SW	0.02	0.04	0.01	0.0	0.0	0.0	0.07	2.61
WSW	0.0	0.0	0.0	0.0	0.0	0.0	0.0	0.0
W	0.01	0.0	0.0	0.0	0.0	0.0	0.01	1.25
WNW	0.0	0.0	0.0	0.0	0.0	0.0	0.0	0.0
NW	0.0	0.0	0.0	0.0	0.0	0.0	0.0	0.0
NNW	0.0	0.0	0.0	0.0	0.0	0.0	0.0	0.0
Total	0.08	0.10	0.03	0.05	0.04	0.0	0.30	4.35

Table 8. Winter (Oct-Feb) frequencies of winds.

Direction toward which the wind blows	Frequency, % For winds having speeds (in m/s) of: 0.5-2.0	2.1-3.5	3.6-5.5	5.6-9.0	9.1-12.0	> 12	Totals by direction	Av speed
			Stability Category A					
N	0.56	0.38	0.10	0.20	0.0	0.0	1.24	2.97
NNE	0.43	0.38	0.20	0.18	0.03	0.0	1.22	3.40
NE	0.43	0.23	0.28	0.10	0.0	0.0	1.04	3.06
ENE	0.48	0.41	0.66	0.87	0.33	0.03	2.78	5.41
E	0.33	0.33	0.26	0.23	0.0	0.0	1.15	3.65
ESE	0.41	0.23	0.28	0.18	0.0	0.0	1.10	3.40
SE	0.66	0.26	0.33	0.26	0.0	0.0	1.51	3.28
SSE	0.69	0.26	0.46	0.20	0.08	0.0	1.69	3.54
S	0.89	0.28	0.31	0.56	0.05	0.0	2.09	3.79
SSW	0.61	0.61	0.59	0.51	0.03	0.0	2.35	3.91
SW	0.48	1.35	1.58	1.33	0.20	0.03	4.97	4.80
WSW	0.41	1.91	2.22	1.28	0.38	0.13	6.33	4.94
W	0.05	0.46	0.79	0.46	0.15	0.0	1.91	5.18
WNW	0.0	0.0	0.0	0.0	0.0	0.0	0.0	0.0
NW	0.0	0.0	0.0	0.0	0.0	0.0	0.0	0.0
NNW	0.15	0.05	0.03	0.03	0.0	0.0	0.26	2.63
Total	6.58	7.14	8.09	6.39	1.25	0.19	29.64	4.31

Table 8, continued.

				Stability Category B				
N	0.26	0.69	0.15	0.28	0.05	0.0	1.43	3.85
NNE	0.31	0.31	0.38	0.13	0.05	0.03	1.21	4.06
NE	0.13	0.18	0.23	0.15	0.03	0.0	0.72	4.34
ENE	0.18	0.13	0.10	0.05	0.0	0.03	0.49	3.79
E	0.05	0.08	0.18	0.13	0.0	0.0	0.44	4.67
ESE	0.23	0.15	0.03	0.10	0.0	0.0	0.51	3.09
SE	0.13	0.03	0.15	0.03	0.03	0.0	0.37	3.96
SSE	0.08	0.18	0.28	0.18	0.05	0.0	0.77	4.83
S	0.97	0.43	0.36	0.36	0.05	0.0	2.17	3.32
SSW	1.35	0.94	0.61	0.99	0.05	0.0	3.94	3.77
SW	0.43	0.46	0.38	0.69	0.0	0.0	1.96	4.38
WSW	0.0	0.03	0.03	0.0	0.0	0.0	0.06	3.68
W	0.0	0.0	0.0	0.0	0.0	0.0	0.0	0.0
WNW	0.0	0.0	0.0	0.0	0.0	0.0	0.0	0.0
NW	0.08	0.13	0.13	0.03	0.0	0.0	0.42	3.37
NNW	0.41	0.31	0.15	0.20	0.0	0.0	1.07	3.29
Total	4.61	4.10	3.16	3.32	0.31	0.06	15.56	3.86
				Stability Category C				
N	0.38	0.51	0.38	0.59	0.28	0.0	2.14	5.09
NNE	0.31	0.46	0.56	0.64	0.26	0.03	2.26	5.35
NE	0.26	0.38	0.43	0.87	0.15	0.03	2.12	5.53

Table 8, continued.

ENE	0.18	0.48	0.36	0.38	0.15	0.10	1.65	5.49
E	0.13	0.18	0.26	0.05	0.0	0.0	0.62	3.57
ESE	0.05	0.15	0.05	0.13	0.03	0.0	0.41	4.82
SE	0.18	0.10	0.20	0.03	0.05	0.0	0.56	3.86
SSE	0.36	0.28	0.38	0.15	0.05	0.0	1.22	3.76
S	0.97	0.74	0.59	0.71	0.10	0.0	3.11	3.93
SSW	1.99	1.20	0.94	0.54	0.28	0.0	4.95	3.44
SW	1.71	2.04	1.35	0.79	0.13	0.0	6.02	3.51
WSW	0.18	0.31	0.20	0.20	0.0	0.0	0.89	3.89
W	0.0	0.0	0.0	0.0	0.0	0.0	0.0	0.0
WNW	0.03	0.05	0.0	0.0	0.0	0.0	0.08	2.22
NW	0.31	0.20	0.13	0.03	0.0	0.0	0.67	2.62
NNW	0.43	0.36	0.36	0.31	0.03	0.0	1.49	3.87
Total	7.47	7.44	6.19	5.42	1.51	0.16	28.19	4.12
			Stability Category D					
N	0.10	0.05	0.18	0.43	0.33	0.0	1.09	7.07
NNE	0.15	0.18	0.26	0.54	0.18	0.03	1.34	6.09
NE	0.13	0.20	0.28	0.66	0.10	0.05	1.42	6.07
ENE	0.28	0.33	0.41	0.56	0.03	0.08	1.69	5.17
E	0.18	0.20	0.15	0.20	0.13	0.0	0.86	5.00
ESE	0.05	0.20	0.28	0.08	0.05	0.0	0.66	4.56
SE	0.13	0.18	0.08	0.13	0.0	0.0	0.52	3.81

Table 8, continued.

SSE	0.28	0.38	0.23	0.38	0.03	0.0	1.30	4.27
S	0.36	0.48	0.61	0.89	0.13	0.0	2.47	5.04
SSW	1.12	0.77	0.31	0.69	0.10	0.0	2.99	3.70
SW	1.35	1.50	0.61	0.46	0.13	0.03	4.08	3.39
WSW	0.33	0.94	0.48	0.51	0.0	0.03	2.29	4.11
W	0.0	0.03	0.0	0.0	0.0	0.0	0.03	2.80
WNW	0.03	0.08	0.10	0.0	0.0	0.0	0.21	3.41
NW	0.10	0.23	0.05	0.08	0.0	0.0	0.46	3.44
NNW	0.10	0.08	0.08	0.13	0.0	0.0	0.39	4.26
Total	4.69	5.83	4.11	5.74	1.21	0.22	21.80	4.53
			Stability Category E					
N	0.03	0.0	0.0	0.03	0.0	0.0	0.06	4.28
NNE	0.0	0.0	0.0	0.0	0.0	0.0	0.0	0.0
NE	0.03	0.0	0.0	0.0	0.03	0.0	0.06	5.90
ENE	0.05	0.03	0.03	0.03	0.0	0.0	0.14	3.59
E	0.10	0.05	0.03	0.08	0.0	0.0	0.26	3.79
ESE	0.03	0.08	0.0	0.05	0.0	0.0	0.16	3.92
SE	0.03	0.0	0.08	0.03	0.0	0.0	0.14	4.43
SSE	0.03	0.10	0.18	0.15	0.0	0.0	0.46	4.85
S	0.13	0.05	0.15	0.20	0.0	0.0	0.53	4.61
SSW	0.20	0.18	0.10	0.41	0.0	0.0	0.89	4.72
SW	0.18	0.23	0.15	0.20	0.0	0.03	0.79	4.38

Table 8, continued.

WSW	0.03	0.28	0.20	0.20	0.0	0.0	0.71	4.50
W	0.0	0.0	0.0	0.0	0.0	0.0	0.0	0.0
WNW	0.08	0.03	0.0	0.0	0.0	0.0	0.11	1.67
NW	0.03	0.0	0.05	0.0	0.0	0.0	0.08	3.31
NNW	0.0	0.05	0.0	0.0	0.0	0.0	0.05	2.80
Total	0.95	1.08	0.97	1.38	0.03	0.03	4.44	4.38
			Stability Category F					
N	0.03	0.0	0.0	0.0	0.0	0.0	0.03	1.25
NNE	0.0	0.0	0.0	0.0	0.0	0.0	0.0	0.0
NE	0.0	0.03	0.0	0.0	0.0	0.0	0.03	2.80
ENE	0.0	0.03	0.03	0.0	0.08	0.0	0.14	7.60
E	0.0	0.0	0.0	0.0	0.0	0.0	0.0	0.0
ESE	0.0	0.03	0.0	0.0	0.0	0.0	0.03	2.80
SE	0.0	0.0	0.0	0.0	0.0	0.0	0.0	0.0
SSE	0.0	0.0	0.0	0.03	0.03	0.0	0.06	8.93
S	0.0	0.0	0.0	0.05	0.0	0.0	0.05	7.30
SSW	0.05	0.03	0.0	0.03	0.0	0.0	0.11	3.32
SW	0.05	0.08	0.0	0.0	0.0	0.0	0.13	2.20
WSW	0.0	0.0	0.0	0.0	0.0	0.0	0.0	0.0
W	0.03	0.0	0.0	0.0	0.0	0.0	0.03	1.25
WNW	0.0	0.0	0.0	0.0	0.0	0.0	0.0	0.0
NW	0.0	0.0	0.0	0.0	0.0	0.0	0.0	0.0
NNW	0.0	0.0	0.0	0.0	0.0	0.0	0.0	0.0
Total	0.16	0.20	0.03	0.11	0.11	0.0	0.61	4.69

Table 9. Summer (March-September) frequencies of winds.

Direction toward which the wind blows	Frequency, % For winds having speeds (in m/s) of: 0.5-2.0	2.1-3.5	3.6-5.5	5.6-9.0	9.1-12.0	> 12	Totals by direction	Av speed
			Stability Category A					
N	0.40	1.41	0.98	0.15	0.0	0.0	2.94	3.40
NNE	0.27	1.23	1.97	0.78	0.02	0.0	4.27	4.37
NE	0.51	0.98	1.23	0.38	0.0	0.0	3.10	3.79
ENE	0.42	0.42	0.51	0.18	0.0	0.0	1.53	3.49
E	0.36	0.67	0.47	0.09	0.0	0.0	1.59	3.22
ESE	0.58	0.40	0.47	0.11	0.0	0.0	1.56	3.07
SE	0.80	0.42	0.29	0.09	0.0	0.0	1.60	2.60
SSE	0.45	0.36	0.43	0.07	0.0	0.0	1.31	3.08
S	0.58	0.33	0.47	0.22	0.0	0.0	1.60	3.37
SSW	0.42	0.85	0.83	0.67	0.0	0.0	2.77	4.18
SW	0.31	0.74	0.38	0.25	0.0	0.0	1.68	3.58
WSW	0.15	0.15	0.04	0.0	0.0	0.0	0.34	2.32
W	0.0	0.0	0.0	0.0	0.0	0.0	0.0	0.0
WNW	0.04	0.04	0.0	0.0	0.0	0.0	0.08	2.03
NW	0.13	0.15	0.13	0.0	0.0	0.0	0.41	2.86
NNW	0.33	0.80	0.18	0.04	0.0	0.0	1.35	2.79
Total	5.75	8.95	8.38	3.03	0.02	0.0	26.13	3.55

Table 9, continued.

				Stability Category B:				
N	0.16	0.42	1.16	0.94	0.02	0.0	2.70	5.08
NNE	0.27	0.58	2.06	1.72	0.0	0.0	4.63	5.16
NE	0.11	0.34	0.67	0.56	0.0	0.0	1.68	4.90
ENE	0.16	0.31	0.09	0.09	0.0	0.0	0.65	3.28
E	0.16	0.07	0.04	0.05	0.0	0.0	0.32	2.95
ESE	0.24	0.04	0.07	0.07	0.0	0.0	0.42	2.96
SE	0.33	0.04	0.0	0.02	0.0	0.0	0.39	1.72
SSE	0.13	0.07	0.07	0.04	0.0	0.0	0.31	3.13
S	0.38	0.29	0.29	0.27	0.0	0.0	1.23	3.72
SSW	0.53	0.71	0.63	0.53	0.0	0.0	2.40	3.91
SW	0.22	0.71	0.53	0.05	0.0	0.0	1.51	3.34
WSW	0.02	0.09	0.04	0.0	0.0	0.0	0.15	3.06
W	0.0	0.0	0.0	0.0	0.0	0.0	0.0	0.0
WNW	0.0	0.0	0.0	0.0	0.0	0.0	0.0	0.0
NW	0.13	0.31	0.07	0.0	0.0	0.0	0.51	2.65
NNW	0.29	0.65	0.36	0.05	0.0	0.0	1.35	3.10
Total	3.13	4.63	6.08	4.39	0.02	0.0	18.25	4.21
				Stability Category C				
N	0.05	0.47	1.32	2.90	0.18	0.11	5.03	6.38
NNE	0.15	0.98	1.56	2.52	0.11	0.09	5.41	5.72
NE	0.13	0.81	1.32	0.40	0.02	0.04	2.72	4.47

Table 9, continued.

ENE	0.45	1.56	0.85	0.18	0.0	0.0	3.04	3.33
E	0.24	0.38	0.27	0.09	0.0	0.0	0.98	3.32
ESE	0.29	0.25	0.20	0.02	0.0	0.0	0.76	2.79
SE	0.27	0.02	0.07	0.07	0.0	0.0	0.43	2.84
SSE	0.51	0.09	0.15	0.07	0.0	0.0	0.82	2.54
S	0.20	0.36	0.98	0.53	0.07	0.0	2.14	4.82
SSW	0.18	0.63	0.62	0.56	0.05	0.0	2.04	4.62
SW	0.47	0.60	0.36	0.04	0.0	0.0	1.47	2.86
WSW	0.11	0.20	0.02	0.0	0.0	0.0	0.33	2.39
W	0.0	0.0	0.0	0.0	0.0	0.0	0.0	0.0
WNW	0.04	0.07	0.0	0.0	0.0	0.0	0.11	2.24
NW	0.16	0.25	0.07	0.0	0.0	0.0	0.48	2.54
NNW	0.02	0.22	0.18	0.09	0.02	0.0	0.53	4.39
Total	3.27	6.89	7.97	7.47	0.45	0.24	26.29	4.66
			Stability Category D					
N	0.0	0.15	0.42	0.81	0.18	0.04	1.60	6.71
NNE	0.13	0.67	0.91	0.62	0.04	0.16	2.53	5.35
NE	0.36	1.57	1.34	0.45	0.05	0.02	3.79	3.97
ENE	0.89	4.00	1.95	0.20	0.0	0.02	7.06	3.25
E	0.78	1.63	0.33	0.07	0.0	0.0	2.81	2.69
ESE	0.20	0.40	0.22	0.16	0.02	0.0	1.00	3.75
SE	0.09	0.07	0.13	0.02	0.0	0.0	0.31	3.37
SSE	0.42	0.34	0.43	0.04	0.0	0.0	1.23	3.03

Table 9, continued.

S	0.16	0.60	0.98	0.81	0.05	0.0	2.60	4.92
SSW	0.20	0.33	0.16	0.25	0.04	0.0	0.98	4.23
SW	0.15	0.25	0.0	0.0	0.0	0.0	0.40	2.22
WSW	0.13	0.31	0.0	0.0	0.0	0.0	0.44	2.34
W	0.0	0.0	0.0	0.0	0.0	0.0	0.0	0.0
WNW	0.09	0.05	0.02	0.05	0.0	0.0	0.21	3.37
NW	0.05	0.02	0.02	0.02	0.0	0.0	0.11	3.23
NNW	0.0	0.0	0.04	0.05	0.0	0.0	0.09	6.08
Total	3.65	10.39	6.95	3.55	0.38	0.24	26.16	3.93
			Stability Category E					
N	0.0	0.0	0.04	0.02	0.0	0.0	0.06	5.47
NNE	0.0	0.05	0.0	0.0	0.0	0.0	0.05	2.80
NE	0.0	0.04	0.09	0.0	0.0	0.0	0.13	4.01
ENE	0.11	0.33	0.0	0.0	0.0	0.0	0.44	2.41
E	0.27	1.18	0.16	0.0	0.0	0.0	1.61	2.71
ESE	0.0	0.27	0.07	0.02	0.0	0.0	0.36	3.39
SE	0.04	0.04	0.04	0.0	0.0	0.0	0.12	2.87
SSE	0.02	0.16	0.11	0.0	0.0	0.0	0.29	3.36
S	0.11	0.27	0.33	0.04	0.0	0.0	0.75	3.58
SSW	0.02	0.20	0.02	0.0	0.0	0.0	0.24	2.82
SW	0.05	0.04	0.02	0.0	0.0	0.0	0.11	2.41
WSW	0.04	0.02	0.0	0.0	0.0	0.0	0.06	1.77
W	0.02	0.0	0.0	0.0	0.0	0.0	0.02	1.25

Table 9, continued.

WNW	0.0	0.0	0.0	0.0	0.0	0.0	0.0	0.0
NW	0.0	0.0	0.0	0.0	0.0	0.0	0.0	0.0
NNW	0.0	0.0	0.0	0.0	0.0	0.0	0.0	0.0
Total	0.68	2.60	0.88	0.08	0.0	0.0	4.24	3.00
			Stability Category F					
N	0.0	0.0	0.02	0.0	0.0	0.0	0.02	4.55
NNE	0.0	0.0	0.0	0.02	0.0	0.0	0.02	7.30
NE	0.02	0.0	0.0	0.0	0.0	0.0	0.02	1.25
ENE	0.0	0.0	0.0	0.0	0.0	0.0	0.0	0.0
E	0.0	0.02	0.0	0.0	0.0	0.0	0.02	2.80
ESE	0.0	0.02	0.0	0.0	0.0	0.0	0.02	0.80
SE	0.0	0.0	0.0	0.0	0.0	0.0	0.0	0.0
SSE	0.02	0.0	0.0	0.0	0.0	0.0	0.02	1.25
S	0.0	0.0	0.0	0.0	0.0	0.0	0.0	0.0
SSW	0.0	0.0	0.0	0.0	0.0	0.0	0.0	0.0
SW	0.0	0.02	0.02	0.0	0.0	0.0	0.04	3.68
WSW	0.0	0.0	0.0	0.0	0.0	0.0	0.0	0.0
W	0.0	0.0	0.0	0.0	0.0	0.0	0.0	0.0
WNW	0.0	0.0	0.0	0.0	0.0	0.0	0.0	0.0
NW	0.0	0.0	0.0	0.0	0.0	0.0	0.0	0.0
NNW	0.0	0.0	0.0	0.0	0.0	0.0	0.0	0.0
Total	0.04	0.06	0.04	0.02	0.0	0.0	0.16	3.41

in Table 6. Tables 7, 8, and 9 show the relative uniformity of average wind speed between stability categories.

Also, for certain wind directions, higher wind-speed ranges occur relatively frequently in stability categories that are traditionally thought to occur at low windspeeds. In part, this is due to the mechanics of extracting stabilities from wind-speed traces. The present state of the art precludes using more sophisticated techniques. A summary of these stability wind-rose tables for winter and summer is shown in Table 10.

HUMIDITY AND FOG

The only humidity records taken routinely at NTS are made at Yucca Flat. The climatological summary, Table 1, shows typically high humidities in early morning, with significantly lower readings in the afternoon. The reported averages reflect the desert climate -- an annual-average 4:00 a.m. value of 53% and a 4:00 p.m. value of 23%. Fog is a rare occurrence at NTS. Fog is present fewer than six days per year in southern Nevada.[5] Most of these cases occur in winter, but the trend is not pronounced.

Program of Onsite Meteorological Measurements

A CLIMET 013-1 wind-sensing system is operated on a 10-m tower at "Area 410 Basin NW." This location is northwest of the LLL assembly buildings. The starting speed of the CLIMET system is less than 0.5 m/s. Recordings are made on strip charts and the unit is serviced every two weeks by National Oceanic and Atmospheric Administration personnel.

Long-Term (Routine) Diffusion Estimates

Due to the nature of Area 410 activities, there are no routine releases of ionizing radiation or other potentially harmful pollutants. Hence, no estimates of long-term diffusion were made in our study.

Table 10. Summary of wind frequency tables by stability categories, based on records for 1968. Directions are those toward which the wind blows.

Wind statistic	Stability category A	B	C	D	E	F
Winter[a] season						
Most frequent direction	WSW	SSW	SW	SW	SSW	ENE, SW
Frequency, %	6.3	3.9	6.0	4.1	0.9	0.1, 0.1
Speed, m/s	5.0	3.8	3.5	3.4	4.7	7.6, 2.2
Least frequent direction	WNW, W	W, WNW	W	W	NNE, W	7 sectors[b]
Frequency, %	0	0	0	<0.1	0, 0	0
Speed, m/s	0	0	0	2.8	0, 0	0
Highest average speed, m/s	5.4	4.7	5.5	7.1	5.9	7.6
Direction	ENE	E	NE	N	NE	ENE
Frequency, %	2.8	0.4	2.1	1.1	<0.1	0.1
Lowest average speed, m/s	0	0	0	3.4	0, 0	0
Direction	WNW, W	W, WNW	W	SW	NNE, W	7 sectors[b]
Frequency, %	0	0	0	4.1	0, 0	0
Summer[c] season						
Most frequent direction	NNE	NNE	NNE	ENE	E	SW
Frequency, %	4.3	4.6	5.4	7.1	1.6	<0.1
Speed, m/s	4.4	5.2	5.7	3.3	2.7	3.7
Least frequent direction	W	W, WNW	W	W	WNW→NNW	9 sectors[b]
Frequency, %	0	0	0	0	0	0
Speed, m/s	0	0	0	0	0	0
Highest average speed, m/s	4.4	5.2	5.7	6.7	5.5	4.6
Direction	NNE	NNE	NNE	N	N	N
Frequency, %	4.3	4.6	5.4	1.6	<0.1	<0.1
Lowest average speed, m/s	0	0	0	0	0	0
Direction	W	W, WNW	W	W	WNW→NNW	9 sectors[b]
Frequency, %	0	0	0	0	0	0

[a] October through February.

[b] Direction divided into 16 sectors each 22.5° wide.

[c] March through September.

Short-Term (Accident) Diffusion Estimates

Arithmetic-average and probability maps of exposure (time-integrated ground level concentrations of radioactive particles) were obtained from the instantaneous point source (IPS) code developed by Peterson.[6] The input data were the tower winds observed near Super Kukla. The generalized diffusion equation for surface exposure concentration under an explosion's cloud centerline is

$$\psi_s = \frac{Q}{\pi \sigma_{y_I} \sigma_{z_I} u} \exp - \left(\frac{h^2}{2\sigma_{z_I}^2} \right)$$

where ψ_s = surface exposure, in units of $Q \cdot s/m^3$.

Q = source term, assumed unity in this report.

σ_{y_I} = instantaneous crosswind horizontal standard deviation, in m.

σ_{z_I} = instantaneous vertical standard deviation, in m.

u = horizontal windspeed at cloud center, in m/s.

h = height of cloud center above ground, in m.

The IPS code uses Walton's[7] scale-dependent diffusion approach to determine σ_{y_I}; σ_{z_I} is obtained from the equation $\sigma_{z_I} = (2K_x t)^{1/2}$, where K_z, the vertical diffusion coefficient, is a stability-dependent input parameter, and t is travel time downwind. Scaling equations developed from observations of explosions were used to determine the height and geometry of the stabilized cloud. The calculations in this section include surface exposures and deposition from a "puff" of gases and particles that have no appreciable fall velocity (radius less than ~5 μm). Fallout of larger particles, which could produce substantially higher depositions, is not included.

Three types of accidents have been postulated, and this report presents contour maps of radioactive exposure presented for all types. These accidents are:

- The dispersal of plutonium by detonation of 68 kg (150 lb) of high explosives (HE),
- a criticality accident involving 10^{19} fissions of uranium-235 (equivalent to about a 140-lb high-explosives detonation), and
- an inadvertent 100-ton fission explosion.

For accidents (a) and (b), the explosive yields are nearly equal. Hence, it is assumed that their resulting cloud geometries are the same, and one set of exposure-contour maps covering both these accidents is presented in Figs. 6, 7, and 8. Each of these figures gives radioactive exposures calculated on the basis of annual, winter, and summer wind data, respectively. Half of the maps on each time period show the arithmetic

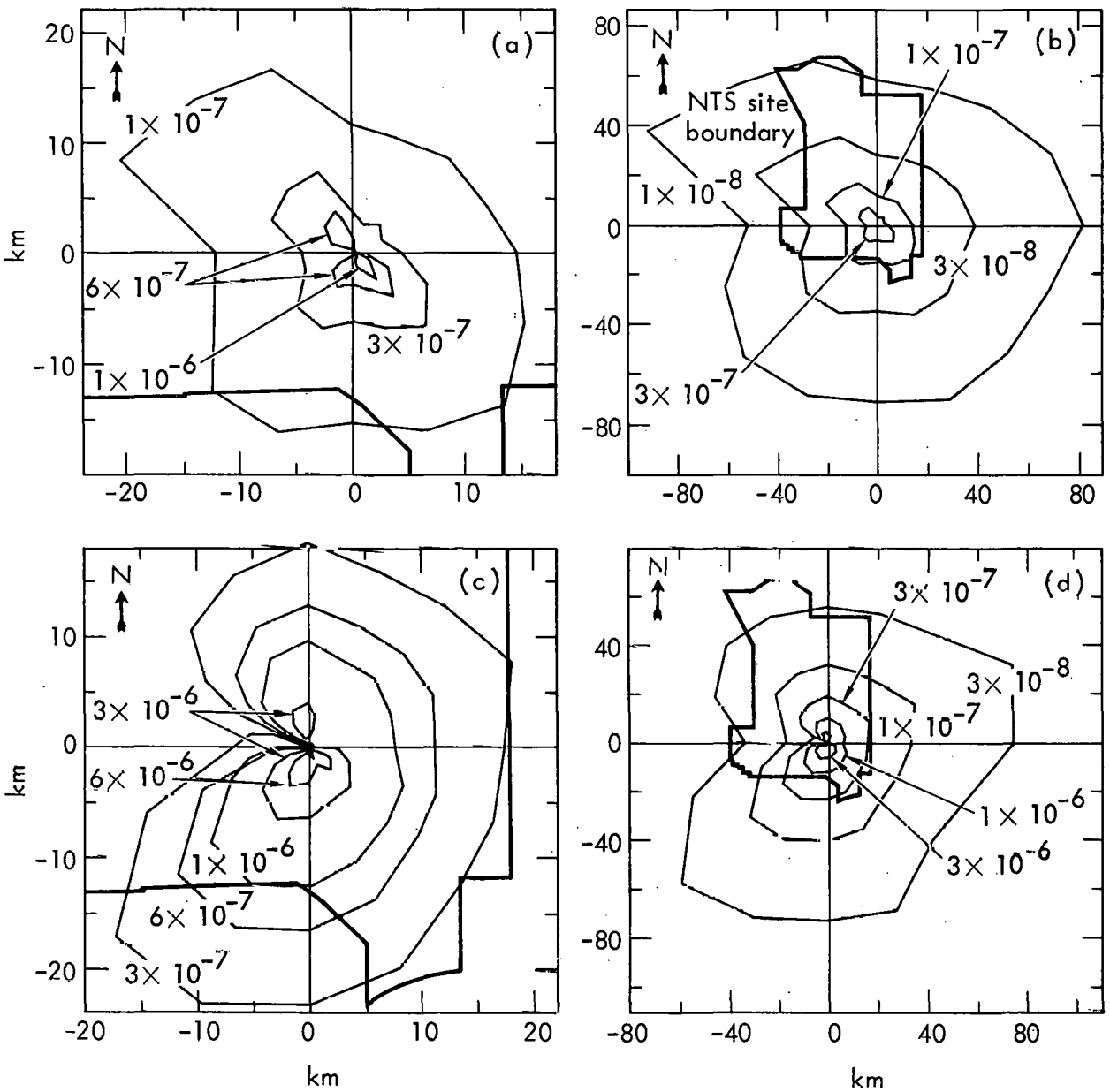

Fig. 6. Relative exposures (in s/m^3) around Area 410 for HE or criticality accident, based on annual wind data: (a) and (b) average exposures at near and far perspectives, respectively; (c) and (d) exposure limits exceeded 5% of the time at near and far perspectives, respectively.

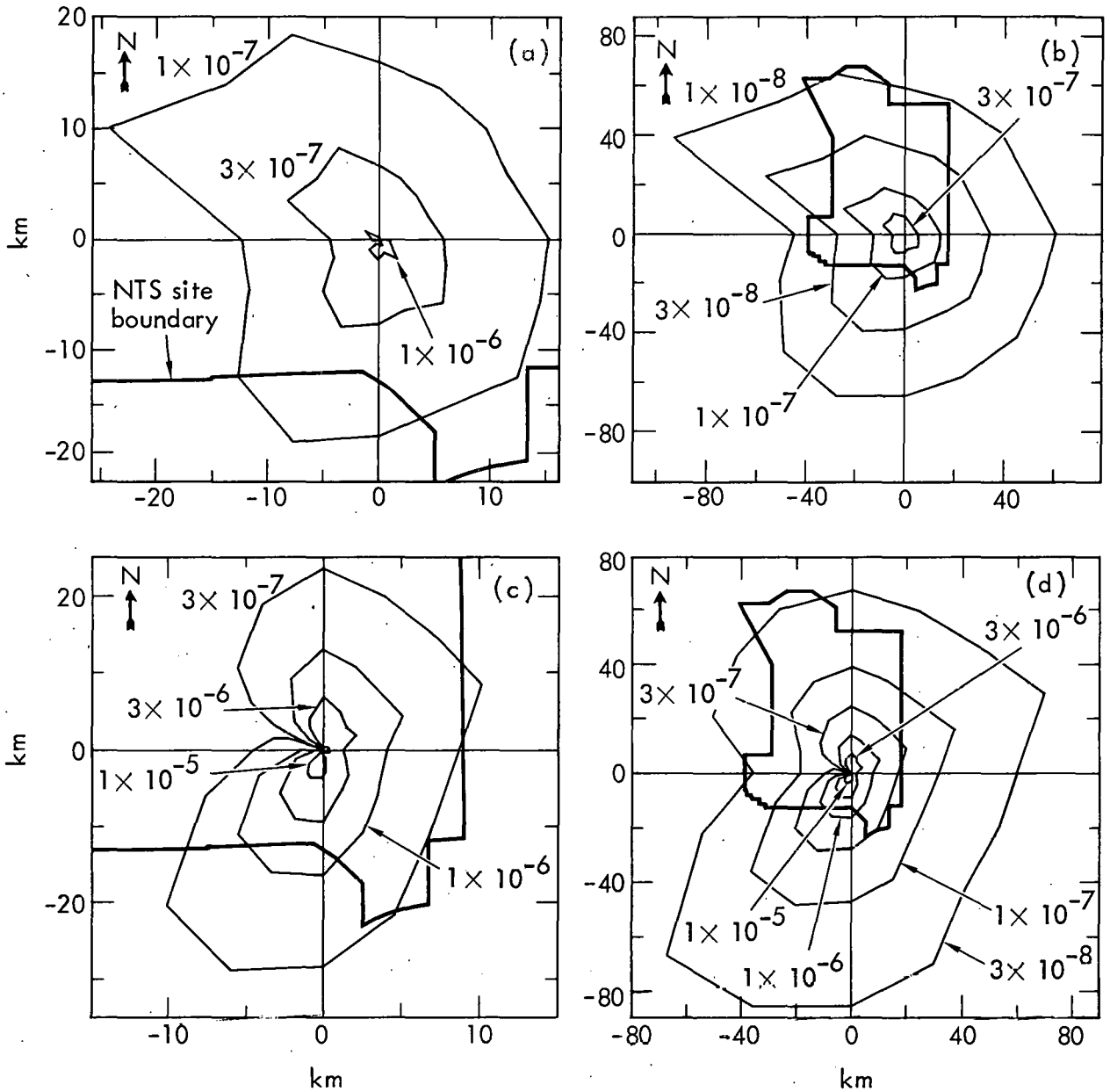

Fig. 7. Relative exposures (in s/m^3) around Area 410 for HE or criticality accident, based on winter (October-February) wind data: (a) and (b) average exposures at near and far perspectives, respectively; (c) and (d) exposure limits exceeded 5% of the time at near and far perspectives, respectively.

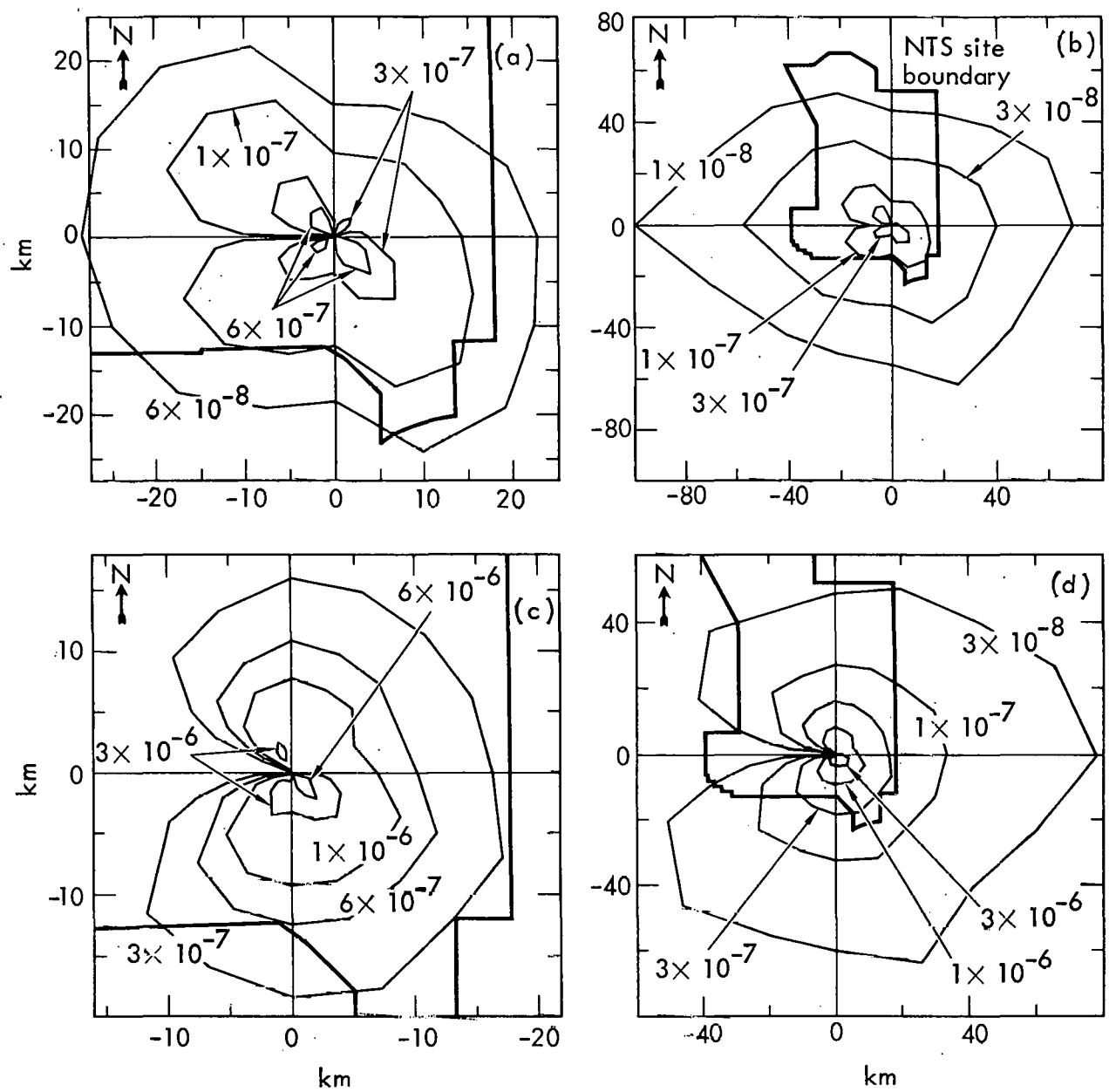

Fig. 8. Relative exposures (in s/m^3) around Area 410 for HE or criticality accident, based on summer (March-September) wind data: (a) and (b) average exposures at near and far perspectives, respectively; (c) and (d) exposure limits exceeded 5% of the time at near and far perspectives, respectively.

average exposures, and the other half were computed allowing a 5% probability that the specified exposures will be exceeded. The latter maps are prepared by assuming a lognormal distribution of exposure and omitting the top 5% of the distribution. Hence, one random accident out of twenty will result in exposures greater than shown on the map. Both close-up and distant maps are presented for each of the average and 5% cases within each time period, with the distant map showing exposures as far as 80 km from Area 410. Also, the NTS site boundary is sketched on the contour maps.

The IPS code depletes the puff with distance according to the deposition velocity, which was assumed to be 0.01 m/s. The product of the exposure and the deposition velocity yields deposition, in units of m^{-2}. Hence, multiplying the exposure-contour values by 0.01 m/s gives surface-deposition contour values. All atmospheric stability categories, weighted by their relative frequencies, were included by the code when it calculated the maps. The specific exposure values for each contour are entered on the diagrams.

The annual average maps have a nearly circular distribution, with a slight diminution of exposures toward the west and west-southwest. The annual 5% maps show a northeast-southwest elongation with diminished values toward the west-northwest. The average and 5% exposure contours of winter are close to those of the annual maps in both shape and magnitude. The northeast-southwest elongation is more pronounced in the winter 5% maps. This is due to wind and stability conditions that favor higher exposures when the wind direction is from the NE and SW.

In the summer, the average exposure pattern shows a general east-west elongation. However, the 5% contours for the same period are nearly circular except for zero exposure values toward the west. The zero values are due to the fact that only one wind toward the west (from the east) was observed in the summer of 1968. The probability routine in the IPS code is unable to treat one case.

The direction toward which exposure at the site boundary is greatest is referred to as the "critical azimuth." Table 11 presents the directions and relative exposures where the critical azimuth crosses the site boundary, as well as those at the closest site boundary (to the south). Note that the critical-azimuth values are less than 20% greater than exposures to the south. Exposure values at various distances to 100 km are presented in Table 12.

Table 11. Relative exposures[a] at the site boundary's intersection with the critical azimuth and at the closest point of the boundary that would result from an HE or criticality explosion.

	Arithmetic av			95%-probable limit		
	Annual	Winter	Summer	Annual	Winter	Summer
Direction of the critical azimuth	SSW	SSW	SE	SSW	SSW	S
Exposure, s/m^3	1.5×10^{-7}	1.8×10^{-7}	1.0×10^{-7}	1.1×10^{-6}	1.7×10^{-6}	5.7×10^{-7}
Direction of the closest site boundary	S	S	S	S	S	S
Exposure, s/m^3	1.3×10^{-7}	1.6×10^{-7}	9.4×10^{-8}	9.5×10^{-7}	1.5×10^{-6}	5.7×10^{-7}

[a]Deposition values (in units of m^{-2}) are 1/100 of exposure values.

100-TON FISSION EXPLOSION

A 100-ton fission explosion would generate a stabilized cloud center at about 1800 m above the surface. This altitude is well beyond the valid range for the power-law wind profile, used to adjust wind speeds at 10 m above the surface to those at the approx 200-m cloud-center height for an HE or criticality accident. Hence, we prepared new input data, using the 1968 upper-air wind conditions observed twice-daily at Yucca Flat. These winds are representative of those at Area 410. The corresponding stability categories were determined from these observations and the near-surface to cloud, center-temperature profile.

The frequencies and average speeds of these upper-air winds as a function of the direction toward which the wind blows are presented in Table 13. The average speeds are generally greater than those of 10-m winds (listed in Table 4), but by less than a factor of two. Winter wind speeds are greater than summer wind speeds. Such behavior is consistent with usual winds in middle latitudes. The wind frequencies at 1800 m also differ from those at 10 m. For the 1800-m winds, the most frequent directions are toward the SSW and SW in both winter and summer. (The 10-m winds show a pronounced reversal toward the NNE in summer.)

The frequencies of stability categories affecting a 100-ton fission accident are shown in Table

Table 12. Relative exposures (s/m^3) along the critical azimuth at site boundary and other points at distances to 100 km; for HE or criticality accident.

Type of exposure	Critical azimuth	Distance along critical azimuth - km at distances (in km) of: 1	2	5	10	SB[a]	20	50	100
Based on annual data									
arithmetic average	SSW	7.8×10^{-7}	7.5×10^{-7}	4.3×10^{-7}	2.1×10^{-7}	1.5×10^{-7}	8.0×10^{-8}	2.0×10^{-8}	5.8×10^{-9}
95%-probable limit	SSW	7.2×10^{-6}	8.4×10^{-6}	4.7×10^{-6}	1.7×10^{-6}	1.1×10^{-6}	4.5×10^{-7}	7.5×10^{-8}	1.8×10^{-8}
Based on winter data									
arithmetic average	SSW	1.0×10^{-6}	9.3×10^{-7}	5.3×10^{-7}	2.5×10^{-7}	1.8×10^{-7}	1.0×10^{-7}	2.3×10^{-8}	6.6×10^{-9}
95%-probable limit	SSW	1.2×10^{-5}	1.4×10^{-5}	8.3×10^{-6}	2.9×10^{-6}	1.7×10^{-6}	7.5×10^{-7}	1.0×10^{-7}	2.5×10^{-8}
Based on summer data									
arithmetic average	SE	2.2×10^{-6}	1.6×10^{-6}	7.7×10^{-7}	2.9×10^{-7}	1.0×10^{-7}	9.0×10^{-8}	2.1×10^{-8}	5.8×10^{-9}
95%-probable limit	S	3.3×10^{-6}	3.6×10^{-6}	2.2×10^{-6}	8.6×10^{-7}	5.7×10^{-7}	2.5×10^{-7}	4.5×10^{-8}	1.2×10^{-8}

[a]SB = Critical azimuth site boundary: 13.5 km to SSW, 12.5 km to S, 19 km to SE.

Table 13. Frequency and average speeds vs wind direction of winds at 1800 m above ground affecting a 100-ton fission explosion at Area 410 (based on 1968 data).

Direction toward which wind blows	Annual		Winter		Summer	
	Frequency, %	Av speed, m/s	Frequency, %	Av speed, m/s	Frequency, %	Av speed, m/s
N	6.0	8.2	6.5	9.4	5.7	7.4
NNE	4.6	8.7	5.4	9.1	4.0	8.4
NE	4.1	7.8	6.2	8.8	2.9	6.4
ENE	1.8	6.0	1.5	9.0	1.9	4.5
E	1.3	5.6	1.9	6.8	1.0	4.0
ESE	0.7	5.4	0.8	3.0	0.7	7.0
SE	1.5	4.4	0.8	3.5	1.9	4.6
SSE	4.3	5.7	2.7	8.3	5.2	4.8
S	6.6	6.7	2.7	3.7	9.0	7.2
SSW	16.9	9.3	10.8	12.2	20.7	8.4
SW	15.9	9.6	15.8	13.2	16.0	7.4
WSW	7.8	6.6	8.5	8.0	7.4	5.6
W	7.1	6.4	5.8	8.3	7.9	5.6
WNW	5.6	6.5	6.9	7.8	4.8	5.2
NW	10.3	8.4	14.6	9.8	7.6	6.8
NNW	5.6	9.2	9.2	10.8	3.3	6.4
All directions	100.	7.2	100.	8.2	100.	6.2

14. On an annual basis, "D" (neutral) stability occurs over 60% of the time at 1800 m above ground. In the winter, essentially all the stabilities are "D" or "E", with "E" occurring almost 60% of the time, while in the summer "D" stability predominates over 70% of the time. More stable conditions are to be expected in winter, particularly in a desert environment.

A comparison of Table 14 with Table 6 (based on 10-m winds) indicates considerably higher frequencies of stable conditions affecting the 100-ton nuclear accident. This is consistent with daytime observations of lapse rate

Table 14. Frequency of stability categories for 100-ton fission explosion at Area 410 (based on winds at 1800 m above ground).

Stability category	Frequency, %		
	Annual	Winter (Oct-Feb)	Summer (Mar-Sept)
A	0.4	0	0.7
B	4.0	0	6.4
C	6.9	0	11.2
D	61.3	41.9	73.3
E	27.2	57.7	8.3
F	0.2	0.4	0

vs height. Super-adiabatic lapse rates (very unstable) often occur near the surface, especially in a desert environment. At higher levels, the lapse rate usually becomes neutral or slightly stable. Also, it has been observed, upon occasion, that the $\Delta\theta$-method of assessing stabilities (from wind-direction strip charts) has tended to yield stabilities that are too unstable, by about one Pasquill category.

The upper-air winds were used to calculate relative exposures for annual, winter, and summer periods for both the arithmetic average exposure and the 5% probability that specified exposures would be exceeded.

Due to the geometry of the 100-ton fission explosion's stabilized cloud (at about a height of 1800 m above the ground), the gradient of exposure values along a radial is small for both the arithmetic average and the 5% calculations. This small gradient is due to the fact that as the cloud moves downwind, the surface concentrations of a pollutant decrease while the cloud's time in passing increases at a nearly compensating rate. As a result, the exposure at any point during cloud passage is nearly constant.

Instead of calculating exposure values at intervals so small that they greatly exceed the estimated error of the calculations, it is preferable to present the average of exposures out to 100 km, with an indication of the variation about the average. This latter approach has been used in Figs. 9-11. The top number within each sector represents the average of exposure values out to 100 km, in units of 10^{-10} s/m^3.

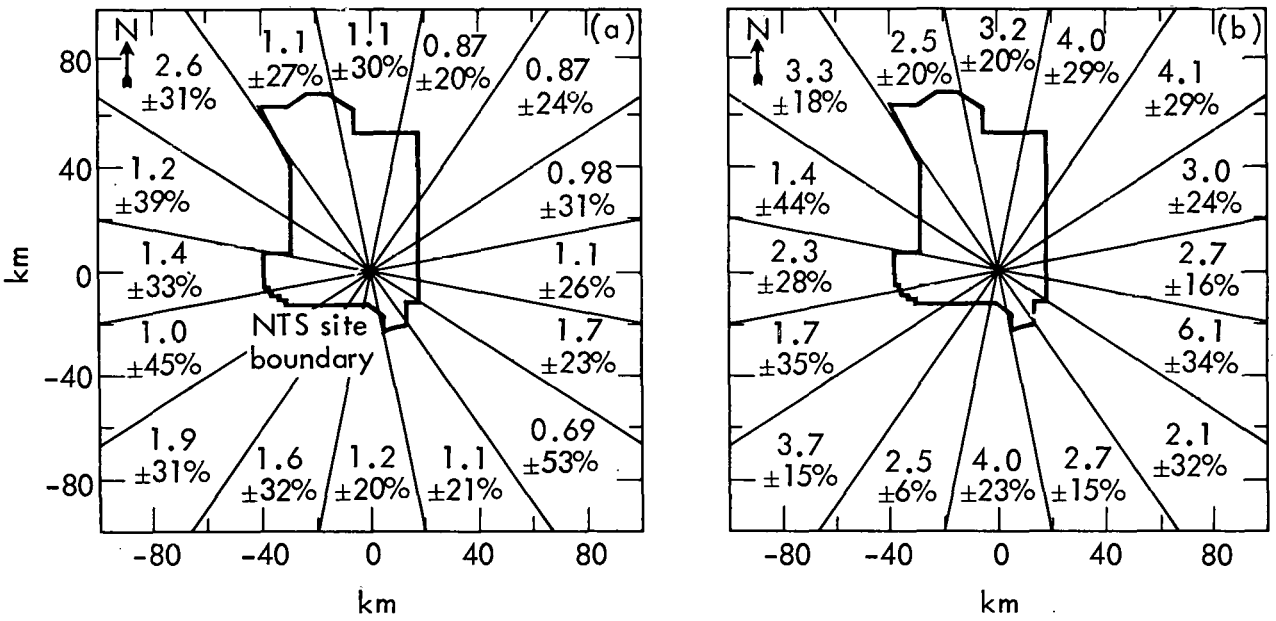

Fig. 9. Relative Exposures (in 10^{-10} s/m^3) for 100-ton fission accident, based on annual wind data. Percentages indicate variation of exposures within each zone up to 100 km from Area 410. Fig. 6a gives the arithmetic average exposures, Fig. 6b gives a limit of exposure exceeded 5% of the time.

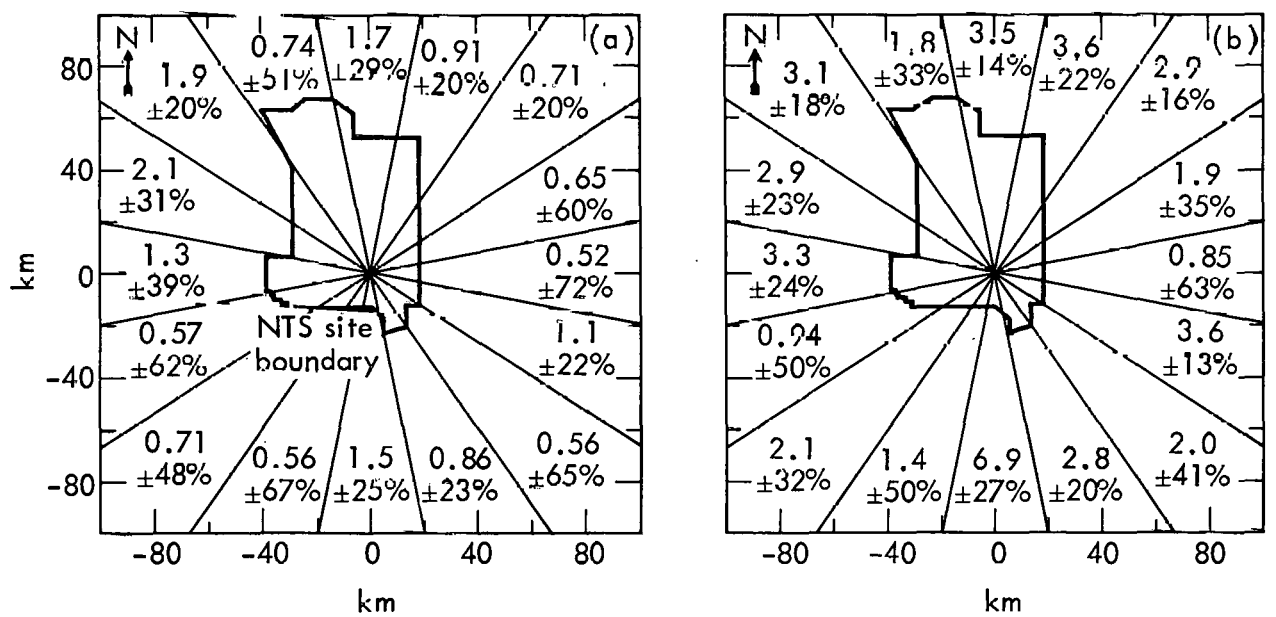

Fig. 10. Relative exposures (in 10^{-10} s/m^3) for 100-ton fission accident, based on winter (October-February) wind data. Percentages indicate variation of exposures within each zone up to 100 km for Area 410. Fig. 6a gives the arithmetic average exposures; Fig. 6b gives a limit of exposure exceeded 5% of the time.

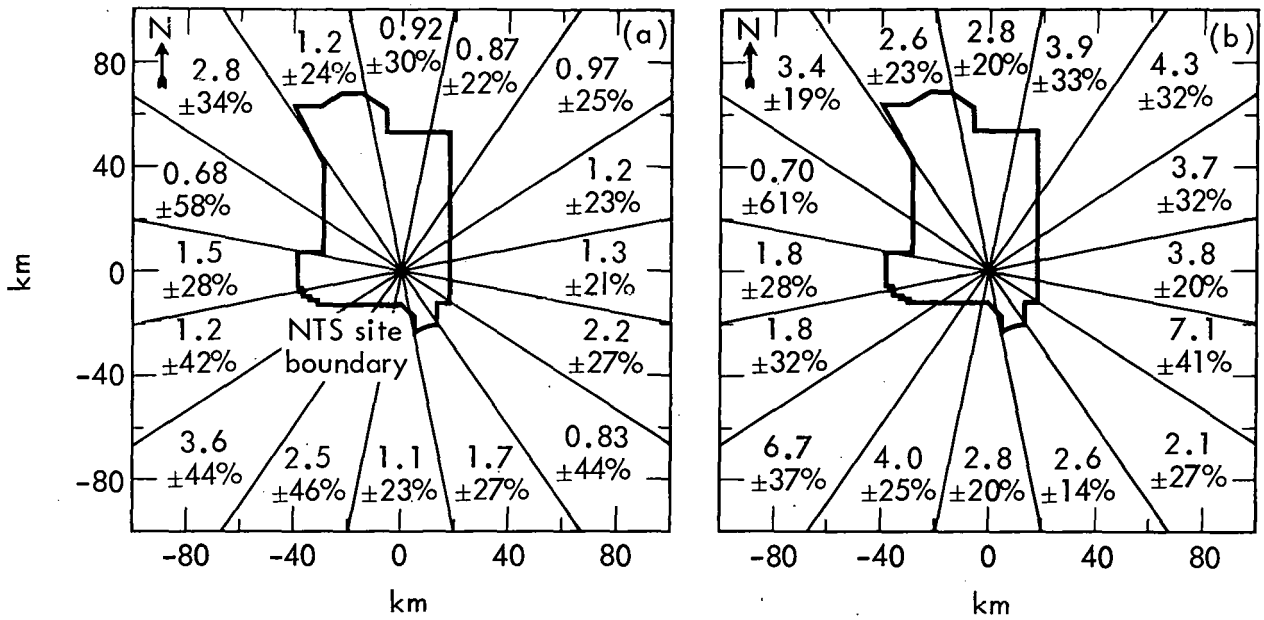

Fig. 11. Relative exposures (in 10^{-10} s/m^3) for 100-ton fission accident, based on summer (March-September) wind data. Percentages indicate variation of exposures within each zone up to 100 km from Area 410. Fig. 6a gives the arithmetic average exposures, Fig. 6b gives a limit of exposure exceeded 5% of the time.

The bottom number is the absolute range of calculated values within each sector, expressed as a percentage. For example, in Fig. 9a, the numbers at the top center indicate an arithmetic average exposure of 1.1×10^{-10} s/m^3, with a range of exposures between 0.8×10^{-10} and 1.4×10^{-10}. On all the charts, the highest value in each sector is less than a factor of two greater than the average (+ 100% and -50% are factors of two from the average). Those sectors with the larger percentages are generally associated with the smaller exposure values during the winter season. Note that the highest annual exposures are toward the NW and ESE for the arithmetic average and 5% values, respectively. During the winter, arithmetic averages are greatest toward the NW and N; 5% values show a maximum toward the S. In summer, maximum values occur toward the SW (arithmetic average) and the ESE and SW (5% values). Surface deposition values, in relative units of m^{-2}, may be obtained by dividing the exposures by v_d (0.01 m/s).

Table 15 gives the relative exposures (s/m^3) at the site boundary along the critical azimuth and at the closest boundary from Area 410, in the event of a 100-ton fission explosion. Table 16 presents relative exposures at various distances along the critical azimuth. Note the uniformity of the arithmetic averages at from 1 to 100 km.

Table 15. Relative exposures[a] at site boundary along the critical azimuth and at the closest boundary for a 100-ton fission explosion.

	Arithmetic average			95%-probable limit		
	Annual	Winter	Summer	Annual	Winter	Summer
Direction of critical azimuth	NW	NW	NW	ESE	S	ESE
Exposure, s/m^3	2.3×10^{-10}	2.0×10^{-10}	9.0×10^{-11}	4.2×10^{-10}	5.0×10^{-10}	4.7×10^{-10}
Closest site boundary	S	S	S	S	S	S
Exposure, s/m^3	9.9×10^{-11}	1.1×10^{-10}	2.6×10^{-10}	3.1×10^{-10}	5.0×10^{-10}	2.2×10^{-10}

[a]Deposition values (in m^{-2}) are 1/100 of exposure values.

Table 16. Relative exposures (in units of 10^{-10} s/m^3) at various distances along the critical azimuth for a 100-ton fission explosion.

	Direction of critical azimuth	Distance along critical azimuth - km						
		1	2	5	10	20	50	100
Annual exposure								
arithmetic average	NW	2.0	2.0	1.9	1.8	1.9	2.5	3.4
95%-probable limit	ESE	4.3	4.2	4.1	4.0	4.2	5.7	8.2
Winter exposure								
arithmetic average	NW	2.2	2.1	1.9	1.7	1.6	1.7	2.1
95%-probable limit	S	5.3	5.2	5.1	5.0	5.2	6.4	8.7
Summer exposure								
arithmetic average	NW	2.0	1.9	1.8	1.8	2.0	2.8	3.7
95%-probable limit	ESE	4.3	4.2	4.2	4.2	4.7	6.6	1.0

References

1. R. F. Quiring, Climatological Data, Nevada Test Site and Nuclear Rocket Development Station, ESSA Research Laboratories, Las Vegas, Nev., Technical Memorandum ERLTM-ARL7, (1968).

2. J. R. McDonald, J. E. Minor, and K. C. Mehta, Development of a Design Basis Tornado and Structural Design Criteria for the Nevada Test Site, Nevada, Lawrence Livermore Laboratory Rept. UCRL-13668 (1975).

3. R. F. Quiring, Wind Summaries for Area 410 Basin NW Station, 1964-1968, private communication (April 26, 1972).

4. D. H. Slade, Ed., Meteorology and Atomic Energy 1968, U.S. Atomic Energy Commission, New Brunswick, New Jersey, Rept. T10-24190 (1968).

5. W. C. Hardwick, Monthly Weather Rev. 101 (10), 763 (1963).

6. K. R. Peterson, "IPS: A Computer Program for Calculating Diffusion and Deposition for an Instantaneous Point Source," Lawrence Livermore Laboratory private communication (1976).

7. J. J. Walton, J. Appl. Meteor. 12 (3), 547 (1973).

FW/gw/ms/gw

Technical Information Department
LAWRENCE LIVERMORE LABORATORY
University of California | Livermore, California | 94550

UCRL-13668

DEVELOPMENT OF A DESIGN BASIS TORNADO

and

STRUCTURAL DESIGN CRITERIA

for the

NEVADA TEST SITE, NEVADA

by

James R. McDonald, P.E.
Joseph E. Minor, P.E.
Kishor C. Mehta, P.E.

FINAL REPORT

prepared for

STRUCTURAL MECHANICS GROUP

Nuclear Engineering Test Division

LAWRENCE LIVERMORE LABORATORY

University of California

Livermore, California

P.O. 5062405

Rev. June 1975

McDONALD, MEHTA and MINOR
Consulting Engineers
Lubbock, Texas

FOREWORD

The development of recommendations for a design basis tornado and structural design criteria for use in evaluating critical facilities at the Nevada Test Site was conducted under Purchase Order No. 5062405 with Lawrence Livermore Laboratory, University of California. Mr. Robert C. Murray of the Structural Mechanics Group, LLL, served as the technical representative for monitoring the project. Dr. James R. McDonald represented the consulting firm of McDonald, Mehta and Minor as principal investigator. Dr. Richard E. Peterson, a meteorologist, also contributed to the technical effort.

TABLE OF CONTENTS

LIST OF ILLUSTRATIONS

LIST OF TABLES

I. INTRODUCTION

The purpose of this document is to prescribe criteria and to provide guidance for professional personnel who are involved with the evaluation of existing buildings and facilities at the Nevada Test Site, Nevada. It is intended that this document be used in the evaluation of critical facilities to resist the possible effects of extreme winds and tornadoes. The document contains two major sections: (1) development of parameters for the effects of tornadoes and extreme winds and (2) guidelines for evaluation and design of structures.

The report presents a summary of the investigations conducted and contains discussions of the techniques used for arriving at the combined tornado and extreme wind risk model. The guidelines for structural design include methods for calculating pressure distributions on walls and roofs of structures and methods for accommodating impact loads from missiles.

II. DEVELOPMENT OF A DESIGN BASIS TORNADO

A. Meteorological Considerations

Tornadoes usually occur in association with vigorous convective cloud systems. For the United States, several distinctive synoptic weather patterns have been shown to favor the development of tornado-producing thunderstorms (Miller 1970)*. The essential ingredients, however, are similar for the various tornado producing cloud configurations: (1) a strong flow of moisture near the surface, (2) a dry air current at middle levels, (3) an intense jet stream at upper levels, and (4) a triggering mechanism, such as daytime heating or an advancing front. Recognition of these necessary elements for tornado formation came initially during the 1950's from detailed post-storm analyses which concentrated on weather patterns over the eastern two-thirds of the nation. Limited analyses have appeared regarding tornadoes in the West (Feris 1970; Fujita 1970, 1972).

As shown by Rasmussen (1967), Nevada lacks sufficient moisture to support the type of tornadic activity experienced in the Central U. S. Moreover, the strong currents (particularly near the surface) which promote long-lasting squall lines (with associated tornadoes) do not develop as extensively over the more irregular terrain of the West, although local low-level jets do occur.

Occasionally, however, moisture may flow into Southern Nevada to enhance the development of thunderstorms. Rasmussen (1967) noted the influx of water vapor into Arizona from the south during the

---

*References may be found in the alphabetically arranged List of References by referring first to author name and then to publication date.

summer months. More recently, Hales (1974) and Brenner (1974) have contended that the Gulf of California acts as a low-level moisture source for the interior Southwest. Mountain thunderstorms in Arizona and Nevada may build within this moist air surge which has been channeled northward. The initial flow northward at times arises from hurricane activity off the west coast of Mexico -- an area second only to the Western Pacific in the production of tropical storms. However, NTS is not effected by strong winds but only moisture from these storms.

During the colder part of the year, occasional funnels may develop through the lifting action of strong Pacific cold fronts and as a result of destabilization accompanying the passage of cold low pressure areas at upper levels.

Dust devils are a frequent form of vortex activity in Nevada. Most of the vortices are relatively small and last only a few minutes; however, some dust devils may reach tornadic proportions (and yet not appear in the records as tornadoes). Fujita (1973) has concluded that strong dust devils are more intense than over 50 percent of confirmed tornadoes; his expected maximum wind for dust devils falls in the F2 classification (113-157 mph). Refer to Appendix A for a table of the Fujita-Pearson Scale.

Superadiabatic lapse rates of temperature in the lowest tens of meters are usually observed during periods of dust devil activity (Ryan and Carroll 1970); therefore, surface characteristics and topography will dictate the likelihood of dust devil development. The vortical motion which becomes organized in these cases originates

in various types of mesoscale flow.

B. Orographic Considerations

Local wind fields along valleys or in the lee of terrain features may yield vortices of greater or lesser intensity than the local norm, depending upon the stability of the air in these local regions (Hallett 1969, Ingram 1973). Thunderstorms developing over the desert or forming in the high country often produce outflow regions spreading over hundreds of square miles, persisting for hours after the onset of the storm (Idso 1974). The leading edge of the colder downdraft air is a very active source for dust devil development (Warn 1952); these vortices are likely to be particularly intense at the intersection of two outflows and where the outflow impinges on moist air.

It has been suggested that there may be some correlation between tornado occurrence and the dewpoint temperature (temperature at which the air is saturated with water) at ground level (Wash 1300). Based on approximately 20 years of records, the mean dewpoint temperature for Ely, Las Vegas, Reno and Winnemucca, Nevada is 28°F. (Adjusted to sea level). The highest mean value for any particular month is 41° at Las Vegas (U.S. Department of Commerce 1968). The contention that dewpoint temperatures are below those necessary for thunderstorm activity is further supported by charts by Dodd (1965). These charts show a standard deviation in addition to the mean monthly values.

C. Tornado Records

Nevada is a large, sparsely populated region in which there have been few tornadoes. In fact, dating from one of the earliest maps of tornado activity (Finley 1884) into the modern era (Court 1970), no tornadoes are noted for the Nevada area until 1953 (Flora 1953). There was another reported tornado occurrence in the late fifties. For the last decade, the average rate of tornado occurrence has been about one tornado per year with many years of no reported tornadoes (NSSFC 1974).

The recorded Nevada tornadoes have appeared chiefly in the vicinity of population centers (mostly near Reno) with an additional few tornadoes being reported in the east and southern tip of Nevada. Undoubtedly, as populations increase in this area and as recreational activity increases, the number of tornadoes seen and reported will result in a more widespread distribution. This anticipated more complete, and, hence, more accurate representation of tornado incidence will probably support the observation that tornado occurrence probabilities are relatively low in this region. The general absence of conditions favorable for tornado formation (Fujita 1973, see especially Fig. 7) also support this observation.

Tornadoes occurring during the period 1959-1973 in Arizona, California, Nevada and Utah (the States which surround the Nevada Test Site) are summarized in Table I. Tornadoes occurring within the 5-degree square surrounding the NTS during the same period are summarized in Table II. Tornado occurrence locations and relative windspeed intensities, presented using Fujita's F-Scale (Fujita 1971), are included in Fig. 1.

TABLE I

TORNADO OCCURRENCES AND INTENSITIES IN FOUR STATE AREA SURROUNDING NTS (1959-73)

[SOURCES: NOAA (Storm Data), NSSFC 1974]

	Tornado Intensity (Fujita 1971)				
STATE	F0	F1	F2	F3	TOTAL
Arizona	23	20	18	4	65
California	18	11	4	-	33
Nevada	8	3	1	-	12
Utah	12	9	5	-	26
Total	61	43	28	4	136

TABLE II

TORNADO OCCURRENCES IN 5-DEGREE SQUARE SURROUNDING NTS (1959-73)
[SOURCES: NOAA (Storm Data), NSSFC 1974]

	Tornado Intensity (Fujita 1971)				
STATE	F0	F1	F2	F3	TOTAL
Arizona	-	2	-	1	3
California	1	1	-	-	2
Nevada	3	-	-	-	3
Utah	-	-	-	-	0
Total	4	3	0	1	8

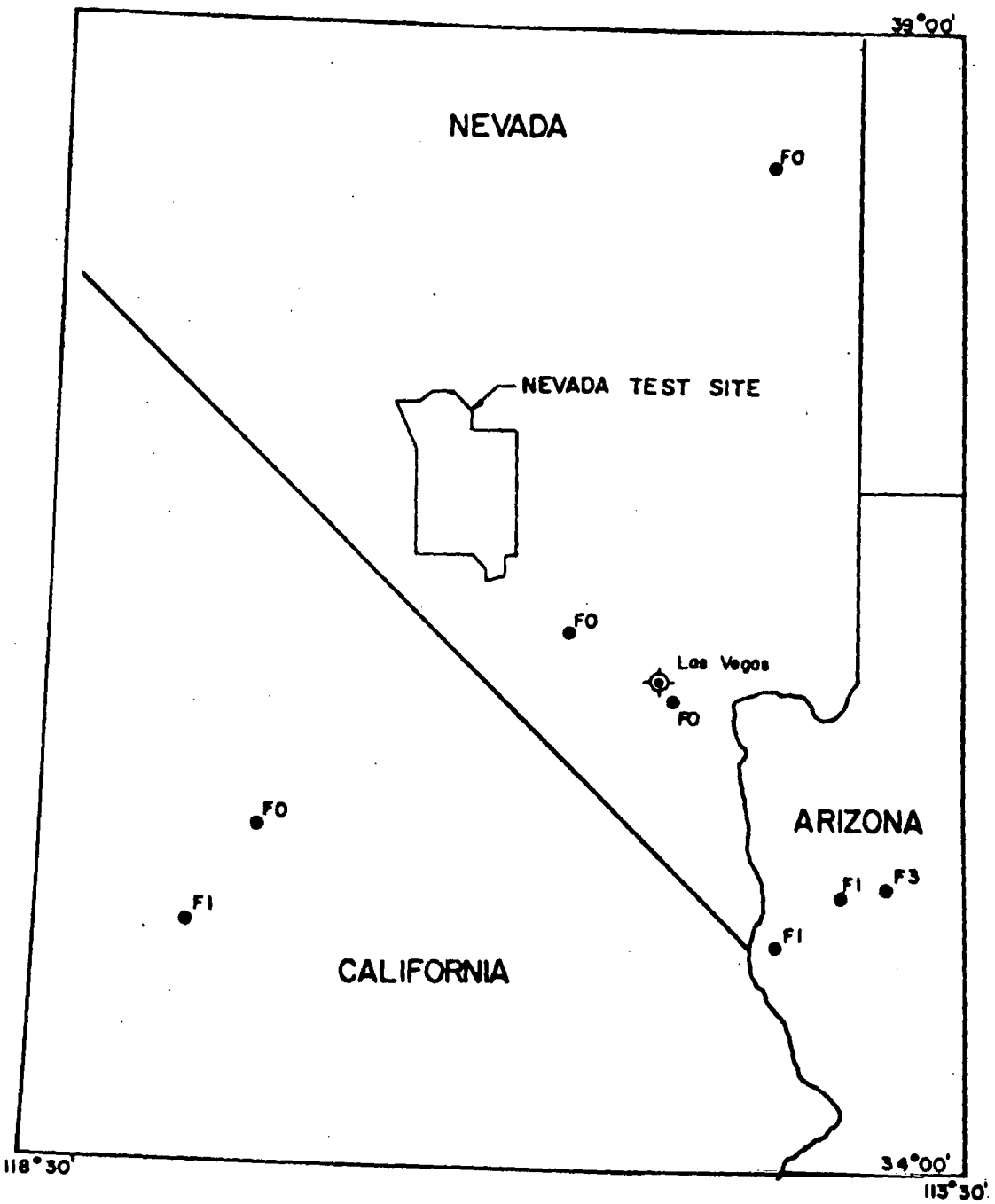

FIGURE 1. TORNADO OCCURENCES IN 5-DEGREE SURROUNDING THE NEVADA TEST SITE

D. Tornado and Extreme Wind Risk Model

The above reviews of the published literature and reviews of both published and unpublished tornado occurrence records indicate that tornadic vortices are uncommon in Nevada due to the absence of sufficient moisture and the interruption of low level flows by terrain irregularities. On the other hand, those tornadoes which do occur may be caused and enhanced more by locally induced flows than by synoptic scale features.

Design standards that are incorporated into building codes do not normally include the effects of tornadoes in their wind load criteria, while some tornado risk models ignore the presence of nontornadic extreme winds. The literature reviews and data evaluations suggest that design basis extreme windspeeds and associated tornado effects for NTS should be developed from available tornado records used in combination with extreme wind data available elsewhere in the literature. Furthermore, the design basis extreme winds and tornado effects should be developed on a probabilistic basis which relates extreme windspeeds with a probability of occurrence.

1. Methodology for Developing the Tornado Portion of the Risk Model

Since tornado intensities are expressed in terms of Fujita-Pearson Scales (FPP-Scales), the tornado risk model was developed on this basis. Four basic steps are involved:

(1) Determination of the mean area of tornado damage based upon tornadoes which occurred in the four state area surrounding NTS.

(2) Determination of the average number of tornadoes per year for each F-Scale intensity classification in a 5-degree square surrounding the NTS.

(3) Calculation of the probability of occurrence of tornadoes exceeding a threshold windspeed within the 5-degree square area.

(4) Determination of the probability that windspeeds in tornadoes will exceed the threshold value.

a. Mean Damage Area

There was an insufficient number of tornado occurrences in a 5-degree square around NTS to make a statistically reliable prediction of the mean damage areas for each F-Scale classification of tornadoes. Although this procedure has been employed in other tornado risk model developments (McDonald 1974, 1974a), a different procedure was employed in the NTS study. In the modified procedure a larger geographical region (consisting of the State of Nevada, and parts of the States of Utah, Arizona, and California) was used to determine a single average damage area for all tornadoes occurring in the four state area. The NSSFC tape (NSSFC 1974) gives a Pearson path length (P_L) and path width (P_W) for most tornadoes in the four state region for the three year period 1971-73. From the P_L and P_W ratings the damage area in square miles was determined for these tornadoes using the median length and width in each Pearson scale classification. The mean damage area for tornadoes in the four state area was then computed from these data.

b. Average Number of Tornadoes Per Year

The number of tornadoes in the 5-degree square was obtained from the master list discussed above. These data are presented in Table II and in Fig. 1. F-Scale ratings were assigned by the authors

on the basis of damage descriptions from Storm Data (NOAA), if they were not provided by the NSSFC computer tape. In some instances the descriptions in Storm Data were vague or non-existent. A conservative F-Scale rating was assigned in these cases. Once these ratings had been made, the average number of tornadoes exceeding any threshold windspeed was determined for the region. The number of tornadoes exceeding the windspeed represented by each F-Scale rating was plotted on semi-log paper (Ref. Fig. 2). A straight line was fitted through the points. From this plot the number of tornadoes exceeding any threshold velocity could be determined. With this information, the average number of tornadoes per year exceeding the threshold velocity was found.

c. Probability of Occurrence

By having the mean damage path area and the average rate of occurrence per year for any arbitrary threshold windspeed, the probability of occurrence of tornadoes having any arbitrary threshold windspeed could be determined by using the relationship

$$P_i = \frac{\lambda_i \overline{A}}{A}, \qquad (1)$$

where:

λ_i is the average rate of tornado occurrence per year for the threshold windspeed V_i (tornadoes/year, from Fig. 2)

$\overline{A}$ is the mean tornado damage path area in sq mi

A is the total area within the 5-degree square surrounding the NTS (sq mi).

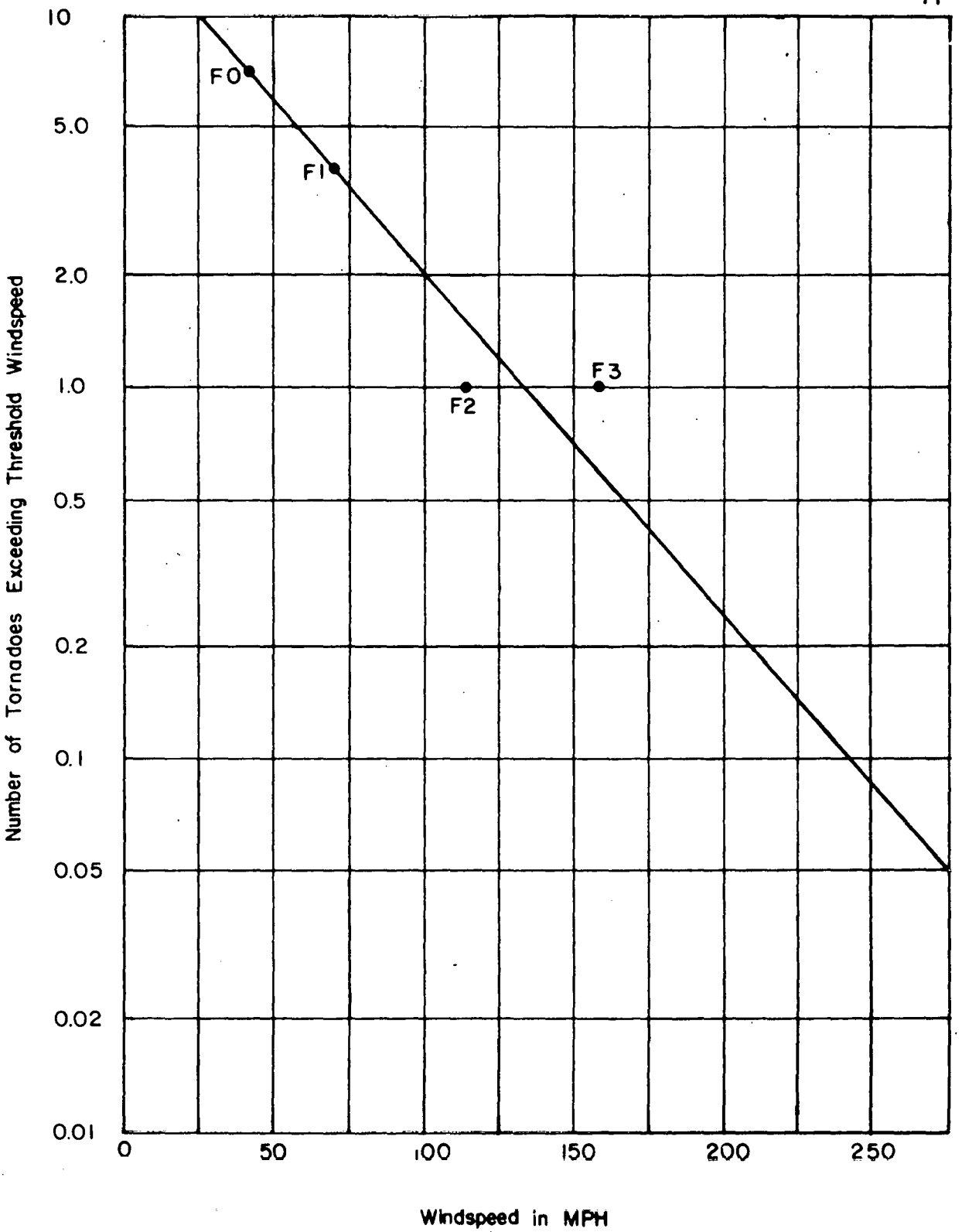

FIGURE 2. NUMBER OF TORNADOES EXCEEDING THRESHOLD WINDSPEEDS

d. Probability of Windspeeds Exceeding a Threshold Value

The probability of winds exceeding a windspeed corresponding to a specific threshold value, V_i, is obtained by taking the cumulative sum of the probabilities of the threshold values higher than the one under consideration.

$$P_E = \sum_{i=i}^{n} P_i \qquad (2)$$

where n is related to the largest threshold velocity considered. Table III contains a summary of the results of the study to determine the tornado occurrence probability distribution.

2. Methodology for Determining the Straight Wind Portion of the Risk Model

The work of Thom (1968) is used to evaluate the probability of straight winds exceeding any threshold value of windspeed. Thom's data specifically excludes tornadoes from the data set.

a. Windspeed Records

The probability distributions for straight winds developed by Thom are based on records of extreme annual fastest mile windspeeds. The records cover a 21 year period and were accumulated at 150 locations in the contiguous United States.

b. Straight Windspeed Distribution

Because winds are bounded at zero and are generally thought of as being unlimited above zero, Thom selected the Fisher-Tippett Type II distribution for straight winds. The data set of annual extreme fastest mile windspeeds for each weather station, after being corrected for elevation and terrain roughness, was fitted to the Fisher-

TABLE III

COMPUTATIONS: TORNADIC WIND OCCURRENCE PROBABILITY DISTRIBUTION

	Threshold Windspeed (mph)					
	50	100	150	200	250	300
Number of tornadoes exceeding threshold windspeed	6.5	2.2	0.8	0.3	0.09	0.03
Number of tornadoes in the threshold interval	4.3	1.5	0.5	0.17	0.058	0.020
Number of tornadoes per year, λ_i	0.28	0.097	0.033	0.011	0.0039	0.0014
Mean damage area, $\bar{A}$ (sq mi)	.39	.39	.39	.39	.39	.39
Geographic area, A (sq mi)	96,000	96,000	96,000	96,000	96,000	96,000
Probability of occurrence of threshold value, P_i (per year)	1.1×10^{-6}	3.9×10^{-7}	1.3×10^{-7}	4.6×10^{-8}	1.6×10^{-8}	5.5×10^{-9}
Probability of exceeding threshold value, P_E (per year)	1.7×10^{-6}	5.9×10^{-7}	2.0×10^{-7}	6.7×10^{-8}	2.1×10^{-8}	5.5×10^{-9}

Tippett Type II probability distribution. The expression for the cumulative probability per year of not exceeding a windspeed value V is

$$F(V) = \exp -(V/\beta)^{-\gamma} \tag{3}$$

where β and γ are chosen to fit the annual extreme fastest mile wind data set for the geographical location under consideration. Thom constructed a special probability paper (See Fig. B1) on which the Fisher-Tippett Type II distribution plots as a straight line. A simple logarithmic transformation of Eqn. 3 puts it in the form

$$y = a + bx, \tag{4}$$

where a and b are parameters that define the straight line relationship. A regression analysis then yields values of the parameters a and b for the best fit straight line through the data points. The β and γ terms in Eqn. 3 are related to the values of a and b. The distributions were fitted to 150 stations to obtain data for the wind probability maps of the United States for mean recurrence intervals of 2, 10, 25, 50 and 100 years (Thom 1968). The mean recurrence interval is given by

$$R = \frac{1}{1 - F(V)} \tag{5}$$

A transformation involving logarithms of the extreme windspeeds can be made to obtain the Fisher-Tippett Type I model. This is the model that was actually used by Thom (1968) in his latest work.

This mathematical model is also known as the Frechet distribution function.

Based on Thom's work, the probability of exceeding a threshold windspeed in one year is given by the expression

$$P_E = 1 - F(V). \tag{6}$$

Since a data set of annual extreme fastest mile winds was not available for the NTS site, the probability distribution (Eqn. 3) was obtained from Thom's wind probability maps. The procedure used is described in Appendix B.

The extrapolation of the straight wind curve into the 200 mph or greater regime must be discussed in terms of confidence limits. There is always some uncertainty as to the line of best fit through the data points. Thus any value quoted from the wind model is the expected value. The expected value is expected to be exceeded half the time and not exceeded half the time. Therefore, there is a band of confidence (or band of uncertainty) associated with any statement from the model. If more data points are used (additional years of records) the band of confidence narrows. However, since the expected value line is extrapolated beyond the data points, as is done in this study, the band of confidence becomes extremely wide.

There may be some upper bound on maximum straight windspeed. A value corresponding to the speed of sound would appear to be one such limit. On the other hand, the upper limit assumed for tornadoes is in the neighborhood of 300 mph (Kessler, 1974; Fujita,

1970, 1972). This limit could be used for straight winds as well. Thus in this study the upper limit windspeed for straight wind is assumed to approach the generally accepted upper limit windspeed for tornadoes.

3. The Risk Model: Combined Effects of Straight Winds and Tornadoes

The combined probability distribution of both tornadoes and straight winds is approximately equal to the sum of the two distributions. The probability of the union of two events is approximately equal to the sum of the probabilities of the individual events, if the probability of their intersection is small (Neville and Kennedy 1966). Values for the straight wind (Fisher-Tippett Type II) distribution, the tornado distribution and the combined distribution are given in Table IV, and are plotted in Figure 3.

TABLE IV

PROBABILITY DISTRIBUTIONS FOR NEVADA TEST SITE
(STRAIGHT WINDS, TORNADOES, AND COMBINED)

Windspeed	Straight Wind Distribution	Tornado Distribution	Combined Distribution
50	4.5×10^{-1}	1.7×10^{-6}	4.5×10^{-1}
100	1.0×10^{-3}	5.9×10^{-7}	1.0×10^{-3}
150	2.4×10^{-5}	2.0×10^{-7}	2.4×10^{-5}
200	1.7×10^{-6}	6.7×10^{-8}	1.8×10^{-6}
250	2.2×10^{-7}	2.1×10^{-8}	2.4×10^{-7}
300	4.0×10^{-8}	5.5×10^{-9}	4.6×10^{-8}

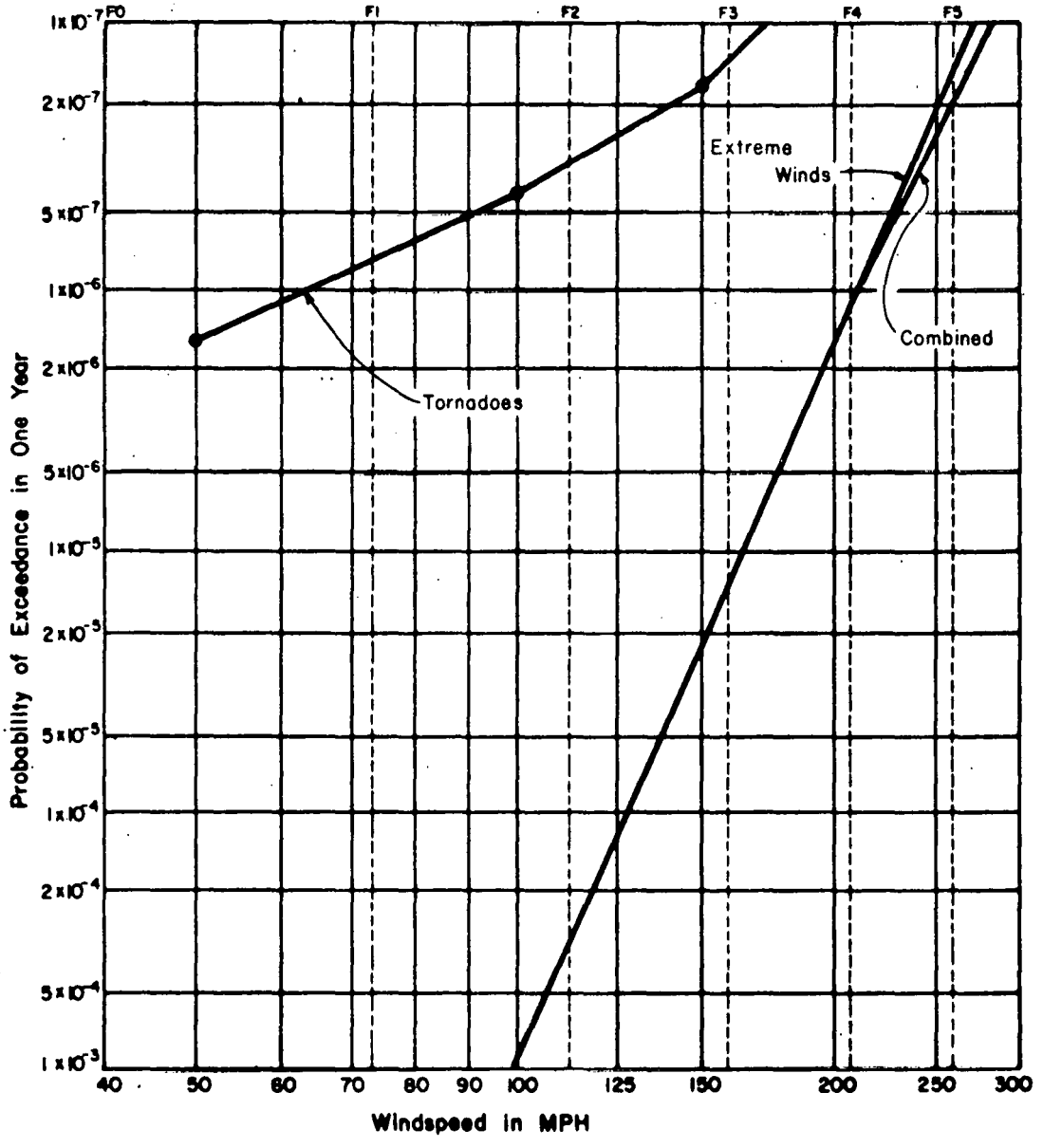

FIGURE 3. PROBABILITY OF EXCEEDANCE vs. WINDSPEED -- NEVADA TEST SITE

E. Tornado and Extreme Wind Parameters at NTS

Determinations of specific tornado and extreme wind parameters for any specific geographic location must involve: (1) the tornado and extreme wind risk model and (2) a definition of the acceptable level of risk for structures and facilities under consideration. The risk model involves the curves developed for NTS as presented in Figure 3. The latter, level of risk definition, is defined by the responsible contractor organization acting in coordination with the Nuclear Regulatory Commission (NRC). In the case of the NTS, the responsible contractor organization (Lawrence Livermore Laboratory) has advanced two levels of risk for evaluating existing facilities at NTS. The levels of risk are stated as 1×10^{-4} and 1×10^{-6} probability of occurrence per year for design tornado and extreme wind parameters.

With the risk model and acceptable levels of risk having been defined, it remains only to develop a listing of specific tornado and extreme wind parameters. Reference to Figure 3 reveals that the maximum design windspeeds associated with the 1×10^{-4} and 1×10^{-6} levels of risk are 130 mph and 210 mph respectively. Note that the tornado windspeeds associated with these levels of risk are relatively small compared with those for straight winds. This fact confirms the more general observations made in the meteorological discussion (Section II), i.e. available data suggest that severe tornadoes are not a significant threat in the area surrounding NTS. Furthermore, this interpretation of the risk model suggests that extreme straight winds should be the governing design parameter as the straight wind

probability curve dominates the combined tornado-straight wind curve (Ref. Fig. 3).

The above interpretations of the risk model (for the levels of risk selected) produce the recommended wind parameters advanced in Table V. For the selected level of risk, the straight wind parameters dominate the design parameters. Atmospheric pressure change is thus not a significant design parameter. The design parameters reflect the effects of straight wind and the missiles which can be produced by these windspeed values.

The design basis missiles advanced in Table V were developed by considering (1) the character of structures at NTS which might, upon failure, contribute to the missile environment and (2) the trajectory predicted by injecting the missiles into an analogous windfield. A computer program developed at Texas Tech was used to determine the expected accelerations, velocities and trajectories of potential missiles injected into the windfield. The following assumptions are made in the computer program:

(1) Aerodynamic drag coefficients of 1.0 and 1.2 are used for cylindrical and parallelpipeds respectively

(2) The missiles assume a nontumbling mode with their largest surface area normal to the relative wind velocity vector

(3) A tornado windfield patterned after the Dallas Tornado of 1957 (Hoecker 1960) is used.

Assumptions 2 and 3 are both conservative. The missiles are likely to tumble because of turbulence. Missiles are more likely to be picked up ty tornadic winds than by straight winds.

TABLE V

RECOMMENDED WIND PARAMETERS -- NTS

RISK: $1x10^{-6}$ Occurrence/year		
Maximum Windspeed*		210 mph
Missiles:	4 x 12, 12 ft long timber, 139 lbs, area 41.7 $in.^2$	90 mph (horizontal) 60 mph (vertical)
	4000 lb automobile	25 mph (tumbling on ground)
RISK: $1x10^{-4}$ Occurrence/year		
Maximum Windspeed*		130 mph
Missile:	2 x 4, 12 ft long timber, 20 lb, area 5.9 $in.^2$	70 mph (horizontal)

*The design basis tornadoes associated with the $1x10^{-4}$ and $1x10^{-6}$ levels of risk will pose no threat to critical facilities designed to withstand the maximum (straight) wind. Hence no parameters for translational, rotational, tangential, radial, or vertical windspeeds, for atmospheric pressure change, or for tornado-generated missiles are advanced.

Four different missiles were considered with the 210 mph windspeed (1×10^{-6} occurrence/year):

(1) Timber plank 4 x 12, 12 ft long at 139 lbs

(2) Steel pipe, Schedule 40, 3 in. dia., 10 ft long at 76 lbs

(3) Utility pole, 13.5 in. dia., 35 ft long at 1490 lbs

(4) Automobile, 4000 lbs.

Results from the computer program showed that only the 4 x 12 timber plank would be sustained in the assumed windfield. The 3 in. dia. pipe and the utility pole were thus ruled out as potential missiles. The automobile is not sustained in the windfield, but could roll or tumble along the ground. Therefore, it was included as a plausible missile. This decision agrees with observations of windstorm damage in the field (McDonald 1974, 1974a).

None of the four missiles would be suspended in the 130 mph windfield (1×10^{-4} occurrence/year). As minimum criteria, the 2 x 4 x 12 ft long timber at 70 mph (horizontal) is recommended.

F. Relationship of Proposed Design Criteria to Criteria in Regulatory Guide 1.76

The AEC Regulatory Guide 1.76 (AEC 1974) suggests a criteria for tornado resistant design in Zone III with the following parameters:

Maximum Horizontal Windspeed	240 mph
Total Pressure Drop	1.5 psi

These criteria are based on a level of risk of 1×10^{-7}, which is considered appropriate for nuclear power plant sites. The technical basis for the Regulatory Guide criteria is contained in WASH-1300 (Markee, Beckerly and Sanders 1974). The technique described in the Wash-1300

report was applied to a 5-degree square region surrounding NTS. For a level of risk corresponding to 10^{-6} the technique predicts a maximum expected tornado windspeed of 150 mph. This compares with a value of 63 mph determined in the present study for the same level of risk.

There are two major differences in the approaches used for determining the tornado risk models:

(1) In calculating the probability of a strike the WASH-1300 report procedure employs a mean tornado damage area of 2.82 sq mi. This differs considerably from the 0.39 sq. mi area determined from tornado records of the four state area surrounding NTS. Smith and Mirabella (1972) found that the mean damage area of California tornadoes (1951-1971) was only 0.11 sq. mi.

(2) The authors of the WASH-1300 report base their intensity-occurrence relationship on a region (Zone III) that is considerably larger than the 5-degree square surrounding NTS.

In general, the study published in the WASH-1300 report represents an attempt to regionalize tornado criteria for the entire United States. The recommendations are admittedly "interim" criteria. The results of the present study represent detailed investigations into both the meteorology of the site and the statistics of the tornado records. The proposed criteria based on the present study are consistent with the spirit of the WASH-1300 report, and they represent a comparable level of safety based on the best information available at the site.

III. GUIDELINES FOR DESIGN LOADS

A. General

This section addresses the translation of tornado and extreme wind parameters from Table V into recommended pressure distributions and missile impact loads on walls and roofs. Because the most significant design parameter is a straight wind, the approach to developing wind induced pressure distributions follows, as a guide, the procedures advanced in the American National Standards Institute Standard, ANSI A58.1-1972 (ANSI 1972). The approaches used in developing missile impact resistant designs follow previously advanced procedures formulated by the nuclear power industry.

Since these guidelines are to be used for evaluating the structural integrity of critical facilities at the Nevada Test Site, it will be assumed in presenting design pressures and missile impact loads that:

(1) the pressures and loads given will be treated as ultimate loads, and

(2) structures will be analyzed and designed by plastic or ultimate strength methods using these ultimate loads.

B. Wind Induced Loads

1. Effective Velocity Pressure

An effective velocity pressure q = 113 psf shall be used as the basic value. This effective velocity pressure is applicable to building heights of 30 ft. or less. For velocity pressures at heights greater than 30 ft. the 1/7 power law shall be applied. The effective velocity pressure at height z is given by

$$q_z = 113\ K_z, \qquad (7)$$

where values of K_z are given in Table VI. Buildings and structures exceeding 200 ft. in height will require special engineering attention which is beyond the scope of these design guidelines.

TABLE VI

VELOCITY PRESSURE COEFFICIENT, K_z

Height Above Ground (ft)	K_z*
$\leq$ 30	1.0
50	1.16
100	1.41
150	1.58
200	1.72

*$K_z = \left(\frac{z}{30}\right)^{\frac{2}{7}}$

Critical structures are to be analyzed and designed by plastic or ultimate strength procedures; hence, the effective velocity for critical structures represents an ultimate loading condition.

2. Design Wind Pressures

Critical structures which by definition must maintain structural integrity at design windspeed should be designed for external pressures

only. (i.e., Do not include atmospheric pressure change associated with tornado.) Design wind pressures are equal to the product of the effective velocity pressure q and appropriate pressure coefficients. External pressure coefficients C_p are used with the effective velocity pressure to obtain design pressures for components according to the equation:

$$p = q\, C_p \qquad (8)$$

Care must be exercised in using Equation 8 as the sign of the design pressure p is very important. A positive value for design pressure (+p) means inward acting pressure, and a negative value for design pressure (-p) means outward acting pressure. The signs for C_p, referenced in ANSI (1972), are self correcting, and appropriate signs should be used in Equation 8 to obtain proper signs for the design pressure p. Building components such as walls and roofs should be designed for maximum inward acting pressures and maximum outward acting pressures. The pressure coefficients presented in this document are taken from the American National Standards Institute, Building Code Requirements for Mimimum Design Loads in Building and Other Structures (ANSI 58.1-1972).

External pressure coefficients C_p depend upon the type of components being considered and the building geometry.

Walls: External pressure coefficients C_p for walls are given in ANSI A58.1, Table 7, p. 19. The windward wall experiences a positive design pressure (+p) while the leeward and side walls experience negative design pressure (-p). The pressure coefficients for the leeward wall depend on the ratio of height to horizontal dimension. At all corners

a local external pressure coefficient of -2.0 shall be used over a small area to account for localized turbulence. These relatively high local pressures are assumed to act on strips of width 0.1w, where w is the least width of the building. These local pressures are not used in combination with other pressures on the walls in the determination of overall loads.

Roofs: Flat, arched, and sloped roofs with winds acting parallel to roof surfaces have negative external pressure coefficients. The values of the coefficients depend on the dimensions of the structure. For buildings with a ratio of wall height to least width of less than 2.5, an external pressure coefficient of -0.7 shall be used for the roof, and the computed pressure shall be assumed uniform over the entire roof area. For buildings in which the height to width ratio is 2.5 or greater, a value of -0.8 shall be used for the entire roof area.

Arched roofs have both positive and negative external pressure coefficients for wind perpendicular to the axis of the arch. The roof area is divided into three parts: windward quarter, center half, and leeward quarter. The magnitude and sign of the pressure coefficients depend upon the rise to span ratio. Coefficients for arched roofs are given in ANSI A58.1, Table 8, p. 19.

Gabled roofs require a pressure coefficient of -0.7 on the leeward slope for wind perpendicular to the gable. The values and signs of external pressure coefficients on the windward slope depend on the slope of the roof and on the ratio of wall height to least width dimension. Values are given in ANSI A58.1, Table 9, p. 19.

At ridges, eaves and 90-degree corners of roofs, local peak external pressures shall be computed using the pressure coefficients given in ANSI A58.1, Table 10, p. 20. These local pressures shall not be used in combination with other roof pressures.

C. Design for Missiles

Critical structures shall be designed to resist the missiles specified in Table V. The missiles are assumed to strike normal to the wall or roof surface with the minimum cross sectional area (on-end). In addition, at critical locations the structure should be checked for damage because of collapse of columns, walls, or rigid

frames resulting from the impact of a tumbling automobile.

1. Penetration Formulas

The penetration of a missile represents a local effect. The prediction of damage includes an estimation of the depth of penetration, the miminum thickness required to prevent perforation and the minimum thickness to preclude spalling. As used in this document, perforation means that the missile passes through the wall or roof target, penetration means that the missile embeds itself in the target.

a. Reinforced Concrete Target

The Modified Petry Formula is recommended for reinforced concrete targets. The depth to which a rigid missile will penetrate a reinforced concrete target of infinite thickness is estimated by the formula:

$$D = 12\ K_p\ A_p\ \text{Log}_{10}\ (1 + \frac{V_s^2}{215{,}000}) \qquad (9)$$

where

D = Depth of penetration (in.)

K_p = Penetration coefficients for reinforced (see Fig. 4 for values)

A_p = Impact pressure (psf); Missile weight (lbs)/contact area (ft^2)

V_s = Missile strike velocity (ft/sec).

When the wall has a finite thickness, the depth of penetration is

$$D_1 = [1 + e^{-4(\frac{T}{D} - 2)}]D \qquad (10)$$

where

T = Thickness of the slab (in.)

e = Base of Natural logarithms

When the wall thickness, T, is 2D, the penetration D_1 = 2D and the wall is just perforated. In order to prevent spalling, the thickness of the wall shall be a minimum of 3D.

b. Steel Target

The Ballistic Research Laboratory (BRL) Formula is recommended for penetration and perforation of steel targets. The steel plate thickness (in.) that will just be perforated is

$$T = \frac{\left(\frac{M_m V^2}{2}\right)}{672 d_m} \tag{11}$$

where

M_m = Mass of the missile (slugs)

V = Velocity of the missile (ft/sec)

d_m = Diameter of the missile (in.)

For an irregularly shaped missile an equivalent diameter is used. The equivalent diameter is the diameter of a circle with an area equal to the circumscribed contact, or projected frontal area of the noncircular missile. The thickness to prevent perforation should be taken as

$$T_p = 1.25T \tag{12}$$

The residual velocity (V_r in ft/sec) after perforation is given by the following equation:

$$V_r = \left[V_s^2 - \frac{1.12 \times 10^6 (d_m T)^{1.5}}{W_m}\right]^{1/2} \tag{13}$$

where

V_s = Strike velocity of the missile (ft/sec)

d_m = Diameter (or equivalent diameter) of the missile (in.)

T = Thickness of the steel plate (in.)

W_m = Weight of the missile (lbs)

Eqn. 13 may be used for estimating the residual velocity of a missile after it has perforated a target. For example, suppose an existing door is not capable of stoping a certain missile. Eqn. 13 could be used to estimate the velocity of the missile after it passes through the door.

2. Structural Response to Missile Impact

When a missile strikes a structural component such as a beam or slab, the failure mechanism may be due to overall structural response rather than penetration. Of the missiles specified in Table V, only the automobile is likely to cause this type of response.

Missile impact may be either elastic or plastic. In the case of elastic impact the missile and target remain in contact for a very short time and then disengage because of elastic interface restoring forces. Plastic impact is characterized by the missile remaining in contact with the target subsequent to impact. Recent impact tests (Stephenson 1975) indicate that both the timber missiles and the automobile result in plastic impact when they strike a solid object such as a concrete wall. For this reason only the plastic impact case is treated in this report.

Several methods are available for estimating the maximum response. The Energy Balance method uses the strain energy of the target at

maximum response to balance the residual kinetic energy of the target (or target-missile combination) resulting from missile impact. An alternative approach, referred to as the Acceleration Pulse Method, is possible, if the target-missile interface loading function is known, and if the dynamic system is modeled as a one degree-of-freedom elasto-plastic system. This latter method is recommended for studying the impact effects of the automobile. The maximum response predicted by the Energy Balance method is 2 to 3 times greater than that predicted by the acceleration-pulse technique. However, the latter values are considered to be more realistic even though they are less conservative.

In experiments with automobile crashes an approximate force-time function for frontal impact has been derived (Bechtel 1973).

$$F(t) = 0.625\ V_s\ W_m \sin 20.06t \tag{14}$$

where

V_s = missile (automobile) strike velocity (ft/sec)

W_m = weight of automibile (lbs)

The function is a sine wave with frequency $\omega = 20.06$ rad/sec and period

$$\begin{aligned} \bar{t} &= 2\pi/\omega \\ &= 0.314 \text{ sec.} \end{aligned} \tag{15}$$

The maximum force occurs at $t = \bar{t}/4 = 0.0785$ sec, when the velocity of the striking automobile is zero relative to the target surface. Under the condition of plastic impact (i.e. target and missile ac-

quire the same velocity after impact) the duration of the impact force is from t = 0 to t = 0.0785 sec. At t = 0.0785 sec the interface force diminishes to zero.

The maximum target response is obtained by writing the equation of motion for a one-degree-of-freedom elasto-plastic oscillator with damping neglected.

$$M'\ddot{y} + R(y) - F(t) = 0 \qquad (16)$$

In this equation

M' = effective mass of the target plus the mass of the missile (lb sec^2/ft)

$R(y)$ = resistance function for the target material (lb)

$F(t)$ = target-automobile interface force function (lb)

For elasto-plastic target response with no other concurrent loads on the target, the resistance function is

$$R(y) = Ky \qquad (0<y<y_{el})$$

$$R(y) = Ky_{el} = R_m \qquad (y_{el}<y<y_{max}) \qquad (17)$$

where

y = the displacement of the target (ft)

y_{el} = the displacement at yield in the target material (ft)

K = stiffness of the target (lb/ft)

R_m = maximum plastic resistance

The above relationships are illustrated in Fig. 5.

The effective target mass during impact varies and generally increases to a maximum at the end of the impact duration. Expressions

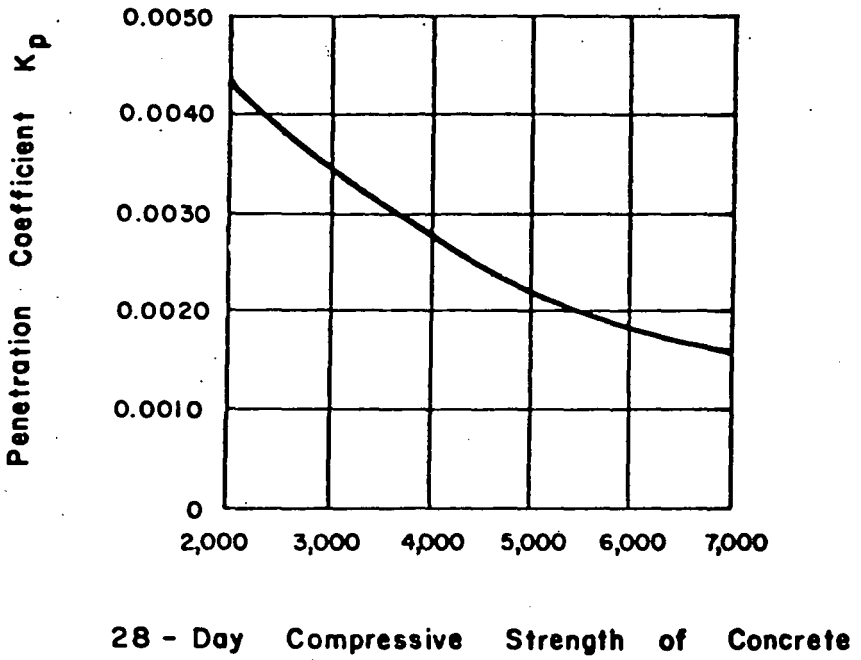

FIGURE 4. VALUES OF PENETRATION COEFFICIENT K_p FOR REINFORCED CONCRETE

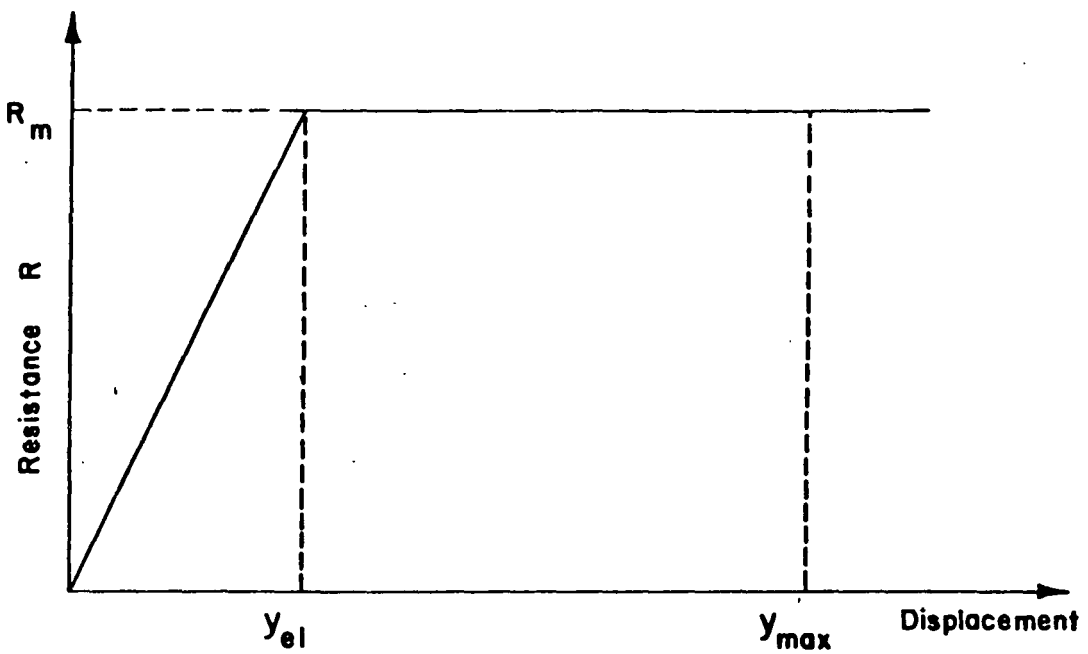

FIGURE 5. IDEALIZED RESISTANCE-DISPLACEMENT FUNCTION FOR DUCTILE MATERIALS

for estimating the average effective mass are given in Table VII.

The equation of motion may be solved by numerical techniques. The problem may be further simplified by replacing the load function given by Eqn. 14 with an equivalent rectangular pulse. The applied impulse is, by definition, the area under the load function. Integrating over the load duration

$$\begin{aligned} I &= \int (0.625\, V_s\, W_m \sin 20.06t)dt \\ &= 0.625\, V_s\, W_m \left[\frac{-1}{20.06} \cos 20.06t\right]_0^{0.0785} \\ &= 0.625\, V_s\, W_m\, (0.05) \end{aligned} \tag{18}$$

Thus an equivalent rectangular pulse is one whose magnitude is $F_1 = 0.625 V_s W_m$ and whose time duration is $t_d = 0.05$ sec.

The Acceleration-Pulse method of numerical integration gives a reasonable solution if the time step Δt is taken less than one tenth the fundamental period of the target. The displacement during the first time step is estimated using the equation

$$y_1 = \frac{1}{2} \ddot{y}_0 \Delta t \tag{19}$$

Displacements in subsequent time steps are obtained from the recurrence relationship

$$y_{t+1} = 2y_t - y_{t-1} + \ddot{y}_t (\Delta t)^2 \tag{20}$$

Once the maximum displacement has been found, the ductility ratio u is calculated

$$u = \frac{y_{max}}{y_{el}} \tag{21}$$

TABLE VII

EFFECTIVE MASS OF TARGET
DURING IMPACT

Concrete Beams:

$$M_e = (D_x + 2T)\,\frac{BT\gamma_c}{g} \qquad (B < D_y + 2T)$$

$$M_e = (D_x + 2T)\,(D_y + 2T)\,T\,\frac{\gamma_c}{g} \qquad (B > D_y + 2T)$$

Concrete Slabs:

$$M_e = (D_x + T)(D_y + T)\,T\,\frac{\gamma_c}{g}$$

Steel Beams:

$$M_e = (D_x + 2D)\,M_x$$

Steel Plates:

$$M_e = D_x\,D_y\,T\,\frac{\gamma_s}{g}$$

D_x = Maximum missile contact dimension in the x-direction (longitudinal direction for beams and slabs)

D_y = Maximum missile contact dimension in the y-direction (transverse to longitudinal direction for beams and slabs)

B = Width of concrete beam (not to exceed $D_y + 2T$)

T = Depth of concrete beam or thickness of concrete slab

M_x = Mass per unit length of steel beam

γ_c = Unit weight of concrete

γ_s = Unit weight of steel

g = Acceleration due to gravity

The maximum recommended ductility ratios to absorb energy of missile impact for various components are given in Table VIII. The ratios should be reduced appropriately if axial loads in addition to lateral impact loads are involved. For reinforced concrete walls, the ductility ratios given in the Table are for low percentage of reinforcement; the ratios should be reduced if higher than recommended percentage of reinforcement is used. Precautions should be taken to prevent premature failure of reinforced concrete wall slab due to diagonal tension, due to punching shear, or due to bond failure. If reinforcing bars are terminated in the tension zone in the wall slab, there could be a reduction in the capacity of the slab. In the case of steel beams the flanges must be thick enough to prevent local buckling.

The Acceleration-Pulse technique is illustrated in an example problem in Section III. D. 5. c.

TABLE VIII

RECOMMENDED DUCTILITY RATIOS

Component	Maximum Ductility Ratio
Steel Beam	15
Concrete Beam or One-Way Slab	10 (with $\rho^* \leq 0.01$)
Concrete Two-Way Wall Slab	20 (with $\rho \leq 0.005$ in each direction)

$^*\rho = \frac{A_s}{bd}$; ratio of steel area to concrete area.

D. Design Example

This example treats the case of reinforced concrete building that might be found at NTS. The example is not modeled after any particular building at the site. Only the design loads are determined. Structural design of the individual components of the building is beyond the scope of these guidelines.

A plan view of the building outline is shown in Fig. 6. Overall dimensions of the building are 92 ft x 56 ft. The wall height is 30 ft in the critical area. The critical nature of functions performed inside the building requires that the structural integrity of the building be maintained. All doors and openings shall be designed to withstand the design windspeeds and the impacts from windborne missiles. A covered walkway separates the critical structure from a non-critical portion of the building which has conventional concrete masonry walls and a steel joist roof system.

1. Design Criteria

The critical portions of the building shall withstand wind loadings equivalent to:

Maximum windspeed, 210 mph

Missiles: Timber with nominal dimensions 4 in. x 12 in. x 12 ft long weighing 139 lbs and traveling at 90 mph (horizontal) and 60 mph (vertical).

Automobile weighing 4000 lbs tumbling at 25 mph.

2. Wind Induced Loads

The effective velocity pressure is q = 113 psf. Since the wall height is less than or equal to 30 ft, no adjustment in q is needed because of height.

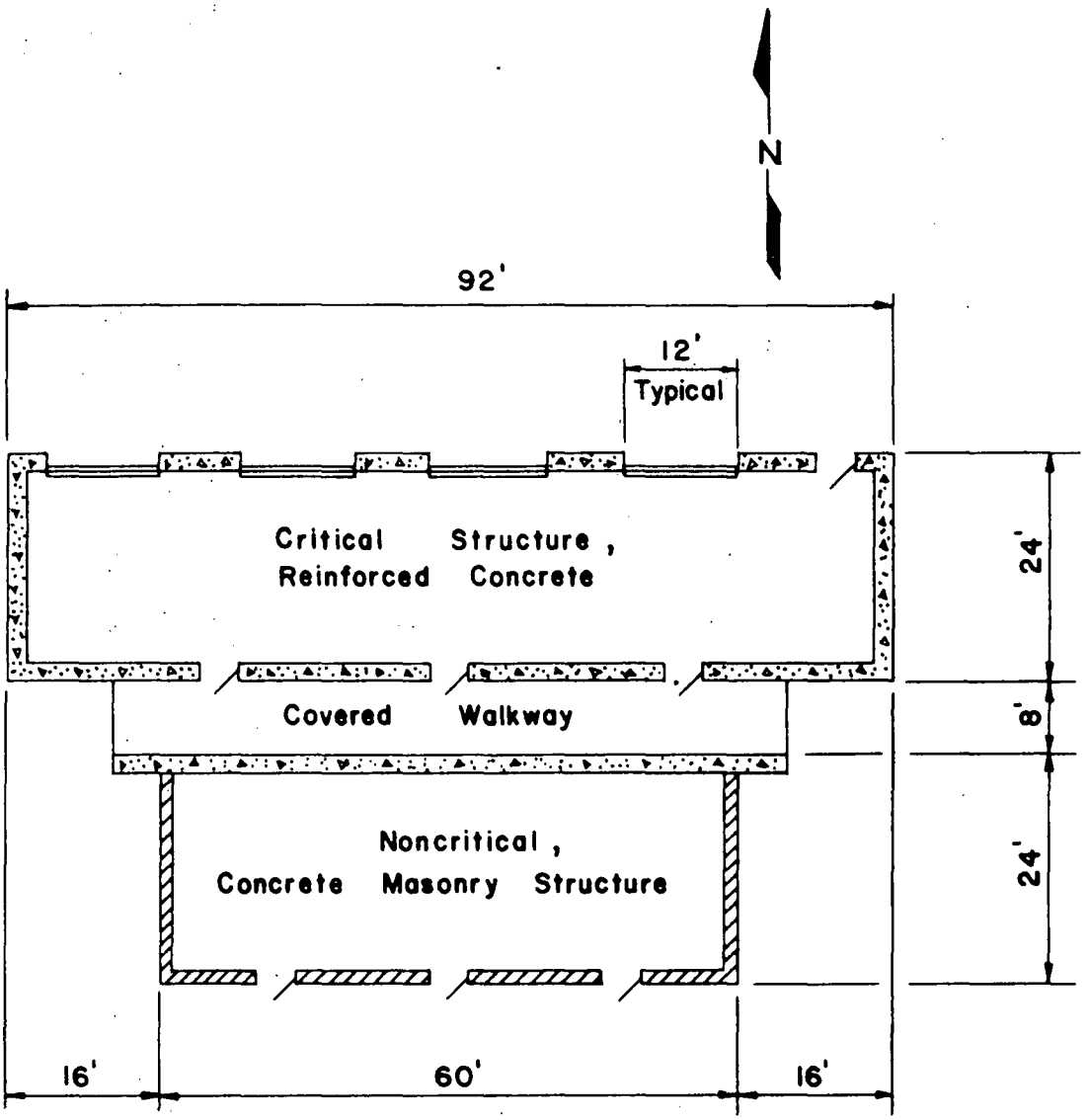

FIGURE 6. PLAN VIEW OF EXAMPLE STRUCTURE

a. External Pressure

From ANSI A58.1, Table 7:

Windward wall: (+0.8)(113) = 90 psf

Leeward wall: (-0.5)(113) = -56 psf

Side wall: (-0.7)(113) = -79 psf

Roof: (-0.7)(113) = -79 psf

b. Local Effects

Wall corners: (-2.0)(113) = -226 psf acting on a strip 5.6 ft wide at outside corner.

Eaves (all around perimeter of roof):
(-2.4)(113) = -271 psf acting on a strip 5.6 ft wide.

Roof corners: (-5.0)(113) = -565 psf acting on an area 5.6 ft x 5.6 ft at all corners.

3. Wind Induced Roof Diaphragm and Shear Wall Loads

The walls are assumed simply supported at the footing and at the roof.

a. Winds from North or South

Diaphragm load: (113)(+0.8 + 0.5) (30)/2 = 2204 plf

Total diaphragm load = 2204(92)

= 203,000 lb

Force per ft on shear walls = $\frac{203,000}{2}(\frac{1}{24})$

= 4229 plf

b. Winds from East or West

Diaphragm load = 113(0.8 + 0.5)(30)/2

= 2204 plf

Total diaphragm load = 2204(24)

= 52,900 lb

Force per ft on shear wall = $\frac{52,900}{2}(\frac{1}{92})$

= 288 plf

4. Controlling Design Wind Loads

a. Walls

1. +90 psf (acting inward)

2. -79 psf (acting outward)

3. -226 psf acting outward on a strip 5.6 wide at each outside corner. This load primarily controls the horizontal steel required to tie the two intersecting walls together. It is not used in combination with other externally applied loads.

4. 4229 plf load on shear walls at east and west end of the building.

5. 288 plf load on shear walls at north and south sides of the building.

b. Roof

1. -79 psf acting upward.

2. -271 psf acting on 5.6 ft wide strip all around the perimeter of the building. This load controls the steel required to anchor the roof slab to the top of the walls. It should not be used in combination with any other loads.

3. -565 psf acting upward on a 5.6 ft x 5.6 ft area at each roof corner. This load also affects the anchorage of the roof slab to the top of the walls. It should not be used in combination with any other loads.

c. Components

1. +90 psf

2. -79 psf

3. Local effects (at wall corners, roof corners and eaves), if the component is located within the areas influenced by the local effects.

5. Missile Induced Loads

Three examples are presented below which illustrate the use of the missile penetration formulas:

a. Reinforced Concrete Target

The Modified Petry Formula should be used to determine the thickness of reinforced concrete required to resist the design timber missile. Assume f'_c = 4000 psi for the concrete.

Determine the minimum thickness of the wall to just prevent perforation:

The Modified Petry Formula is given by Eqn. 9.

$$K_p = 0.0028 \text{ for } f'_c = 4000 \text{ psi (Ref. Figure 4)}$$

$$A_p = \frac{139}{41.7/144} = 480 \text{ psf}$$

$$V_s = 90 \text{ mph} = 132 \text{ fps}$$

$$D = 12(0.0028)(480)\ \text{Log}_{10}\left[\ 1 + \frac{(132)^2}{215{,}000}\ \right]$$

$$= 0.55 \text{ in.}$$

Clearly, missile penetration into a reinforced concrete wall is not critical for this design windspeed.

b. Steel Target:

Determine the thickness of a steel plate in an overhead door to prevent penetration of the design missile:

Neglect deflection of the door and assume the supports are rigid.

$$M_m = \frac{139}{32.2} = 4.32 \text{ slugs}$$

$$V_s = 132 \text{ fps}$$

A = Area of missile = 41.7 in.^{2}

The equivalent circular diameter is

$$d_m = \sqrt{\frac{4A}{\pi}} \qquad (17)$$

$$= \sqrt{\frac{4(41.7)}{\pi}} = 7.29 \text{ in.}$$

The thickness of the plate to just prevent perforation is obtained from the BRL formula

$$T = \frac{\left[\frac{4.32(132)^2}{2}\right]^{2/3}}{672(7.29)} = 0.23 \text{ in.} \quad \text{(Equation 11)}$$

The design thickness should be

$$T_p = 1.25T$$

$$= 0.29 \text{ in.} \qquad \text{(Equation 12)}$$

Suppose the material available for the door cladding is only 1/8 in. thick. Estimate the residual velocity of the design missile after perforation. Use Eqn. 13:

$$V_r = \left[(132)^2 - \frac{1.12 \times 10^6 \, (7.29 \times 0.125)^{1.5}}{139}\right]^{1/2}$$

$$= 102 \text{ ft/sec (70 mph)}$$

c. Structural Response of a Concrete Wall to the Impact of a Tumbling Automobile

Check the adequacy of a 12 in. concrete wall panel when impacted by a 4000 lb automobile (M_v = 124.3 slugs) traveling at 25 mph (36.7 ft/sec). The wall is simply supported at top and bottom and has a height of 15 ft. The point of impact is 5 ft above the base of the wall as shown in Fig. 7.

Assume:

f'_c = 3000 psi

f_s = 40,000 psi

Vertical steel #9 @ 12" o.c.

A_s = 0.99 $in.^2$/ft of wall

Calculate wall parameters (Refer to Fig. 8):

$$d = 12 - 1.31 = 10.69 \text{ in.}$$

$$\rho = \frac{0.99}{10.69(12)} = 0.00772$$

A value of $\rho < 0.5\ \rho_b$ assures adequate ductility of the slab.

$$n = \frac{29 \times 10^6}{(150)^{1.5}\ (33)\sqrt{3000}} = 8.73$$

Use n = 9

Calculate the yield moment M_y on the basis of straight line theory:

$$12(kd)\ \frac{kd}{2} = 8.91\ (10.69 - kd) \qquad (22)$$

$$kd = 3.25 \text{ in.}$$

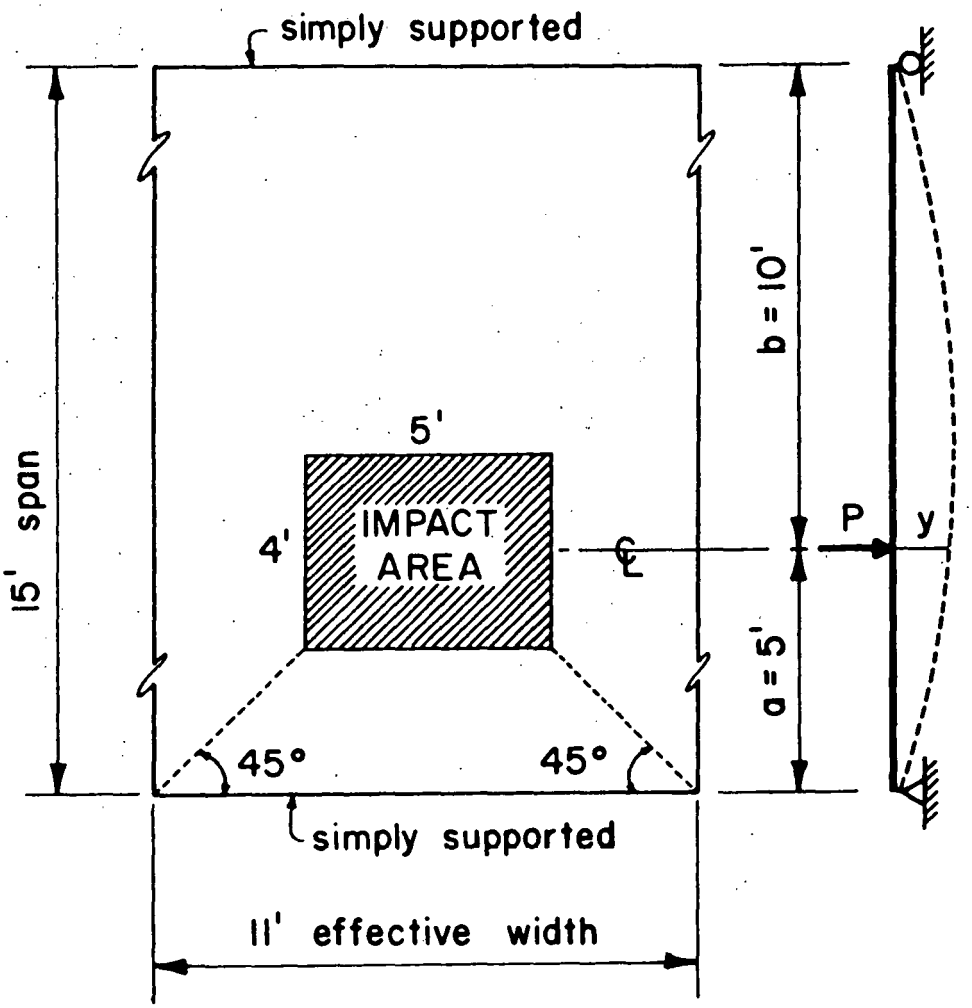

FIGURE 7. STRUCTURAL RESPONSE OF A REINFORCED CONCRETE WALL

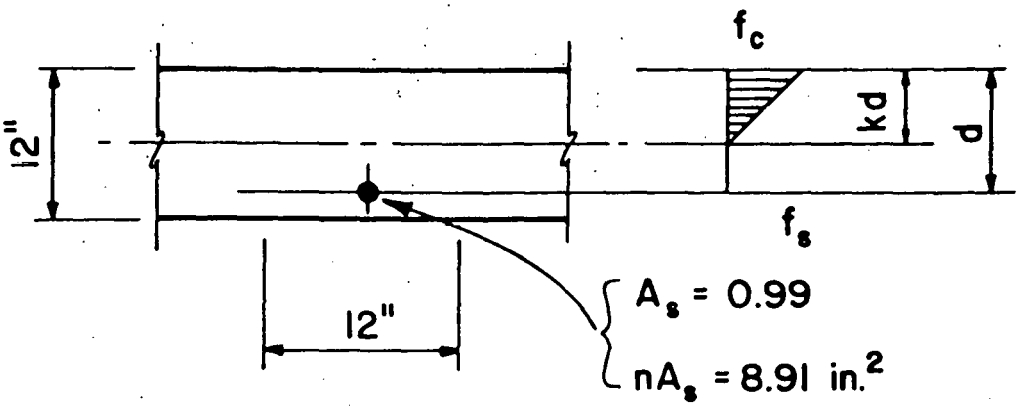

FIGURE 8. REINFORCED CONCRETE WALL CROSS SECTION

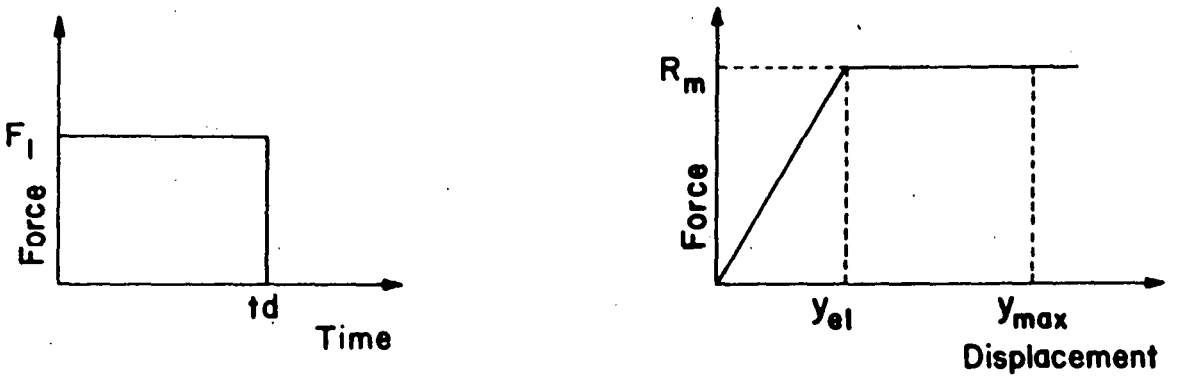

Force - Time Function

Resistance Function

FIGURE 9. FORCE-TIME FUNCTION AND RESISTANCE FUNCTION

$$M_y = f_s A_s jd$$

$$= 40,000\ (0.99)(10.69 - \frac{3.25}{3})$$

$$= 380,400 \text{ in. lb/ft}$$

$$= 3.49 \times 10^5 \text{ ft. lb/11ft width}$$

Check f_c:

$$C = 40,000\ (0.99)$$

$$= 39,600 \text{ lb}$$

$$f_c = 2C/bkd \qquad (24)$$

$$= \frac{2(39,600)}{12(3.25)}$$

$$= 2031 \text{ psi} < f'_c$$

Note that for this cross section

$$M_u = 397,800 \text{ in.lb/ft}$$

$$M_y = 0.96\ M_u$$

Calculate moment of inertia

$$I_0 = \frac{12\ (3.25)^3}{3} + 8.91\ (10.69 - 3.25)^2$$

$$= 630.5 \text{ in}^4/\text{ft}$$

$$= 6936 \text{ in}^4/11 \text{ ft width}$$

Stiffness of one way slab

$$K = \frac{3EIL}{a^2 b^2}$$

$$= \frac{3(3.2 \times 10^6)(6936)(15)}{(5)^2\ (10)^2\ (144)} \qquad (25)$$

$$= 2.77 \times 10^6 \text{ lb/ft} \quad (11 \text{ ft width})$$

The maximum resistance of the slab is

$$R_m = \frac{M_y L}{ab} \qquad (26)$$

$$R_m = \frac{3.49 \times 10^5\ (15)}{(5)\ (10)}$$

$$R_m = 1.05 \times 10^5 \text{ lb}$$

The deflection to produce yield is

$$y_{el} = \frac{R_m}{K}$$

$$= \frac{1.05 \times 10^5}{2.77 \times 10^6} \qquad (27)$$

$$= 0.0378 \text{ ft} \quad (0.45 \text{ in.})$$

For the impact of an automobile the loading is considered to be a rectangular load pulse. The magnitude of the pulse is

$$F_1 = 0.625\ V_s\ W_m \qquad (28)$$

where V_s = strike velocity of the automobile (ft/sec)

W_m = weight of the automobile (lbs)

In this example

$$F_1 = 0.625\ (36.7)(4000)$$

$$= 9.18 \times 10^4 \text{ lb}$$

The duration of the load pulse t_d is 0.05 sec. The load pulse and assumed resistance function are shown in Fig. 9.

The impact is assumed to be plastic. Thus upon impact the velocity of the wall and the automobile are the same and they move together to the point of maximum deflection, y_{max}. The equivalent mass of the slab itself is (Table VII):

$$M_e = (D_x + T)(D_y + T)(T)\frac{\gamma_c}{g} \tag{29}$$

where D_x, D_y = dimensions of the contact area (ft)

γ_c = the unit weight of concrete (lb/ft^3)

g = acceleration due to gravity (ft/sec^2)

T = the thickness of the concrete (ft)

$M_e = 6(5)(1)(150)/32.2$

$= 139.8\ lb.sec^2/ft$

Since the effective mass of the target and the missile move together the total mass is

$$\begin{aligned} M' &= M_e + M_m \\ &= 139.8 + 124.2 \\ &= 264.0\ lb.sec^2/ft \end{aligned} \tag{30}$$

The equation of motion in general terms for this one-degree-of-freedom elasto-plastic system is

$$M'\ddot{y} + R(y) - F(t) = 0 \qquad \text{(Equation 16)}$$

Or, because of the nature of the assumed resistance function

$$M'\ddot{y} + Ky - F_1 = 0 \qquad (0<y<y_{el})$$

$$M'\ddot{y} + R_m - F_1 = 0 \qquad (y_{el}<y<y_{max}) \qquad (31)$$

Substituting appropriate values and rearranging, the equations become

$$\ddot{y} = 347.7 - 1.049 \times 10^4 y \qquad (0<y<0.0378)$$

$$\ddot{y} = 347.7 - 397.7$$

$$= -50.0 \qquad (0.0378<y<y_{max}) \qquad (32)$$

The above equations may be solved by using numerical integration, or the tables and charts in Biggs (1964) can be used to determine y_{max} and the time t_{max} at which it occurs.

The Acceleration-Pulse method is presented in this example. The relationship needed to determine the displacement during the first time step is

$$y_1 = 1/2\ \ddot{y}_0\ (\Delta t)^2 \qquad \textbf{(Equation 19)}$$

Subsequent displacements are given by the recurrsion formula

$$y_{t+1} = 2\ y_t - y_{t-1} + \ddot{y}_t(\Delta t)^2 \qquad \text{(Equation 20)}$$

The period for this equivalent one-degree-of-freedom system is given by

$$\overline{t} = 2\pi\sqrt{\frac{M'}{K}}$$

$$= 2\pi\sqrt{\frac{264.0}{2.77 \times 10^6}} \qquad (33)$$

$$= 0.061 \text{ sec}$$

The time step Δt should be less than $\bar{t}/10$. Use $\Delta t \leq 0.006$ sec. The calculations are summarized in Table IX. The maximum deflection ($y_{max} = 0.127$ ft) occurs at $t = 0.054$ sec. The corresponding ductility ratio is

$$u = \frac{y_{max}}{y_{el}} = \frac{0.127}{0.0378} = 3.36 \qquad \text{(Equation 21)}$$

The ductility ratio is well within the allowable of 10 recommended in Table VIII. Therefore the 12 in. concrete slab is adequate to resist the impact of the 4000 lb automobile traveling at 25 mph.

Note that the wall height used in the calculation of the structural response was not 30 ft as given in the example problem. A 30 ft high wall impacted 5 ft from its support is more likely to experience a shear response failure rather than due to bending. Therefore the 15 ft high wall was used in the example to illustrate the Acceleration Pulse method as outlined in Section C. 2.

TABLE IX

NUMERICAL SOLUTION TO EQUATIONS OF MOTION

Time Step	Ellapsed Time Sec	F_1/M' ft/sec^2	R/M' ft/sec^2	$\ddot{y}$ ft/sec^2	$\ddot{y}\,\Delta t^2$ ft	y ft
0	0	347.7	0	347.7	1.39×10^{-3}	0
1	.002		-7.29	340.4	1.36×10^{-3}	6.95×10^{-4}
2	.004		-28.89	318.8	1.28×10^{-3}	2.75×10^{-3}
3	.006		-63.83	283.9	1.14×10^{-3}	6.08×10^{-3}
4	.008		-111.0	237	9.48×10^{-4}	1.06×10^{-2}
5	.010		-168	180	7.21×10^{-4}	1.60×10^{-2}
6	.012		-232	116	4.63×10^{-4}	2.21×10^{-2}
7	.014		-301	47	1.86×10^{-4}	2.87×10^{-2}
8	.116		-372	-25	-9.84×10^{-5}	3.55×10^{-2}
9	.018		397.7	-50	-2.0×10^{-4}	4.22×10^{-2}
10	.020					4.87×10^{-2}
11	.022					5.50×10^{-2}
12	.024					6.10×10^{-2}
13	.026					6.69×10^{-2}
14	.028					7.26×10^{-2}
15	.030					7.81×10^{-2}
16	.032					8.34×10^{-2}
17	.034					8.85×10^{-2}
18	.036					9.34×10^{-2}
19	.038					9.81×10^{-2}
20	.040					1.03×10^{-1}
21	.042					1.07×10^{-1}
22	.044					1.11×10^{-1}
23	.046					1.15×10^{-1}
24	.048					1.18×10^{-1}
25	.050	347.7	397.7	-50	-2.0×10^{-4}	1.22×10^{-1}

TABLE IX (CONT'D)

NUMERICAL SOLUTION TO EQUATIONS OF MOTION

Time Step	Ellapsed Time Sec	F_1/M' ft/sec^2	R/M' ft/sec^2	$\ddot{y}$ ft/sec^2	$\ddot{y}\,\Delta t^2$ ft	y ft
26	.052	0	397.7	-397.7	$-1.59\text{X}10^{-3}$	$1.25\text{X}10^{-1}$
27	.054	0	397.7	-397.7	$-1.59\text{X}10^{-3}$	$1.27\text{X}10^{-1}$
28	.056	0	397.7	-397.7	$-1.59\text{X}10^{-3}$	$1.27\text{X}10^{-1}$
29	.058	0				$1.26\text{X}10^{-1}$

LIST OF REFERENCES

AEC, 1974: Design Basis Tornado for Nuclear Power Plants, Regulatory Guide 1.76, April 1974.

ANSI, 1972: American National Standard: Building Code Requirements for Minimum Design Loads in Buildings and Other Structures, ANSI A58.1-1972, ANSI, New York, 60 pp.

Bechtel Power Corporation, "Design of Structures for Missile Impact," BC-TOP-9, Revision 1, Bechtel Power Corporation, San Francisco, California July 1973.

Biggs, J.M., Introduction to Structural Dynamics, McGraw-Hill Book Company, New York, 1964.

Brenner, I.S., 1974: A Surge of Maritime Tropical Air-Gulf of California to the Southwestern United States. Mon. Wea. Rev., 102, 375-389.

Court, A., 1970: Tornado Incidence Maps. ESSA Tech. Memo. ERLTM-NSSL 49, 76 pp.

Dodd, A.V., "A real Distribution and Diurnal Variation of Water Vapor Near Ground in the Contiguous United States" Technical Report ES-17, Earth Sciences Division, W.S. Material Command, U.S. Army Natick Laboratories, Natick, Mass., Nov. 1965.

Feris, C., 1970: The Tornado at Kent, Washington. Weatherwise, 23, 75-77, 83.

Finley, J.P., 1884: Report on the Character of 600 Tornadoes. Pap. Signal Serv., No. 7, 29 pp.

Flora, S.D., 1953: Tornadoes of the United States. University of Oklahoma Press, Norman, 221 pp.

Fujita, T.T., 1970: Estimate of Maximum Windspeeds of Tornadoes in Three Northwestern States. SMRP Rpt. No. 72, University of Chicago, 27 pp.

_____, 1971: Proposed Characterization of Tornadoes and Hurricanes by Area and Intensity. SMRP Rpt. No. 91, University of Chicago, 42 pp.

_____, 1972: Estimate of Maximum Windspeeds of Tornadoes in Southernmost Rockies. SMRP Rpt. No. 105, University of Chicago, 47 pp.

_____, 1973: Tornadoes Around the World. Weatherwise, 26, 56-62, 78-83.

Hales, J.E., Jr., 1974: Southwestern United States Summer Monsoon Source -- Gulf of Mexico or Pacific Ocean? J. Appl. Meteor., 13, 331-342.

Hallett, J., 1969: A Rotor Induced Dust Devil. Wea., 24, 133.

Hoecker, W.H., Jr., "Wind Speed and Air Flow Patterns in the Dallas Tornado of April 2, 1957," Monthly Weather Review, Vol. 88, No. 5, pp. 167-180, 1960.

Idso, S.B., 1974: Tornado or Dust Devil: The Enigma of Desert Whirlwinds. Amer. Scientist, 62, 530-541.

Ingram, R.S., 1973: Arizona "Eddy" Tornadoes. NOAA Tech. Memo. NWS WR 91, 9 pp.

McDonald, J.R., 1974: Tornado Risks and Design Windspeeds for the Oak Ridge Plant Site. Institute for Disaster Research, Texas Tech University, Lubbock, Texas, 23 pp.

_____, 1974a: Tornado Risks and Design Windspeeds for the Portsmouth Plant Site. Institute for Disaster Research, Texas Tech University, Lubbock, Texas, 23 pp.

Kessler, Edwin, 1974: "Survey of Boundary Layer Winds with Special Response to Extreme Values," American Institute of Aeronautics and Astronautics, Paper No. 74-586.

Miller, R.C., 1970: Notes on Analysis and Severe-Storm Forecasting Procedures of the Air Force Global Weather Central. TR200 (Rev), AWS USAF.

Neville, A.M. and Kennedy, J.B., Basic Statistical Methods for Engineers and Scientists, International Textbook Company, Scranton, PA, 1966.

NOAA: Storm Data, Monthly Weather Summary by NOAA Environmental Data Service, Asheville, North Carolina (Published since 1956).

NSSFC, 1974: Computer Records of Tornado Occurrences. National Weather Service, Kansas City.

Rasmussen, E.M., 1967: Atmospheric Water Vapor Transport and the Water Balance of North America. Pt. 1. Mon. Wea. Rev., 95, 403-426.

Ryan, J.A., and J.J. Carroll, 1970: Dust Devil Velocities: Mature State. J. Geophys. Res., 75, 531-541.

Thom, H.C.S., 1968: New Distributions of Extreme Winds in the United States," Proc. Structural Div. ASCE, 94, ST7.

U.S. Department of Commerce, "Climatic Atlas of the United States," Environmental Data Service ESSA, June 1968.

Warn, G.F., 1952: Some Dust Storm Conditions of the Southern High Plains. Bull. Amer. Meteor. Soc., 33, 240-243.

APPENDIX A

TABLE OF FUJITA-PEARSON TORNADO SCALE. Characteristics of a tornado can be expressed as a combination of Fujita-scale windspeed and Pearson-scale path length and width. This scale permits us to classify tornadoes between two extreme FPP scales, 0,0,0 and 5,5,5.

F-scale Maximum Windspeed				P-scale Path Length			P-scale Path Width			
Scale	mph	kts	m/s	Scale	miles	km	Scale	ft	yds	meters
F 0.0	40	35	18	P 0.0	0.3	0.5	P 0.0	17	6	5
0.1	43	37	19	0.1	0.4	0.6	0.1	19	6	6
0.2	46	40	21	0.2	0.4	0.6	0.2	21	7	6
0.3	49	43	22	0.3	0.5	0.7	0.3	24	8	7
0.4	52	46	23	0.4	0.5	0.8	0.4	26	9	8
0.5	56	48	25	0.5	0.6	0.9	0.5	30	10	9
0.6	59	51	26	0.6	0.6	1.0	0.6	33	11	10
0.7	63	54	28	0.7	0.7	1.1	0.7	37	13	11
0.8	66	57	30	0.8	0.8	1.3	0.8	42	14	13
0.9	70	60	31	0.9	0.9	1.4	0.9	47	16	14
F 1.0	73	64	33	P 1.0	1.0	1.6	P 1.0	53	18	16
1.1	77	67	34	1.1	1.1	1.8	1.1	59	20	18
1.2	81	70	36	1.2	1.3	2.0	1.2	66	22	20
1.3	84	73	38	1.3	1.4	2.3	1.3	74	25	23
1.4	88	77	40	1.4	1.6	2.6	1.4	84	28	26
1.5	92	80	41	1.5	1.8	2.9	1.5	94	31	29
1.6	96	84	43	1.6	2.0	3.2	1.6	105	35	32
1.7	100	87	45	1.7	2.2	3.6	1.7	118	39	36
1.8	104	91	47	1.8	2.5	4.0	1.8	133	44	40
1.9	109	94	49	1.9	2.8	4.5	1.9	149	50	45
F 2.0	113	98	50	P 2.0	3.2	5.1	P 2.0	167	56	51
2.1	117	102	52	2.1	3.5	5.7	2.1	187	62	57
2.2	121	105	54	2.2	4.0	6.4	2.2	210	70	64
2.3	126	109	56	2.3	4.5	7.2	2.3	235	78	72
2.4	130	113	58	2.4	5.0	8.1	2.4	265	88	81
2.5	135	117	60	2.5	5.6	9.0	2.5	297	99	90
2.6	139	121	62	2.6	6.3	10.2	2.6	333	111	102
2.7	144	125	64	2.7	7.1	11.4	2.7	374	125	114
2.8	148	129	66	2.8	7.9	12.8	2.8	419	140	128
2.9	153	132	68	2.9	8.9	14.3	2.9	470	157	143
F 3.0	158	137	70	P 3.0	10.0	16.1	P 3.0	528	176	161
3.1	162	141	73	3.1	11.2	18.0	3.1	591	197	180
3.2	167	145	75	3.2	12.6	20.3	3.2	665	222	203
3.3	172	149	77	3.3	14.1	22.7	3.3	744	248	227
3.4	177	154	79	3.4	15.9	25.6	3.4	837	279	256
3.5	182	158	81	3.5	17.8	28.6	3.5	940	313	286
3.6	187	162	83	3.6	20.0	32.2	3.6	1054	351	322
3.7	192	167	86	3.7	22.4	36.0	3.7	1183	394	360
3.8	197	171	88	3.8	25.1	40.4	3.8	1326	442	404
3.9	202	175	90	3.9	28.2	45.4	3.9	1489	496	454
F 4.0	207	180	93	P 4.0	31.6	50.9	P 4.0	1670	557	509
4.1	212	184	95	4.1	35.5	57.1	4.1	1874	625	571
4.2	218	189	97	4.2	39.8	64.1	4.2	2102	701	641
4.3	223	194	100	4.3	44.7	71.8	4.3	2354	785	718
4.4	228	198	102	4.4	50.1	80.6	4.4	2646	882	806
4.5	233	203	104	4.5	56.2	90.4	4.5	2967	989	904
4.6	238	207	107	4.6	63.1	102	4.6	3332	1111	1.0 km
4.7	244	212	109	4.7	70.8	114	4.7	3738	1246	1.1
4.8	250	217	112	4.8	79.4	128	4.8	4194	1398	1.3
4.9	255	222	114	4.9	89.1	143	4.9	4704	1568	1.4
F 5.0	261	227	117	P 5.0	100	161	P 5.0	1.0 mi	1760	1.6
5.1	267	232	119	5.1	112	181	5.1	1.1	1971	1.8
5.2	272	236	122	5.2	126	203	5.2	1.3	2218	2.0
5.3	278	241	124	5.3	141	227	5.3	1.4	2482	2.3
5.4	284	246	127	5.4	159	255	5.4	1.6	2798	2.6
5.5	289	251	129	5.5	178	286	5.5	1.8	3133	2.9
5.6	295	256	132	5.6	200	321	5.6	2.0	3520	3.2
5.7	301	261	135	5.7	224	360	5.7	2.2	3942	3.6
5.8	307	267	137	5.8	251	404	5.8	2.5	4418	4.0
5.9	313	272	140	5.9	282	454	5.9	2.8	4963	4.5

APPENDIX B

Windspeed Probabilities
Based on Fisher-Tippett Type II Distribution

For more specific details of the calculations presented herein, reference is made to Thom (1968). The Fisher-Tippett Type II distribution is given by the equation

$$F(V) = \exp\left[-(V/\beta)^{-\gamma} \right] \qquad (B1)$$

where

$F(V)$ is the probability that the windspeed will not exceed the value V in one year.

β, γ are constants to be determined.

Values of β and γ are determined for a specific location from the data presented in the Thom article. Contour maps are presented for annual extreme-mile windspeeds for 2, 10, 25, 50 and 100 year mean recurrence intervals. These values are plotted on the special Fisher-Tippett Type II probability paper (Figure B1) and a best fit straight line is drawn through the points. Then by observing from the curve that

$$F(40) = 0010$$

$$F(100) = 0.999,$$

Equation (B1) may be used to solve for and .

$$0.010 = \exp\left[- (40/\beta)^{-\gamma}\right]$$

$$0.999 = \exp\left[- (100/\beta)^{-\gamma}\right]$$

Values are found to be

$$\beta = 47.22$$

$$\gamma = 9.21$$

Equation (B1) thus becomes

$$F(V) = \exp\left[-\left(V/47.22\right)^{-9.21}\right] \qquad \text{(B2)}$$

where V is expressed in mph.

The probability that the windspeed will exceed a value V is

$$P_E = 1 - F(V) \qquad \text{(B3)}$$

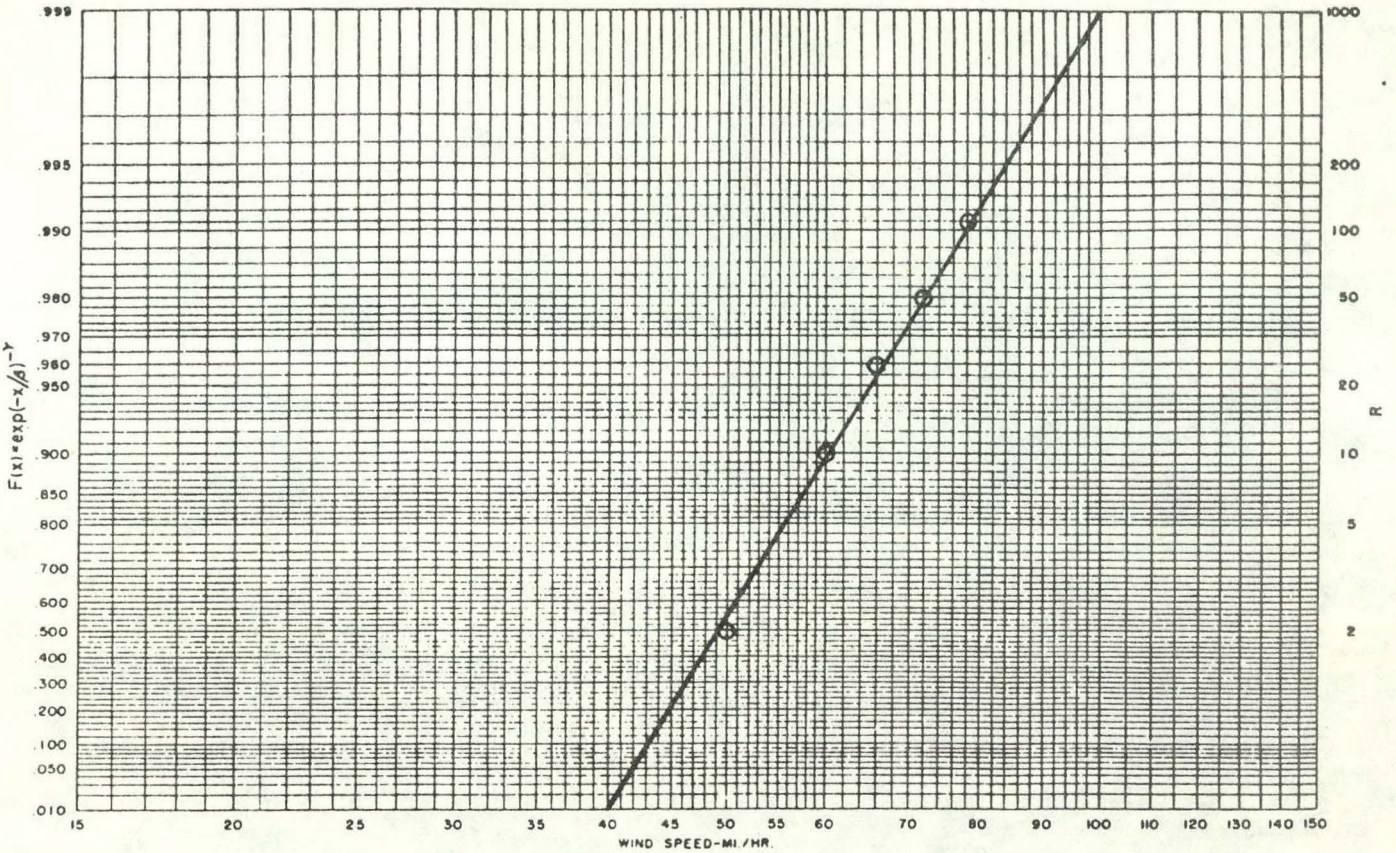

MAXIMUM-VALUE PROBABILITY PAPER, FISHER-TIPPETT TYPE II DISTRIBUTION.

FIGURE B1. FISHER-TIPPETT TYPE II PROBABILITY DISTRIBUTION FOR NEVADA TEST SITE

DISTRIBUTION

Bob Murray	105
TID, File	3
TIC, Oak Ridge, TN	2

SAND76-0407
Unlimited Release
Printed August 1976

IMPACT TESTS of WIND-BORNE WOODEN MISSILES

A. E. Stephenson
Sandia Laboratories
Tonopah Test Range
Tonopah, Nevada 89049

ABSTRACT

A 6-inch concrete and an 8-inch block test panel were impacted by 2 x 4 and 4 x 12 wood missiles at 65 and 85 mph to simulate wind-borne missile impacts of nuclear facilities. The 6-inch concrete test panel was found to be an effective barrier.

SECTION 1

SUMMARY

Tests with two sizes of hypothetical wind-borne wooden missiles impacting reinforced 6-inch (.15 m) thick concrete and 8-inch (.2 m) concrete block test panels have been completed. The objective of the 4-test program was to ascertain the vulnerability of nuclear facility walls to penetration and backface scabbing through mockup test panel tests.

The results are summarized as follows:

MISSILE	VELOCITY	TEST PANEL	RESULTS
2 x 4 x 12 ft. (3.7 m)	65 mph (29 m/s)	6 in. Concrete (.15 m)	No Damage
4 x 12 x 12 ft. (3.7 m)	85 mph (38 m/s)	6 in. Concrete (.15 m)	Hairline Cracks
2 x 4 x 12 ft. (3.7 m)	65 mph (29 m/s)	8 in. Block (.2 m)	Hairline Cracks
4 x 12 x 12 ft. (3.7 m)	83 mph (37 m/s)	8 in. Block (.2 m)	Perforation

This report gives detailed data in the tests completed and the test setup used in obtaining the data.

SECTION 2

TEST DESCRIPTIONS

In this section are described the missiles, test panels, test facility, and the camera setup for all tests. Test results are given in Section 3.

MISSILES:

Two sizes of wooden missiles, postulated to be borne in the vicinity of a nuclear facility, were evaluated. They were a 12-foot (3.7 m) 2 x 4 weighing 16 pounds (7.26 kg) and a 12-foot (3.7 m) 4 x 12 weighing 107 pounds (48.5 kg). Each were Douglas fir.

TEST PANELS:

Test panels were designed to be prototypical of nuclear facility walls. Each 17-feet square (5.2 m) test panel had the same clear span (15 by 15 feet (4.6 m)) thus providing a one-foot (.3 m) simple support on all four sides.

The 6-inch (.15 m) thick concrete test panel had a design strength of 3000 psi (20.7 MPa) with a maximum aggregate size of 3/4-inches (20 mm). Compressive strength as determined from laboratory cured samples (6-inch (.15 m) diameter by 12-inches (.3 m) long) was:

DATE TESTED	AGE-DAYS	STRENGTH - psi
2-6-76	8	2550 (17.6 MPa)
2-12-76	14	2710 (18.7 MPa)
2-26-76	28	3380 (23.3 MPa)
3-8-76	39	3940 (27.2 MPa)
3-8-76	39	3610 (24.9 MPa)

Sieve analysis of the fine and coarse aggregates used in fabrication of the test panel was:

	Percent Finer by Weight	
SIEVE SIZE	COARSE	FINE
1"	100	
3/4"	91.8	
1/2"	51.5	
3/8"	24.0	100
No. 4	5.7	99.6
No. 8	1.6	89.7
No. 16		68.3
No. 30		45.8
No. 50		24.2
No. 100		8.0
No. 200		3.9

The reinforcing bars used in the test panel were No. 4 (.5-inch (12.7 mm) nominal diameter) Grade 40 at 12-inches (.3 m) on center. To climinate debonding and pull-out of the ends of the reinforcing bars, all bars had an 180-degree tensile hook at the panel edges.

The 8-inch (.2 m) concrete block test panel was fabricated within a steel channel support frame. (Note the test panel standing in Figure 1). Reinforcing bars in the test panel were No. 5 (.625-inch (15.9 mm) nominal diameter) Grade 40 on 32-inch (.8 m) centers. The same concrete mix design as used in the fabrication of the 6-inch (.15 m) test panel was used to fill all cells of the block wall. No laboratory cured samples were made for compressive strength tests.

TEST FACILITY:

The test facility, located at the Sandia Laboratories, Tonopah Test Range, includes a missile launcher, a backup structure for support of test panels, and a camera instrumentation system.

A view of the missile launcher is shown in Figure 1. It consists of a launcher rail, a missile guide, and a rocket propelled pusher sled and its brake system.

The launcher rail for the rocket propelled sled is a 130-foot (39.6m), wide flange I-beam mounted on pedestals for aiming the missile at the desired impact location. The desired speed for the missile is attained by selecting a launch position on the rail and the number of rockets (up to four) mounted to the sled. The rockets used are High Velocity Aircraft Rockets (HVAR) with a burn time of 1.25 seconds and an impulse of 5500-pound seconds (24.5 kN-sec.).

At the impact end of the launcher, crushable aluminum honeycomb captures the sled and the rockets, leaving the missile in free flight for 20 feet (6 m) to the test panel.

The fixed backup structure reacts impact loads by means of both its mass (40 tons (36 kg)) and footings that transmit forces to the ground. The 1-foot (.3 m) thick backup structure is 17-feet (5.2 m) square and 8-feet (2.4 m) deep. Grout between the test panel (no grout was used with the concrete block test panel) and the backup structure assures uniform test panel support. Test panels are supported at their bottom by eight 6-inch (.15 m) wide I-beams embedded in the concrete apron. In addition, turnbuckle and cable ties hold the test panel against the backup structure.

High speed motion photography was used extensively in each test to obtain the motion of the missile before, during, and after impact. The cameras were positioned on the frontface normal to the flight of the missile and at the rear of the test panel to observe scabbing and debris motion. The framing rate for the cameras was 3000 frames per second with 10 KHz timing superimposed to facilitate data reduction. These films are available for viewing upon request to Sandia Laboratories, Tonopah Test Range, Tonopah, Nevada.

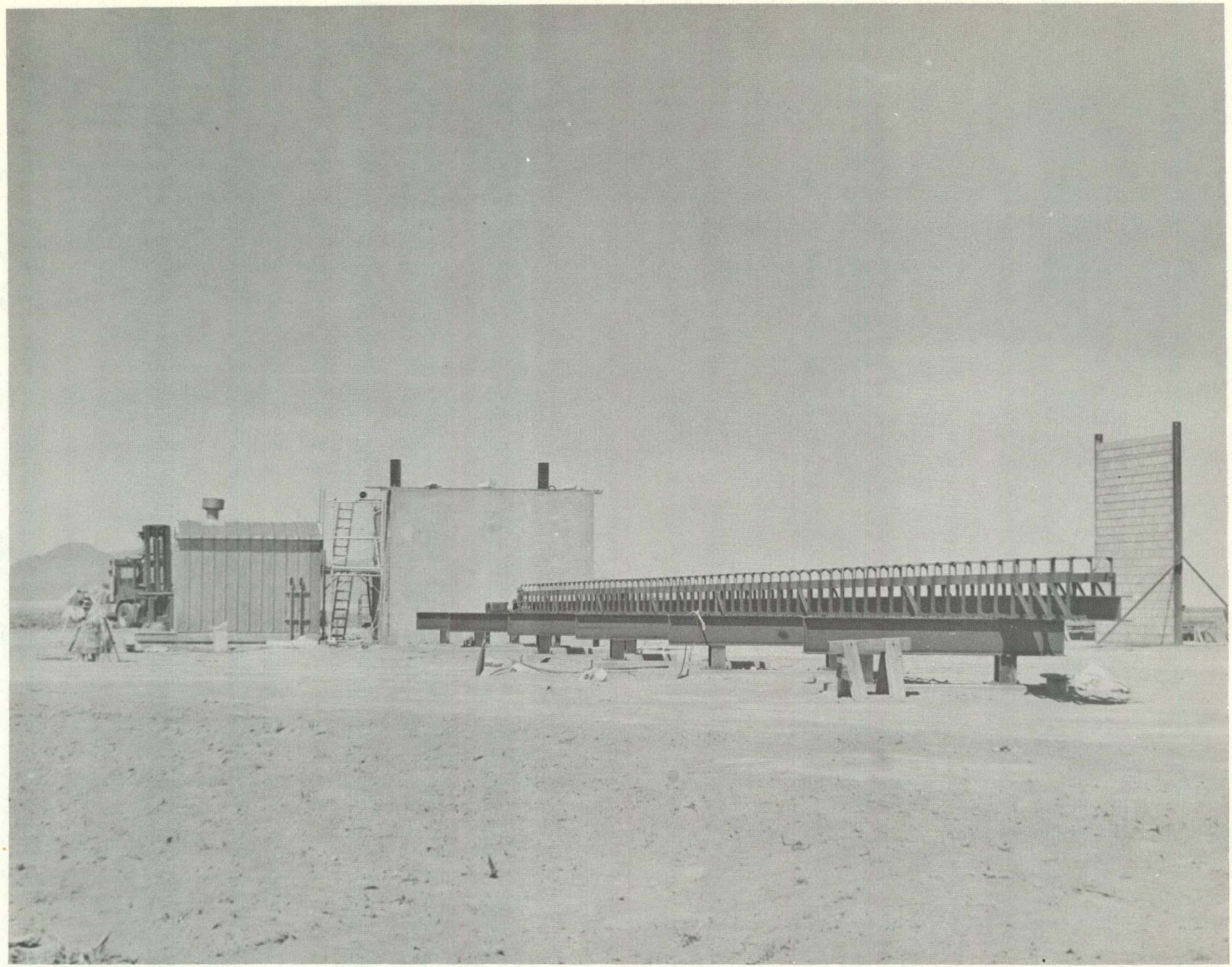

FIGURE 1 - Overall View of Test Facility

SECTION 3

TEST RESULTS

The objective of this test program was to evaluate prototypical test panels to the impact of hypothetical wind-borne wooden missiles.

TEST VELOCITIES:

To meet the program objective, postulated velocities of 70 mph (31 m/s) and 90 mph (40 m/s) were selected for the 2 x 4 and 4 x 12 missiles respectively. All tests were conducted at the middle of the test panel at a point between reinforcing bars with the missile impacting normal to the test panel.

IMPACT DAMAGE:

Test panel and missile damage resulting from the four tests conducted is as follows:

TEST 1 — A 2 x 4 at 65 mph (29 m/s) was impacted in the center of the 6-inch (.15 m) concrete test panel. Neither the 2 x 4 (Figure 2) nor the test panel showed any damage as a result of the test. The missile did fail, however, from column loading at a point 2 feet (.6 m) from the impact end. The impact end of the 2 x 4 did not show effects of the impact loading.

TEST 2 — A 4 x 12 at 85 mph (38 m/s) was on the same test panel and at the same impact location as Test 1. The panel survived the test with only a minor hairline backface (Figure 3) crack. The missile, on the other hand, deformed 23 inches (.58 m) (Figure 4).

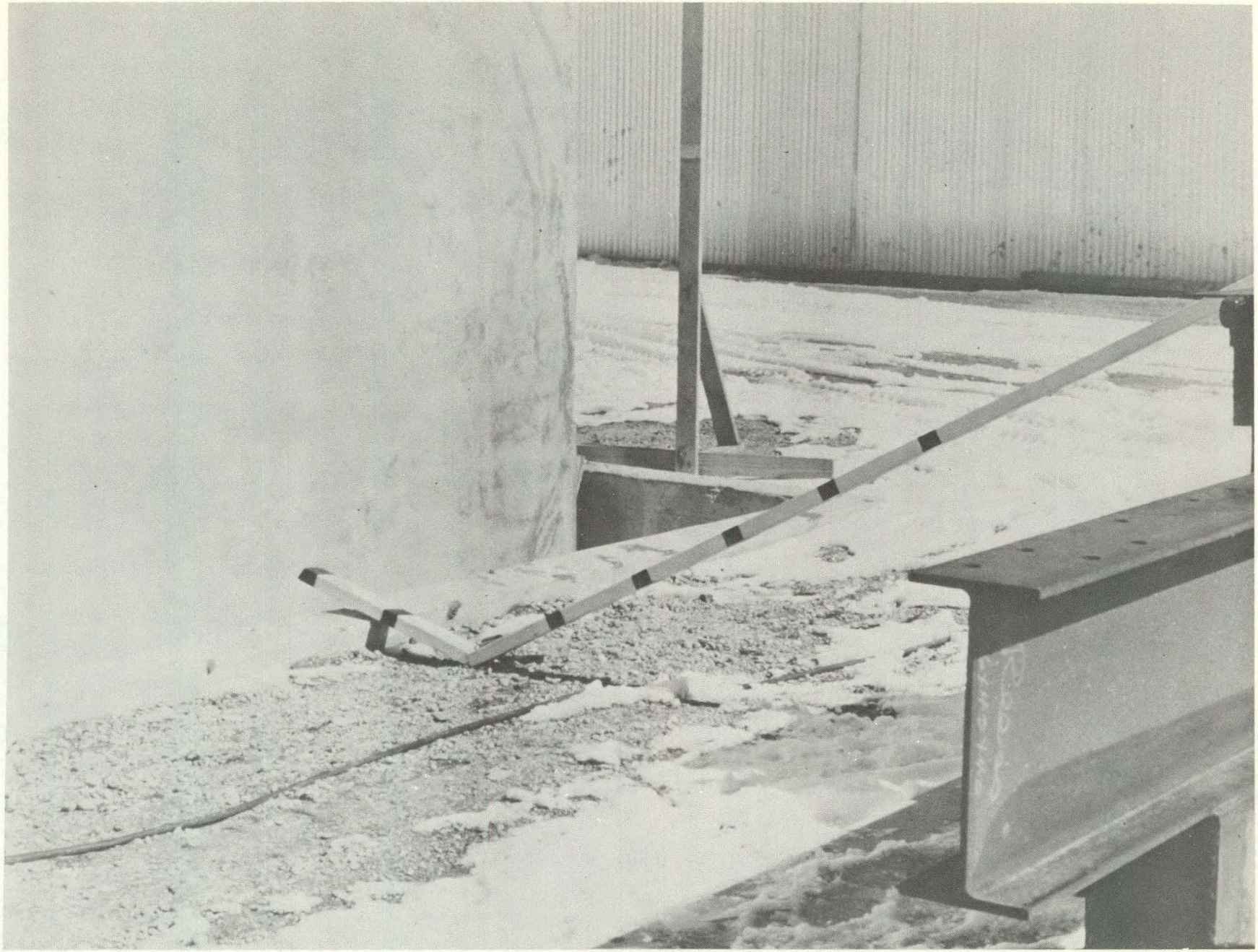

FIGURE 2 - Te - 2 x 4 Post Test

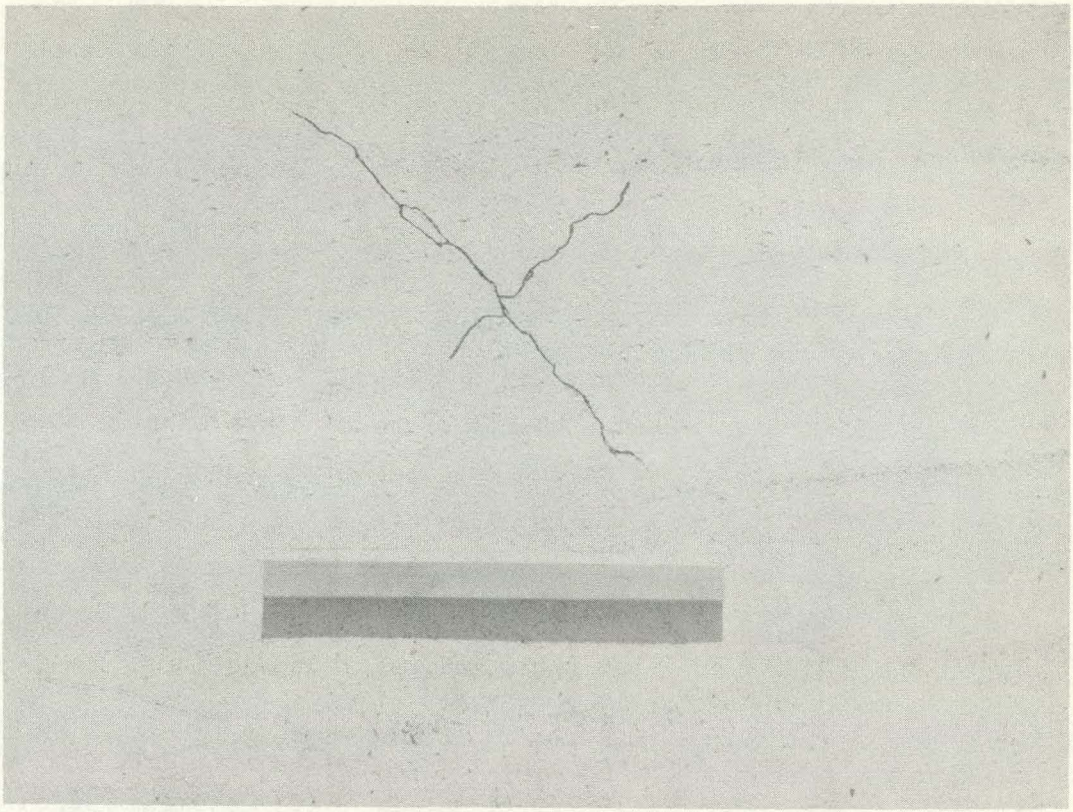

FIGURE 3 - Backface Test 2 - 4 x 12 at 85 mph

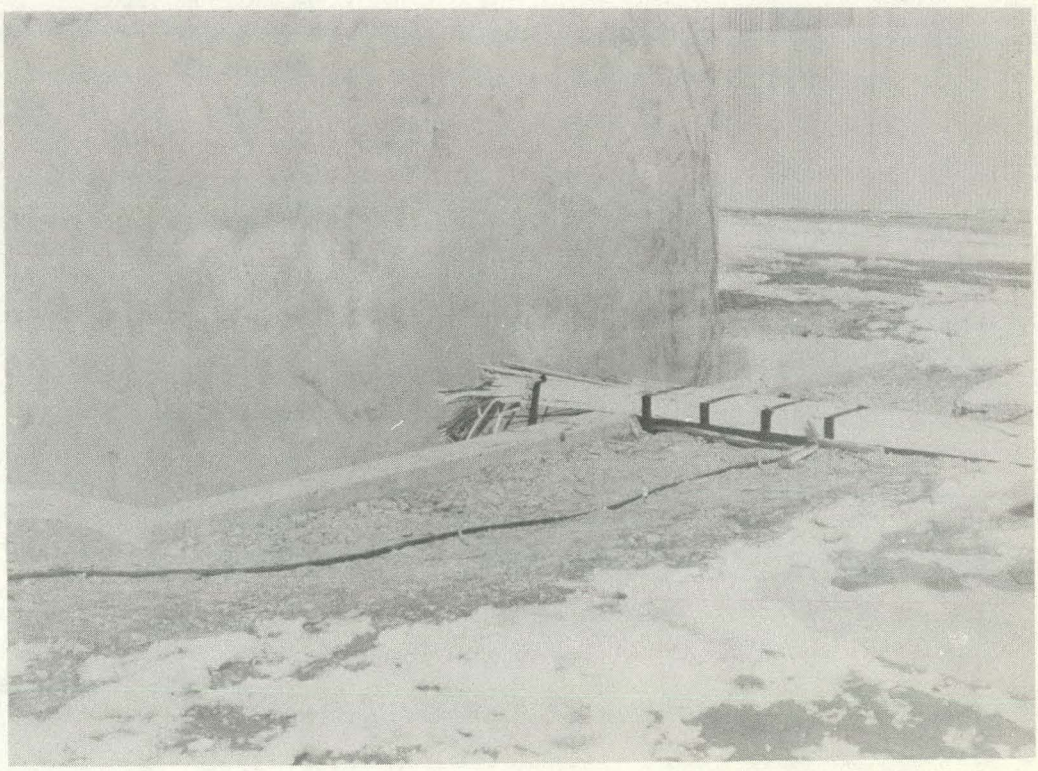

FIGURE 4 - Missile Test 2 - Post Test

TEST 3 — A 2 x 4 was impacted at 65 mph (29 m/s) at the center of the 8-inch (.2 m) concrete block test panel. A small indentation of approximately 1/8-inches (3 mm) (Figure 5) resulted on the frontface and a hairline crack on the backface (Figure 6). No damage was done to the missile.

TEST 4 — A 4 x 12 at 83 mph (37 m/s) was impacted on the same block wall and at the same impact location as the previous test. The missile perforated the test panel (Figure 7 and 8).

It is clear from the post test examination of the 2 x 4 wooden missiles that insufficient kinetic energy was available to either exceed the strain energy of the missile or to produce significant test panel damage. The impact ends of both 2 x 4's from Tests 1 and 3 were unspoiled at the test velocity of 65 mph (29 m/s).

The post test examination of the 4 x 12 from Test 2 clearly indicates sufficient strain energy was developed within the missile to deform it. At virtually the same impact velocity in Test 4, the block test panel failed in shear. The impact end of the missile was unspoiled yet with numerous longitudinal fractures of the missile. The block test panel was weakened from the impact of Test 3 thus making it virtually impossible to compare the relative strength of the block test panel with the missile. The same multiple hit testing occurred with the block wall panel in Reference 3, where the block test panel was weakened from a previous test and the panel failed in shear when hit by the wooden missile. It too was virtually unspoiled at the impact end when tested at 105 mph (47 m/s). A third test on the same block test panel in Reference 3 was conducted at another location than the previous two tests resulting in a shear failure of the test panel and longitudinal cracks without impact end deformation. This test was conducted at 100 mph (44.7 m/s), at a point 2.5 feet (0.76 m) below the damage area of the previous tests.

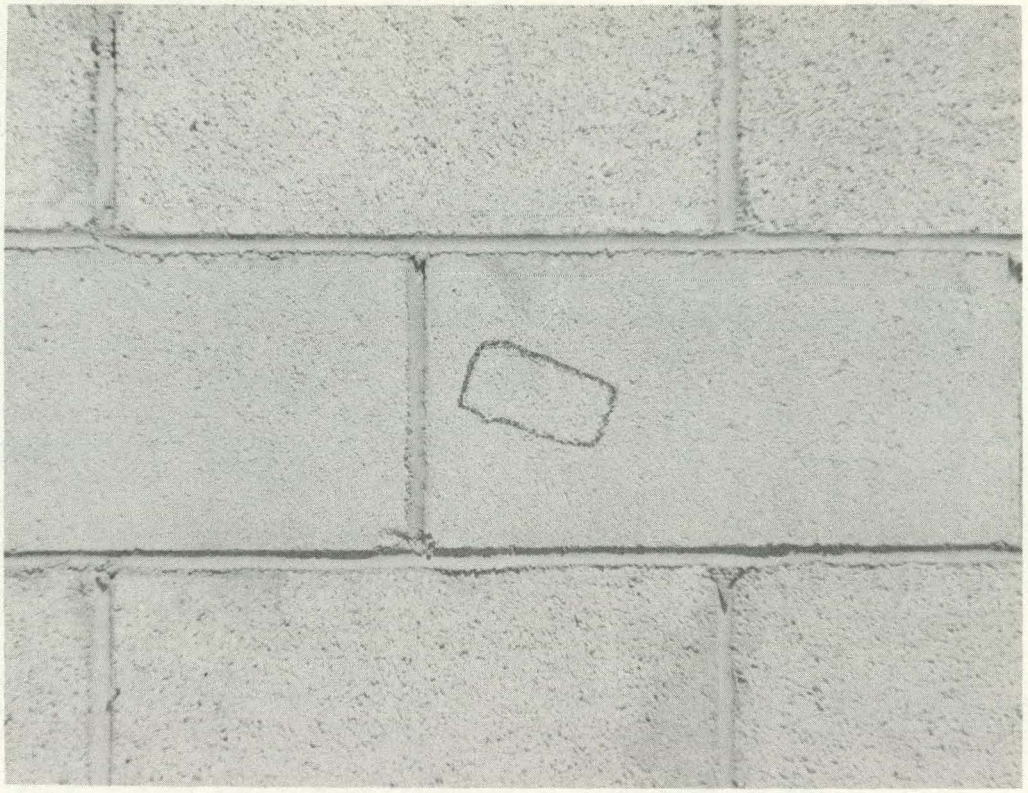

FIGURE 5 - Frontface Test 3 - 2 x 4 at 65 mph

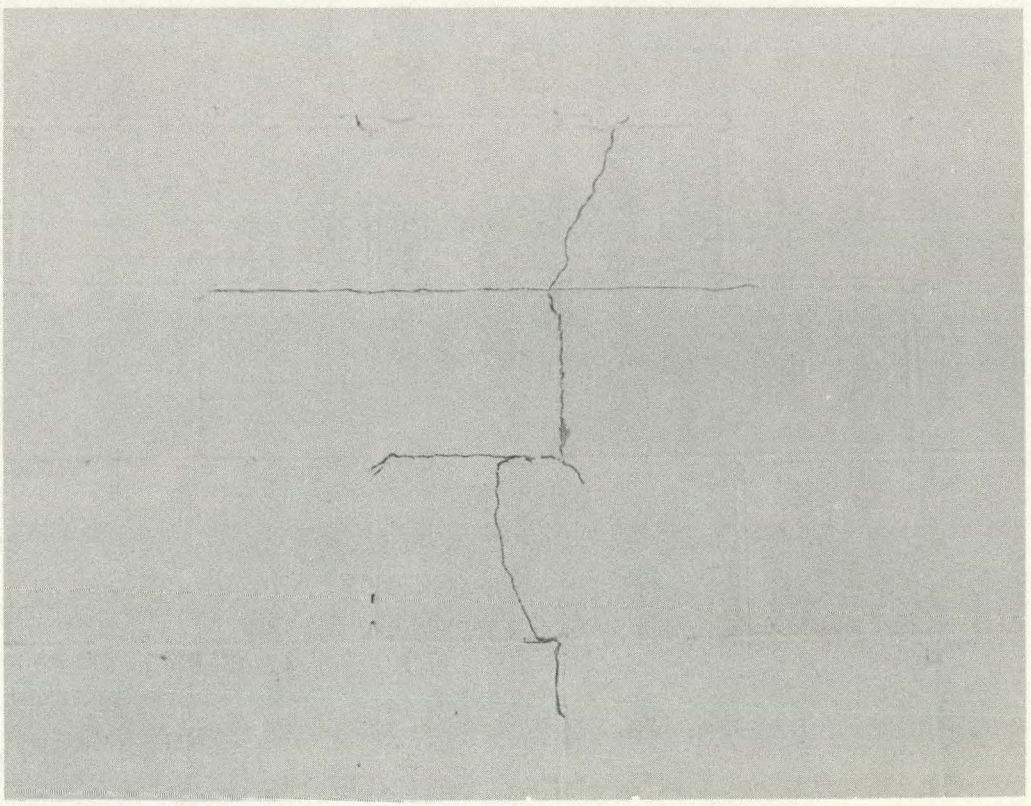

FIGURE 6 - Backface Test 3 - 2 x 4 at 65 mph

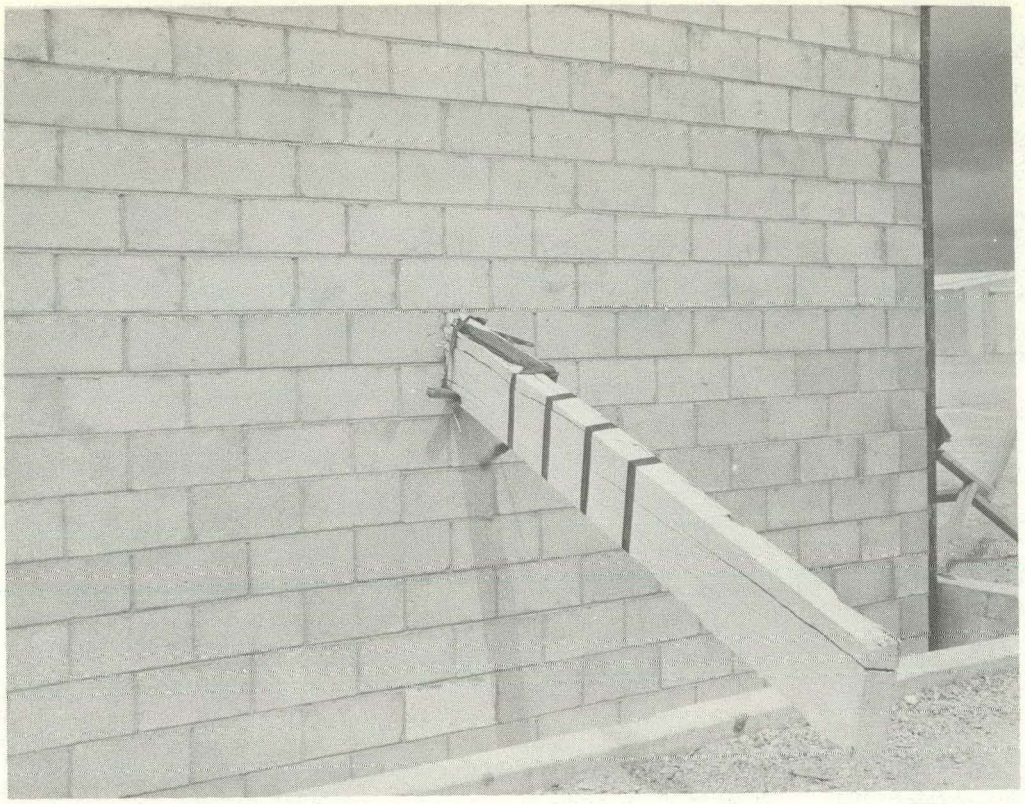

FIGURE 7 - Frontface Test 4 - 4 x 12 at 83 mph

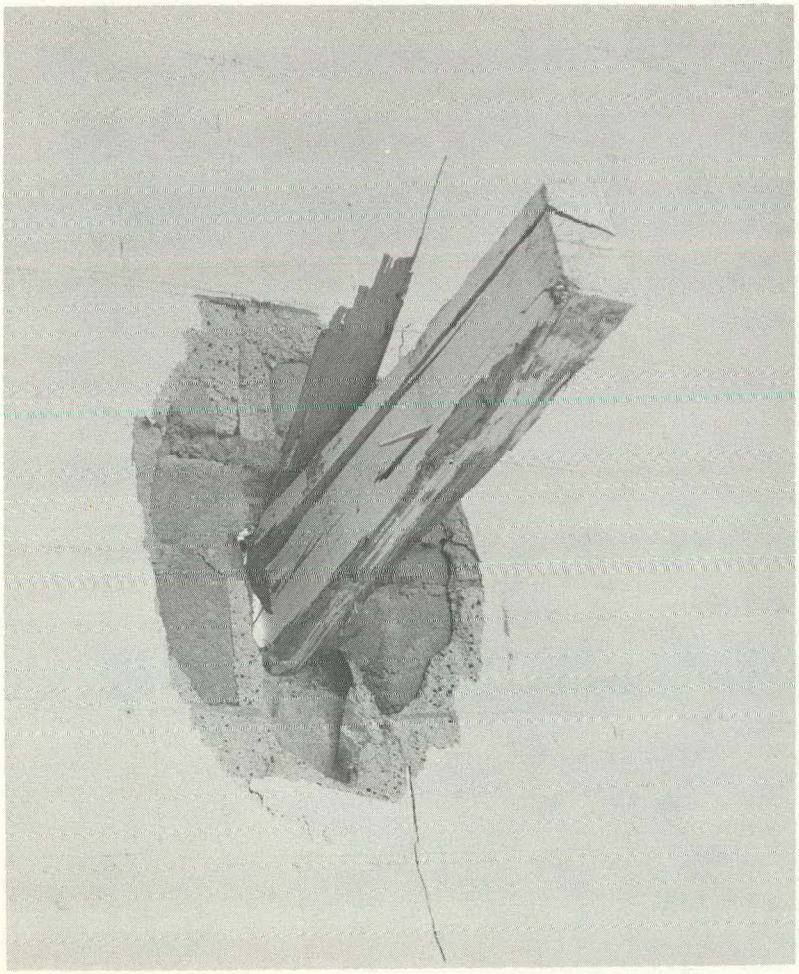

FIGURE 8 - Backface Test 4 - 4 x 12 at 83 mph

Within the range of parameters tested, the 6-inch (.15 m) concrete wall is an efficient barrier to the 2 x 4 and 4 x 12 wooden missile. The concrete block wall, on the other hand, is not a recommended barrier to the 4 x 12 wooden missile.

SECTION 4

DATA COMPARISONS

Several full-scale and scale test programs have been conducted by others wherein wooden missiles have been impacted into concrete and block test panels. A brief summary of these data are shown in Table 1. Comparison of these data with the work reported herein indicate similar damage results. The concrete barriers are effective in deterring the wooden missile whereas the 8-inch filled concrete block test panels are penetrated and many generate backface spall products.

TABLE 1

MISSILE	WEIGHT	VELOCITY	TARGET	PENETRATION	REF.
4 x 12 x 12 ft. (3.7 m)	108 lb. (50 kg)	191 mph (85.4 m/s)	16 in. (.4 m) Concrete	0	5
4 x 12 x 12 ft. (3.7 m)	108 lb. (50 kg)	200 mph (89.4 m/s)	16 in. (.4 m) Concrete	0	5
4 x 12 x 12 ft. (3.7 m)	108 lb. 50 kg)	240 mph (107 m/s)	16 in. (.4 m) Concrete	0	6
35 ft. (10.7 m) Utility Pole	1500 lb. (630 kg)	139 mph (62 m/s)	12 in. (.3 m) Concrete	0 (1)	4
35 ft. (10.7 m) Utility Pole	1470 lb. (657 kg)	139 mph (62 m/s)	18 in. (.46 m) Concrete	0 (1)	4
2 x 12 x 12 ft. (3.7 m)	50 lb. (22.7 kg)	105 mph (47 m/s)	8 in. (.2 m) Block	3 in. (76 mm) (2)	3
2 x 12 x 12 ft. (3.7 m)	53 lb. (24 kg)	100 mph (44.7 m/s)	8 in. (.2 m) Block	5.5 in. (140 mm) (2)	3
3 3/8 in. (86 mm) Pole	23 lb. (10.4 kg)	180 mph (80.5 m/s)	6 in. (.15 m) Concrete	0	2
3 3/8 in. (86 mm) Pole	23.2 lb. (10.5 kg)	176 mph (78.7 m/s)	4.5 in. (.1 m) Concrete	0 (2)	2
3 3/8 in. (86 mm) Pole	23.4 lb (10.6 kg)	290 mph (129.6 m/s)	4.5 in. (.1 m) Concrete	0 (2)	2
8 in. (.2 m) Pole	201 lb. (91 kg)	204 mph (91.2 m/s)	12 in. (.3 m) Concrete	0	1
8 in. (.2 m) Pole	199 lb. (90.3 kg)	300 mph (134 m/s)	12 in. (.3 m) Concrete	0	1
8 in. (.2 m) Pole	200 lb. (90.7 kg)	334 mph (149.3 m/s)	24 in. (.6 m) Concrete	0	1

(1) Slight Cracks on backface

(2) Backface Spall

REFERENCES

(1) Vassallo, F. A., 1975: Missile Impact Testing of Reinforced Concrete Panels, Calspan Corp., HC-5609-D-1.

(2) White, M. P., 1976: "Missile Tests of Quarter-Scale Reinforced Concrete Barriers", A symposium on Tornadoes Assessment of Knowledge and Implications for Man, 22-24 June, 1976, Lubbock, Texas.

(3) Clark, J. E., 1976: Tornado Missile Impact Barrier Evaluation, Sandia Laboratories, R422202.

(4) Stephenson, A. E., 1976: Full-Scale Tornado-Missile Impact Tests, EPRI, Interim Report, NP-148.

(5) Stephenson, A. E., 1975: Tornado Vulnerability - Nuclear Production Facilities, Sandia Laboratories, RS 9333/13.

(6) Stephenson, A. E., 1975: Addendum to Tornado Vulnerability - Nuclear Production Facilities, Sandia Laboratories, R423595.


G

APPENDIX G

HYDROLOGY OF THE 410 AREA (AREA 27) AT THE NEVADA TEST SITE

GENERAL

Geography

Geology

Precipitation

SURFACE HYDROLOGY

ABLE AREA

BAKER AREA

SUBSURFACE HYDROLOGY

Figures

APPENDIX G

HYDROLOGY FOR THE 410 AREA (AREA 27)

GENERAL

Geography

The 410 Area (Area 27) is located in the south central portion of the Nevada Test Site (see Fig. 1). The area comprises a drainage basin formed by Skull Mountain on the west, Hampel Hill on the east, and on the north by a ridge running east-west between Hampel Hill and Skull Mountain. The southern end of the basin slopes southwest toward Rock Valley and the northern end of the Amargosa Desert. Elevation ranges from 1800 m on Skull Mountain to approximately 1300 m at the southern boundary of the 410 Area.

Geology

The general soil characteristics at the Nevada Test Site described by Romney[1] indicate the soil in this type of terrain to be alluvial deposits containing unconsolidated parent materials low in clay content. This soil can be classified as silty, sandy gravel according to the Unified Soil Classification System[2] and identified by the group symbol, GM.

Although soils of this type range in permeability from moderately slow to moderately rapid, the soil in this area has been found to be well drained with medium permeability.

The vegetative cover of the 410 Area is very sparse and mainly consists of tumbleweed-type shrubs spaced at 60-90 cm apart and growing to about 30-60 cm in height.

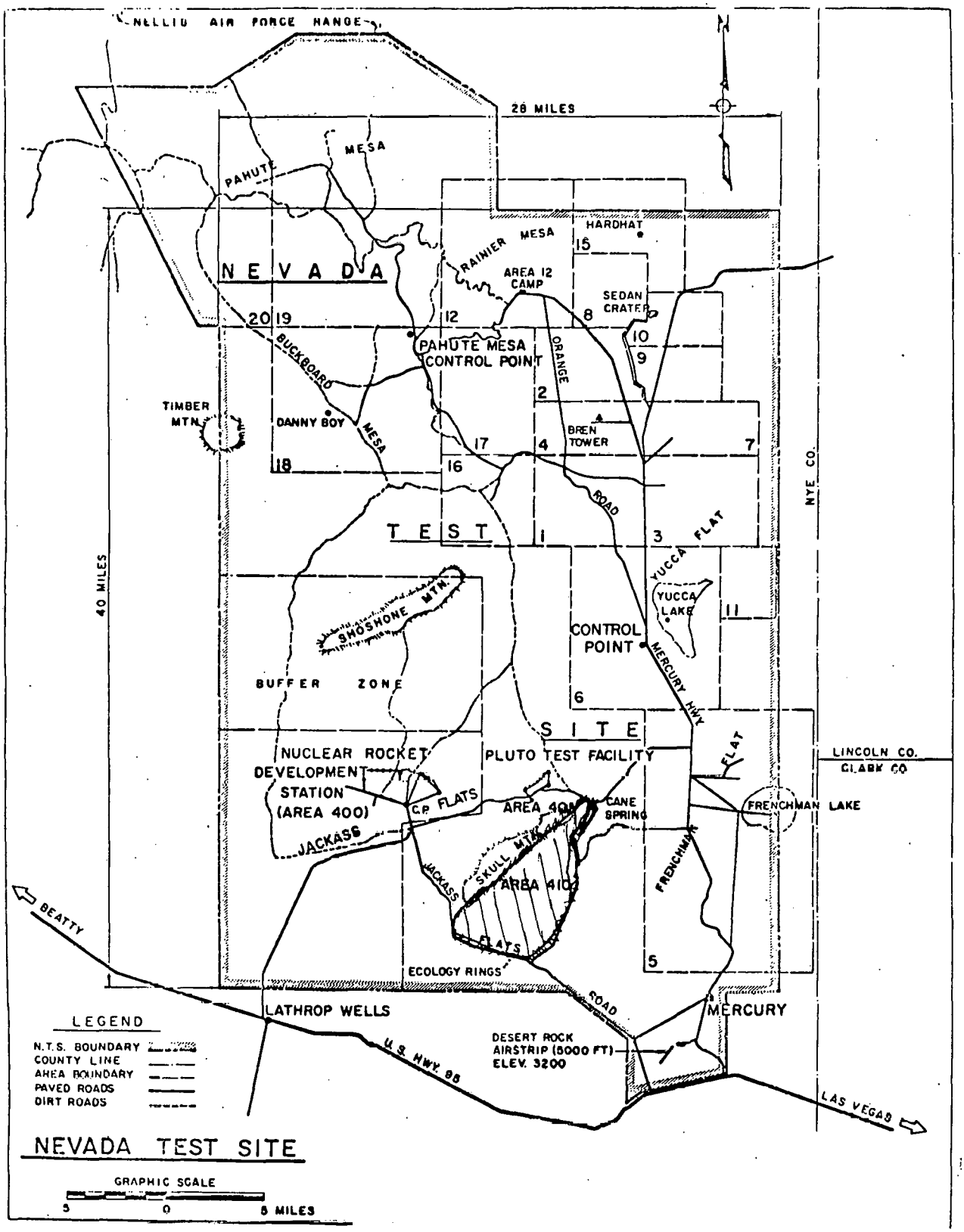

Fig. 1. Map of Nevada Test Site.

Precipitation

Precipitation in an arid climate varies in intensity and duration according to season. Winter rains are of long duration, low intensity, and tend to cover broad areas. Often winter precipitation is snow in the higher elevations. In February 1969, approximately 32 mm of warm rain fell in 24 h on an existing 250-mm-deep snow cover in Area 410. Even though this was only a 20% flood, it was sufficient to cause runoff. No damage was recorded.

Summer rains are normally of short duration, high intensity, and affect small areas. These rains cause late summer flash floods. On July 29, 1968, 43 mm of rain was recorded in 1 h at Cane Springs rain gauge but no damage was recorded for the Able or Baker sites.

The annual precipitation cycle for Cane Springs shows a maximum in February, a secondary maximum in July, a minimum in September, and a secondary minimum in May, (see Fig. 2).

Data taken over 11 years at the Cane Springs Recording Station show an annual average precipitation of 183 mm with 37 days per year having measurable precipitation.

SURFACE HYDROLOGY

The Rational Formula

The rational formula[3] for predicting flood runoff will be used in this assessment. It is:

$$Q = CIA$$

where

Q = peak runoff

C = runoff coefficient

I = average rainfall intensity for a duration equal to the period of concentration

A = area of the drainage basin.

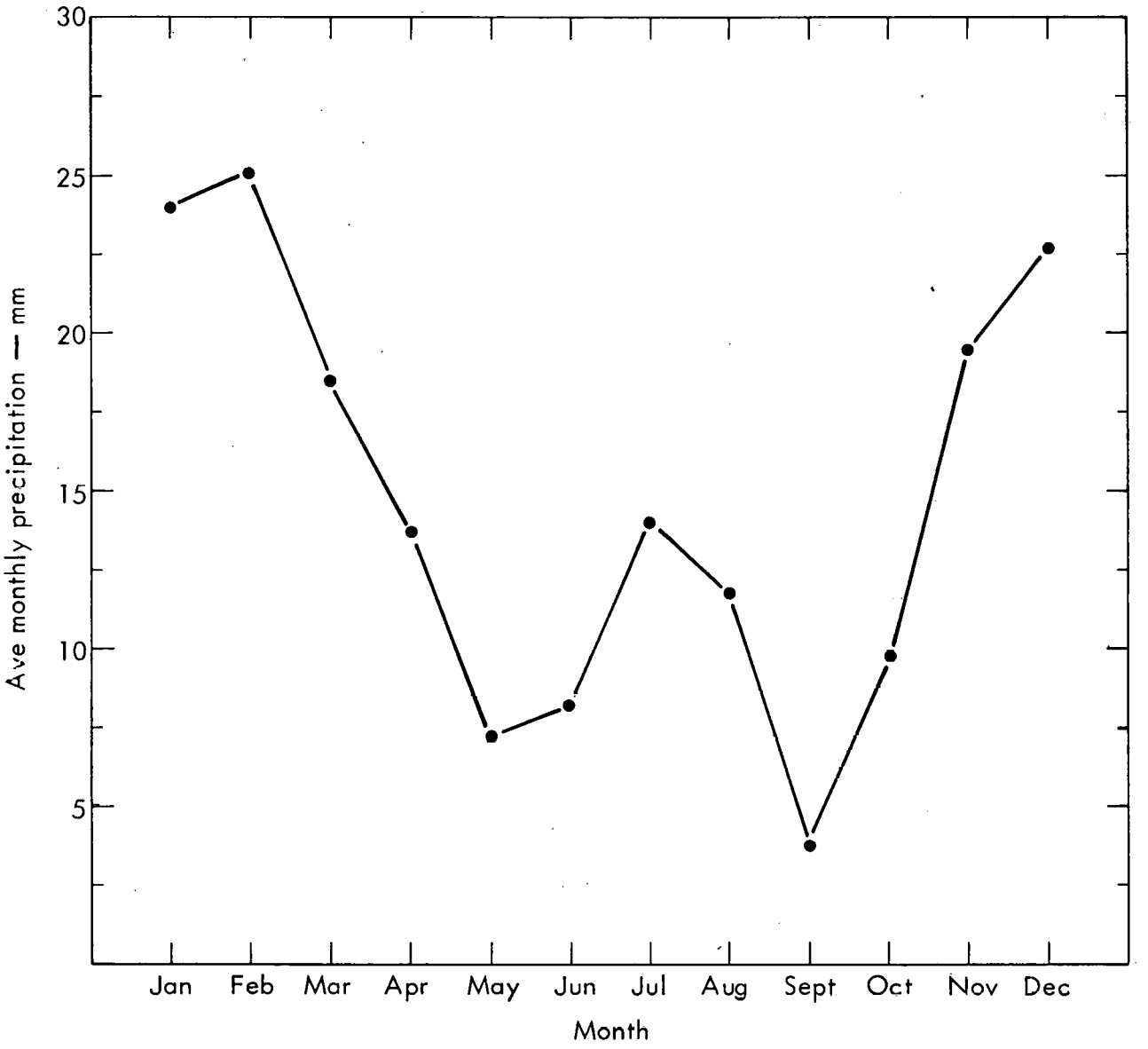

Fig. 2. Annual precipitation cycle at Cane Springs (11 yr record).

This formula is applicable to small drainage areas (less than 2.6×10^7 m^2) where few, if any, rainfall and runoff records are available. The formula does not take into account the variability of the rainfall rate and the infiltration capacity of the soil. However, the maximum runoff (flood) will occur at a point in time when the entire drainage area is contributing to the runoff. The time it takes to reach this point is called the time of concentration and varies with ground vegetation, maximum overland flow length, and slope.

The rainfall intensity must then be figured based on the time of concentration and the desired frequency. This can be done by starting with a base storm of desired frequency and 1 h duration. The intensities for other durations, equal to the time of concentration, may be obtained using the rainfall intensity duration curve shown in Fig. 3.

The 100 year or 1% probability storm intensity for the NTS was obtained from a rainfall frequency atlas for Nevada.[4] The 1 h storm intensity was found to be 25 mm/h.

In order to provide a worst-case condition for this flood analysis, it was assumed that the storm happened in the late winter with snow still on the ground. It was determined that the snow would contribute 10% additional precipitation equivalent and, because the ground would be semi-frozen, much of the precipitation will appear as runoff. Thus, a value of 28 mm/h is used as the base storm to obtain the rainfall intensity for the time of concentration for each drainage area considered.

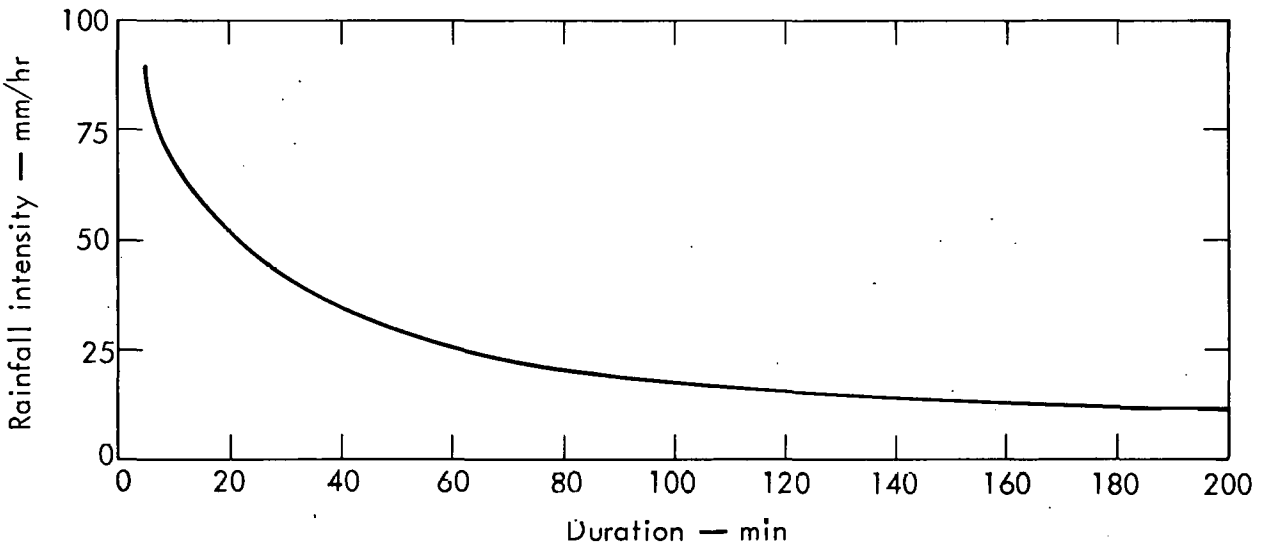

Fig. 3. Rainfall intensity – duration curve for 100 yr (1% probability) storm at Nevada Test Site.

The runoff coefficients for the soil type found in the 410 Area ranges from 15% to 65% depending on vegetation and ground hardness. Due to the scarce vegetation and the semi-frozen nature of the soil, a runoff coefficient of 45% was chosen.

ABLE AREA

The Able site is located in an 88 acre drainage basin north of Hill 4341, draining to the southwest, see Fig. 4. There are four major drainage channels in the area, see Fig. 5.

Channel 1-A drains the runoff from the main access road and paved area southeast of Buildings 5140 and 5130. It is a 0.15-m-deep earth channel with a 1.22-m-wide top that slopes 2% toward the southwest corner of the Site, see Fig. 6. The maximum capacity of Channel 1-A (0.15 m^3/s) would not be exceeded during the 1% probable flood due to its small drainage area.

Channel 2-A runs northeast along Building 5140, makes a 90° turn around the end of Building 5140 and ends. This channel is not much more than a low area at the edge of the pavement. Because of the small slope of this channel, its maximum capacity is low, 0.04 m^3/s. Runoff will probably pond instead of flowing freely. Since there is only 6 cm clearance between the channel and the door of the building, the channel should be redefined, similar to Channel 1-A.

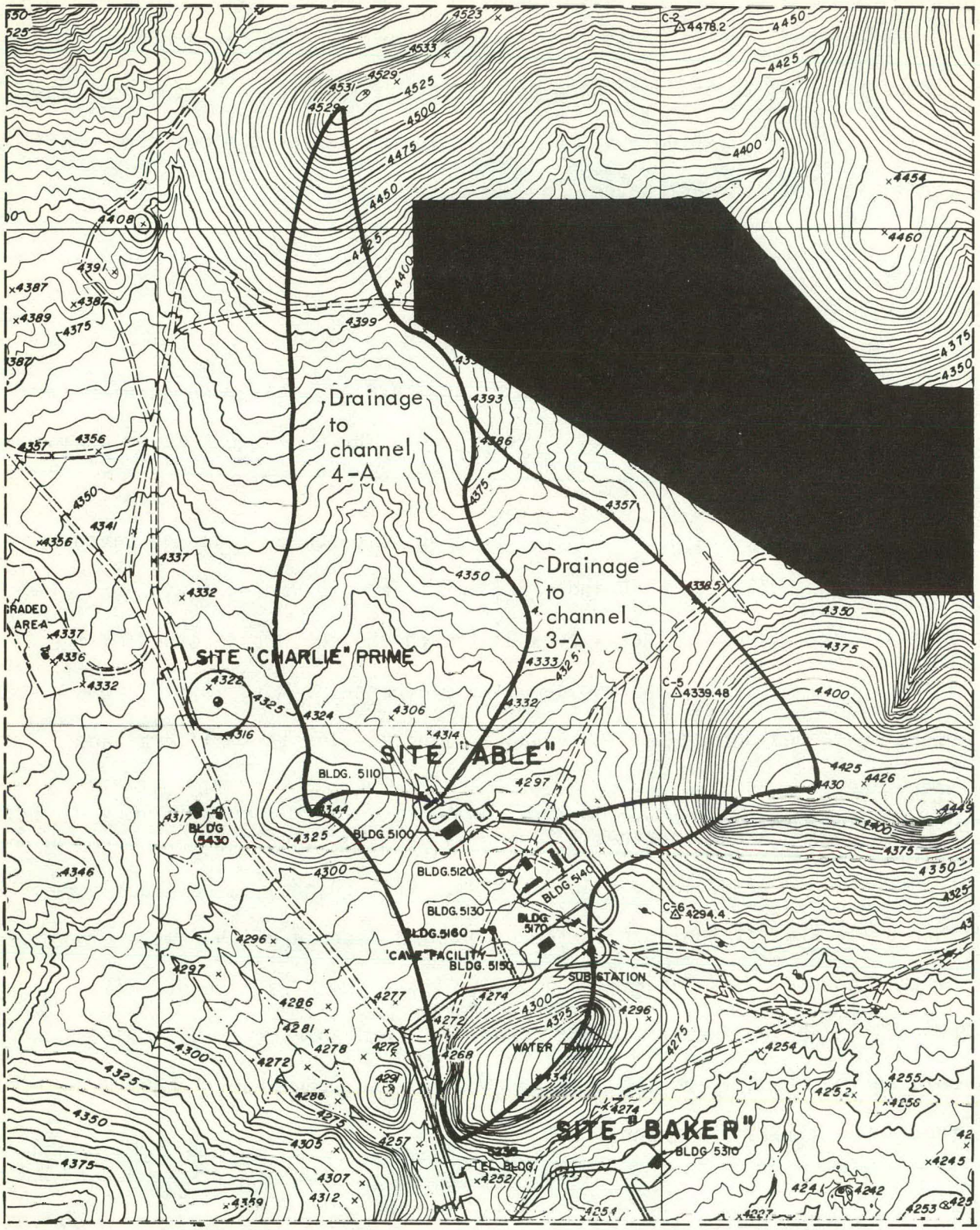

Fig. 4. Able Area drainage basin.

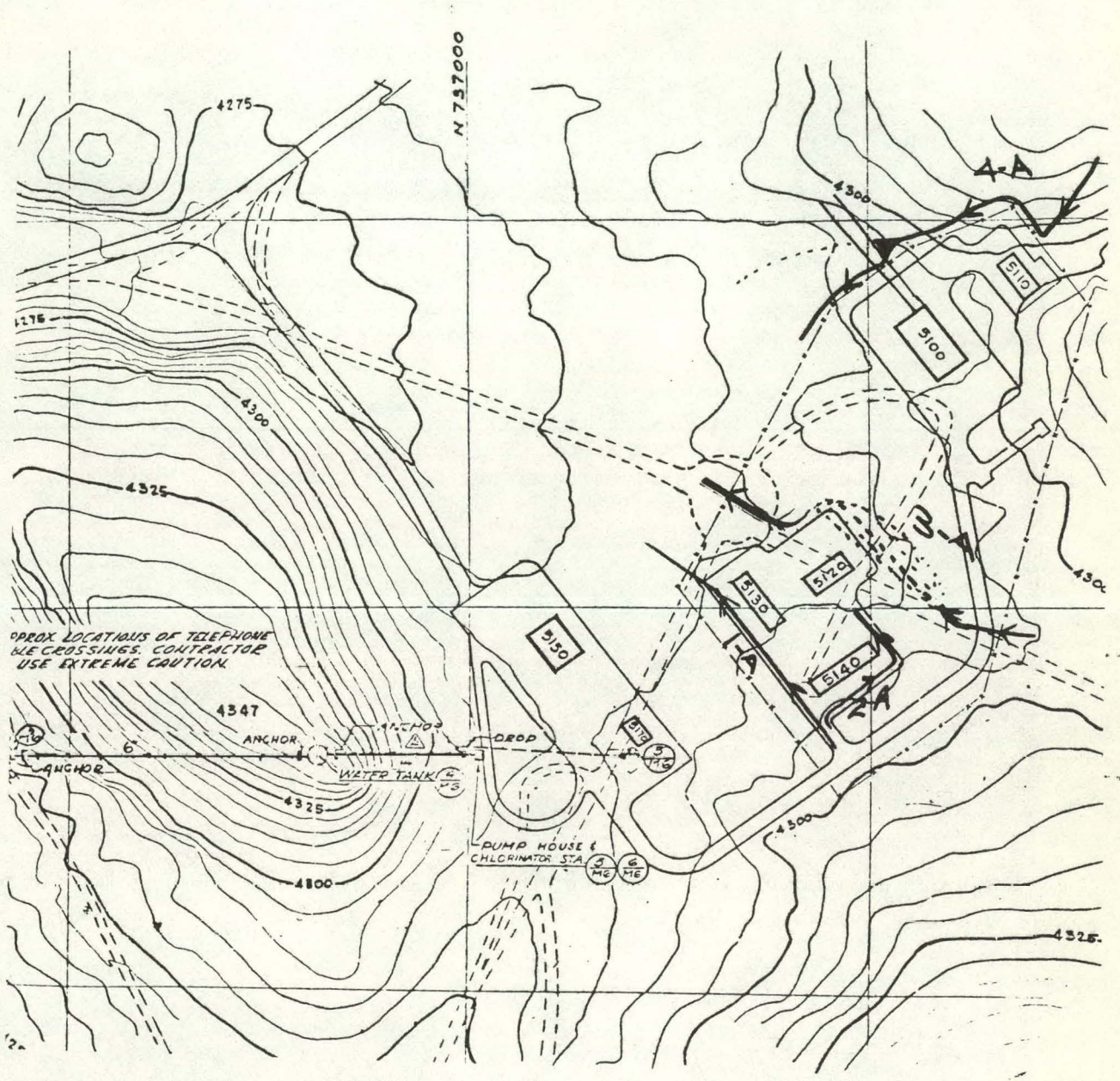

Fig. 5. Able Area drainage system.

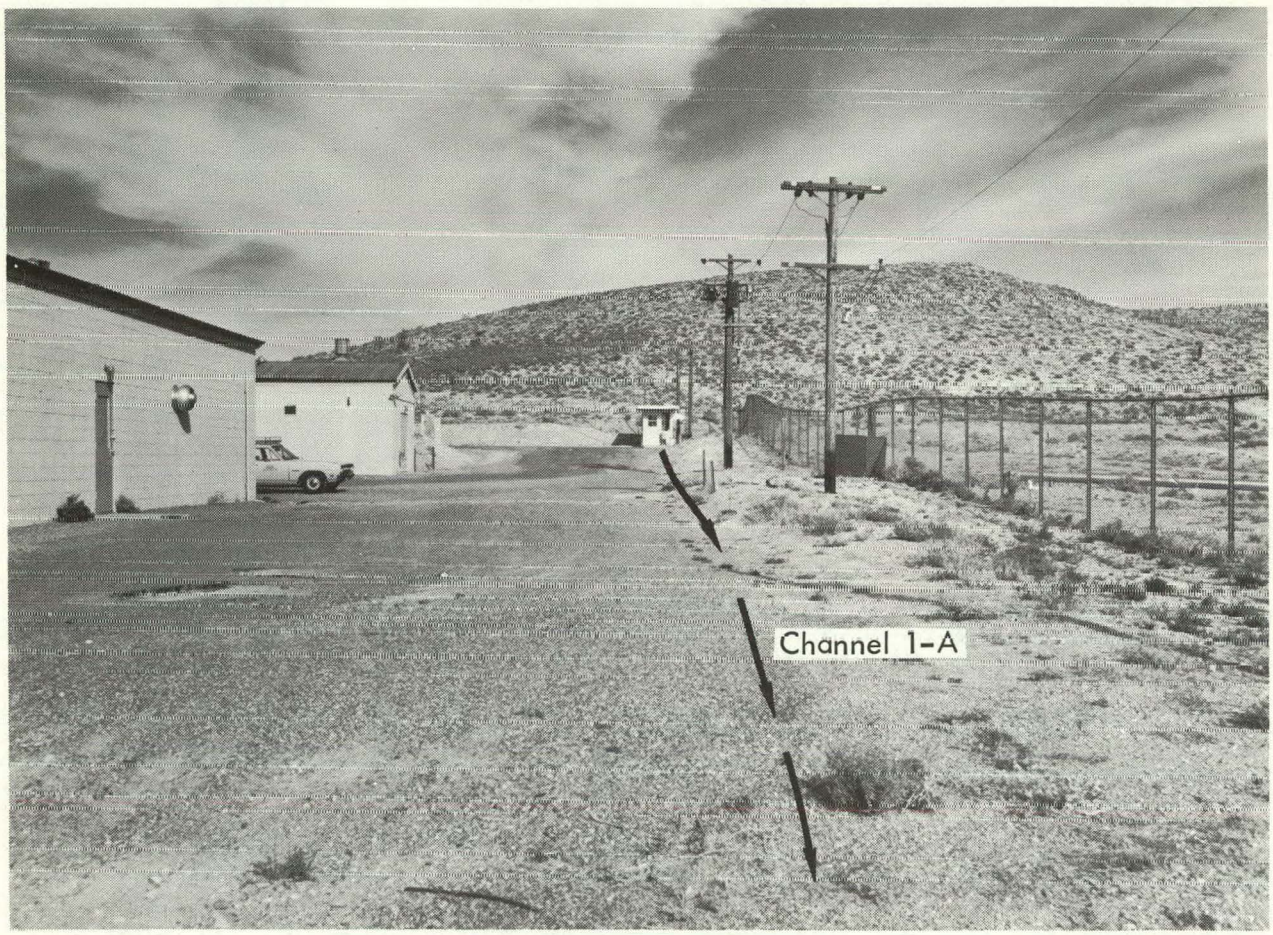

Fig. 6. Channel 1-A by B-5130 and B-5140.

Channel 3-A drains a 28 acre basin north of the Able site. A natural channel funnels the runoff to a culvert under the main access road into Channel 3-A. The culvert has partially collapsed under the road and will not handle the flood flow entering Channel 3-A. The water will back up until it tops over the road and possibly wash it out.

The design plans show Channel 3-A to be a shallow channel running across the Site, exiting southwest of Building 5120. This channel is almost filled with sand due to weathering, see Fig. 7. The channel ends about 6 m from the culvert outlet, see Fig. 8.

Runoff water will sheet flow from this point and follow the Site grade. The sheet flow will be shallow enough not to damage any of the buildings and will accumulate and flow off site in the remaining end of Channel 3-A, southwest of Building 5120, see Fig. 9.

Channel 4-A is a diversion of a natural channel draining the 40 acre basin northwest of Building 5110. This channel is about 1.2 m deep at the turn where the natural channel enters Channel 4-A and follows the fence to a road leaving the 5100 Area, see Fig. 10. There used to be a double culvert that allowed the water to flow under the road and continue in Channel 4-A. In June 1975, the culvert collapsed under the weight of a loaded truck. A decision was then made to fill and stabilize the road, see Fig. 11. The water will now back up until it tops the road and flows over to a 3.7-m-wide trapezoidal channel running along the fence. The elevation of 5100 will prevent any flooding due to runoff in this area.

The existing channels should be maintained routinely to remove vegetation and silt.

The calculations for this analysis are included as Attachment A to this Appendix.

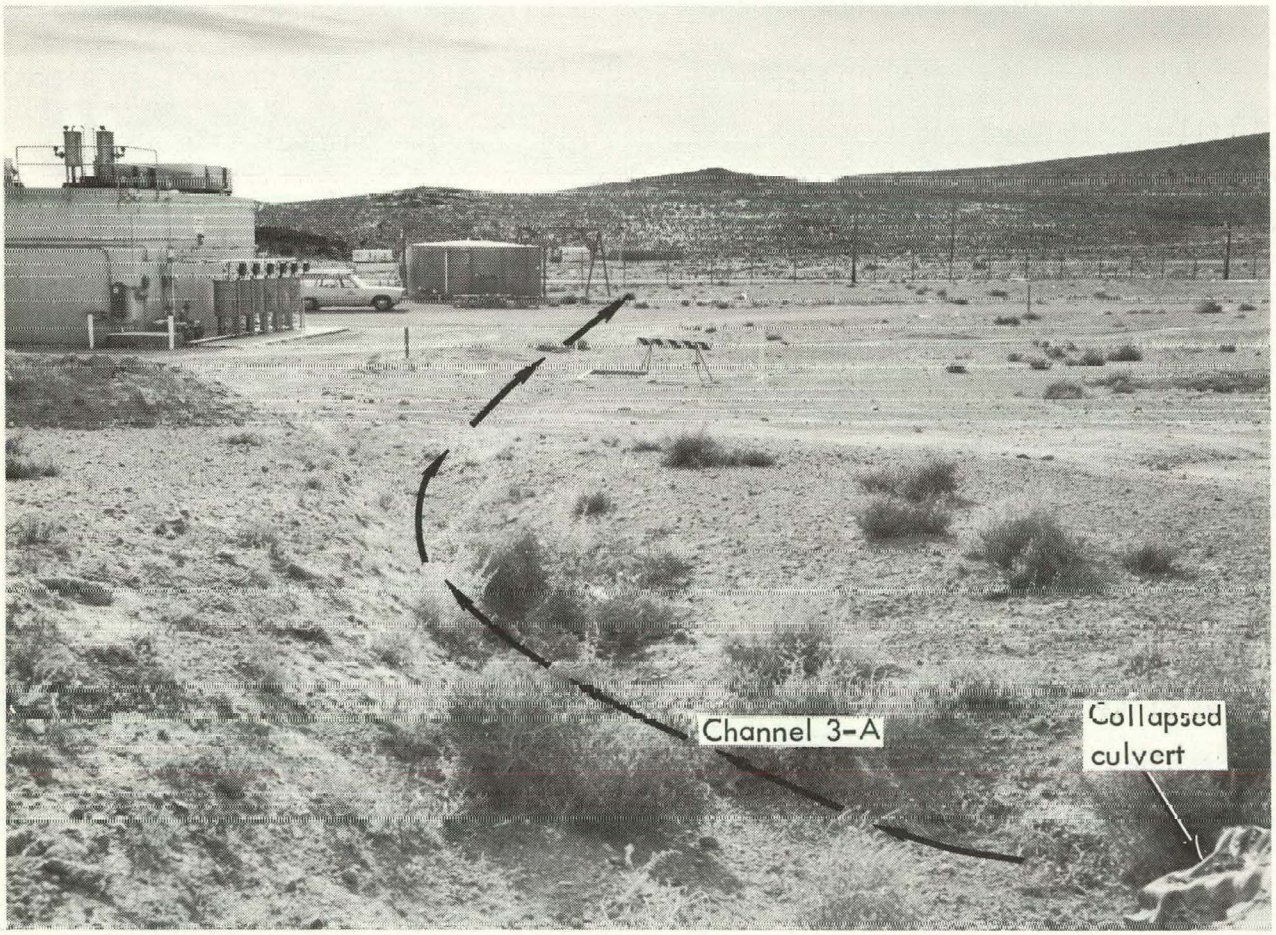

Fig. 7. Channel 3-A near B-5120.

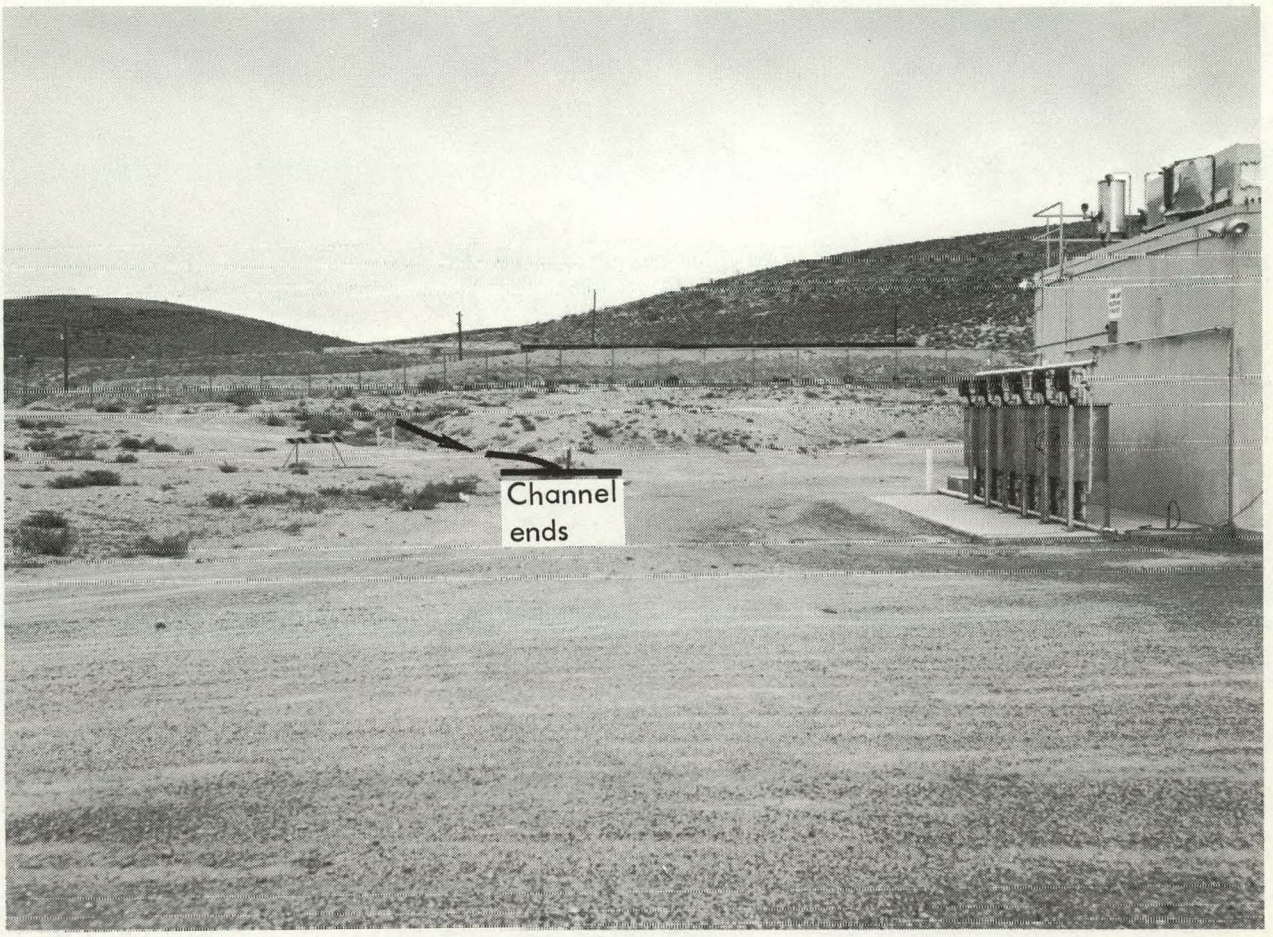

Fig. 8. Channel 3-A ends near B-5120.

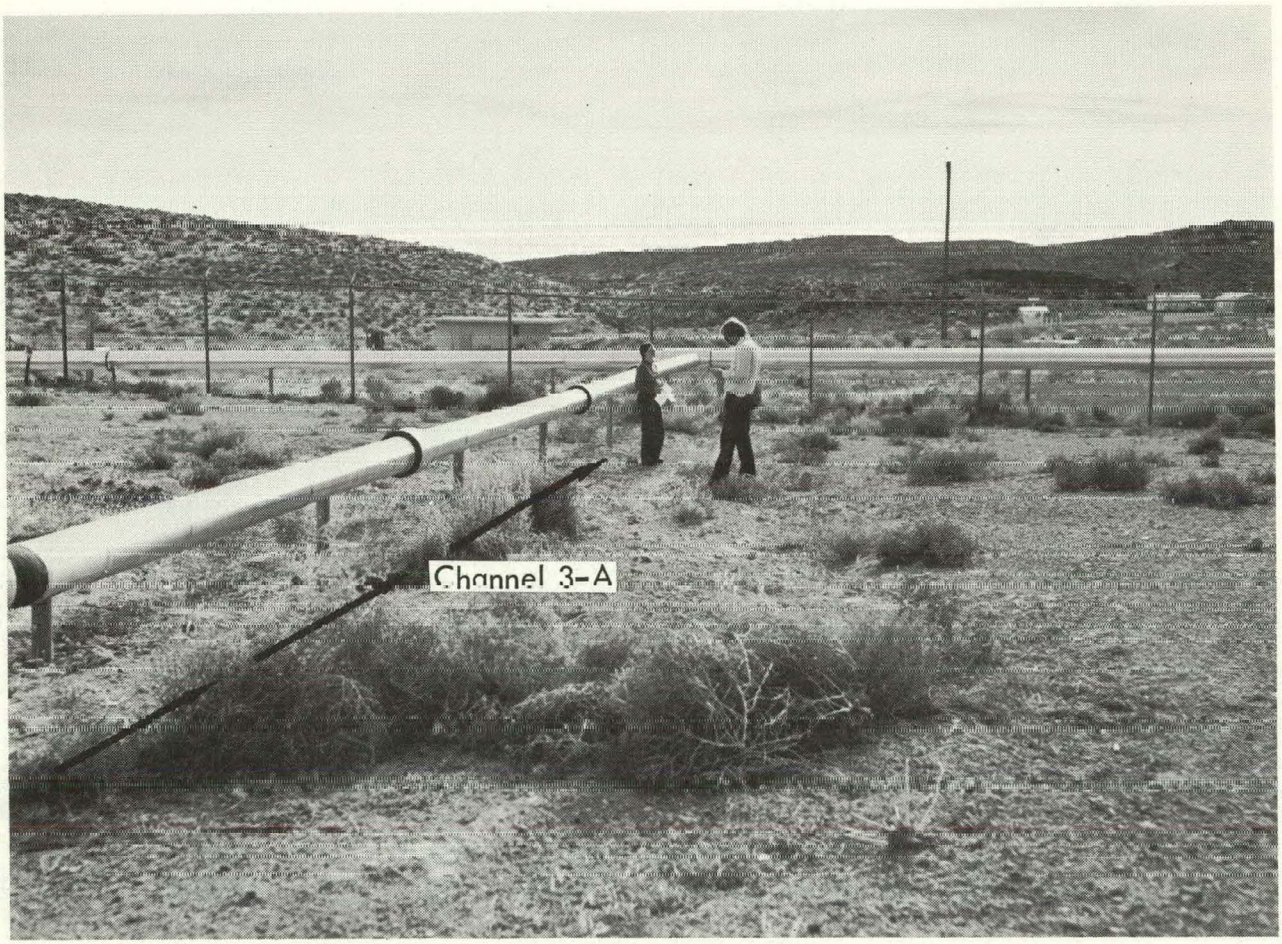

Fig. 9. Channel 3-A flowing off Able site.

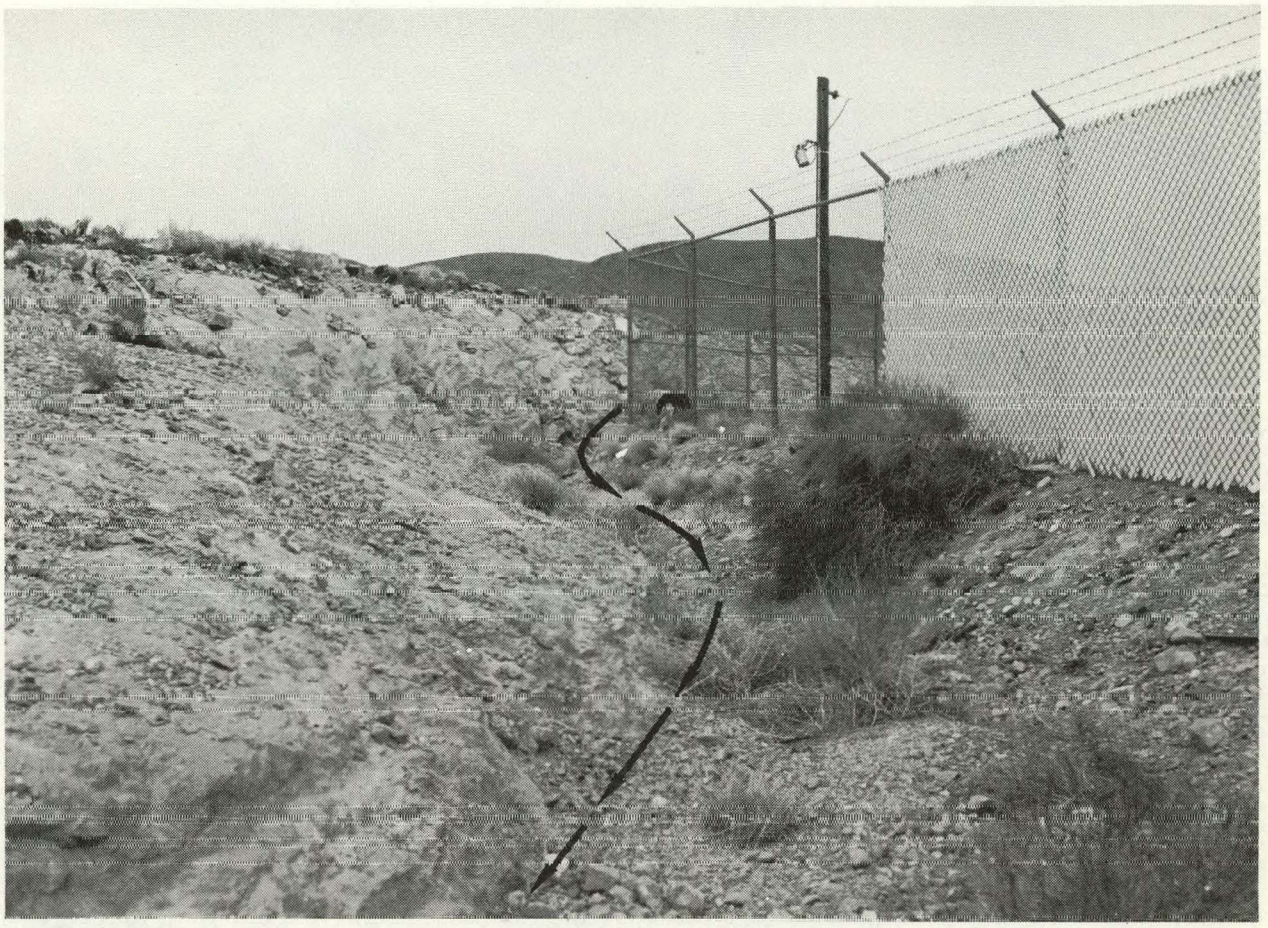

Fig. 10. Beginning of Channel 4-A by B-5110.

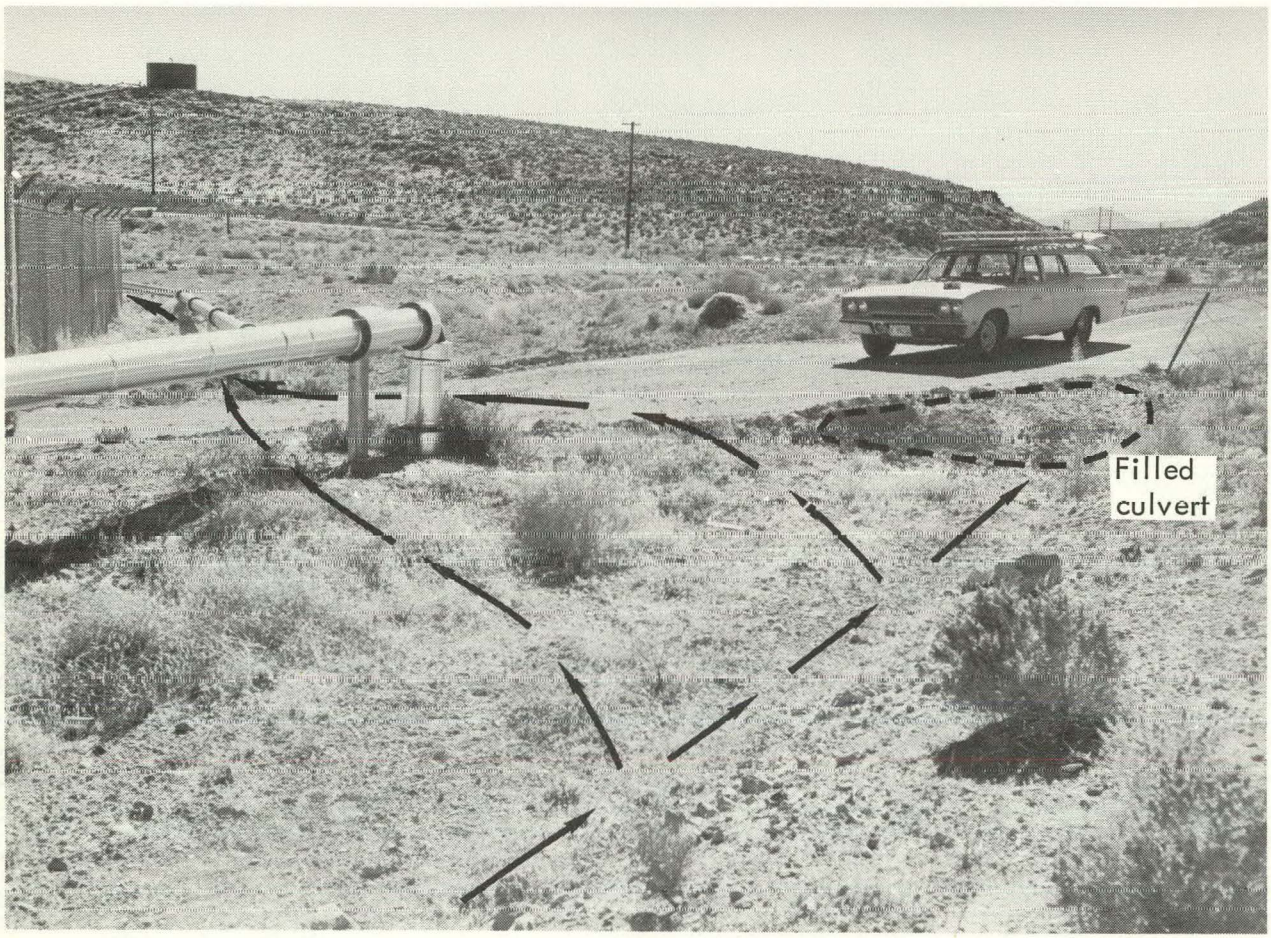

Fig. 11. Channel 4-A crosses road to B-5100.

BAKER AREA

The Baker Area is situated in a 2.8×10^5 m^2 drainage basin south of Hill 4341 and west of Hampell Hill, see Fig. 12. There are five important drainage channels in the area, see Fig. 13.

Channel 1-B drains a portion of the area of Hill 4341 upon which the water tower is located. The channel passes through a 61-cm-CMP (corrugated metal pipe) culvert under the security road and continues about 9 m before making a 90° turn, see Fig. 14. This channel runs parallel to the fence and ends abruptly at the north corner of the fence, see Fig. 15. The flood flow, 0.06 m^3/s, through the culvert and into the channel seems small but, at a velocity of 0.9 m/s and depth of 0.15 m in the channel, it could be enough to undercut and wash away the soft-earth berm at the bend. This would allow the water to drain to the paved area of 5310. This paved area is completely level, see Fig. 16.

The concrete apron is sloped 2% to give a 12 cm elevation at the bay doors of Building 5310. Before the water could build up to a 12 cm depth, it would flow into Channel B-2 around Building 5310 or into the road.

Channel B-2 runs around Building 5310 and behind the two storage Butler buildings. Channel B-2 starts as a 15-cm-deep depression around the north-east side of Building 5310, (see Fig. 17) and continues as such to Building 5306. At Building 5306, a one-half section of CMP culvert was used to line the ditch to its exit at the security fenceline.

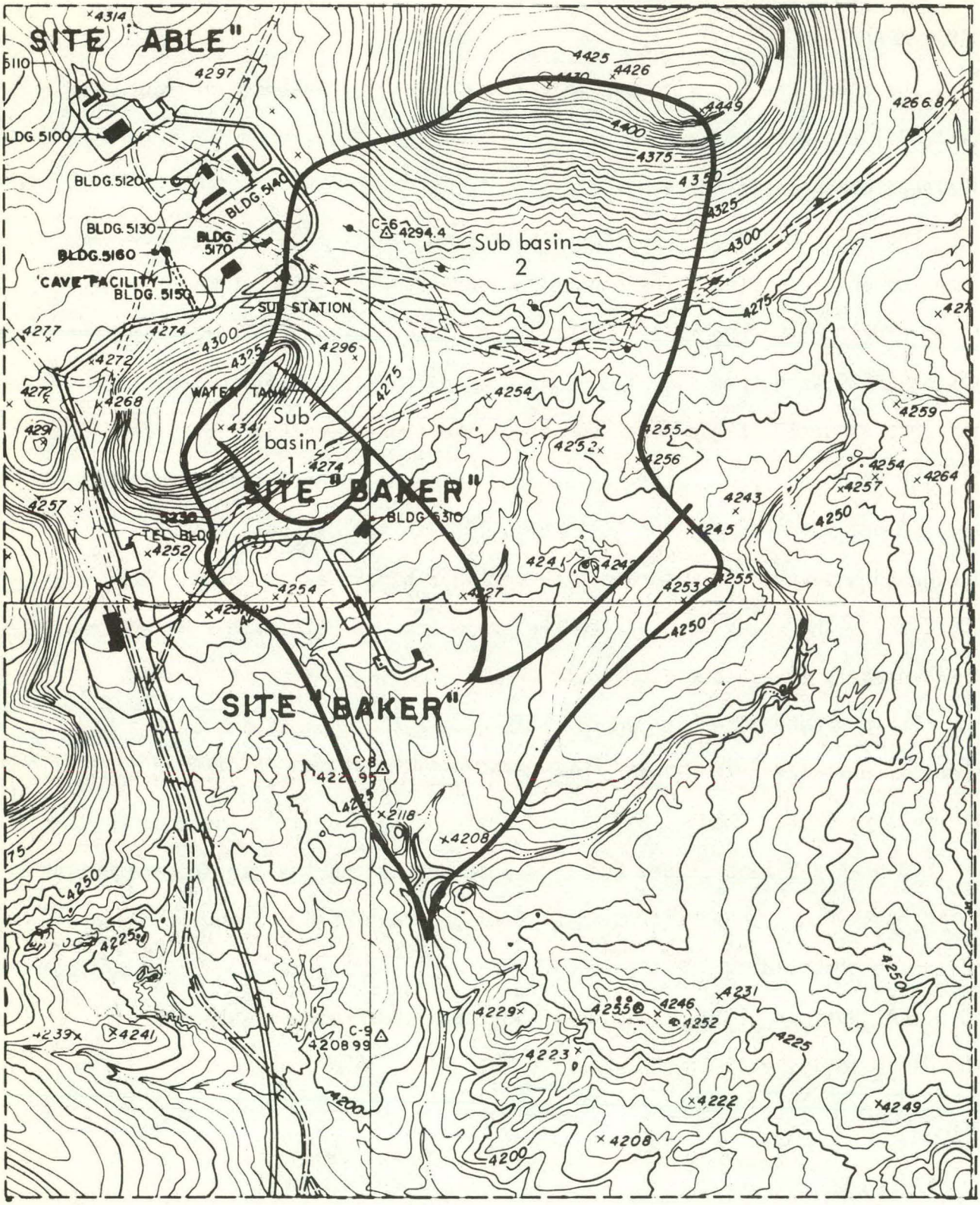

Fig. 12. Baker Area drainage basin.

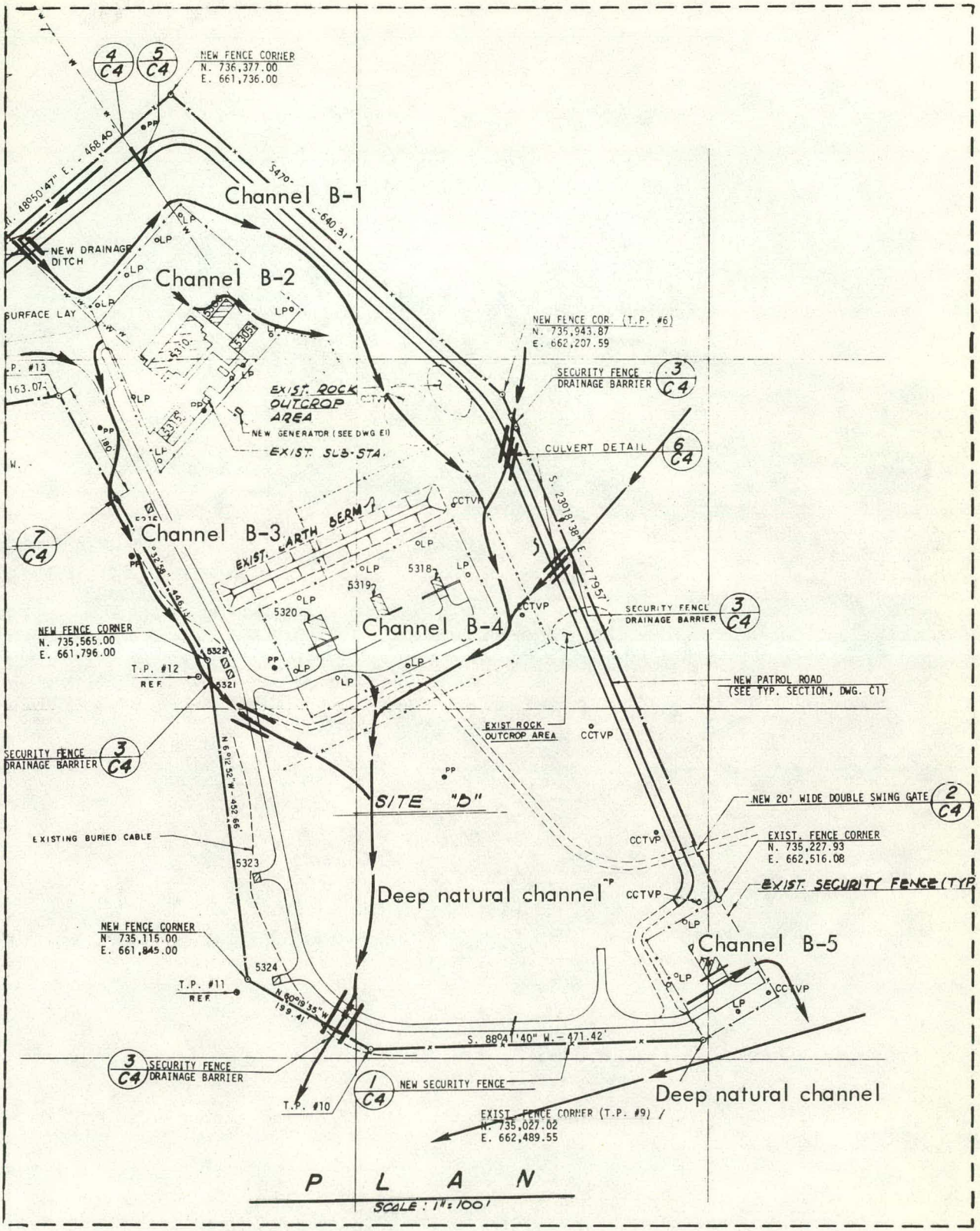

Fig. 13. Baker Area drainage system.

Fig. 14. Channel B-1 near B-5310.

Fig. 15. Abrupt end of Channel B-1 near B-5310.

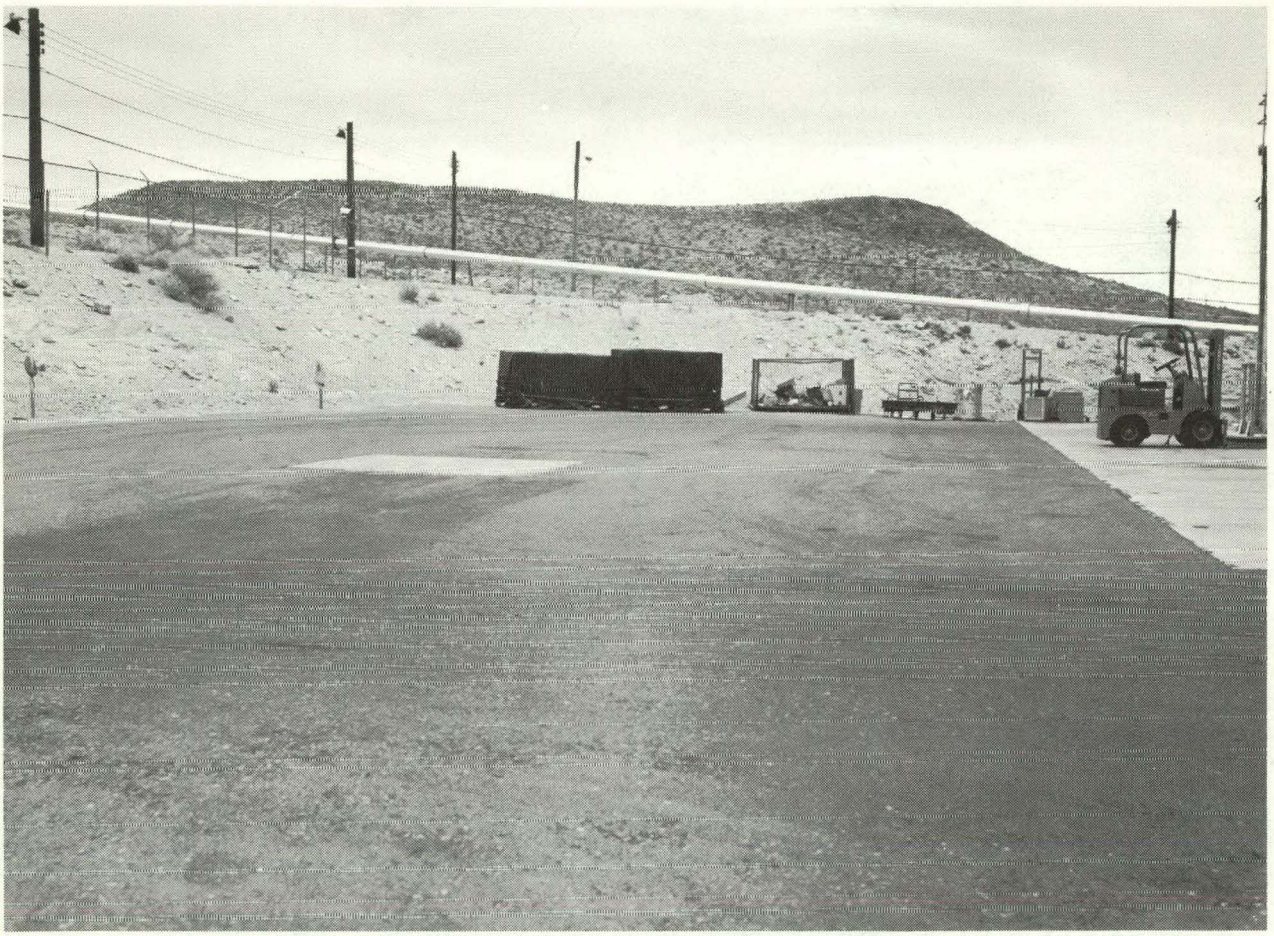

Fig. 16. Paved area by B-5310.

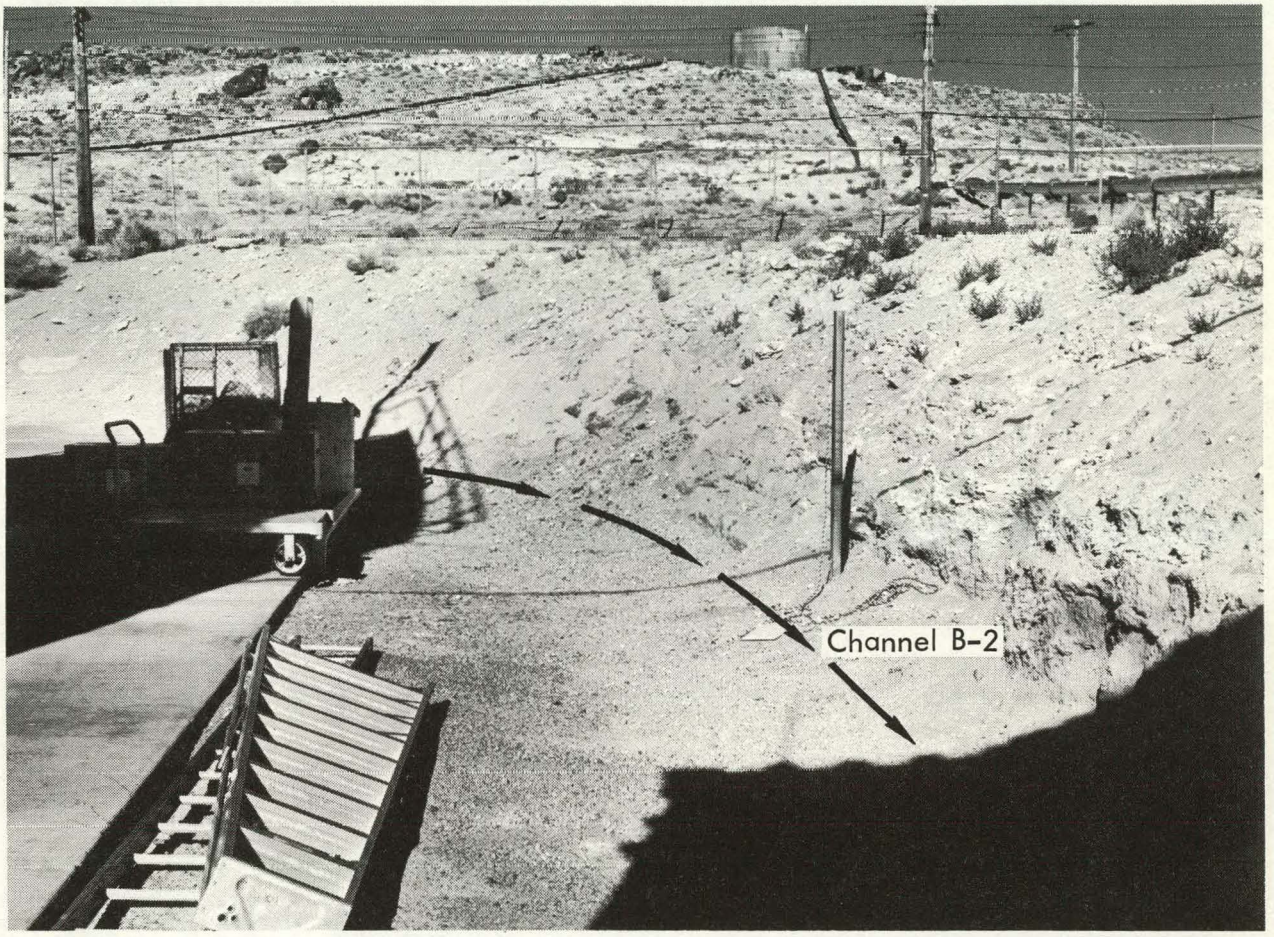

Fig. 17. Channel B-2 around B-5310.

Channel B-2 has the capacity to handle a flow of 0.17 m^3/s which would not be a problem during a rainstorm. The only flooding potential of Building 5310 would be caused by the failure of the 3 x 10^5-ℓ water tank on top of Hill 4341. This volume of water would exceed the drainage capacity of any of the channels around Building 5310.

Channel B-3 runs along the lower road and drains the rest of Hill 4341 and the road area from the Site entrance. This channel passes under the road through a 61-cm-CMP culvert just south of the 5318-20 Complex, see Fig. 18. The culvert was found to be half filled with dirt and weeds. The channel continues in a southeasterly direction to join a deep, natural drainage channel flowing off-site. Channel B-3 does not pass near any critical buildings and will not pose a flooding danger. The culvert and culvert entrances should be maintained to prevent undercutting or possibly washing out of the road.

Channel B-4 drains the largest area in the Baker site. It diverts water around the bunker complex, specifically Building 5318 through which flood water would normally drain.

Two main streams from the drainage area contribute most of the surface runoff to Channel B-4. These are channeled through two, 61-cm-CMP culverts under the dirt security road, see Fig. 19. They are joined by the drainage from Channels B-1 and B-2 from the 5310 Area. Channel B-4 collects all this water in a broad wash, diverts it around the southeast corner of the fence and through a 91-cm-diam culvert to join the deep natural ditch flowing south off-site. The elevation of 5318 and the earth inside the southeast corner of the fence eliminate any flooding potential to the buildings. However, the tendency of the water to follow its natural course has caused undercutting of the fence posts which should be reinforced and maintained.

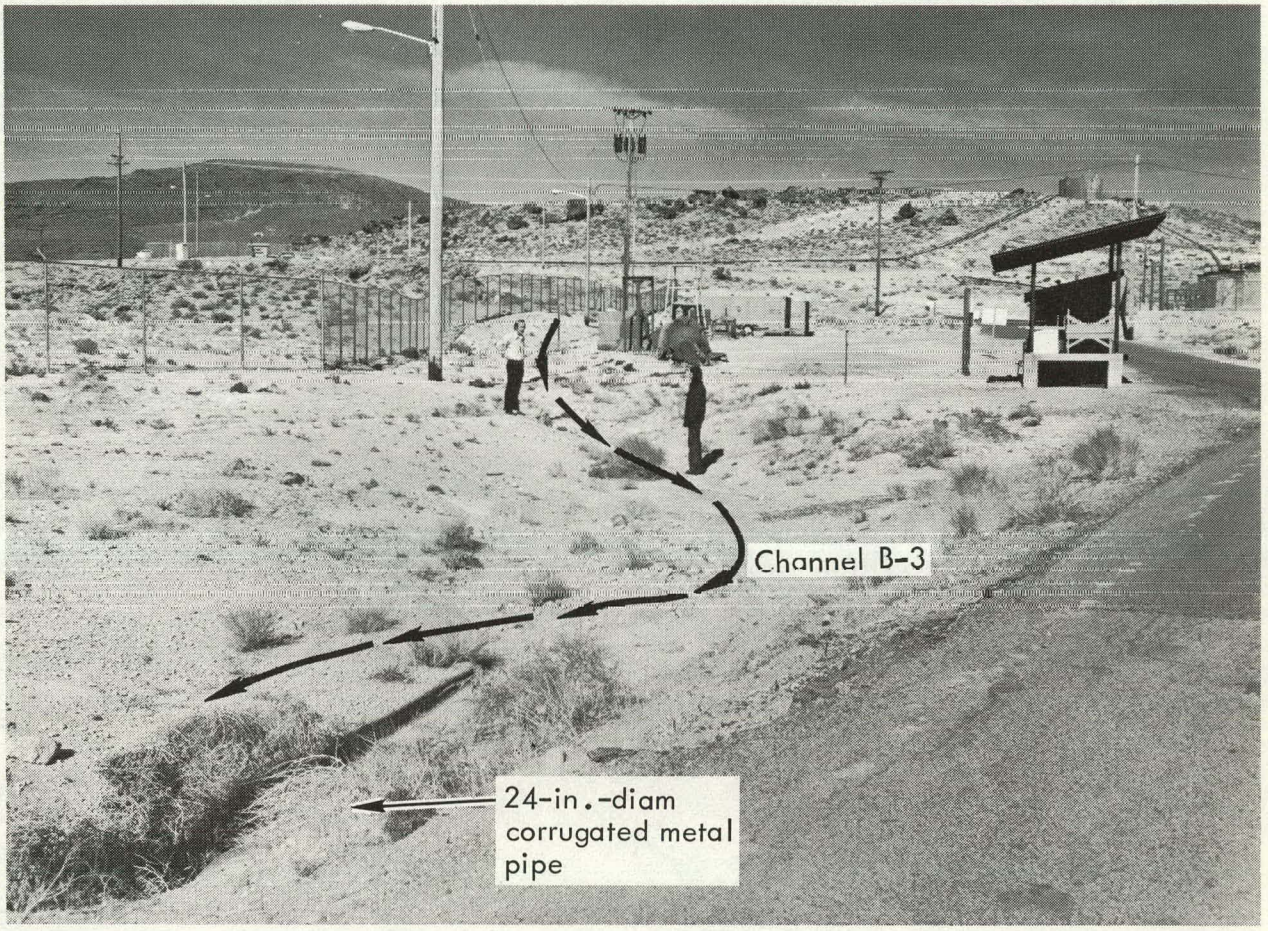

Fig. 18. Channel B-3 parallel to Baker site road.

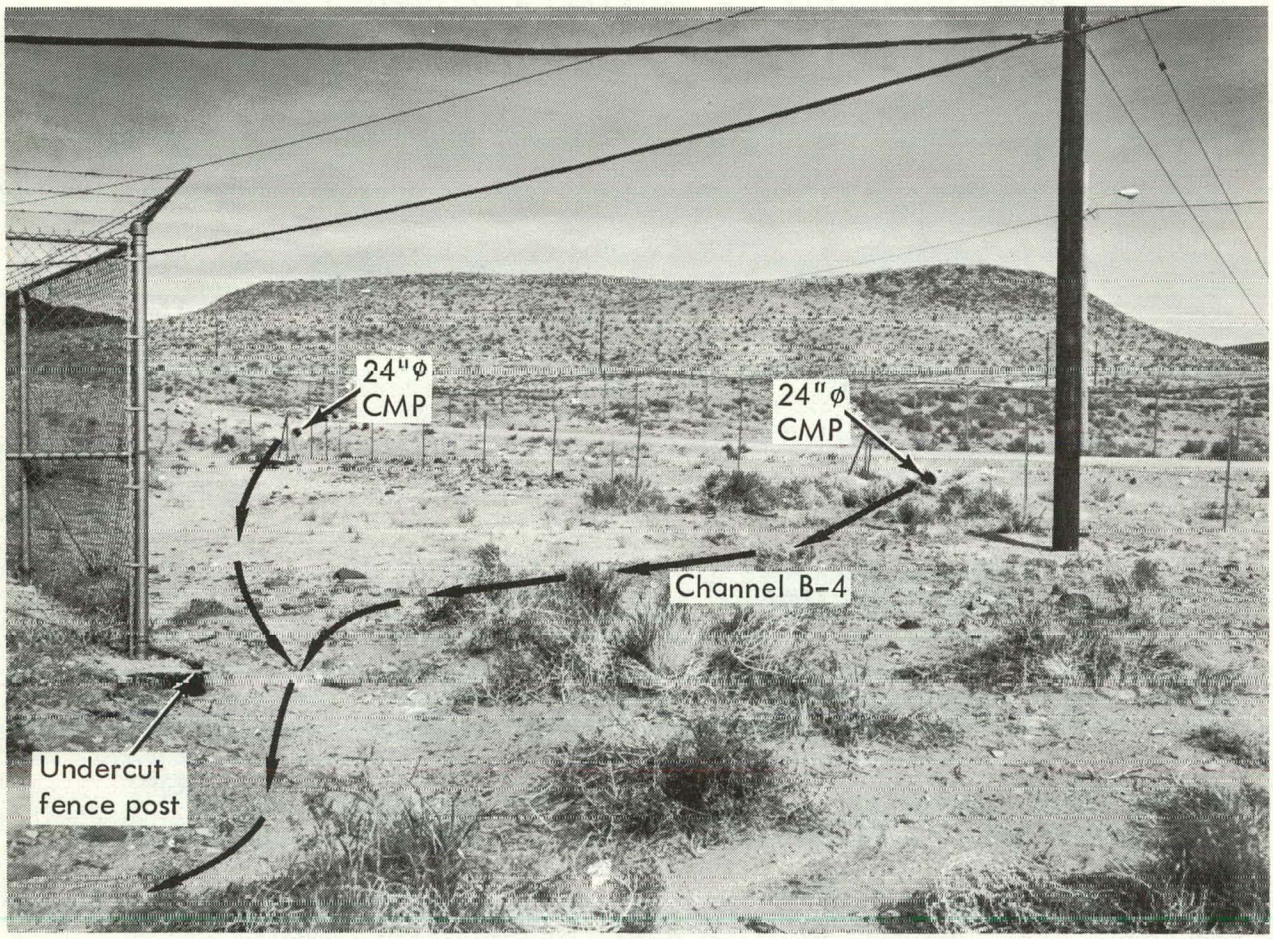

Fig. 19. Channel B-4 near B-5318, B-5319, and B-5320.

The flood flow of 1.44 m^3/s will top over the road at the 91-cm-diam culvert but will not backup enough to cause any damage to the bunkers. Run-off from the bunker complex itself is drained through a culvert and joins the deep natural channel south of the complex. The grading of the area and the elevation of the bunkers prevent flooding.

Bunker 5325 has only what little runoff is generated in its area. The water flows along the edge of the pavement toward the northeast side of the fence, see Fig. 20. There is a drainage grate in the fence; however, it has not been maintained and has silted up causing a 10 cm rise from the channel, see Fig. 21. The water would pool in a low spot but would top out the rise of the road before flooding the bunker. This rise should be removed to allow the runoff to flow freely into a second deep natural drainage ditch flowing west.

The existing drainage channels as designed are adequate to prevent flooding from natural rainstorm. The 90° bend in Channel B-1 should either be reinforced or a deflection placed in the culvert exit so that the culvert will not wash away. The end of Channel B-1 should be cleared and joined with the drainage along the security road. In general, all the channels and culverts should be routinely maintained to remove vegetation and silt.

The calculations for this analysis are included as Attachment B to this Appendix.

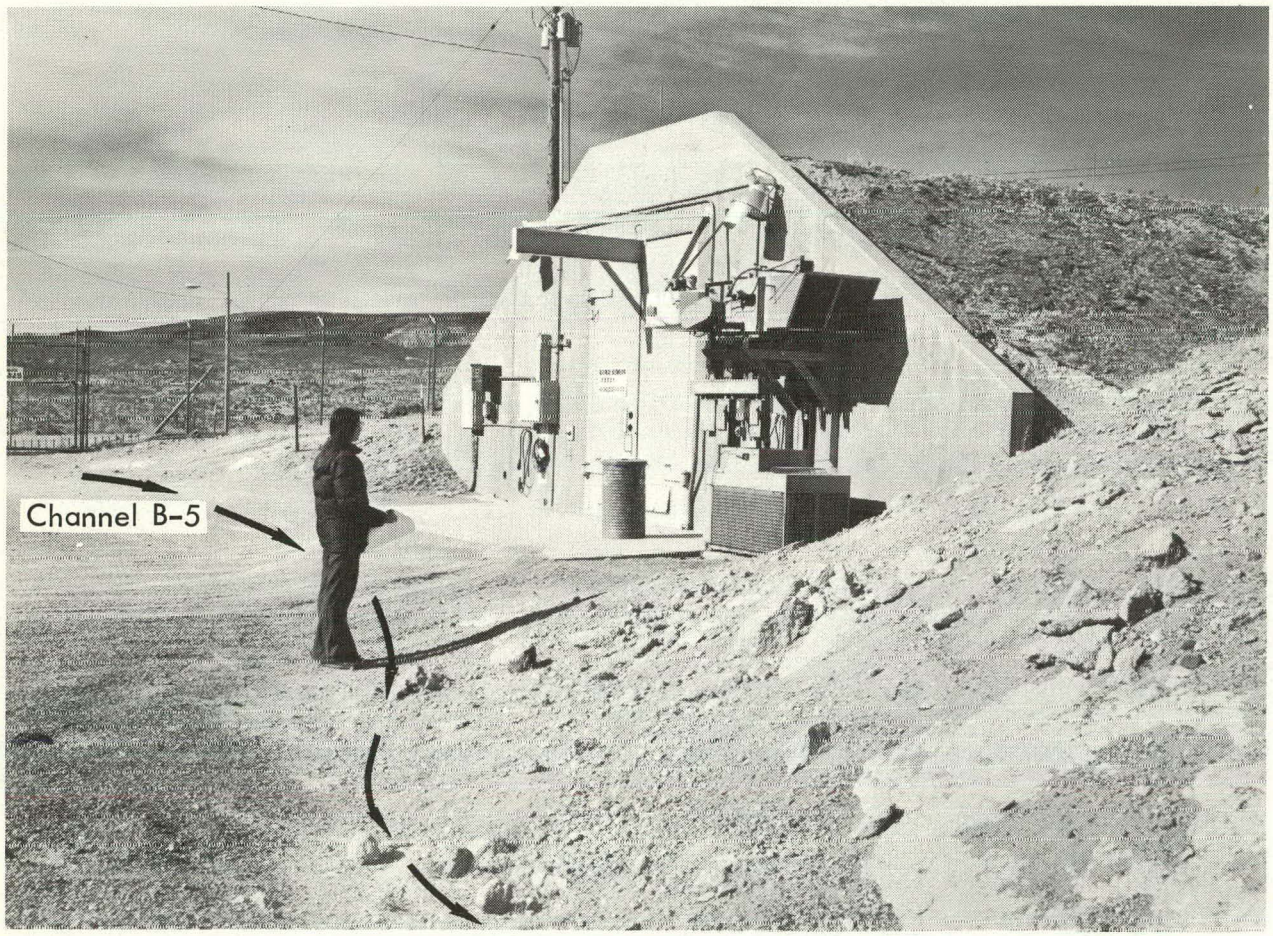

Fig. 20. Channel B-5 near B-5325.

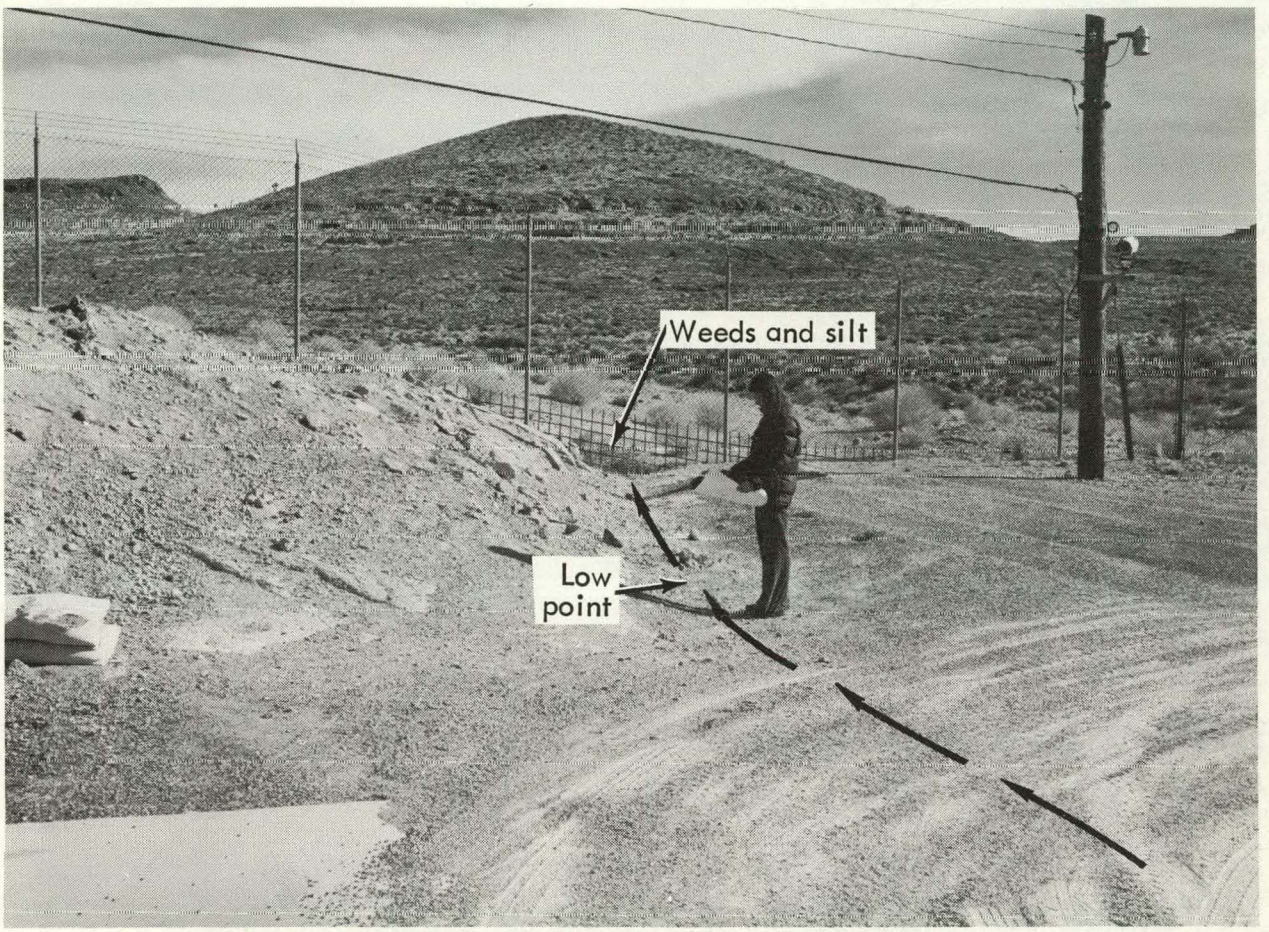

Fig. 21. Channel B-5 at B-5325.

SUBSURFACE HYDROLOGY

The USGS Test Well F, located at Nevada State Coordinates N731,853; E.661,153 was completed in 1962 at a depth of 1040 m.[6] It penetrates three tuff aquitards, (Wahmonie, Salyer, and Pavitt Spring) and ends in Paleozoic dolomite.

The Wahmonie Formation extends from the subsurface to a depth of about 337 m. It consists of ash-fall tuff, tuffaceous sandstone, and lithic tuff. The Salyer Formation consists of volcanic brecia, tuff, and tuffaceous sandstone and extends from 339 m to 452 m. The Pavitt Spring Formation, 452 m to 957 m, consists of calcareous claystone and siltstone, massive tuff, fluvial and lucustrine tuffaceous deposits, conglomerates, limestones, and dolomite.

The major carbonate aquifer extends from 957 m to 1040 m and consists of fractured Paleozoic dolomite.[7]

The general trend is for infiltration to percolate downward to the aquifer. There is, however, some water trapped by an aquitard. This "perched" water was observed in Test Well F at 23 m.[8] Additional perched water was found at lower depths.

The static water level of the aquifer was 529 m below the surface.[9]

Soil borings[10] were taken in the 410 Area before construction of facilities. The deepest of these were drilled 21 m. Sand and gravel are prevalent in the first 15 m. Beyond 15 m, tuff was encountered but water was not found in any of the borings.

With the closest subsurface water at 23 m, there is no chance of flooding due to the subsurface water level.

References

1. E. M. Romney, et al, "Some Characteristics of Soil and Perennial Vegetation in Northern Mojave Desert Areas of the Nevada Test Site," Laboratory of Nuclear Medicine and Radiation Biology (1973).

2. G. B. Sowers and G. F. Sowers, Introductory Soil Mechanics and Foundations, The McMillan Co., New York (1968).

3. Handbook of Concrete Culvert Pipe Hydraulics, Portland Cement Association, Skokie, Illinois (1964) p.29.

4. J. F. Miller, R. H. Frederick, and R. J. Tracey, NOAA Atlas 2, Precipitation-Frequency Atlas of the Western United States, Volume VII - Nevada, U.S. Department of Commerce, Silver Springs, Maryland (1973).

5. R. F. Quiring, Climatological Data Nevada Test Site and Nuclear Rocket Development Station, ESSA Research Laboratories Technical Memorandum - ARL 7 (1968) p.V-8.

6. R. D. Carroll, Interpretation of Geophysical Logs, Test Well F, Nevada Test Site, United States Department of Interior, Technical Letter NTS-54 (1963).

7. William Thordarson, et al, Records of Wells and Test Holes in the Nevada Test Site and Vicinity (through December 1966), United States Department of Interior Geological Survey, Open File Report TEI-872 (1967).

8. Lewis R. West and Murray S. Garber, Abridged Log of Ground-Water Test Well F, 410 Area, Nevada Test Site, Nevada, United States Department of the Interior, Geological Survey, Technical Letter NTS-12 (1961).

9. J. L. Winograd, W. Thordarson, and R. A. Young, Hydrology of the Nevada Test Site and Vicinity, Southern Nevada, U.S.G.S. Open File Report (August 1971).

10. Soils Reports for Area 410, Nevada Test Site, on file at LLL-Nevada Engineering and Construction office.

ATTACHMENT A

CALCULATIONS FOR ABLE SITE HYDROLOGY

FLOOD FLOW HYDROLOGY

I. Drainage to Channel 3-A

Area = 28 acres

Overland flow = 1650 ft

Slope = 10%

Max storm = 1.1 in./hr

Runoff factor = 45%

Concentration time = 17 min

17 min storm intensity = 2.25 in./hr

$Q = CIA = 0.45 \times 2.25 \times 28 = 28$ cfs ($0.79\ m^3/s$)

II. Drainage to Channel 4-A

Area = 40 acres

Overland flow = 2797 ft

Slope = 7%

Max storm = 1.1 in./hr

Runoff factor = 45%

Concentration time = 25 min

25 min storm intensity = 1.85 in./hr

$Q = CIA = 0.45 \times 1.85 \times 40 = 33$ cfs ($0.93\ m^3/s$)

FLOOD FLOW HYDRAULICS

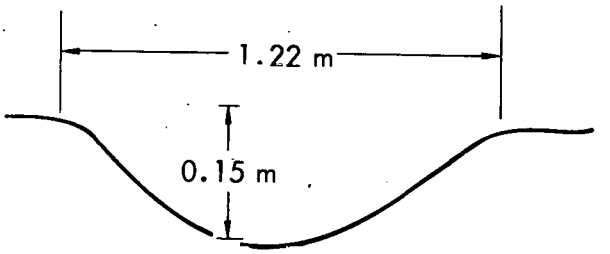

Channel 1-A

Channel 1-A

Top width = 1.22 m n = 0.025

Depth = 0.15 m

Slope = 0.02 m/m

Maximum capacity = $\frac{1.00^{*}}{n} AR^{2/3^{**}} \sqrt{S} = \frac{1.00}{0.025} (0.12)(0.1)^{2/3} \sqrt{0.02} = 0.15\ m^3/s$

**Formula for A & R

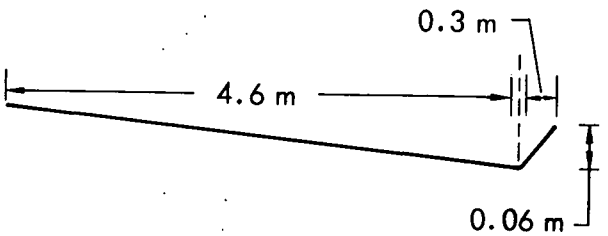

Channel 2-A

Channel 2-A

Top width = 4.9 m

Depth = 0.06 m

Slope = 0.004 m/m

n = 0.020

Maximum capacity = $\frac{1.00^{*}}{n} AR^{2/3**} \sqrt{S}$ =

$$\frac{1.00}{0.020}\left[(0.27)(0.03^{2/3})\right]+\left[(0.02)(0.03^{2/3})\right]\sqrt{0.004} = 0.04\ m^3/s$$

*Mannings constant = 1.00 for metric units from HEC-2 Water Surface Profiles, Programmers Manual (June 1973) p. 36.

**Formula for A and R in V. T. Chow, Open-Channel Hydraulics, McGraw-Hill Book Company, New York (1959) pp. 21 and 129.

ATTACHMENT B

CALCULATIONS FOR BAKER SITE HYDROLOGY

FLOOD FLOW HYDROLOGY (See Fig. B-1)

I. Flood Flow to Culvert

Above Building 5310 = Sub-Basin 1

Area = 1.3 acres slope @ 17%

Max hr 1% storm = 1.1 in./hr

Overland flow length = 370 ft

Concentration time = 9 min

Max 9 min 1% intensity = 2.75 in./hr

Runoff factor = 45%

Q = CIA = 1.61 cfs (0.05 m^3/s)

II. Flood Flow[1] to Building

5318 = Sub-Basin 2

Area = 50.56 acres

Overland flow length = 1900 ft

Max 1 hr 1% storm intensity = 1.1 in./hr

Concentration time = 16 min

Max 16 min 1% storm intensity = 2.25 in./hr

Runoff factor = 45%

Q = CIA = 51 cfs (144 m^3/s)

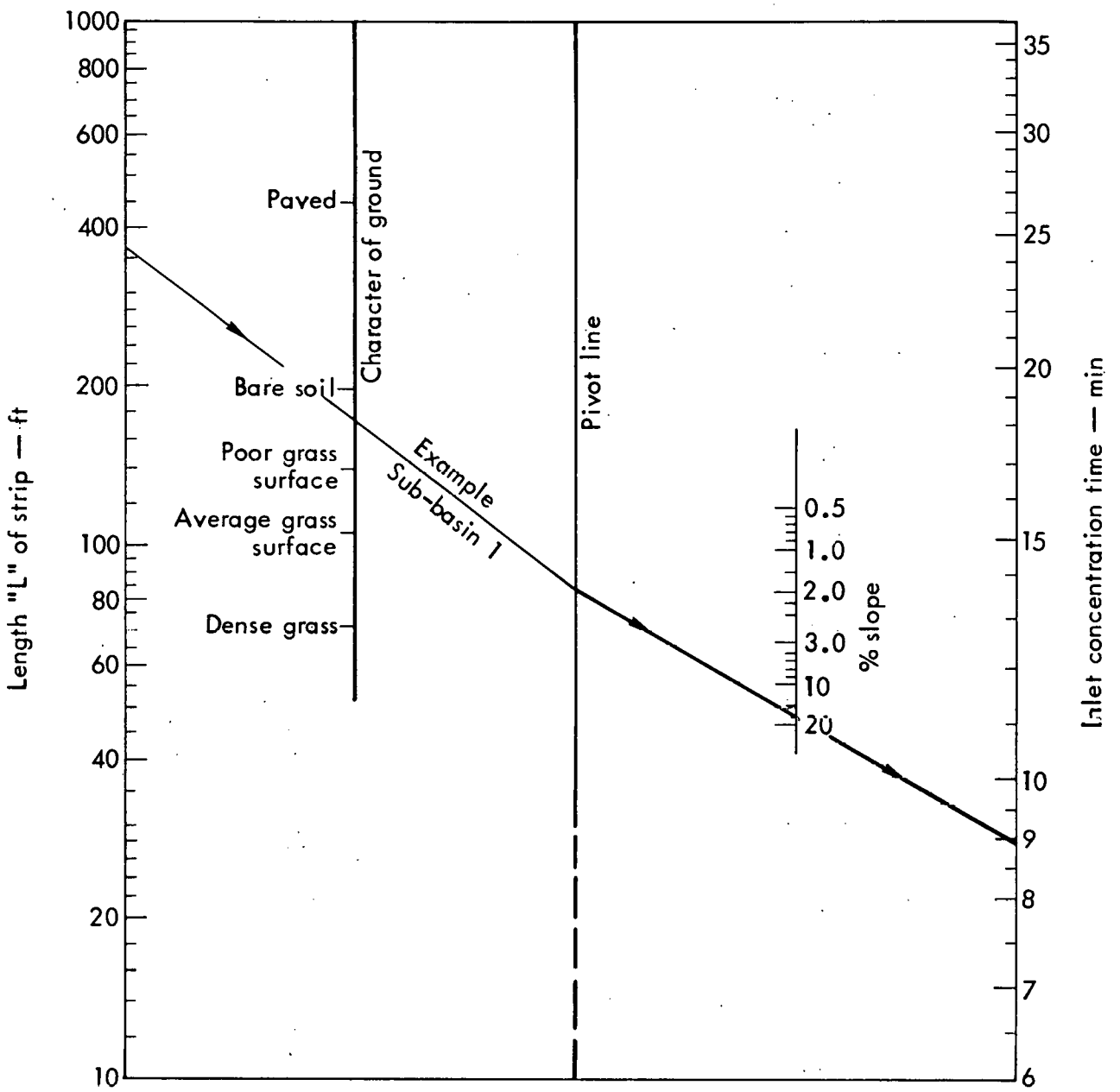

Fig. B-1. Overland flow time.

FLOOD FLOW HYDRAULICS

Channel B-1

Runoff to culvert = 1.61 f^3/s

24 in. Ø CMP culvert
n = 0.024 S = 1%

Flowing full:

$$Qf = \frac{1.49}{n} AR^{2/3} \sqrt{S} = \frac{1.49}{0.024} (3.14)(0.5)^{2/3} \sqrt{0.01} = 12 \text{ } f^3/s$$

$$V = \frac{Q}{A} = \frac{12}{3.14} = 3.82 \text{ f/s}$$

For flood flow:

$$\frac{Q}{Q_f} = \frac{1.6}{12} = 0.13$$

From graph[2] (Fig. B-2)

$$\frac{d}{D} = 0.24$$

$$\frac{V}{V_f} = 0.69$$

$$V = 0.69(3.8) = 2.6 \text{ f/s}$$

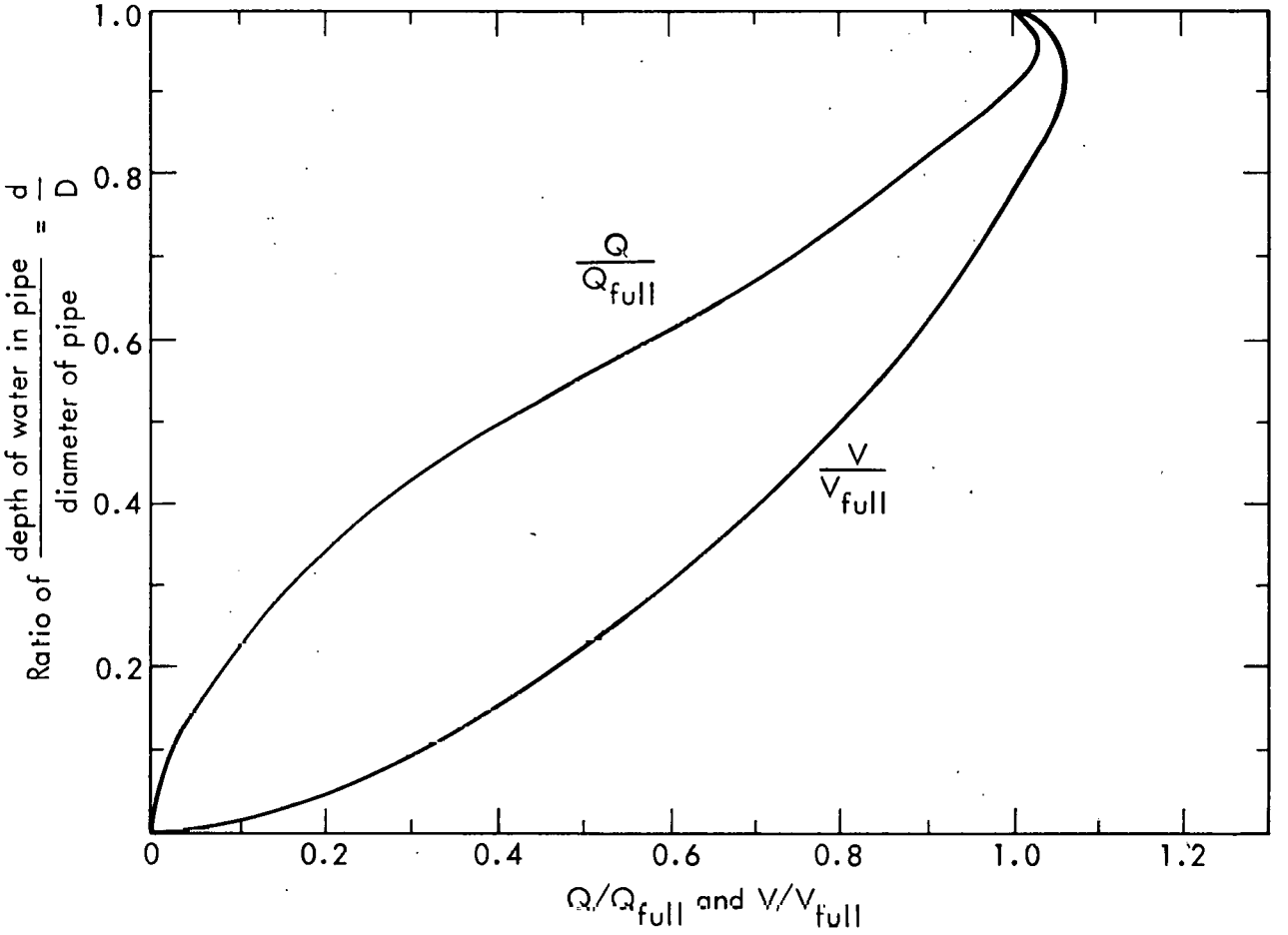

Fig. B-2. Hydraulic characteristics of circular pipes flowing partly full.

Channel B-1

$$AR^{2/3} = \sqrt{2}\, y^{2.5} =$$

$$Q \frac{n}{1.49} \sqrt{S} = \frac{(1.61)(0.025)}{(1.49)(0.1)}$$

$y = 0.52$ ft

$$\text{Velocity} = \frac{Q}{A} = \frac{1.61}{2(0.5)}2 = 2.5 \text{ f/s}$$

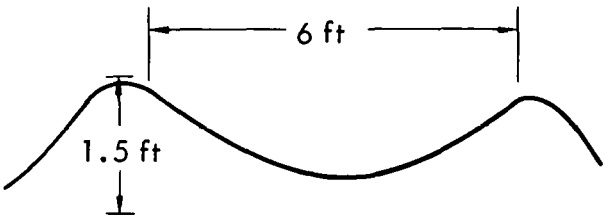

Channel B-1

Channel B-2

1st Section

$$Q\text{max} = \frac{1.49}{0.025} AR^{2/3} S^{1/2} =$$

$$\frac{1.49}{0.025}\left[\frac{2}{9}\sqrt{6}\ (6.5)^{1.5}\right]\sqrt{0.01} = 6.88 \text{ f}^3\text{/s}$$

Channel capacity = 6.88 f^3/s

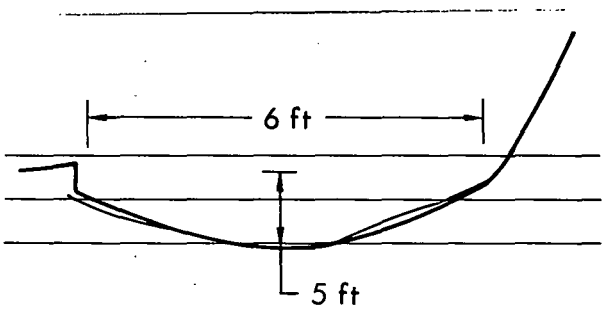

Channel B-2 , 1st section

2nd Section

$$Q = \frac{1.49}{0.024}\left(\frac{TTy^2}{2}\right)\left(\frac{y}{2}\right)2/3\ \sqrt{0.01} = 6.14 \text{ f}^3\text{/s}$$

Channel capacity = 6.14 f^3/s

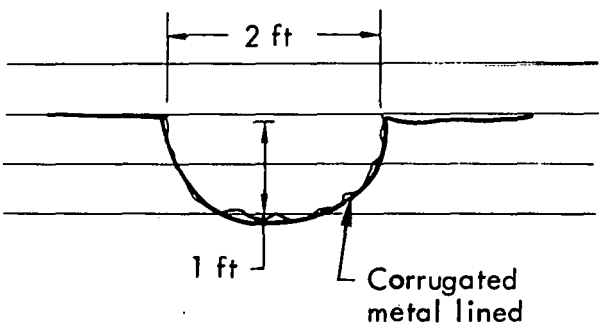

Channel B-2, 2nd section

Channel B-4 culvert

Runoff to culvert = 5.1 cfs

24 in. Ø CMP culvert

n = 0.024 S = 0.02

Maximum flow (under pressure):[4]

$$Q = A\sqrt{\frac{2gH}{K}}$$

A = area of opening = 7 ft^2

H = pressure head = 1 ft max to top of road

K = total less coefficient = 1.5

$$Qmax = 7\sqrt{\frac{2(32)(1)}{(1.5)}} = 46 \text{ cfs}$$

Flood flow = 51 cfs so will top over road.

References

1. E. E. Seelye, Data Book for Civil Engineers, Design, John Wiley and Sons, New York (1960).

2. V. T. Chow, Open-Channel Hydraulics, McGraw-Hill Book Co., New York (1959) pp. 21 and 129.

3. R. K. Linsley and J. B. Franzini, Water-Resources Engineering, 2nd Ed., McGraw-Hill Book Co., San Francisco (1972) p. 273.

4. Training Document No. 6, Applications of the HEC-2 Bridge Routines, Hydraulic Engineering Center, U.S. Army Corps of Engineers (June 1974) p. 9.